OTS: 60-11,918

JPRS: 5024

July 26, 1960

PROBLEMS ON THE THEORY OF HEAT RESISTANCE OF ALLOYS

- USSR -

Distributed by:

OFFICE OF TECHNICAL SERVICES
U. S. DEPARTMENT OF COMMERCE
WASHINGTON 25, D. C.

~~Price: $4.00~~

U. S. JOINT PUBLICATIONS RESEARCH SERVICE
205 EAST 42nd STREET, SUITE 300
NEW YORK 17, N. Y.

JPRS: 5024

CSO: 3910-N

PROBLEMS ON THE THEORY OF HEAT RESISTANCE OF ALLOYS

[Following is a translation of excerpts from Trudy Instituta Fiziki Metallov -- Voprosy teorii Zharoprochnosti metallicheskikh Splavov (Works of the Institute of Physics of Metals -- Problems of the Theory of Heat Resistance of Metal Alloys), No. 4, 1958, pages 3-94 and 101-162]

Work of the Institute of Physics of Metals of the Ural Affiliate of the Academy of Sciences USSR, on the Theory of Heat Resistance of Alloys

By V. I. Arkharov

It is unnecessary to explain the importance of improving (increasing) the mechanical properties of metals used for various machine parts, mechanisms, apparatus, and structures subjected to high-temperature heating under service conditions. Naturally, in addition to heat resistance, such materials must also meet other requirements; in particular, their cost must be sufficiently low, the raw materials for them must not be scarce, and they must readily yield to various operations in the process of mechanical, thermal, and other types of treatments when used for the fabrication of parts and components of installations.

The importance of the problem dealing with the correspondence of the characteristics of the mechanical properties of a material under certain test methods to the behavior of the same material under real service conditions is conceded; in this case, the shapes and dimensions of the product, the vibrations, the sharp and frequent changes in thermal loads, etc., acquire a substantial and sometimes decisive role.

The specific nature of deformations of materials

at high temperature introduces into the problem of their selection and characterization additional factors which strongly complicate the picture as compared to a similar selection and characterization of materials subjected to deformation under normal temperatures (such as the load duration factor).

The introduction of a newly created material sometimes proves unsuccessful due to the fact that, though meeting all specifications, it is actually almost useless because of its failure to satisfy what is apparently only a minor requirement, whose importance could not have been foreseen because of our incomplete understanding of the nature of deformation of materials at high temperatures.

In this connection we must understand the great difficulties to be encountered in an empirical investigation of new materials subjected to deformation at high temperatures.

On the basis only of experimental data on the required composition of the material, on the methods of production and processing, and on the permissible ranges of service conditions, the researcher will seldom achieve his object. Even if the object is attained after having concluded numerous unsuccessful variants, there always arises a doubt as to whether one variant close to those tested had not been left unchecked; whether that one could not have produced better results; whether its effect had therefore been lost for practical purposes because of the impossibility of investigating too many variants.

Such a situation is caused by the absence of sufficiently clear concepts of the physical mechanism of deformation phenomena in materials at high temperatures. It is obvious that the correct evaluation of the role played by individual factors which provide material with the ability to resist deformation at high temperatures (in short, its "heat-resisting" properties), and the evaluation of the importance of those or other service conditions on the behavior of the material in service, etc., depends on the completeness of our knowledge.

Thus, solid-state physics and, in particular, both physics of metals and metallography face the important problem -- the creation and elaboration of the <u>theory of heat resistance of materials</u>. This includes a great

number of problems and the most important is to determine the following: (a) the mechanism of high-temperature plastic deformation in monocrystals; (b) the dependence of mechanical properties of the crystal on the atomic interaction within the lattice; (c) the influence of structural nonuniformity of real solids on the mechanism of the development of deformation in them and on their mechanical properties*; (d) the influence of nonuniformity of concentration in real solids on their mechanical properties.

The problem of studying the mechanism of some physical phenomenon is often more easily solved on materials under conditions which are different from those used in practice but in which the resulting phenomena are more contrastible and more readily traced in detail. In other words, the phenomena under study are better represented on materials under conditions specially selected for the investigation. The relationship revealed must then, of course, be checked on materials under conditions employed in practice, which is immeasurably easier to accomplish after the model study had been carried out.

At first sight, model studies seem to be unconnected with those in practice. However, this idea is erroneous. Related to practical objects, the results of these investigations give a more general and therefore more valuable solution of the practical problems set forth than does a similar investigation conducted from the very beginning on a material employed in practice but in which the mechanism under study is not so clearly apparent and the relationships revealed in the test are not so singularly defined nor as accurate as on the prototypes of the material.

Of course, here as in other similar problems, a reasonable compromise can be found by selecting the model

*We have in mind the influence of the extent of polycrystallization, the mosaics of the crystallites (and a subcrystallite structure in general), the heterophase of the alloy and the heterogeneity of a single-phase crystal, and, particularly, the influence of various phases of aging of alloys, etc.

material that is closest to that used in practice*.

In the wide scope of work conducted in the Soviet Union for finding ways to improve the heat resistance of materials needed for the new techniques, a substantial part of this work to create a general theory of heat resistance and its details is conducted in many scientific institutions. A share of this work is being conducted by the Institute of Physics of Metals of the Academy of Sciences USSR (AN SSSR), Ural Branch, where some of the basic problems on the theory of heat resistance are worked out, namely, the problems associated with two aspects of the mechanism of high-temperature deformation: 1) the localization of the processes of high-temperature plastic deformation on structural nonuniformities in a deformed solid; and 2) the internal adsorption of some dissolved admixtures on the same nonuniformities. The combined influence of these phenomena on the heat resistance of the material is particularly important because they are both localized in the same regions of the alloy. Actually, deformation develops in the regions where the composition of the alloy -- due to internal adsorption -- is substantially different from that of an average composition determined through a chemical analysis for the entire mass (or the entire volume). The fact that the influence of internal adsorption depends on the preceding heat treatment is also important in this case. It follows from this that the "small" impurities, frequently not even accounted for by the analysis, may noticeably alter the heat resistance of the alloy to various degrees, depending on the treatment. It can be assumed that the main factor which determines the heat resistance of a crystal is the interatomic bond in its lattice. This bond varies with the composition of the solid solution. However, the heat resistance of a real polycrystalline body is determined by the interatomic bonds, that is, in those regions of the body where deformation originates and develops. And since the internal adsorption can change the composition in these regions quite substantially, their interatomic bonds may prove to be greatly different from those existing in the lattice of a solid body which has the average composition of the given alloy. This important fact must be

*For instance, to study the general problems of heat resistance, we have used ferrum-chromium-nickel alloys of the heat-resistant type, close in composition to those used in practice but more simple.

remembered when studying the influence of the composition of the alloy on the interatomic bonds in it and on its heat resistance, since this may cause the incompleteness and the ambiguity of the results of such an investigation.

The above considerations form the basis of the complex work on the theory of heat resistance conducted in the Institute during the period 1949-1954. At present the first phase of this work is completed. The results obtained make it possible to assume that our suppositions on the role of localization of deformation on the structural nonuniformities and of the internal adsorption of impurities on them were to some degree correct. With respect to such nonuniformities as intergranular coupling in polycrystalline alloys (under certain deformation conditions), this role becomes substantial, and there is reason to assume that the heat resistance is influenced by the localization of deformation and by the internal adsorption of impurities on finer structural nonuniformities -- on cells of subcrystallite structure (further work is planned in this direction).

Thus, the immediate problem set forth by the team of scientific workers of the Institute was solved. In this connection there arose the need of summing up the results obtained at the completion of the first phase of the study of the problem of the theory of heat resistance, to which this collection of articles is devoted.

The article by V. I. Arkharov and M. B. Yakutovich (2)* gives a developed substantiation of the investigations conducted in the Institute on the problem of heat resistance and a detailed elucidation of the general leading idea of the entire complex of these investigations.

The works described in the article by V. I. Arkharov, I. P. Polikarpova, S. I. Ivanovskaya, and N. P. Chuprakova (3), and the article by V. I. Arkharov and A. A. Pen'tina (4) are devoted to the elucidation of the adsorption activity of admixtures of a number of elements (molybdenum, tungsten, niobium, titanium, aluminum, and boron) in ferrum-chromium-nickel austenite. The first article describes the investigation of the diffusional mobility of one of the main components of the

*The numbers of the references (in parentheses) correspond to the order of the articles in the collection (see index).

alloy (nickel) in the intergranular transitional zones -- a characteristic important for heat resistance, since plastic deformation has a diffusion mechanism.

A confirmation of this fact is obtained by analyzing the experimental data on high-temperature relaxation of stresses. This analysis is given in the article by G. N. Kolesnikov and A. I. Moiseyev (10); the article by G. N. Kolesnikov, A. I. Moiseyev, and M. V. Yakutovich (9) is devoted directly to the experimental work on measuring the relaxation of stresses. The correlation between the data on intergranular diffusional mobility of nickel and the data on the relaxation of stresses in the tested alloys, which confirms the basic assumptions concerning the mechanism of high-temperature deformation as well as the role of internal adsorption in this case, is given in the article by V. I. Arkharov, S. I. Ivanovskaya, G. N. Kolesnikov, and A. I. Moiseyev (11). The article by V. S. Averkiyev, G. N. Kolesnikov, A. I. Moiseyev, and M. V. Yakutovich (8) gives the description of the methods of measuring high-temperature relaxation of stresses. The article by V. A. Pavlov, E. S. Yakovleva, and M. V. Yakutovich (5) relates the basic experimental data on the influence of small admixtures of "horophile" (active with respect to internal adsorption) elements on the creep of solid solutions. It has been shown in this work that at low stresses, when deformation is considerably localized in the intergranular transitional zones, such an admixture has a strenthening effect. At high stresses, when deformation is mainly of a displacive nature and extends over the entire volume of the crystallite, the role of internal adsorption of a small admixture in the intergranular zones comes to naught, and in some cases, at high stresses, a small admixture can reduce the resistance of the material to flow. Additional data on this problem are contained in the article by M. G. Gaydukov and V. A. Pavlov (14), as well as in the article by E. S. Yakovleva (6).

The article by E. S. Yakovleva (7) accounts for the results obtained in attempting to get a microinterferometric confirmation of changes and of distribution of deformation over the grain of the metal in alloying it with small admixtures. The first very small additions markedly influence deformation, which is (at low stresses) localized at the intergranular boundaries. Further increase in the concentration of the admixture introduces a thickness of crystallites into the deformation process

and raises the flow rate. These results also agree with the basic hypothesis on the influence of internal adsorption of admixtures on the heat resistance, and supplement this hypothesis with indications on the range of conditions of deformation where the internal adsorption plays a substantial role.

In the course of investigating the relaxation of stresses in some alloys, there was detected a peculiar effect of "negative relaxation", which consisted of a build-up of stresses in time rather than the usual, natural droop of stresses. This effect was explained on the basis of an assumption of the phase transformation's taking place -- under conditions of relaxation testing -- in the material as the specific volume is reduced (12). This effect obtained further confirmation in the work by M. G. Gaydukov and V. A. Pavlov (13).

The article by V. I. Arkharov (16) is devoted to discussing the possibility of practicing the basic idea of this complex of studies on subcrystallite structural nonuniformities, and particularly on those which occur and develop during aging. If we take into consideration the fact that most heat-resistant alloys can be classified as aging, the problem of the influence of internal adsorption of admixtures structural nonuniformities on the heat resistance of an alloy develops into a problem of major significance. Thus, in essence, is mapped the program of an important section of remaining work connected with the creation of the theory of heat resistance; this program is the logical development of works already conducted in the Institute and stated in this collection.

* * *

Heat Resistance and Internal Adsorption in Polycrystalline Alloys*

I. General Considerations on the Mechanism of Plastic Deformation at Low and Elevated Temperatures and on Internal Adsorption in Solid Alloys

By V. I. Arkharov and M. B. Yakutovich

Raising the heat resistance of a polycrystalline alloy consists in preventing and encumbering the elementary processes of plastic deformation at elevated, possibly much higher, temperatures. This can be attained, on the one hand, by preventing or encumbering the nucleation of the elementary act of plastic deformation and, on the other, by preventing its propagation and development (the formation of a build-up process consisting of new nucleation of elementary acts and their propagation in groups).

*This article is based on a report written by V. I. Arkharov made on behalf of the entire group of workers of the Institute of Physics of Metals of the Academy of Sciences USSR, Ural Branch (IFM UFAN), which had participated in the works on heat resistance produced during the period 1948-1953 (the report was read at the Scientific Technical Session on Heat-Resistant Alloys in Moscow, 1953); the text has been supplemented in accordance with the results of the works conducted in 1954.

M. V. Yakutovich, who had taken direct part in these works in the first part of the above period and had kept in touch with them during the second part of the same period, is responsible, together with V. I. Arkharov, for the scientific idea which was the basis of all works on the theory of heat resistance carried out during this time in the IFM UFAN. This idea consists of a presentation of the combined influence of two factors on plastic deformation: (1) localization of plastic deformation on structural nonuniformities; and (2) internal adsorption of dissolved impurities on the same nonuniformities.

It is obvious that, to prevent plastic deformation, we must know:

(1) the mechanism of nucleation of the elementary act of plastic deformation;

(2) the conditions favorable and unfavorable to the nucleation;

(3) the localization sites of these conditions;

(4) the propagation mechanism of the elementary act of plastic deformation;

(5) the conditions favorable and unfavorable to its expansion; and

(6) the distribution of these conditions in a polycrystalline aggregate.

1. Nucleation Mechanism of Plastic Deformation

It can be assumed (1) that in the basis of the elementary act of plastic deformation in general and at high temperatures in particular lies the act of atomic displacement from the lattice point to the nearest interstice in the region of the lattice elastically most distorted; such a displacement occurs under the influence of fluctuation of thermal motion and represents an elementary act of diffusion directed by the acting stress. The act of displacement may develop further by means of a repetition of similar acts performed by the adjoining atoms, in which the force effect of distortion created in the lattice by the first displacement subsequently spreads. Thus, the elementary act of plastic deformation of the displacive type can develop and expand, covering the region of either a larger or smaller lattice. For a directed propagation of an elementary deformation process it is necessary to have a field of stresses which is created by external effects on the polycrystalline body and which has certain directions within the limits of the region in the lattice considerably exceeding the normal interatomic distance.

With this mechanism of nucleation of the elementary act, the conditions favorable to its nucleation are the distortions available in the lattice beforehand and reducing the energy barrier; the latter must be overcome so that

the atom can be displaced from the lattice point. The atomic displacements, including also the first displacement, constitute the elementary act of plastic deformation. In order to direct them in a certain manner, it is necessary that the favoring initial distortions are oriented in a certain manner, or that they are not oriented unfavorably. Obviously, the conditions favorable to the nucleation of elementary acts of plastic deformation are most probably encountered in regions where there are in general lattice distortions which are not oriented; for instance, near the structural nonuniformities. First, we may refer here to the intergranular transitional zones (roughly described as intergranular "boundaries"); we may also refer to the interlump zones on the "boundaries" of the lumps of the subcrystallite structure in general (distortion zones surrounding the submicroscopic inclusions of different sizes up to individual foreign atoms, etc.). And we may also refer to the distortion zones which are to some degree oriented; for instance, the boundaries of twin crystals, traces of slippage which had earlier taken place in this crystal under the influence of different effects, and so forth. In view of the fact that in the regions of these uniformities there are distortions of a disordered, complex nature, there will always be found among these distortions such that will enhance the nucleation of the elementary act of plastic deformation, an act which is oriented* according to the field of acting stresses.

2. The Mechanism of Inhibition of the Elementary Act of Plastic Deformation

Parallel with the nucleation of the elementary act of plastic deformation we must also discuss the conditions which inhibit (end the propagation of) the act which had already originated. The most favorable conditions "relay" the displacements from one atom to the adjoining one -- in a regular lattice where each preceding displacement causes the one which follows, since at each subsequent displacement the periodic field of the lattice becomes distorted to such an extent that the atom which adjoins the distortion is pushed out from its "energy pit".

---

*In other words, the first atomic displacement will occur in a direction in which the displacement of the second atom caused by the first displacement, as well as all the following displacement, will be composed into a displacive process directed according to the field of stresses.

Thus, since the elementary act of plastic deformation had already started, it will propagate in a regular lattice to a macroscopic distance. To inhibit and stop this process we must disturb the regularity of the lattice. When the process of plastic deformation approaches the region of this disturbance, the next atomic displacement will create a distortion of the lattice which, being superposed on the earlier disturbance and thereby being diminished, will prove to be insufficient to push out the next atom from its energy pit. The relaying process of displacement will be interrupted here; the process of plastic deformation will be inhibited -- at least in this sector of the propagation front.

The causes disturbing the regularity of the lattice are:

(a) the fluctuation of thermal motion; and

(b) prolonged distortion of the lattice due to causes existing beforehand, long before the elementary process of plastic deformation had approached this region.

The chaotic state (disordered state) of the thermal motion makes it difficult to achieve the regular sequence of relaying the displacive effects from one atom to another in the propagation process of the displacive plastic deformation. The thermal displacements create short-term local distortions of the lattice which may become sizable to the extent that the will interrupt the relay of displacements which forms the displacive process, provided such a distortion (fluctuation) originates the moment the relay approaches the given region of the lattice.

The influence of fluctuation of the thermal motion on the propagation of the displacive processes depends on the frequency of the fluctuations in time and space. Since the fluctuations increase their frequency in time and space with the rise in temperature, the elementary processes of the displacive plastic deformation diminish in size and approach the elementary act of diffusion at a sufficiently high temperature. At this temperature, the macroscopically visible plastic deformation is made up of elementary diffusion acts, not interrelated by a definite regular space-time sequence.

In this sense, plastic deformation at high temperatures may be called diffusion ductility.

The influence of the second cause on the propagation and development of displacive processes depends on the nature of the space distribution of the initial distortions in the lattice, on the distances between the sites of distortion, and on the expanses of these sites. In particular, if these sites are the nodes or the interstices of the lattice replaced by foreign atoms (in solid solutions), the propagation of the displacive process depends on the concentration of the solid solution.

3. The Development of Plastic Deformation as a Dialectical Unity of Opposite Factors

In examining the conditions of nucleation of elementary processes of plastic deformation, as well as the conditions of their inhibition, we find that the physical nature of the influence of structural nonuniformities of a polycrystalline body on the course of the deformation phenomena becomes profoundly dialectical: these nonuniformities bring about the nucleation of the processes of plastic deformation and cause the inhibition of these processes.

Thus, the development of processes of plastic deformation reflects the struggle of these two opposites. The rise in the number of nonuniformities in a unit of volume of a crystalline medium facilitates the nucleation of the deformation processes, making their occurrence more frequent in time and space. At the same time the rise in the number of nonuniformities leads to a reduction in the expanses between them where the undistorted lattice makes possible the propagation of each originating displacive process; as a result the development of plastic deformation is curtailed. Obviously, the different "denseness" of the distributed nonuniformities leads to various combinations of their stimulating and paralyzing influence on the development of plastic deformation; at a certain nearness the predominance of one of the two struggling factors will be evident, while at some other denseness the other factor will predominate. This picture will look particularly simple in a case when the distortion regions of the lattice near the nodes (or the interstices) replaced by foreign atoms in solid solutions act as structural nonuniformities.

The displacive processes can develop without hindrance in an undistorted lattice of a completely pure solvent, but the stimulus to their nucleation is lacking.

There is such a stimulus in the presence of a low concentration of the dissolved component; the displacive processes which originate can develop comparatively freely, since obstruction in the form of replaced nodes which are encountered is rare.

As the concentration increases, obstructions to the propagation of the displacive processes become more frequent and deformation is hampered. However, as the concentration becomes very high (this becomes particularly distinct in the case of a system with a continuous series of solid solutions) in a crystalline lattice, the degree of distortion declines again, and the distribution density of the disturbance sites and -- at some concentration -- the deformability of the crystal rise again.

Along with the influence of the distortions earlier originated in the lattice we must also take into account the distortions which originate in the very development process of plastic deformation in the crystal. The passage of every subsequent elementary displacive process through the region of the lattice where the preceding elementary displacive process had passed and had been halted prior to it becomes difficult because of the distortions which had remained in this region; the distortions extend also to the regions adjoining the one where the distortion which had halted the preceding elementary displacement is localized. Thus, as the subsequent elementary displacive processes are being inhibited, the distortions of the lattice build up and their inhibitive influence on the further development of plastic deformation increases. This is the essence of the strengthening phenomena in deformation.

Thermal motion enhances the discharge of the inhibited displacive processes and the decline in the lattice distortions caused by them: the deformed crystal resoftens. The resoftening processes develop with the intensification of thermal motion, i.e., with a rise in temperature. The dialectical struggle of opposites -- strengthening and resoftening -- is therefore characteristic for high-temperature plastic deformation; the picture of high-temperature deformation appears as a result of the struggle of these opposites.

Besides the influence of the concentration of the solid solution on the development processes of plastic deformation we must also take into account the influence

of the deformation rate; in other words, the magnitude of the acting stresses. Both these factors determine the greater or smaller degree of participation of the entire volume of the crystallite in plastic deformation and the localization of the latter in the regions of structural nonuniformity.

Higher deformation rates enhance the development of overstresses on nonuniformities, and greater acting stresses are favorable to the development of the displacive processes within the entire volume of the crystallite where nonuniformities of all sizes are distributed.

At low stresses (at slow-rate deformation), particularly at elevated temperatures, deformation is localized to a greater degree at the structural nonuniformities, without exceeding the bounds of the regions nearly adjoining these nonuniformities.

The resoftening factor has the same tendency: at high deformation rates, resoftening is unable to take place at the degree at which it is accomplished during slow deformation, when the removal of strengthening at the region where deformation begins makes it impossible to propagate the deformation process to the adjoining region (i.e., to develop into a displacive process) and deformation becomes localized in the region of structural nonuniformities.

4. Localization Mechanism of Plastic Deformation at the Intergranular Boundaries

Among the variety of causes of lattice distortion in polycrystalline bodies there are such whose action is most stable with respect to time (those that resist to a substantial degree the balancing influence of thermal motion) and at the same time appear to be the strongest (cause the greatest distortions). This is the influence of the neighborhood of adjoining crystallites with strongly differing orientations, which distorts the lattice. At the articulation of such crystallites -- as has been pointed out earlier (2-6) -- there must be transition (intergranular) zones, generally of polyatomic thickness; the arrangement of atoms in these zones is only partly coordinated and the degree to which the order is disturbed increases at the transverse transition from the crystallite to the central zone (from both sides), where the lattice is

distorted to its maximum. According to the crystallographic nature of nets arranged parallel to the joint boundary in both of the adjoining crystallites, the degree of lattice distortion in such a transverse transition depends on the location (with respect to the crystallographic axes in the net-plane) of the region of the intergranular zone on which the transverse transition can be traced. In some of these regions, the transverse transition through this zone can be achieved while maintaining most of the coherency in the arrangement of the atoms; in other regions, this transition is accompanied by an almost complete loss of coherency in the central zone.

Without going into a more detailed description of the constitution of the intergranular transitional zone (2-6), we can conclude that as long as there exists an intergranular transitional zone it will contain regions with an atom arrangement considerably different from a regular crystalline lattice and, consequently, with excess potential energy. We will call this energy the excess energy of intergranular transitional zones, as distinct from the incorrect concept "surface energy of intergranular boundaries", which is frequently applied. The nucleation of the elementary acts of plastic deformation in the intergranular transitional zones, as well as the initiating elementary diffusion acts, is eased -- depending on the thickness of the crystallite -- due to this excess energy, to a degree which increases with the rise in temperature. This means that with the increase in temperature the plastic deformation processes (at stresses not too high) will concentrate to a greater and greater degree in the intergranular transitional zones and in the adjoining layers of the crystalline lattice of both crystallites linked through the zone.

At the same time we must take into account the fact that with a macroscopic uniform stressed state of a single-phase polycrystalline material there occur overstresses in the boundary zones, the adjoining sites of differently oriented regions of the media which are anisotropic by their elastic properties. This also leads to a localization of the origination of plastic deformation processes in the intergranular transitional zones.

The fact (as mentioned above) that the resoftening processes are intensified with the rise in temperature is of utmost importance. At low temperatures, when the

strengthening factor is substantial, plastic deformation which had originated and had begun to develop in the intergranular zone, strengthening the adjoining regions, is passed on deep down the crystallite to where the material is not yet hardened; consequently, deformation may begin at lower stresses. At elevated temperatures, due to weakening which immediately follows plastic deformation, the latter is not passed on deep down the crystallite, since the stresses there are lower than in the overstressed intergranular zones, while the activation energy is higher due to the absence of a distorted lattice.

5. Experimental Proof of Localization of Plastic Deformation in Intergranular Conjunctions at High Temperatures

The tendency of plastic deformation processes to localize in intergranular conjunctions is shown experimentally. The elongation of macrocrystalline aluminum at various temperatures was investigated in the tests conducted by M. V. Yakutovich and E. S. Yakovleva (7). The elongation of a bicrystal* of aluminum led to the formation of a "node" near the intergranular conjunction (i.e., the transverse dimensions of the specimen were found greater than in its other parts along the axis). The deformation at the same rate at 400° showed no formation traces of a "node" near the intergranular conjunction.

The flow at 550° under a constant stress of 0.144 kg/mm^2 has led to the localization of deformation (kinks) in the boundary zones of the crystallites. To confirm the localization of plastic deformation at the intergranular conjunction at high temperatures, we can cite certain observations of a similar localization in creepage tests and a considerable rise in creep strength at the coarsening of the grain.

6. Intergranular Internal Adsorption

The presence of excess energy in the intergranular transitional zones may also cause another phenomenon independently of the localization of the deformation processes.

*The intergranular transitional zone was arranged across the tensile stress (force).

In the presence of foreign atoms in a crystal, namely, atoms of an impurity dissolved in the crystal in a low concentration (considerably lower than the solubility of this impurity at this temperature), the processes of self-diffusion will rearrange these foreign atoms in the lattice.

It may turn out that the atoms of certain (so-called "horophile") elements, which are present in the crystal as impurities, may get into the intergranular transitional zone by means of self-diffusion and replace the atoms of the solvent in this zone, partly reducing the excess energy of the zone. This reduction may be caused by the fact that the atoms of this impurity will be of a different size than those of the solvent, and also because the interaction forces between the atom of the impurity and that of the solvent differ from the interaction forces between two atoms of the solvent. Consequently, getting into the intergranular zone by means of self-diffusion, the atom of the admixture will be found in a more stable (equilibrium) state as compared to the atom of the solvent which had been replaced. It will take a greater activation energy to recover this impurity atom from its position in the intergranular transitional zone and to send it to the nearest less distorted lattice than for a similar transfer of the solvent atom. Therefore, the impurity atoms getting into the intergranular zone (which is where the solvent atoms also get in) by means of self-diffusion will stay there longer than the solvent atoms; consequently, the concentration of the admixture in the intergranular transitional zone will be increased. This phenomenon, which is analogous to the Gibbs effect on the free interface of two different media, we called (2, 8, 9, 10) intergranular internal adsorption*.

Due to the intergranular internal adsorption, the concentration of certain impurities in the intergranular transitional zones, which are positively active with respect to internal adsorption (in the conception just

*The concept of intergranular internal adsorption may be extended to any case of structural nonuniformity in solids; the lower the excess local energy related to such structural nonuniformity the weaker will be the internal adsorption.

stated) and which are called for short horophile admixtures, may, due to the intergranular internal adsorption, become very high, although in the crystallite mass (and upon the average over the entire volume of the polycrystalline body) the concentration may be very low with respect to both the absolute value and the solubility at this temperature.

In accordance with the conception of the structure of the intergranular transitional zone, which unites continuously and smoothly by each of its sides with the corresponding crystallite, the rise in concentration of the horophile admixture is smoothly accomplished, with each of two sides attaining a maximum in the central part of the zone, where the arrangement of the atoms is most distorted, as compared to a regular lattice, and, consequently, the excess energy is at its maximum. In this central part of the transition zone the concentration* of the horophile admixture may even exceed the solubility which is determined for the macroscopic volume of the body, since the crystalline lattice is almost completely disturbed in this part of the zone. As for the parts of the transitional zone situated nearer to each of the two crystallites being joined by it, the arrangement of the atoms approaches a regular lattice; in these parts the concentration gradually decreases, changing smoothly to the central concentration common to the entire volume of the body -- where the lattice turns out to have almost no visible distortions. Considering the entire intergranular transitional zone as a whole, we can speak of its mean value of increased concentration; this value must be related with the solubility, i.e., with the maximum high concentration of this horophile element which can be held by the crystalline lattice of the solvent. Such a correlation between the adsorptive increased concentration and the solubility is caused by the fact that solubility is determined by the nature of interatomic interactions in the crystalline lattice, and in a intergranular transitional zone, considered as a whole, we do have a crystalline lattice, though it is distorted.

The structural details of transcrystallite

*For such thin layers of a substance as the "central part of the transitional zone" we can speak of concentration only if we bear in mind the expanse of these layers along the zone.

transitional zones, their expanse across, the degree of distortion of the crystalline lattice in them, and, consequently, their excess energy are distinguished according to the varieties in relative crystallographic orientation. The excess energy also causes diversities in the level adsorptive increase of concentration in the zones. For a large volume of polycrystalline material, in the absence of a distinctly manifested uniformity in the orientations of the crystallites (i.e., in the absence of a highly perfected texture), the intergranular internal adsorption will display itself to a greater or smaller degree throughout, and we can speak of an averaged increase of concentration of the horophile admixture in the transitional zones as well as of the averaged value of the "thickness" of the zones and their excess energy.

The variation in concentration in the transitional zones, which, generally speaking, may attain high levels, can considerably change the properties of a solid solution and the development conditions of the plastic deformation processes in these zones, depending on the mass of the crystallites.

With a change in temperature, the concentration of the horophile admixture in intergranular transitional zones, estimated on the average, will vary according to the variation in solubility, which depends on the temperature. Sufficiently rapid changes of temperature may cause the occurrence of supersaturation phenomena of the solid solution in these zones, and may even cause its decomposition, despite the fact that for the polycrystalline alloy as a whole the concentration of this admixture is low and there remains considerably less solubility with all the temperature variations considered.

This fact raises even more the importance of internal adsorption for the development of deformation processes. In investigating the problem on the influence of the concentration of any alloying element and, in particular, of a small admixture, we must define more accurately the formulation of this problem with respect to the horophile activity of this element. Due to internal adsorption on various structural nonuniformities, the true distribution of a given component in the alloy can be found very uneven, and then the mean concentration, which is calculated for the entire volume (more accurately, for the entire mass of the alloy) will not correctly characterize the ability of the

alloy to resist deformation. This ability will be determined by what the true concentration in the sectors is, where plastic deformation begins, and to what extent the deformation processes in these sectors are localized. To pass judgement on the heat resistance of an alloy we must know the influence of internal adsorption on the distribution of the concentration of the alloying elements, as well as the influence of the deformation rate on the localization degree of deformation at the structural nonuniformities.

7. Experimental Proof of the Phenomena of Intergranular Internal Adsorption and Its Influence on the Properties of a Polycrystalline Alloy

Despite the great difficulties of exposing and confirming experimentally the intergranular internal adsorption (which is due to the thinness of the layers where the variation in the concentration of the dissolved admixtures occur), we have already accumulated some experimental material which either directly or indirectly proves the existence of this phenomenon and makes it possible to make a number of conclusions on its nature, its variability under the influence of various factors, and its importance in the properties of alloys.

Without aiming to give a detailed review of the experimental data in this article, we will enumerate only the most important ones.

1. An analysis of the surface layer of an intergranular fracture of steel containing a small impurity of molybdenum showing an increased concentration of the latter by comparison with the average content in the entire mass of steel (11).

2. An analysis of the surface layer in the specimens of a platinum-silver alloy hardened from a temperature for the maximum solubility of silver showing a substantially increased concentration of silver by comparison with the mean value of 0.5 percent (12).

3. A great number of observations of intergranular diffusion; the influence caused by impurities contained in the alloy in which the diffusion is observed (4, 13-19)*.

*See also the article by V. I. Arkharov, S. I. Ivanovskaya, I. P. Polikarpova, and N. P. Chuprakova in this collection.

of special interest to us in this series of investigations would appear to be the investigation of the intergranular diffusion of silver in a solid solution of palladium in iron (20).

4. The dependence of the parameter of a crystalline lattice of a solid solution containing a horophile admixture on the grain size; this dependence shows that when the grain breaks down, a portion of the impurity which had been dissolved in the mass of the grain goes to the newly formed intergranular zones (when the grain subsequently coarsens, it returns into the mass of the grains). The effect was detected on a number of alloys with copper as the basic material (21), as well as on Ag-Ti alloys (22).

5. A micro X-ray analysis of polycrystalline solid solutions (silver and aluminum) showing the enrichment of the intergranular transitional zones with silver (23).

6. Selective oxidation of small impurities on the surface of the specimens of a number of solid solutions (24, 25).

7. A chemical analysis of the products of a microsection etching of some polycrystalline alloys (26, 27) showing that the concentration of certain dissolved impurities in the intergranular transitional zones differs from the mean concentration.

A more detailed review of these data has been published by one of the authors of this article (4, 8, 10). It should be noted that the investigations of the intergranular diffusion and the influence caused by certain dissolved admixtures, as well as the investigation of the parameter of the lattice as a function of the grain size, were also conducted on alloys of a heat-resistant type; they also have confirmed the phenomena of intergranular internal adsorption. These investigations are described by the articles in this collection*.

In addition, there is experimental proof of the assumption expressed by one of us on the possibility of

*See the articles by V. I. Arkharov, S. I. Ivanovskaya, I. P. Polikarpova, N. P. Chuprakova, as well as those by B. I. Arkharov and A. A. Pen'tina.

internal adsorption on thinner structural nonuniformities, -- that is, on the conjunctions ("boundaries") of the mosaic lumps of the crystallites (28, 29); obviously, such phenomena may occur on structural nonuniformities which originate in the crystals of supersaturated solid solutions in the process of their breakdown (4, 23, 30-33). This phenomenon may be of particular importance in the formation of heat-resistant properties in alloys*.

II. The Importance of Structural and Concentration Nonuniformities for the Heat Resistance of Alloys

1. The Basic Idea of a Plan to Increase the Heat of Alloys -- Using the Internal Adsorption of Small Impurities

In the light of the general ideas stated, and as a result of their comparison and coordination, there came into being the basic idea for possible ways of increasing the heat resistance of alloys used as ground work conducted in the Institute of Physics of Metals of the Academy of Sciences USSR (AN SSSR), Ural Branch; this work is described in the contents of the articles in this collection. The idea can be formulated in the following fundamentals.

1. Plastic deformation in a polycrystalline system originates, as a rule, mainly on the boundaries of crystallites (in the intergranular transitional zones). Since at high temperatures hardening caused by plastic deformation is directly followed by resoftening, the plastic deformation processes (at stresses not too high, i.e., at slow deformation) localize in the boundary zones and do not propagate into the mass of the crystallites.

2. Intergranular transitional zones are regions of substantial distortion in a lattice, even when the entire polycrystalline body is in an unstressed state. The peculiar effect of internal adsorption occurs in them as the result of the excess energy; it is similar to the Gibbs effect on the interface of phases (Gibbs phase rule) and may lead to a substantial variation in the chemical composition as compared to the mean composition of the entire

*See the article by V. I. Arkharov in this collection.

alloy.

As for the variation in the composition, it changes the properties of the solid solution, and in particular, the ability to resist the development of plastic deformation processes. Thus, it will appear that the properties of the solid solution are changed in the boundary zones of the crystallites, i.e., in the sites where the plastic deformation processes are principally localized.

3. With the rise in temperature, the elementary processes of plastic deformation become smaller in size, and they approach the elementary act of diffusion: displacive plastic deformation gradually (with the rise in temperature) "degenerates" into diffusion ductility*. Heat resistance is thus associated with the diffusion mobility of atoms in a solid solution, where the diffusion phenomena are of preferential importance in those regions of the solid solution which are adjacent to the structural heterogeneity, particularly, in the regions adjacent to the boundaries between crystallites, that is, in the intergranular transition zones.

The main factor which determines the diffusion mobility of atoms in a crystalline lattice are the interatomic bond forces. However, this factor alone is insufficient for heat resistance. The heat resistance of an alloy of a given chemical composition depends, in addition to it, on a certain content of structural nonuniformities in this composition. In the absence of these nonuniformities, it would become necessary to increase the interatomic bond forces so as to completely prevent the nucleation of an elementary act of plastic deformation, since every act which originates in an undistorted lattice develops on a macroscopic scale in view of the fact that there are no obstacles to its propagation. The presence of structural nonuniformities makes this condition (dependence) unnecessary and permits it to be replaced by a condition of maximum possible intensification of interatomic bonds by means of selecting the corresponding basic components.

*This does not exclude the fundamental possibility of displacive processes at high temperatures in cases when the effective stresses are high. However, at slow deformation (effective stresses being not too high), as the temperature increases, the displacive processes become smaller to the degree the effective stresses become lower.

4. The heat resistance of a solid solution may be raised by introducing into the alloy such soluble admixtures which, being horophile and being concentrated in the distortion regions of the lattice, at the structural nonuniformities (primarily -- in the intergranular transitional zones), hinder the completion of the diffusion (to be more exact -- the self-diffusion) processes of which the high-temperature plastic deformation of the alloy is composed.

5. In the very way the problem of the nature of heat resistance is generally formulated we can observe the thorough diversity of structural nonuniformities in the alloy: beginning with the most sharply pronounced nonuniformities on the conjunctions of the crystallites (i.e., intergranular transitional zones); proceeding further to the elements of subcrystallite structure -- including the intragranular finely dispersed inclusions of crystalline particles of extraneous phases, the interlump zones of mosaic, slippage traces, the boundaries of twin crystals, the "pre-transitional" density regions of concentration in supersaturated solid solutions (at their initial stages of aging), the regions of nonuniformity in concentration in unsaturated solid solutions, and, finally, the surroundings of individual dislocations of the lattice of various sizes; and continuing down to the hole in the lattice, the atom wedged in the interstice or the foreign atom which replaces the basic component atom in the node of the lattice.

The above presentations on the localization of the processes of plastic deformation, on the reduction of them (at an increased temperature) to diffusion processes, and on internal adsorption and its influence on the self-diffusional mobility of atoms in regions adjoining the structural nonuniformity are valid to one degree or another with respect to the structural nonuniformity of each type. From this position we face the construction of the theory of heat resistance in the most general way.

6. Proceeding to more specific aspects of the problem as applied to various types and groups of alloys, i.e., to each "basic" chemical composition of alloys, we must examine a number of detailed factors, pertaining to which, are:

(a) the interatomic bond which determines the diffusional mobility (in this case we must consider the

dependence of the interatomic bond on both the concentration and composition of the solid solution; at the site of nucleation and localized development of the diffusion plasticity both concentration and composition may differ from those of the alloy as a whole);

(b) the optimum dispersion degree of the structural nonuniformities at which the inhibiting effect of these nonuniformities on the development of the plastic deformation processes is evident (for alloys of various types, this dispersiveness may be attained at a different stage of heterogeneity);

(c) the degree of the horophile activity of various components of the solid solution (in this case we must consider a possible difference in this degree with respect to the structural nonuniformities of various scales and dispersiveness, a possibility of "competition" of various horophile admixtures present at the same time in the solid solution as well as the dependence of the results of this competition on the absolute and relative amount (concentration) of the competing horophile admixtures in the solid solution).

7. In order to ease the approach to the problem of experimental investigation of the questions set forth, and to verify the expressed hypothesis on the nature of heat resistance, it is sensible to narrow somewhat the general problem in the first phase of the study, and investigate, first of all, the localization phenomena of plastic deformation, its diffusional nature, and internal adsorption applicable to more sharply pronounced structural nonuniformities, such as intergranular transitional zones.

In addition to the general importance of such an investigation for the creation of a general theory of heat resistance, there can also be a more immediate problem -- that of finding methods for additional alloying of heat-resistant alloys in order to give them increased heat resistance by means of horophile admixtures.

In formulating the problem this way, we take as a base an alloy with a chemical composition which already provides a sufficiently high level of heat resistance within the crystallite; the horophile admixture which works (by means of adsorption) in the intergranular transitional zones raises the heat resistance of the alloy to a

level exceeding that attained in this chemical composition of the alloy (without the horophile admixture).

8. Parallel to the importance that the investigation of the influence of internal adsorption on plastic deformation may have for finding ways of improving the heat resistance of alloys, this investigation may also have another value. It may bring to light the reasons for the difference in the heat resistance of alloys of an identical composition in basic alloying elements but containing various small impurities unaccountable for by chemical analysis, which are capable, as previously stated, of exerting a strong influence on the heat resistance, when these unaccountable impurities are horophile active. Obviously, the differences in the heat-resistant properties will not be equally evident in the various states of these alloys after these have undergone different treatments, since the internal adsorption will in this case be realized to an unequal degree.

The presence of certain unaccounted for strongly horophile impurities in the alloy may paralyze the effect of the admixtures introduced on purpose in the composition of the alloy, calculating on their being horophile, while they "cannot compete" with the more horophile impurities that cannot be accounted for.

From this viewpoint we are able to plan ways of exposing similar cases capable of creating the false impression of a negative result in the tests by using certain alloying admixtures, the useful effect of which could not be brought out because of their being overlapped by the adsorption influence of other unaccounted for impurities, while, eliminating the latter from the tested composition, a positive result may be obtained.

These considerations point to the necessity of detailing the chemical analysis of alloys for a greater number of admixtures and also of setting up analysis on the horophile activity of a number of admixtures which can possibly be used for one or another category of alloys.

In addition to the factor of horophile activity which determines the true and uneven distribution of the concentration of the alloying elements in the alloy in accordance with the given nature of distribution of structural nonuniformities in it (the sizes and shape of

the crystallites, the micro- and submicroscopic inclusions of other phases, the nature of the mosaic substructure, the pre-transitional heterogeneity, etc.), to evaluate the heat resistance of an alloy, we must define still more accurately the deformation rate and the magnitude of effective stresses*.

Alloys may have a high heat resistance at low deformation rates due to a favorable distribution of concentration which paralyzes the development of localized processes of diffusional ductility. At the same time these alloys may show a low heat resistance at a high rate of deformation, since they have no sufficient resistance to the development of displacive processes of plastic deformation which propagate into the crystallites.

In accordance with all examined aspects of the phenomenon of high-temperature plastic deformation of alloys, there is reason to assume that internal adsorption may be of the greatest importance, primarily for slow-moving deformation processes (creep).

2. The Works of the Institute of Physics of Metals of the Academy of Sciences USSR (AN SSSR), Ural Branch, on the Study of the Problem of Heat Resistance

Some experimental investigations along the above lines were conducted in the laboratories for mechanical properties of materials and diffusion of the Institute of Physics of Metals of the Academy of Sciences USSR (AN SSSR), Ural Branch. The contents and results of these investigations are set forth in the articles of this collection.

The following are the basic divisions of these complex investigations:

A. Measurements of creep in austenitic alloys having a ferrum-chromium-nickel base and small dissolved impurities of certain elements, and also of aluminum alloys with small concentrations of alloying elements;

*See the article by V. A. Pavlov, E. S. Yakovleva, and M. V. Yakutovich in this collection.

B. Measurements of relaxation of stresses at high-temperature elongation of austenitic alloys having the same compositions as those tested for creep*;

C. The investigation of the diffusional mobility of nickel in the intergranular transitional zones in the same austenitic alloys by means of analyzing the unevenness (of intergranular nature) of the frontal diffusion of nickel in these alloys, on the unevenness of diffusion (the procedure is described in article 34). Parallel to this there were also conducted auxiliary investigations (measurement of continued hardness, measurement of unevenness in the distribution of plastic deformation in the microstructure of polycrystalline alloys, determination of intergranular internal adsorption in the same austenitic alloys using the method of measuring the parameter of the crystal lattice with the variation in the dimensions of the crystallites, and others).

One general explanation, important in principle, must be made with respect to the materials selected for the investigation in the works on heat resistance conducted by the Institute of Physics of Metals Academy of Sciences, Ural Branch (IFM UFAN). Basically, these materials are single-phase solid solutions: either ferrum-chromium-nickel austenite with small dissolved impurities or aluminum with small dissolved impurities.

We consider that an alloy attains its greatest possible heat resistance at a certain (specific for each alloy) degree of heterogeneity in structure: this still does not imply that every heat-resistant alloy must be heterophase. A detailed study of this question is given in other articles (4)**. We must then note here, that the phenomena of nucleation, development, and deceleration of the elementary acts of plastic deformation take place in the regions of the crystalline lattice adjoining the structural nonuniformities at any degree of heterogeneity of the alloy (including also cases with heterophase materials). In these regions there are distortions of the

*The test methods are described in the article by V. S. Averkiyev, G. I. Kolesnikov, A. I. Moiseyev, and M. V. Yakutovich in this collection.
**In addition, see the article by V. I. Arkharov in this collection.

lattice and nonuniformities in the chemical composition. But these regions pertain to the solid solution, and the analysis of the phenomena of high-temperature deformation in heat-resistant alloys inevitably leads to the examination of the elementary processes which take place in the regions of the single-phase solid solution. Therefore, in order to investigate high-temperature deformation, tests must be conducted using polycrystalline single-phase solid solutions where the structural nonuniformities are the intergranular conjunctions ("boundaries"). These nonuniformities are of the same type and are more clearly pronounced; in these alloys, therefore, it is most easy to study high-temperature deformation as well as the influence of structural and chemical nonuniformities in the crystal on the deformation. The notions obtained can further be extended to cover alloys with more complex nonuniformities, able to provide an optimum heat resistance. The selection of material in our investigations was thus specified by the problem of such a "model study" of the basic phenomena of high-temperature deformation, at which the study of these phenomena would be most simple, though the materials selected are, of course, not heat-resistant. Molybdenum, tungsten, titanium, and niobium, introduced into the alloys either individually or in combinations, were used as admixtures. The alloys were melted in sufficiently large quantities that they could be investigated using various methods in accordance with those indicated in the sections.

* * *

The results obtained from the various parts of the whole, complex investigation are summarized at the conclusion of each article of this collection. From this summary we may draw the following general conclusions.

1. The investigations of intergranular diffusion of nickel in ferrum-chromium-nickel austenitic alloys with additions of certain elements, as well as the investigations of the variations in the parameter of the crystal lattice of these alloys during the variation of the grain size, show that such admixtures as molybdenum, tungsten, niobium, titanium, aluminum, and boron dissolved in solid solutions of ferrum-chromium-nickel are horophile (positively active with respect to intergranular internal adsorption).

2. The deformation has a tendency to localize in intergranular transitional zones at creep with low deformation rates.

3. High-temperature plastic deformation at creep and relaxation of stresses is accomplished basically by the mechanism of diffusion ductility*.

4. Intergranular internal adsorption of the investigated horophile admixtures affects the diffusion mobility of the basic components (in any case -- of nickel) in the intergranular transitional zones.

5. The observed influence of the small dissolved impurities on the ability of the alloys to resist high-temperature deformation in creep with small stresses** and during the relaxation of stresses*** can be explained on the basis of our hypothesis that the localization of deformation is the determining factor of the heat resistance in alloys and of the internal adsorption of impurities on the intergranular boundaries; these experimental data thus confirm our hypothesis (taking into account the role of the deformation rate).

6. The role of the processes which develop in the mass of each crystallite substantially increases at high deformation rates, and the role of the structural and concentration nonuniformities which localize in the intergranular transitional zones accordingly decreases; these experimental data determine the range of conditions of deformation within which the hypothesis expressed is of consequence.

7. There is a possibility of considerably expanding the applicability of the above hypothesis -- by means of extending the basic conceptions of both localization of deformation and internal adsorption -- from the most crude

---

*See the articles in this collection by G. N. Kolesnikov and A. I. Moiseyev, as well as those by V. S. Averkiyev, G. N. Kolesnikov, A. I. Moiseyev, and M. V. Yakutovich.
**See the article in this collection by V. A. Pavlov, E. S. Yakovleva and M. V. Yakutovich.
***See the article in this collection by V. I. Arkharov, S. I. Ivanovskaya, G. N. Kolesnikov, and A. I. Moiseyev.

structural nonuniformities of the intergranular transitional zones to the finer nonuniformities of subcrystallite structure; in particular, to the mosaic constitution of the crystallites and to the "pre-transitional" formations of the decomposing supersaturated solid solution. These considerations map out a program for further studies on the improvement of the theory of heat resistance.

8. On the basis of both the results of the experimental studies cited in the articles of this collection and the general theoretical considerations cited here and in the last article of the collection -- and considering also the results of the studies made by other scientific teams working on the development of other aspects of the general theory of heat resistance -- it seems that we are in a position at this phase of our work to point out in a very general way the conditions which determine the heat resistance of an alloy. These are as follows:

(a) an optimum degree of structural nonuniformity created in the alloy of a given composition by means of both heat treatments and mechanical treatments;

(b) an optimum unevenness in the distribution of concentration of components at these structural nonuniformities created (on the basis of utilizing the phenomena of internal adsorption broadly recognized as the result of compensation of energy nonuniformities of any type and size by means of uneven concentrations);

(c) a conformity of thus created structural and chemical unevenness to the conditions of distribution of acting stresses over the volume of the alloy (to the nature of the mechanical service conditions of the material);

(d) sufficient time stability of the structural and chemical unevenness thus created in the alloy.

The most primary condition is the selection of components of the alloys both qualitatively and quantitatively so as to ensure a sufficiently strong interatomic bond in the localization region of the deformation processes, as well as in the other parts of the alloy, in accordance with the level of the acting stresses.

BIBLIOGRAPHY

1. Arkharov, V. I., Izv. AN SSSR, OTN (News of the

Academy of Sciences USSR, Department of Technical Sciences), No. 11, 1951.

2. Arkharov, V. I., Tr. In-ta fiziki metallov UFAN SSSR (Works of the Institute of Physics of Metals of the Academy of Sciences USSR, Ural Branch), Issue 8, Sverdlovsk, Press of the Academy of Sciences USSR, Ural Branch, 1946.

3. Jg. M. Burgers, Proc. of Phys. Soc. (London), 52, 23, 1940.

4. Arkharov, V. I., Works of the Institute of Physics of Metals of the Academy of Sciences USSR, Ural Branch (UFAN SSSR), Issue 16, Press of the Academy of Sciences USSR, 1955.

5. Klassen-Neklyudova, M. B., and Kontorova, T. A., UFN (Progress in Physical Sciences), Vol. 22, 1939.

6. Hargrews, F., and Hill, R., J. Inst. of Metals, Vol. 41, 1929.

7. Yakovleva, E. S., and Yakutovich, M. V., Dokl. AN SSSR (Reports of the Academy of Sciences USSR), Vol. 90, 1953.

8. Arkharov, V. I., Works of the Institute of Metals of the Academy of Sciences USSR, Ural Branch, Issue 12, Press of the Academy of Sciences USSR, Moscow-Leningrad, 1950.

9. Arkharov, V. I., Tr. konferentsii po metallovedeniyu v Sverdlovske v 1950 g. (Works of the Conference on Metallography, Sverdlovsk, 1950), Uralnitomash, Sverdlovsk, Mashgiz (State Scientific and Technical Press for Literature on Machinery), 1951.

10. Arkharov, V. I., Works of the Institute of Physics of Metals of the Academy of Sciences USSR, Ural Branch, Issue 14, Press of the Academy of Sciences USSR, Ural Branch, Moscow, 1954.

11. Arkharov, V. I., Gol'dshteyn, T. Yu., Works of the Institute of Physics of Metals of the Academy of Sciences USSR, Ural Branch, Issue 11, Sverdlovsk, Press of the Academy of Sciences USSR, Ural Branch, 1950.

12. Arkharov, V. I., Somova, Ye. V., and Chukina,

T. P., Reports of the Academy of Sciences USSR, Vol. 76, No 2, 1951.

13. Arkharov, V. I., Yefremova, K. A., Ivanovskaya, S. I., Shtol'ts, A. K., and Yunikov, B. A., Works of the Institute of Physics of Metals of the Academy of Sciences USSR, Ural Branch, Issue 16, Press of the Academy of Sciences USSR, 1955.

14. Arkharov, V. I., Ivanovskaya, S. I., Skornyakov, N. N., Works of the Institute of Physics of Metals of the Academy of Sciences USSR, Ural Branch, Issue 16, Press of the Academy of Sciences USSR, 1955.

15. Arkharov, V. I., and Gol'dshteyn, T. Yu., Reports of the Academy of Sciences USSR, Vol. 66, 1949.

16. Arkharov, V. I., Yefremova, K. A., Ivanovskaya, S. I., Shtol'ts, A. K., Yunikov, B. A., Reports of the Academy of Sciences USSR, Vol. 89, 1953.

17. Arkharov, V. I., Ivanovskaya, S. I., and Skornyakov, N. N., Reports of the Academy of Sciences USSR, Vol. 89, 1953.

18. Barnes, R. S., Nature, Vol. 166, 1950.

19. Achter, M. R., and Smoluchowsky, R., J. of Appl. Physics, Vol. 22, 1951.

20. Arkharov, V. I., and Yunikov, B. A., Reports of the Academy of Sciences USSR, Vol. 94, 1954.

21. Arkharov, V. I., and Skornyakov, N. N., Reports of the Academy of Sciences USSR, Vol. 89, 1953.

22. Arkharov, V. I., and Vangengeym, S. D., "Fizika metallov i metallovedeniye" (Physics of Metals and Metallography), 4, No 3, 1957.

23. Arkharov, V. I., Varskoy, B. N., and Skornyakov, N. N., Reports of the Academy of Sciences USSR, Vol. 89, 1953.

24. Dobinski, S., Nature, Vol. 141, 1938.

25. Dobinski, S., and Smoluchowski, M., Nature, Vol. 144, 1939.

26. Andreyev, I. A., and Polin, I. V., Tr. TsNII transp. Mashinostr. (Works of the Central Scientific Research Institute of Transport Machine Building), No. 1, 1947.

27. Dean. G. R., and Davey, W. R., Trans. A. S. M., Vol. 26, 1938.

28. Bolotov, I. Ye., and Kozmanov, Yu. D., Reports of the Academy of Sciences USSR, Vol. 95, 1954.

29. Bolotov, I. Ye., Kozmanov, Yu. D., and Timofeyev, A. N., ZhTF (Journal of Technical Physics), Vol. 35, 1955.

30. Arkharov, V. I., and Gol'dshteyn, T. Yu., Works of the Institute of Physics of Metals USSR, Ural Branch, Issue 11, 1950.

31. Arkharov, V. I., Vangengeym, S. D., Magat, L. M., and Polikarpova, I. P., Journal of Technical Physics (ZhTF), Vol. 24, 1954.

32. Magat, L. M., and Noskova, N. I., Physics of Metals and Metallography, 1, 1955.

33. Arkharov, V. I., and Noskov, N. I., Physics of Metals and Metallography, 2, 1956.

34. Arkharov, V. I., and Ivanovskaya, S. I., "Zav. lab." (Plant Laboratory), No. 6, 1951.

* * *

The Investigation of Irregularities in Frontal Diffusion of Nickel in Polycrystalline Ferrum-Chromium-Nickel Alloys

By V. I. Arkharov, S. I. Ivanovskaya, I. P. Polikarpova, and N. P. Chuprakova

The basic scientific idea from which we proceeded in setting up this investigation is rooted in the fact that the processes of plastic deformation in a polycrystalline material at high temperatures develop primarily in the boundary zones of the crystallites (in the zones adjoining the intergranular boundaries). These processes are composed of elementary processes similar in scale to the elementary diffusion acts in a crystal lattice.

In this connection, there occurs a notion that heat resistance is related to the diffusional mobility of atoms in the boundary zones where the solid solution has an increased alloying ability due to internal adsorption (1)*. Hence arises the necessity of investigating the diffusion processes in alloys; particularly, the nature of diffusion of the alloying elements. For the object of study of ferrum-chromium-nickel alloys we selected chromium, nickel, cobalt, and manganese as the alloying elements.

In view of the fact that a direct study of the diffusion processes in very thin boundary layers (of the order of 100-1000 A) is extremely difficult, we have attempted to study the processes of diffusion by a method that investigates the frontal diffusion, i.e., the diffusion moving with its leading edge through a great number of crystallites and intergranular zones.

The investigation of the metallographic pattern of a number of elements (such as nickel, chromium, cobalt, manganese, etc.) diffused in austenitic ferrum-chromium-nickel alloys has shown that it is possible to develop

*See also the article by V. I. Arkharov and M. V. Yakutovich in this collection.

metallographically only the diffusion of nickel and cobalt, since only in these cases did we observe formations of narrow edges along the grain boundaries of the austenite, apparently of the solid solution enriched by the diffusible element (2, 3, 4).

In the diffusion of chromium and manganese, an even diffusion front was observed.

The fact that chromium and manganese diffuse at the same rate through both the mass of the grain and the boundary regions, while nickel and cobalt diffuse predominantly along the grain boundaries, points to the unequal activity of different elements (at their diffusion) with respect to the grain boundaries of austenite.

Since nickel has produced a more distinct metallographic pattern of preferential diffusion along the intergranular boundaries forming clearly pronounced projected points (edges) of the diffusion front, our further attention was concentrated on the study of the frontal diffusion of nickel in various austenitic alloys.

It was of primary importance to clear up the question of how the admixture of elements which may be regarded surface-active* affects the diffusional mobility of the atoms of nickel.

A considerable part of the study is therefore devoted to the problem of the influence of additions of molybdenum, titanium, niobium, aluminum, tungsten, and boron on the diffusional mobility of nickel along the grain boundaries.

I. The Metallographic Analysis of the Diffusion of Nickel in Ferrum-Chromium-Nickel Alloys

1. The Composition of the Tested Alloys

*By analogy with the phenomenon of the change in the rate of diffusion of silver along the grain boundaries in copper alloys under the influence of small admixtures of beryllium (5), as well as with the deceleration in the diffusion of nickel in alloys of iron with a small admixture of molybdenum or boron as compared to the diffusion of nickel in iron (4).

The investigation was conducted on ferrum-chromium-nickel monophase austenitic alloys containing 20 or 40 percent Cr and 10 to 40 percent Ni with some of the following admixtures: 0.24 - 5.0 percent Mo; 0.01 - 1.9 percent Ti; 0.25 - 2.0 percent Nb; 0.13 - 1.0 percent Al; 0.20 - 4.0 percent W; 0.01 - 0.05 percent B.

In addition, tests were run on ferrum-chromium-nickel austenitic alloys with 20 percent Cr and 20 percent Ni containing admixtures of two elements:

(1) niobium (0.5 percent) and titanium (0.1 - 0.6 percent);
(2) niobium (0.4 - 0.5 percent) and molybdenum (0.2 - 1.43 percent);
(3) aluminum (0.5 percent) and titanium (0.2 and 0.8 percent); and
(4) aluminum (0.05 and 0.5 percent) and niobium (0.3 and 1.0 percent).

The content of base elements in the investigated alloys is given in Table 1.

These alloys were melted primarily in the Laboratory of Precision Alloys of the Institute of Physics of Metals of the Academy of Sciences USSR, Ural Branch; some of them were melted in the Central Scientific Research Institute for Ferrous Metals.

2. The Technique of Investigation and Testing Conditions

The specimens of the investigated alloys, 10 mm thick, were cut from forged rods which, as a rule, were subjected to a preliminary treatment: heating to 1250°, holding for 1 hour, and quenching in water. At one end of the specimen, two to four hollows (2.2 - 2.5 mm in diameter and 9 mm deep) were drilled. The hollows were etched for about 10 to 15 minutes with aqua regia in order to remove the surface layer which had been deformed during the mechanical treatment; they were then washed with water, then with alcohol, and were thoroughly dried in a blast of air; they were then filled with the powder of the metal designed for diffusion in this test.

Nickel was employed in the form of file dust obtained by means of a thin barette file from an electrode

nickel plate. Electrolytic types of chromium and manganese were used, and the cobalt was made by reduction from hydroxide at the plant. These elements were ground to a fine powder in an agate mortar. The holes of the hollows were clogged up with iron plugs. The specimens were then subjected to heating in the following variants: 750° and holding for 50 - 100 hours; 850° and holding for 16 hours; 950° and holding for 8 hours; 1100° and holding for 2 hours; and 1250° and holding for 1 hour. This was followed by quenching in water. The polished section was made on the cross-sectional plane of the specimen through the hollows filled with nickel on the side opposite the plugs. The results of the microscopic investigations are given in Figures 1 - 8.

In most of the cases, the microsections were etched with a reagent consisting of a mixture: four g $CuSO_4$, 20 cm^3 HCl, and 20 cm^3 H_2O (Figures 1 - 4,h); in some cases, the reagents used were either a solution of picric and hydrochloric acids in alcohol (Figure 4,i) or aqua regia [1 : 3] (Figure 5,c).

Table 1

The Content of the Basic Elements in the Investigated Alloys

No. of alloy	Conventional brand of alloy*	Carbon	Chromium	Nickel	Molybdenum	Titanium	Niobium	Aluminum	Tungsten	Boron
	Alloys without admixtures									
1	Cr20Ni11	0,05	20,35	10,60	—	—	—	—	—	—
2	Cr19Ni11	0,09	18,70	10,50	—	—	—	—	—	—
3	Cr20Ni10	0,09	19,50	10,10	—	—	—	—	—	—
4	Cr21Ni20	0,06	21,10	20,30	—	—	—	—	—	—
5	Cr20Ni20	0,025	19,95	20,00	—	—	—	—	—	—
6	Cr20Ni21	0,084	19,73	20,70	—	—	—	—	—	—
7	Cr20Ni35	0,023	20,24	34,92	—	—	—	—	—	—
8	Cr20Ni40	0,05	20,04	39,85	—	—	—	—	—	—
9	Cr18Ni39	0,06	17,70	39,40	—	—	—	—	—	—
10	Cr38Ni37	0,10	38,50	37,20	—	—	—	—	—	—
11	Cr20Ni80	—	19,52	79,86	—	—	—	—	—	—
	Alloys with an admixture of molybdenum									
12	Cr19Ni20Mo0.2	0,048	19,22	20,10	0,24	—	—	—	—	—
13	Cr20Ni20Mo0.7	0,031	20,10	20,20	0,65	—	—	—	—	—
14	Cr20Ni20Mo1.2	0,01	20,48	20,30	1,20	—	—	—	—	—
15	Cr21Ni10Mo1	0,05	20,90	10,20	0,90	—	—	—	—	—
16	Cr16Ni10Mo1	0,02	16,10	10,00	1,00	—	—	—	—	—
17	Cr18Ni10Mo2	0,04	17,50	10,00	2,10	—	—	—	—	—
18	Cr20Ni10Mo3	0,11	20,30	9,80	2,59	—	—	—	—	—
19	Cr18Ni20Mo3	0,04	18,20	19,70	2,97	—	—	—	—	—
20	Cr20Ni11Mo4	0,08	19,61	10,80	4,07	—	—	—	—	—
21	Cr20Ni16Mo4	0,07	20,10	16,40	4,20	—	—	—	—	—
22	Cr20Ni10Mo5	0,23	19,59	10,30	5,49	—	—	—	—	—
23	Cr19Ni20Mo0.2	0,048	19,22	20,01	0,24	—	—	—	—	—

*Cr -- chromium; Ni -- nickel; Mo -- molybdenum; Ti -- titanium; W -- tungsten; Nb -- niobium; Al -- aluminum; B -- boron.

Table 1 (continued)

No. of alloy	Conventional brand of alloy	Carbon	Chromium	Nickel	Molybdenum	Titanium	Niobium	Aluminum	Tungsten	Boron
24	Cr20Ni20Mo0.6	0,031	20,10	20,20	0,65	—	—	—	—	—
25	Cr20Ni20Mo1.2	0,01	20,48	20,30	1,20	—	—	—	—	—
26	Cr20Ni20Mo4.7	0,064	19,47	19,98	4,65	—	—	—	—	—
27	Cr18Ni20Mo5	0,05	18,41	19,97	5,00	—	—	—	—	—
28	Cr20Ni36Mo1	0,028	20,27	36,00	1,30	—	—	—	—	—
29	Cr17Ni40Mo3	0,08	17,20	40,40	2,84	—	—	—	—	—
30	Cr20Ni39Mo3	0,05	20,35	38,90	2,56	—	—	—	—	—
31	Cr38Ni39Mo2	0,11	37,50	38,80	1,85	—	—	—	—	—
32	Cr19Ni37Mo3	0,043	18,60	37,20	0,25	—	—	—	—	—
	Alloys with an admixture of titanium									
33	Cr20Ni20Ti0.01	0,026	19,59	19,68	—	0,01	—	—	—	—
34	Cr20Ni18Ti0.1	0,024	20,25	18,45	—	0,09	—	—	—	—
35	Cr20Ni20Ti0.4	0,05	20,15	20,38	—	0,37	—	—	—	—
36	Cr20Ni20Ti0.4	0,058	20,00	20,14	—	0,42	—	—	—	—
37	Cr21Ni20Ti1.9	0,05	20,95	20,45	—	1,47	—	—	—	—
38	Cr19Ni36Ti0.2	0,063	18,50	36,43	—	0,24	—	—	—	—
39	Cr20Ni36Ti0.5	0,068	20,00	35,76	—	0,50	—	—	—	—
40	Cr21Ni40Ti0.1	0,06	21,24	40,11	—	0,08	—	—	—	—
41	Cr21Ni40Ti0.3	0,05	20,56	40,24	—	0,3	—	—	—	—
42	Cr21Ni40Ti0.6	0,06	21,04	39,98	—	0,57	—	—	—	—
	Alloys with an admixture of niobium									
43	Cr20Ni19Nb0.3	0,029	19,59	18,92	—	—	0,25	—	—	—
44	Cr20Ni21Nb0.5	0,025	19,93	20,62	—	—	0,50	—	—	—
45	Cr19Ni20Nb0.5	0,031	18,90	19,61	—	—	0,47	—	—	—
46	Cr19Ni20Nb1.0	0,05	19,10	19,98	—	—	1,10	—	—	—
47	Cr19Ni20Nb2	0,08	19,45	20,20	—	—	2,02	—	—	—
48	Cr20Ni36Nb0.2	0,038	19,87	35,60	—	—	0,20	—	—	—
49	Cr20Ni36Nb0.5	0,065	19,55	35,68	—	—	0,51	—	—	—

Table 1 (continued)

No. of alloy	Conventional brand of alloy	Carbon	Chromium	Nickel	Molybdenum	Titanium	Niobium	Aluminum	Tungsten	Boron
	Alloys with an admixture of aluminum									
50	Cr20N120A10.1	0,035	20,20	19,85	—	—	—	0,13	—	—
51	Cr19N120A10.5	0,036	19,45	19,70	—	—	—	0,47	—	—
52	Cr20N120A11	0,033	20,48	20,00	—	—	—	1,00	—	—
	Alloys with an admixture of tungsten									
53	Cr19N120W0.2	0,041	19,48	20,20	—	—	—	—	0,20	—
54	Cr19N120W1.26	0,041	19,02	19,96	—	—	—	—	1,26	—
55	Cr19N120W2.8	0,05	18,94	19,96	—	—	—	—	2,80	—
56	Cr18N111W1	0,11	17,50	10,50	—	—	—	—	0,80	—
57	Cr18N111W2	0,09	18,20	10,50	—	—	—	—	1,80	—
58	Cr19N110W4	0,06	18,80	10,40	—	—	—	—	3,80	—
59	Cr20N121W1	0,07	19,97	21,10	—	—	—	—	0,98	—
	Alloys with an admixture of boron									
60	Cr21N120B0.05	0,05	20,50	20,45	—	—	—	—	—	0,049
61	Cr20N125B0.05	0,045	20,35	25,26	—	—	—	—	—	0,047
62	Cr20N140B0.05	0,05	20,45	40,11	—	—	—	—	—	0,047
63	Cr20N140B0.01	0,05	20,35	40,11	—	—	—	—	—	0,01
64	Cr20N140B0.01	0,055	20,80	39,85	—	—	—	—	—	0,01

Table 1 (conclusion)

No. of alloy	Conventional brand of alloy	Carbon	Chromium	Nickel	Molybdenum	Titanium	Niobium	Aluminum	Tungsten	Boron
	Alloys with admixtures of molybdenum and niobium									
65	Cr20Ni12NbO.4MoO.2	0,037	19,97	20,56	0,17	—	0,40	—	—	
66	Cr20Ni12ONbO.5MoO.7	0,030	19,75	20,24	0,70	—	0,51	—	—	
67	Cr20Ni12lNbO.4Mol.4	0,023	20,29	21,04	1,43	—	0,40	—	—	
	Alloys with admixtures of titanium and niobium									
68	Cr19Ni12ONbO.5Ti0.1	0,045	19,20	19,96	—	0,11	0,48	—	—	
69	Cr20Ni12lNbO.5Ti0.2	0,021	19,65	20,62	—	0,23	0,50	—	—	
70	Cr19Ni12lNbO.5Ti0.6	0,026	18,95	20,91	—	0,60	0,49	—	—	
	Alloys with admixtures of titanium and aluminum									
71	Cr21Ni120Al0.5Ti0.2	0,018	21,0	20,3	—	0,24	—	0,55	—	
72	Cr21Ni120Al0.5Ti0.8	0,018	21,0	20,3	—	0,76	—	0,55	—	
	Alloys with admixtures of niobium and aluminum									
73	Cr20Ni119Al0.5NbO.3	0,037	20,2	18,89	—	—	0,29	0,52	—	
74	Cr20Ni120Al0.6Nbl.0	0,037	20,0	19,7	—	—	0,98	0,63	—	

The ring-shaped diffusion zones obtained around the holes filled with nickel were examined microscopically; that is the shape of the diffusion front was examined and the thickness of the diffusion zones was measured by means of a preliminary calibrated ocular ruler. An examination was then made of the microstructure of these zones.

In addition, the microhardness of the diffusion zone was measured on some specimens by the PMT-3 instrument.

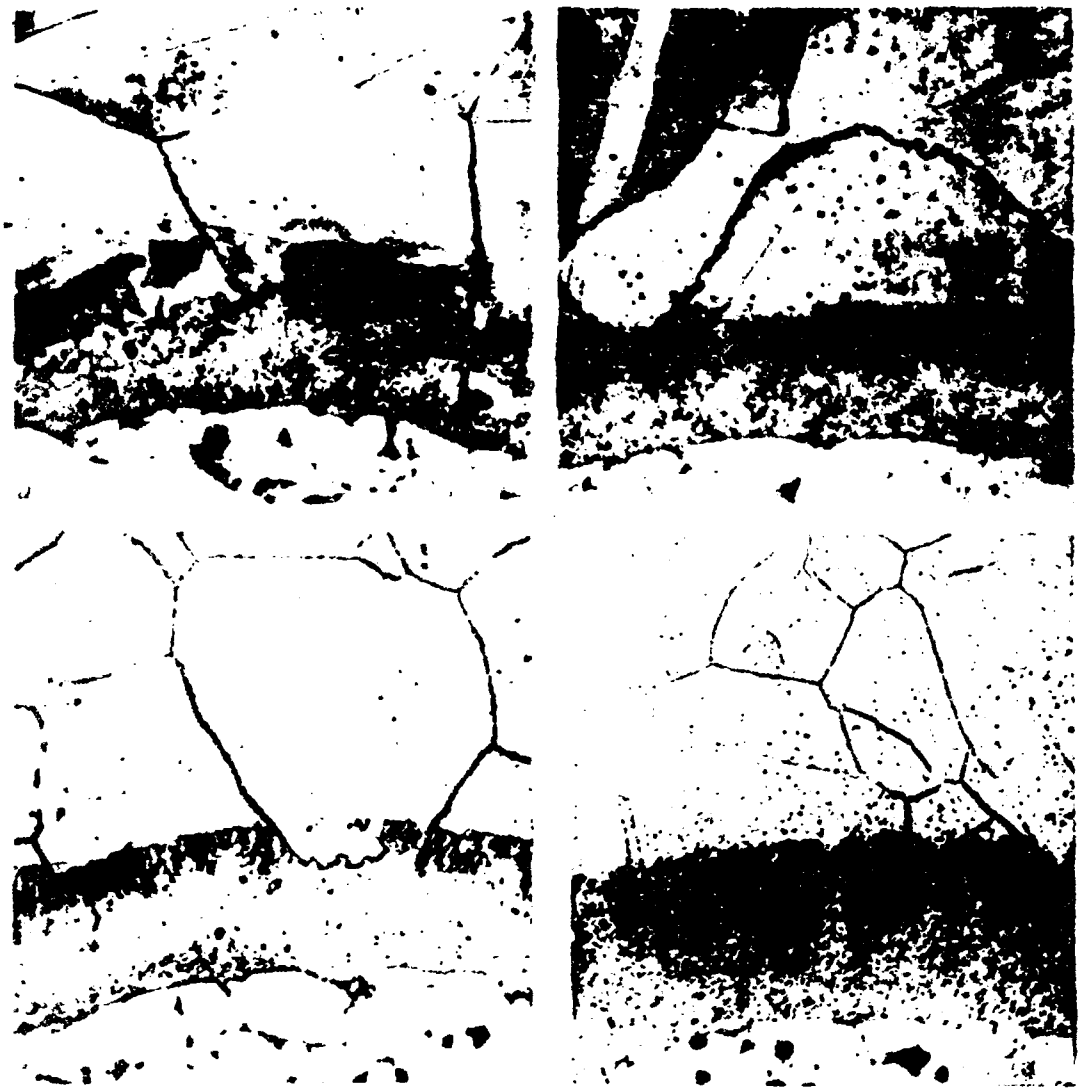

Figure 1. Diffusion temperature 850°, holding time 16 hours (130). (a) Alloy type Cr20Ni120Ti0.01; (b) alloy type Cr20Ni120Mo0.2; (c) alloy type Cr20Ni120Mo1.2; (d) alloy type Cr20Ni120Nb0.5; (e) Cr20Ni135

3. Examination Results of the Shape of the Diffusion Front

Both the shape of the diffusion front and the microstructure of the diffusion zone of nickel depend markedly on the diffusion temperature. The most distinct pattern was observed at the diffusion temperature of 1100° for a period of 2 hours. In this case, the diffusion zone of nickel consists of a "compact" layer adjacent to the edge of the hole filled with nickel and of a continuation of the compact portion of the zone, which includes the projecting points along the grain boundaries, sometimes enveloping the grains in the form of a "shell" (see, for example, Figure 4b).

At a diffusion temperature of 950° for 16 hours, and more rarely of 900° for eight hours, there originates in the base metal of the specimen at the border of the section near the nickel clog a layer with a striped appearance (Figures 1 and 3a), somewhat different from the appearance of the microstructure of the layer that forms at a temperature of 1100° (Figure 4b-e).

Figure 2. Alloy type Cr20Ni20Mo1.4. Diffusion temperature 750°, holding time 90 hours (X130)

The characteristic pattern of the microstructure of the diffusion zone obtained at 850° is that the continuation of the "compact" layer is composed of very fine, long veins along the grain boundaries (Figure 1a-e) are quite different from the projections of the diffusion front formed at 1100° (Figure 4b) and, all the more, at 1250° (Figure 5b).

At a temperature of 850°, very thin projections form in all examined austenitic alloys either with or without specially introduced admixtures. Thus, for instance, Figure 1 gives a microstructure of the diffusional zone in an alloy with titanium; Figure 1bc in alloys with molybdenum; Figure 1d in alloys with niobium.

The sharp difference between the pattern of the diffusional front obtained at 750° (Figure 2) and 850° (Figure 1) as compared to the one obtained at 1100° and 1250° indicates that at lower temperatures the diffusion rate of nickel along the boundaries is very much increased, while the "lateral" diffusion (from the boundary zone in the cross-sectional direction deep down the grain) is rather insignificant.

Consequently, at temperatures of 750° to 850° the diffusion of nickel takes place apparently in a very narrow boundary zone, and the penetration depth of the projections of the diffusional front revealed by etching along the boundaries is greater than the depth revealed after heating at much higher temperatures.

Provisional measurements were made by us at a 154X magnification of the very thin and long projections formed at the diffusion temperature of 750 - 850° along the boundaries. The actual diffusion of nickel along the grain boundaries extends much further -- in the form of a fine net, distinct at great magnifications.

As a result of the diffusing of nickel at a temperature of 950° for eight hours (Figure 3), the microstructure of the diffusional zone differs somewhat from that observed at 850 and 1100°.

The characteristic feature of the diffusion zone obtained at 950° is an uneven border of the "compact" layer; that is, this layer forms short and wide projections in the regions within the grain which are removed from the

boundaries, and at the same time forms projections along the boundaries (Figure 3a-c). Such diffusional projections are sometimes also observed along the boundaries of the twin crystals (Figures 2 and 3d).

At temperatures ranging from 750 to 950° the diffusion of nickel thus takes place not only along the boundaries of the crystallites, where the distortions in the crystal lattice are great, but also along the twin crystal boundaries where there are considerably fewer distortions of the crystal lattice than at the boundaries of the randomly oriented crystallites.

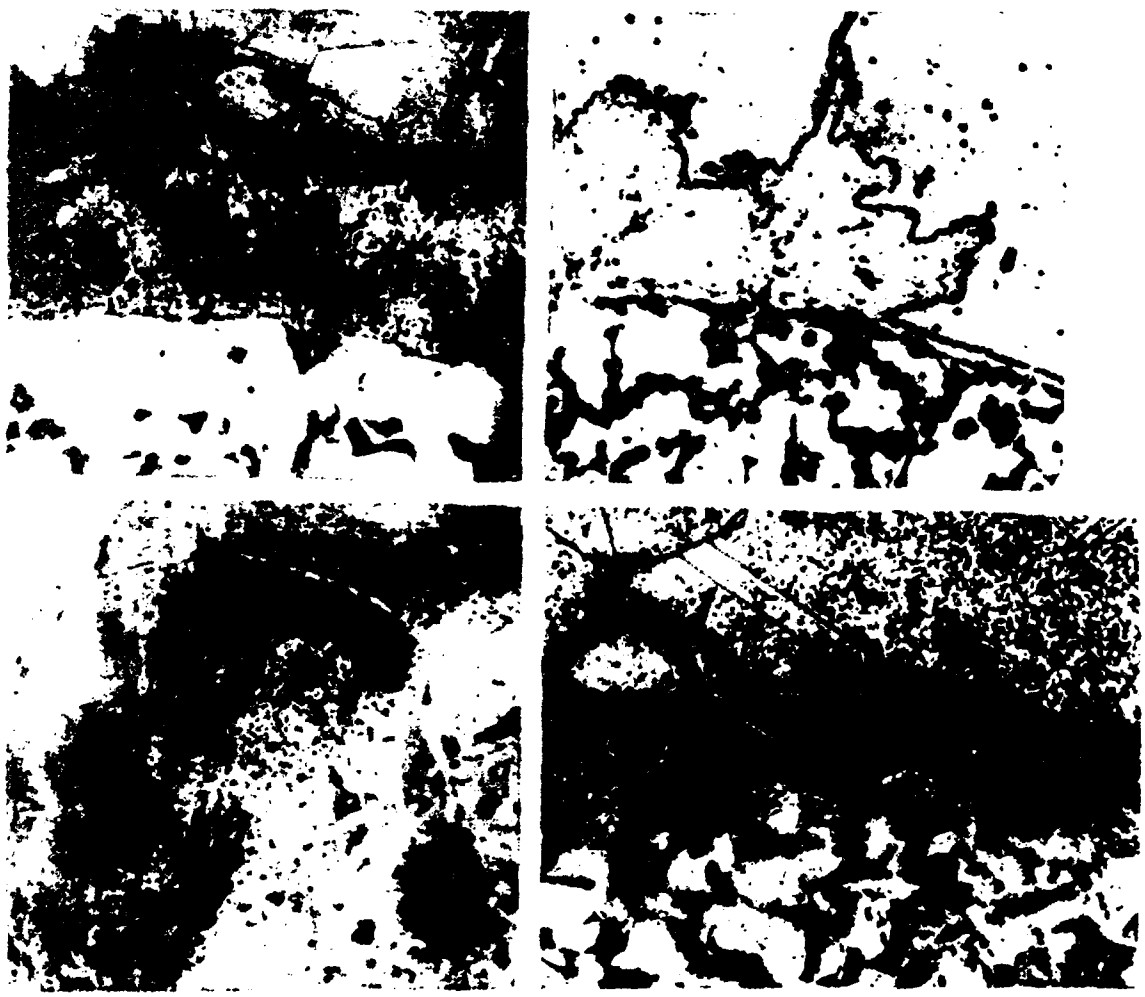

Figure 3. Diffusion temperatures 950°; holding time 8 hours (X130). (a) alloy type Cr20Ni12Nb0.5; (b) alloy type Cr20Ni35Mo0.3; (c) alloy type Cr20Ni25B0.05; (d) alloy type Cr21Ni40Ti0.3

At a 1100° temperature no diffusion was observed along the boundaries.

[illegible] diffusion of [illegible] at [illegible] a different [illegible] pattern. [illegible] the diffusion zone [illegible] quite even front in the portions within the [illegible], with the projections along the boundaries of the crystallites [illegible] distinctly (Figure [illegible]-1).

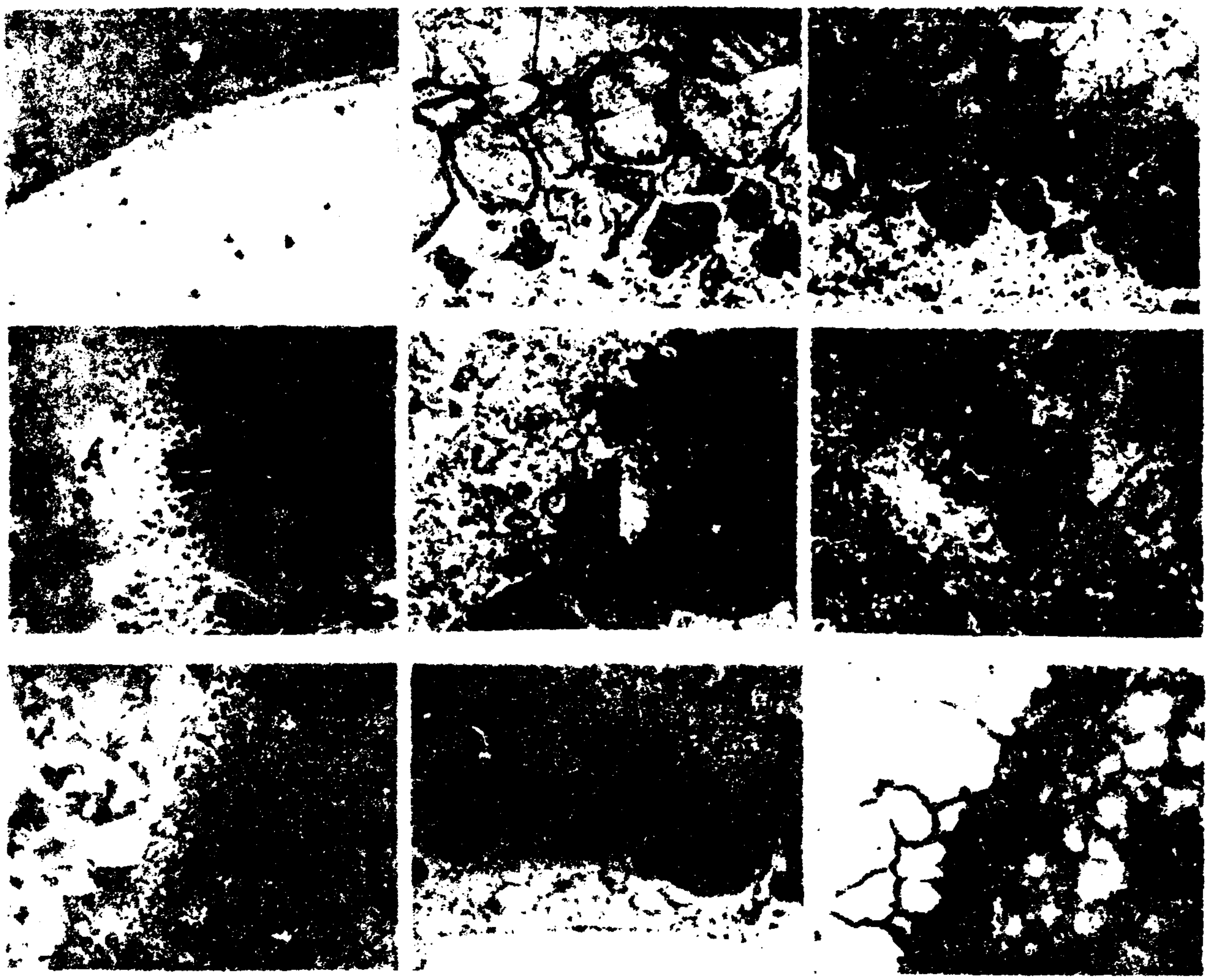

Figure 4. Diffusion temperature 1100°; holding time 2 hours (X150).
(a) Alloy type Cr20Ni21Nb0.5; (b) alloy type Cr20Ni11; (c) alloy type Cr20Ni10; (d) alloy type Cr19Ni11; (e) alloy type Cr21Ni20; (f) alloy type Cr21Ni10Mo1; (g) alloy type Cr20Ni10Mo3; (h) Cr20Ni20Ti0.01; (i) alloy type Cr20Ni20

At a 1100° diffusion temperature the "compact layer" appears more bright and uniform.

At a 1250° temperature all examined austenitic alloys, either with or without admixtures, have a diffusional front without a distinctly pronounced boundary. This makes it possible to draw the conclusion that at 1250° the rates of diffusion of nickel along the grain boundaries and through the grains become evened out, and we observe a diffusional zone with either an even front (Figure 5a) or with a front in which rare, individual, wide, and washed-out projections may be detected (Figure 5b).

The best etchant for exposing the diffusion layer turned out a reagent consisting of a mixture of four cm^3 $CuSO_4$, 20 cm^3 of HCl, and 20 cm^3 H_2O. This reagent etches distinctly the diffusion layer, producing a dark constituent on a light background (see, for instance, Figure 4cdg).

Obviously, the light background corresponds to the solid solution with a high concentration of nickel as confirmed by the roentgenographic investigations described below.

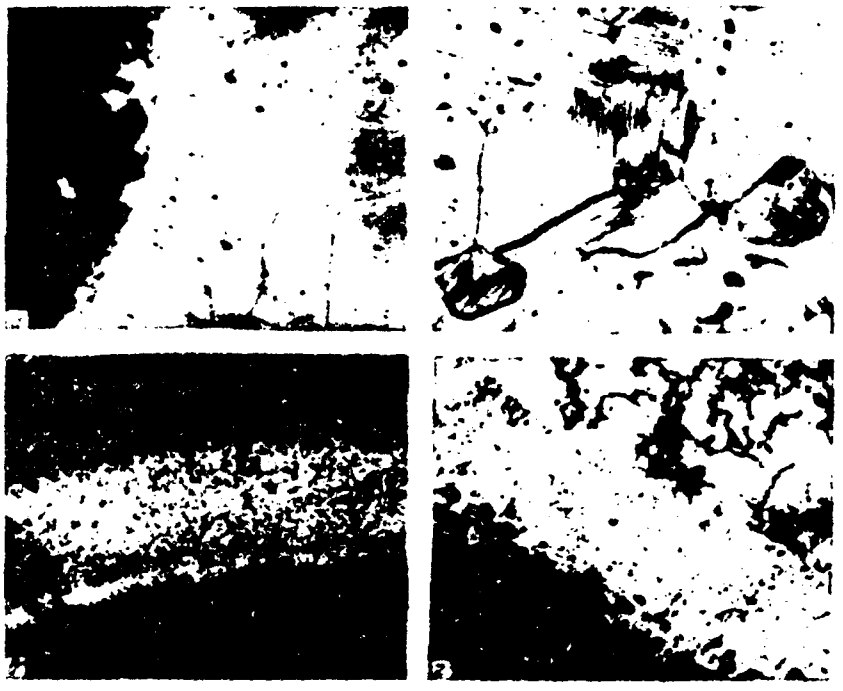

Figure 5. Diffusional temperature 1250°; holding time 1 hour (X130).
(a) Alloy type Cr17Ni40Mo3; (b) alloy type Cr18Ni10Mo2; (c) alloy type Cr20Ni20Mo5; (d) alloy type Cr20Ni16Mo4

The dark component in the "compact portion" of the light layer has an uneven random arrangement; we therefore conventionally call this portion of the diffusional zone the "compact layer".

Along the projection axis of the diffusional front, over the grain boundaries, we see dark "veins", which, as a rule, correspond either to the boundary contours of the austenitic grains (Figures 4cdg and 8) or to the polyhedron boundaries of the solid solution in the compact layer (Figure 4d).

After the microsection is repolished and repeated by etched, the "dark veins" along the boundaries, as well as the dark "inclusions" in the compact layer (Figure 4g), are eaten away and produce the impression of looseness (pores).

4. The Results of Determining the Microhardness of the Diffusion Layer

The specimens of two alloys were taken in order to determine the microhardness of the diffusion layer. A Cr19Ni11 specimen (Table 1, alloy 2) was examined after a diffusion at 1100° and a prolonged holding for 12 hours.

The specimens of the Cr20Ni36Mo1 alloy (Table 1, alloy 28) were examined after heatings at 850, 950, 1100, and 1250° temperatures and 16, eight, two and one hour holding times, respectively, and quenching in water.

The microhardness of the diffusion zone was measured on the PMT-3 instrument at a $\underline{P}$ = 50-g load and at a 485 magnification.

The microhardness measurement results, each of which were obtained as an arithmetical mean of many measurements, are given in Table 2.

Table 2

The microhardness of the specimens after nickel had been diffused into them

The region measured	Microhardness values				
	Cr19Ni11 alloy after heating at 1100°	Cr20Ni36Mo1 alloy after heating at °C temperatures			
		850	950	1100	1250
Austenite grain (specimen metal)	100	104	112	104	104
Diffusional zone:					
Compact layer of diffusion zone	72 : 76	68	72	69	97
Projections along the boundary	60 : 67	-	-	-	-
Electrolytic nickel (before grinding)	65	-	-	-	-

As we can see from Table 2, the microhardness of both the compact layer and the projections along the boundaries of the crystallites in the diffusional zone is intermediate between that of the specimen metal and that of metallic nickel. At the diffusion of nickel in an austenitic chromium-nickel alloy (at temperatures ranging from 850 to 1100°), the concentration of nickel in the solid solution of the diffusional zone increases. As a result, the microhardness becomes reduced as compared to the initial solid solution. At a diffusional temperature of 1250°, the microhardness of the diffusional zone approaches the magnitude of that specific for the initial metal. Obviously, at 1250°, the diffusion of nickel proceeds more intensively over the entire front, creating a smoother concentration gradient of nickel in the solid solution as compared to the diffusion at temperatures ranging from 850 to 1100°. The microhardness at the projection regions along the grain boundaries makes it possible to assume that the projections represent the solid solution of a considerably increased concentration of nickel, as opposed to its concentration in the austenite of the initial metal.

It should be noted that the measurement of the microhardness of the projections of the diffusional front offered certain difficulties, on account of its rather narrow area of the measurement regions. This explains the fact that two microhardness values for the projections (60 : 67) and two for the diffusion zone (72 : 76) are given in Table 2; these values are arithmetical means of 8 and 15 measurements, respectively.

5. Examination Results of the Diffusion Zone Obtained by Magnetic Metallography Method

In order to make a more detailed examination of the diffusional zone formed at the diffusion of nickel into ferrum-chromium-nickel austenitic alloys, we employed the method of magnetic metallography (N. I. Yeremin, Central Scientific Research Institute of Heavy Machinery, TsNIITMash, Moscow).

This method is carried out by means of applying a magnetic emulsion to the polished section.

We took a specimen of the Cr19Ni11 alloy (Table 1, alloy 2) with the intergranular diffusion of nickel

distinctly pronounced on the microstructure of the polished section (Figure 8a). Figures 6 and 7 show the polished section before and after the application of the ferromagnetic emulsion. As we can see, the magnetic emulsion precipitates on the diffusional zone (on both the compact layer and the projections) with the same degree of intensity. Figures 6b and 7 show that the intergranular projections of the diffusion front are ferromagnetic.

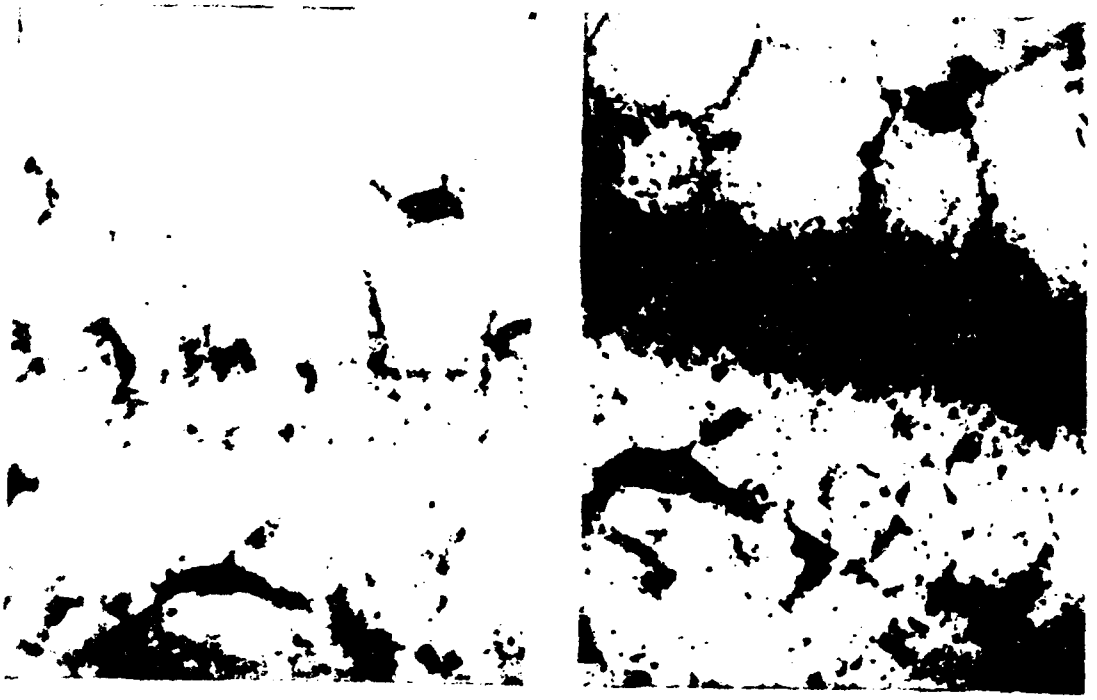

Figure 6. Area of polished Section I, alloy Cr19Ni11, before the application of the magnetic emulsion (a), and after (b) (X138).

This confirms our conclusion, based on the results of metallographic examinations, that the intergranular projections of the diffusional front represent zones of increased concentration of nickel which had become ferromagnetic as a result of it, as distinct from the nonmagnetic austenite of the alloy.

6. Evaluation Method for the Diffusional Mobility of Nickel Along the Grain Boundaries

It has been established by the examination of the microstructure that the diffusion zone of nickel consists of two parts: a compact layer adjacent to the nickel and the extension of this layer which consists of branched, more or less narrow, and long projections along the boundaries of the crystallites of the saturable basic alloy.

The tests have shown that the thickness of the diffusional layer and the degree to which the "intergranular effect" is pronounced depend on the composition of the alloy as well as on the presence of various admixtures in it. These observations were helpful in finding more concrete qualitative characteristics of the diffusion of nickel. In order to make a comparative evaluation of the diffusional mobility of nickel atoms in alloys with different base elements -- nickel and chromium as well as different admixtures (molybdenum, titanium, niobium, etc.) -- we introduced a ratio of the thickness of the portion of the diffusional layer containing the projections along the grain boundaries to that of the compact portion of the diffusional layer. This ratio has been called the coefficient of diffusional mobility of nickel along the grain boundaries $\underline{a}$. A high value of this ratio characterizes the increased diffusional mobility of nickel atoms along the grain boundaries (Figure 4b-e) while the tendency of coefficient $\underline{a}$ to approach zero means the decrease of diffusional mobility down to the complete liquidation of the intergranular effect when $\underline{a} = 0$ (Figure 5cd).

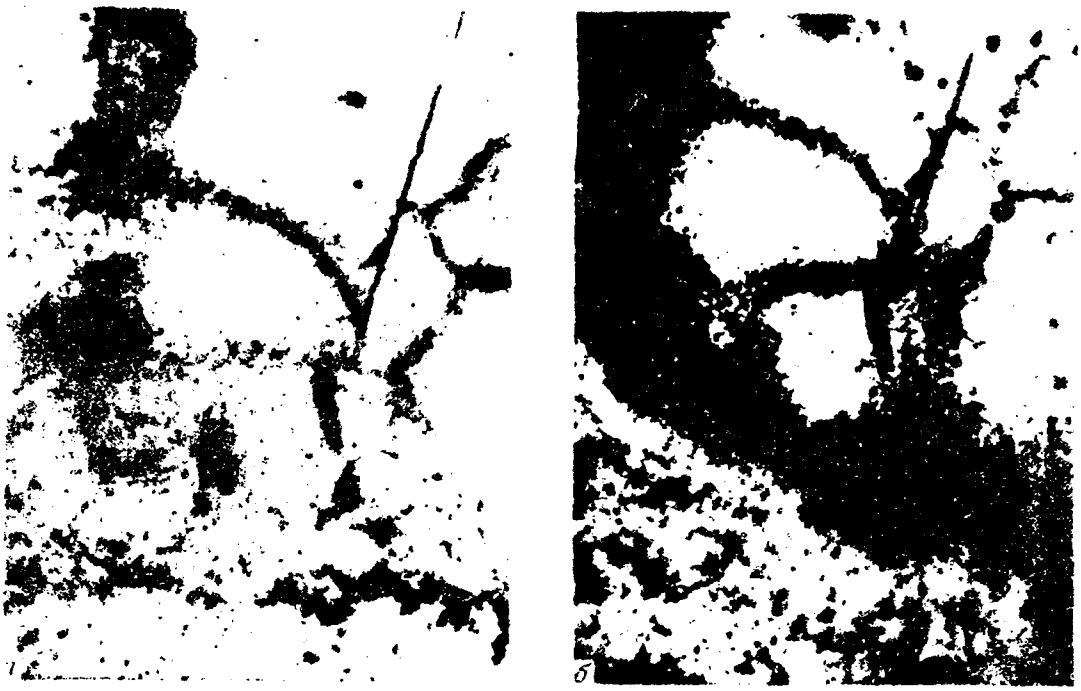

Figure 7. Area of polished Section II, alloy N19N11*, before the application of the magnetic emulsion (a), and after (b) (X120).

The introduction of coefficient a has made it possible to make a qualitative (roughly true) comparison of the diffusional mobility of nickel atoms along the intergranular boundaries, to trace the influence of the admixtures (molybdenum, titanium, tungsten, etc.) on this mobility, and, finally, to establish a certain correspondence between the degree of the diffusional mobility of nickel in the alloys under study and the mechanical characteristics of their heat resistance**.

However, it should be noted that the value of the coefficient of diffusional mobility of nickel a fluctuates within a wide range -- often for one and the same specimen

*Translator's note: The original text has N19N11, but this is apparently an error or a misprint: the correct brand name is Cr19N11.
**See the article by V. I. Arkharov, S. I. Ivanovskaya, L. N. Kolesnikov, and A. I. Moiseyev in this collection.

and still more for the specimens of one and the same alloy.

The coefficient a depends on the degree of distortion in the intergranular zones of the alloy and the degree of internal adsorption of the impurities. Both of these depend most strongly on the interrelated orientation of the crystallites connected by this zone.

Consequently, the effect of the increased intergranular mobility of nickel evident in the projection of the diffusional front also depends, within a wide range, on this interrelated orientation. In addition, importance may be attached to the segregation of the alloying elements*, which leads to the effect of intergranular diffusion being pronounced in a different degree in various sectors over the volume of one and the same specimen.

However, despite the strong fluctuation in the values of the measured coefficients a of diffusional mobility, the averaging of these values from a sufficiently great number of measurements made it possible to obtain an idea of the influence exerted on the diffusional mobility of nickel by the factors sought (alloying elements, temperature, etc.) in both qualitative and roughly quantitative terms. We will therefore not dwell upon the results of the numerous measurements, but will confine ourselves to the conclusions stated below.

7. Measurement Results of Diffusional Mobility of Nickel in the Alloys Under Examination

We have investigated the diffusional front of nickel in austenitic alloys (without admixtures) containing either 20 or 40 percent chromium, where the nickel content varied from 10, 20 and 40 to 80 percent. The intergranular effect (projections of the diffusional front along the boundaries of the crystallites) was observed neither in the Cr40Ni40-type alloy (Table 1, alloy 10) nor in that of Cr20Ni80 (Table 1, alloy 11).

The intergranular effect was distinctly pronounced in the Cr20Ni10-, Cr20Ni20-, and Cr20Ni40-type alloys.

*Molybdenum, as we know, is particularly exposed to such segregation.

For example, for one melt series, without admixtures, the coefficient of diffusional mobility of nickel along the boundaries came down from values of 1.5 - 2.5 for Cr20Ni10-type alloys to those of 1.2 - 1.6 for the Cr21Ni20-type alloy and to 1.0 - 1.36 for the Cr18Ni39 type; in the Cr38Ni37- and Cr20Ni80-type alloys the coefficient a was equal to zero.

From the examined additions of molybdenum to the chromium-nickel austenitic alloys, ranging from 0.24 to 5.0 percent (Table 1, alloys 12-32), the highest additions of molybdenum at temperatures of 1100 and 1250° reduce most strongly the diffusional mobility of nickel (Table 3).

Table 3

The diffusional mobility of nickel a in austenitic alloys with the admixture of some elements

No. of alloy	Conventional brand of alloy	Mean value of the coefficient a at diffusional temperatures		No. of alloy	Conventional brand of alloy	Mean value of the coefficient a at diffusional temperatures	
		850°	1100°			850°	1100°
5	Cr20Ni20	—	2,2	35	Cr20Ni20Ti0.4	--	0,7
13	Cr20Ni20Mo0.7	—	3,8	37	Cr21Ni20Ti1.9	—	0,0
12	Cr19Ni20Mo0.2	—	3,3	43	Cr20Ni19Nb0.25	—	0,0
14	Cr20Ni20Mo1.2	—	1,8	45	Cr19Ni20Nb0.5	—	0,7
21	Cr20Ni16Mo4	—	0,4	46	Cr19Ni20Nb1.0	—	1,1
22	Cr20Ni10Mo5	—	0,1	47	Cr19Ni20Nb2	—	1,7
26	Cr20Ni20Mo4.7	—	0,25	50	Cr20Ni20Al0.1	2,5	2,2
27	Cr18Ni20Mo5	—	0,0	51	Cr19Ni20Al0.5	0,5	2,1
33	Cr20Ni20Ti0.01	—	2,8	52	Cr20Ni20Al01*	1,7	1,0
34	Cr20Ni18Ti0.1	—	2,3				

*Translator's note: Apparently the decimal has been left out in the original.

The additions of titanium, niobium, and aluminum (Table 1, alloys 33-42, 43-49, and 50-52) quite markedly reduce the diffusional mobility of nickel along the boundaries within a specific range of concentration and temperature.

From the examined additions of titanium, 0.01 - 1.9 percent (Table 1, alloys 33-42), the strongest influence on the shape of the diffusional front of nickel was exerted by the addition of 1.9 percent Ti at a diffusional temperature of 1100°; in this case there is no diffusion of nickel whatsoever along the boundaries of the crystallites. Niobium is most effective when added in amounts of the order 0.25 - 0.5 percent at a diffusional temperature ranging from 1100 to 1250°; it reduces the diffusional mobility of nickel along the boundaries. At considerably lower temperatures (950 - 750°) the diffusional mobility of nickel increases in the indicated alloys.

On the other hand, the most effectively acting addition of aluminum (0.5 percent) strongly reduces the diffusional mobility of nickel at 850° (see Table 3).

All examined additions of tungsten (0.2 - 4.0 percent) (Table 1, alloys 53-59) moderately reduce the diffusional mobility of nickel along the boundaries of the crystallites; alloys containing 1.26 - 4.0 percent tungsten show the lowest coefficient ($\underline{a}$ = 0.9 - 1.5).

The additions of boron exerted the least noticeable influence on the diffusional mobility of nickel.

Diffusing nickel in high-nickel alloys on the basis Cr20Ni35-40 (chromium 20 percent, nickel 35-40 percent) with various admixtures, the coefficient of diffusional mobility $\underline{a}$ is pronounced less.

In examining the diffusional mobility of nickel in alloys on the basis of Cr20Ni20 with admixture combinations of niobium and molybdenum or titanium, as well as combinations of aluminum with niobium or titanium, no additional effect of these additions was observed. These alloys may serve as an example to confirm the possibility of competition of various surface-active (horophile) impurities with respect to their being saturated by the intergranular zones of the alloy; the adsorption of one of the impurities may in some cases predominate (6).

Table 4

The diffusional mobility of nickel a in alloys with combined admixtures*

No. of alloy	Conventional brand of alloy	Mean value of coefficient a at diffusional temperatures	
		950°	1100°
68A	Cr19Ni20Nb0.3Ti0.1**	0.70	0.5
43	Cr20Ni19Nb0.3	0.25	0.0
34	Cr20Ni18Ti0.1	0.90	2.3
65	Cr20Ni21Nb0.4Mo0.2	4.50	0.7
45	Cr19Ni20Nb0.5	2.80	0.7
12	Cr19Ni20Mo0.2	1.50	3.3
73	Cr20Ni19Al0.5Nb0.3	1.20	0.0
51	Cr19Ni20Al0.5	0.80	2.1
43	Cr20Ni19Nb0.3	0.25	0.0
72	Cr21Ni20Al0.5Ti0.8	0.80	0.0
51	Cr19Ni20Al0.5	0.80	2.1
36A	Cr19Ni19Ti0.8***	1.00	0.4
5	Cr20Ni20	4.2	2.1

*As compared to the diffusional mobility of nickel in alloys with the same admixtures taken separately.
**The alloy contained 18.90 percent Cr; 19.60 percent Ni; 0.15 percent Ti; and 0.25 percent Nb.
***The alloy contained 19.95 percent Cr; 20.00 percent Ni; and 0.79 percent Ti.

As an example, Table 4 gives the average values of the coefficient of diffusional mobility of the atoms of nickel a for four groups of alloys with the combined admixtures of the following elements: niobium and titanium, niobium and molybdenum, and, finally, aluminum and titanium. The values of the coefficient a for the base-alloy (Cr20Ni20) are given for comparison.

It is obvious from Table 4 that the combined admixture of two elements for any of the four alloys (Nos. 68A, 65, 73, and 72) was composed in such a way that, in two alloys of the same base adding the same elements, the coefficient a at a high temperature (1100°) of either one of them considerably differs; for example, for alloys 43 and 34, the coefficient a was 0.0 and 2.3; for alloys 45 and 12 it was 0.7 - 3.3; for alloys 51 and 36A it was 2.1 and 0.4; and for alloys 43 and 36A it was 0.0 and 2.1

In alloys with a combined admixture of the above elements, the coefficient a at a diffusion temperature (1100°) as a rule dropped, its value approaching to that of the coefficient a for an alloy with one of the elements taken individually. Here, in all three alloys where niobium was used in the combined admixture (in amounts ranging from 0.3 to 0.5 percent), at a diffusion temperature of 1100°, niobium "subdued" the influence of the other competing element (titanium, molybdenum, and aluminum), and the coefficient a decreased.

At much lower temperatures of diffusion (950°) a similar relationship in the reduction of coefficient a was observed only in the alloy with the combined admixture of niobium and titanium. In the other alloys with a combined admixture, the diffusional mobility either increased considerably as compared to that of the alloys with one of the admixture (alloys with niobium and molybdenum as well as with niobium and aluminum) or remained at the same level (alloy with titanium and aluminum). This means that the adsorption effect of niobium becomes paralyzed at reduced diffusional temperatures in an alloy with a combined admixture (niobium-molybdenum and niobium-aluminum).

Thus, the additions of molybdenum and aluminum without niobium display the adsorption effect weakly, whereas in the presence of niobium they paralyze its effect.

II. X-Ray Diffraction Examination of the Diffusion Zone of Nickel

An X-ray diffraction examination was carried out in order to clarify the nature of the diffusional zone of nickel with the projections along the grain boundaries.

A special specimen of the Cr19Ni11 alloy (Table 1, alloy 2) was prepared for the X-ray examination. A hollow 6 mm in diameter and 13 mm deep was drilled in the 15 x 15 x 15-mm specimen. A 4 x 4 x 7-mm insert was made separately of the same alloy as the basic specimen. Both the insert and the hollow were deeply etched to remove the deformed layer. The insert was placed into the hollow and the clearance between the insert and the surface of the hollow was filled with nickel powder, tightly packed; the hollow was clogged up with an iron plug.

The diffusion of nickel took place at a 1100° temperature over a period of 12 hours. A longitudinal, slightly inclined cut was then made near one of the longitudinal planes of the insert. Thus, the plane of the cut passed through the diffusion zone at a slight angle of inclination (approximately perpendicular to the direction of the diffusional flux). This cut is exhibited in Figure 8a showing the diffusional zone corresponding to the variation in depth; the lower portion of the picture shows the area nearer to the compact diffusional layer; the upper portion of the picture shows the "projections" along the grain boundaries which in this section represent a net along the grain boundaries of the basic metal (austenite).

The X-ray diffraction examination was carried out by the method of filming the stationary polycrystalline specimen (polished section) in the monochromatic K-radiation of iron. The X-ray pictures produced various sectors of the inclinced cut of the diffusional zone which can be seen in Figure 8a, beginning with the region near the nickel clog (see Table 5, Sector No. 1) and ending with sectors in the area untouched by the diffusion, the polyhedron austenite -- the basic metal of the specimen (Sectors 14-17).

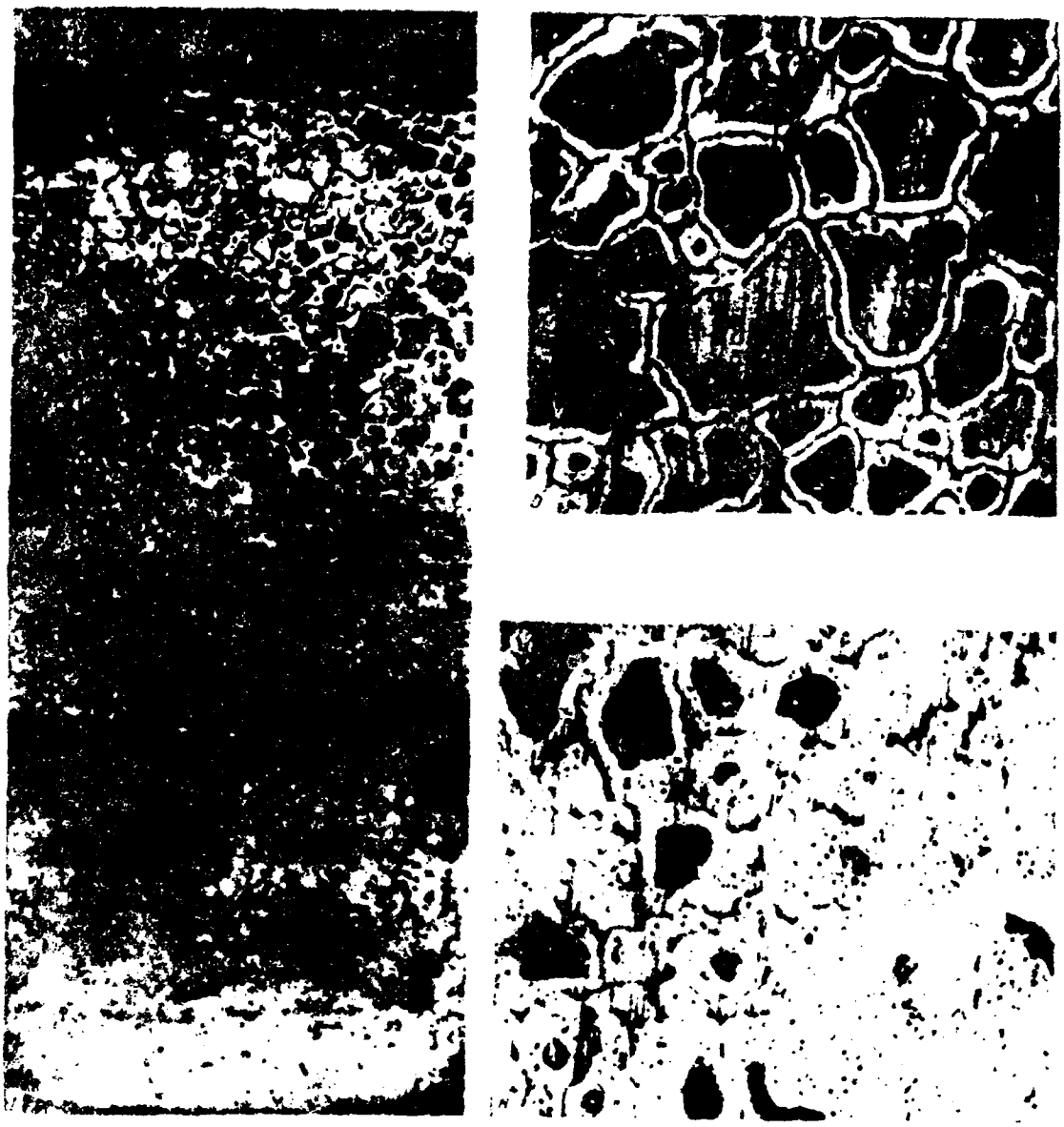

Figure 8. The diffusional zone examined roentgenographically. (a) Microstructure of the oblique cut (X50); (bc) microstructure details (X130)

Examination of the X-ray pictures obtained shows that on some of the roentgenograms (Sectors 1, 2, 6, 9, and 10) there are two line systems, each of which corresponds to a face-centered cubic lattice; these two lattices differ in parameters. A lattice parameter was determined from each of the two line systems on said roentgenograms by extrapolating the lattice parameter values for each individual line at a 90° angle. Obviously, two line systems on one and the same roentgenogram resulted when the primary beam illustrated the microstructure sectors containing simultaneously both the cross sections of the projections of the diffusional front and the polyhedrons of austenite between these projections (Figure 8b). But in cases in which the primary beam illuminated the sectors of the polished section filled with either diffusive projections (Figure 8c) or only with polyhedrons of austenite, there resulted one line system*.

*One line system may also result when the illuminated polished section contains, basically, sectors of one type (either austenite or cross sections of diffusive projections) in the presence of small sectors of another type; in this case, the latter produce very weak lines on the roentgenograms which blend into the background and are therefore almost imperceptible.

Table 5

The values of the lattice parameters of the solid solution of the diffusion zone, A

The numbers of the sectors of the picture	A_1	A_2	The numbers of the sectors of the picture	A_1	A_2
Nickel	3,512	—	9	3,513	3,535
1	3,510	3,544	10	3,522	3,540
2	3,520	3,540	11	—	3,558
3	—	3,542	12	—	3,555
4	—	3,542	13	—	3,560
5	—	3,542	14	—	3,570
6	3,521	3,544	15	—	3,565
7	—	3,542	16	—	3,574
8	—	3,542	17	—	3,576

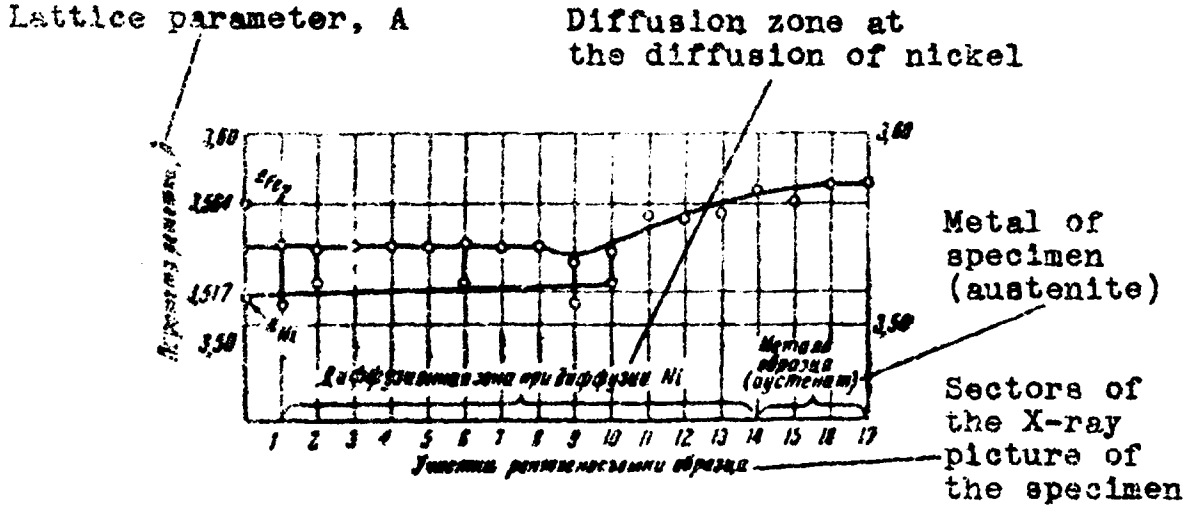

Figure 9. Variation curves of the lattice parameter of the solid solution of the diffusional zone.

Figure 5 gives the values of the lattice parameters for the various sectors of the diffusional zone. In cases of one-line systems, one parameter ($\underline{A}_1$) is given, and in cases of two-line systems, two parameters ($\underline{A}_1$ and $\underline{A}_2$).

Figure 9 shows curves mapped out on the basis of the examination results given in Figure 5.

The data obtained make it possible to draw the following conclusions:

(a) in some sectors (in the central portion of the section) within the range of the illuminated area there are two solid solutions of different concentrations, one of which corresponds to the intergranular projections of the diffusional front, and the other of which is contained in the sectors between these projections. The slight blur of the lines indicates thatthe possible drop in concentration between the diffusional projection and the grain must be very sharp;

(b) in all cases when two values of the lattice parameters for one and the same photographed sector are obtained, the value corresponding to that of the solid solution, richer in nickel (the lower value corresponds to the projections of the diffusional front), must be approximately constant along the entire length of the diffusional zone.

It follows from this that the concentration of nickel is approximately the same along the projection of the diffusional front, dropping sharply at the end of the projection as well as sideways toward the mass of the grain.

Conclusions

1. Disclosure was made of a phenomenon of preferential diffusional mobility of nickel along the intergranular boundaries in ferrum-chromium-nickel austenitic alloys; this explains the formation of distinctly pronounced projections of the diffusional front along the crystallites of austenite. According to the data of the investigations conducted by different methods (microstructural, X-ray diffraction, magnetic metallography, and the microhardness measuring method), the diffusional zone of nickel (the intergranular projections and the compact layer) represent a solid solution of a much higher nickel concentration, as compared to the initial austenite of the alloy, showing a sharp drop in

concentration toward the mass of the grain and the end of projections. This is confirmed by the fact that in the diffusion zones the etching properties of the solid solution, the lattice parameter, and the microhardness are reduced, whereas the magnetic properties are increased.

2. The degree to which the diffusional mobility of nickel along the grain boundaries evident is evaluated by us according to the microstructure of the diffusional zone (coefficient a); it represents a structure-sensitive characteristic which varies strongly, depending probably on the reciprocal orientation of the given pair of crystallites, at their conjunction where the diffusional mobility is determined, and on the nonuniformity of the specimen (the segregation of the alloying elements).

Having taken sufficient measurements and having averaged the coefficient a of the diffusional mobility, we obtained both qualitative and roughly quantitative ideas concerning the influence exerted on the diffusional mobility of nickel by such factors as the admixture of alloying elements (the chemical nature of the admixture, amount, etc.), the temperature of the test, etc.

3. In analyzing the diffusion of nickel into austenitic alloys, mainly of a Cr20Ni20 base (20 percent chromium and 20 percent nickel), with the admixture of such elements as niobium (0.25 - 2.0 percent); aluminum (0.13 - 1.0 percent); titanium (0.01 - 1.9 percent); molybdenum (0.24 - 5.0 percent); tungsten (0.2 - 4.0 percent) and boron (0.01 - 0.05 percent) we found that all these admixtures reduce the intergranular diffusional mobility of nickel to one extent or another. The most effective influence here is that of niobium (at low and medium contents within the range under study), aluminum (medium contents), and titanium and molybdenum (at high contents); tungsten is less effective; and the most feeble influence is exerted by boron.

The amount of the admixture, which reduces most of all the degree of diffusional mobility, depends on temperature.

4. The nature of the projections of the diffusional front varies depending on the temperature regions of the diffusion. At low diffusion temperatures (750 - 960°), the projections originate in the form of very long and thin veinlets extending far down into the specimen of austenite, along the boundaries of the polyhedrons; in the temperature

regions of 950 - 1100°, the projections appear as narrow strips with distinctly outlined contours turning deep into the austenite along the intergranular boundaries and forming characteristics loops around the polyhedrons of the austenite, the nearest to the compact diffusional front.

At a temperature of 1250° and above, the projections of the front are rare, wide, and blurred down to complete smoothing of the diffusional front.

BIBLIOGRAPHY

1. Arkharov, V. I., Tr-dy In-ta fiziki metallov YFAN SSSR (Works of the Institute of Physics of Metals of the Academy of Sciences USSR, Ural Branch), Issue 16, Press of the Academy of Sciences USSR, 1955.

2. Arkharov, V. I., Yefremova, K. A., Ivanovskaya, S. I., Shtol'ts, A. K., and Yunikov, B. A., Works of the Institute of Physics of Metals of the Academy of Sciences USSR, Ural Branch, Issue 16, Press of the Academy of Sciences USSR, 1955.

3. Arkharov, V. I., and Ivanovskaya, S. I., Works of the Institute of Physics of Metals of the Academy of Sciences USSR, Ural Branch, Issue 16, Press of the Academy of Sciences USSR, 1955.

4. Arkharov, V. I., Yefremova, K. A., Ivanovskaya, S. I., Shtol'ts, A. K., and Yunikov, B. A., Dokl. AN SSSR (Reports of the Academy of Sciences USSR), 89, No. 2, 1953.

5. Arkharov, V. I., and Gol'dshteyn, T. Yu., Works of the Institute of Physics of Metals of the Academy of Sciences USSR, Ural Branch, Issue 11, Sverdlovsk, Press of the Academy of Sciences USSR, Ural Branch, 1950.

6. Arkharov, V. I., Ivanovskaya, S. I., and Skornyakov, N. N., Reports of the Academy of Sciences USSR, 89, No. 4, 1953.

* * *

The Influence of Internal Adsorption on the Variation of the Crystal Lattice Parameter of a Heat-Resistant Alloy at the Change of the Grain Size

By V. I. Arkharov and A. A. Pen'tina

The chemical and structural nonuniformities of the alloy are of great importance in decelerating the processes of plastic deformation. A certain optimum of these nonuniformities is required to raise the heat resistance of one or another alloy*.

One of the earlier published studies cites the introduction of a hypothesis on the existence of an effect, called the intergranular internal adsorption, which is analogous to the Gibbs effect on the free interface of two different media. This hypothesis has by now obtained some experimental confirmation. The existence of the above phenomenon results in the fact that the concentration of some impurities (called horophile) in the intergranular transitional zones is increased in comparison with their average concentration in the alloy. At sufficient soaking this concentration attains a certain level at a given temperature and relationship of the orientations of the grains.

The nonuniform distribution in the concentration of the horophile element may exert a substantial influence on the heat-resistant properties of the alloy.

In many alloys the parameter of the crystal lattice of the solid solution markedly depends on the concentration of the impurity. In polycrystalline specimens of such solid solutions, the variations of the distribution in the concentration of the impurity -- due to its being horophile -- may be observed during the roentgenographic measurement of the lattice parameter, particularly when measuring the grain size. The smaller the grain size is, the larger will be the

*See the article by V. I. Arkharov and M. B. Yakutovich in this collection.

total volume of the intergranular transitional zones; the greater the amount of the diffusible horophile impurity in them, the greater will the corresponding variations of concentration in the mass of the grain be, and, consequently, the more will the parameter of the crystal lattice vary. The variation in the parameter will be directed toward either its decrease or its increase, depending both on the chemical composition of the constituents of the solid solution and on the correlation of their atomic radii.

It should be noted that the diffraction pattern on the roentgenogram reflects both the state and structure of the grain mass, whereas the intergranular transitional zones do not in view of the fact that, first, the total volume of these zones is small in comparison with the total mass of all grains and, second, the crystal lattice in these zones is strongly distorted.

Consequently, the precision measurement of the parameter of the crystal lattice may be used as a method for studying the intergranular internal adsorption aiding the determination of the horophile activity of some element or another.

The Technique of the Investigation

For this investigation certain alloys were selected from those tested by other methods described in the other articles of this collection. The composition of the alloys is given in Table 1.

Table 1

The chemical composition of the alloys, percent (of an iron-base)

Conventional make of steel	Cr	Ni	C	Mn	Si	Mo	Nb	Ti
Cr20Ni20	19,95	20,00	0,025	0,30	0,06	—	—	—
Cr20Ni20	21,10	20,30	0,080	0,07	0,15	—	—	—
Cr20Ni20Mo0.6	20,10	20,20	0,031	0,22	0,014	0,65	—	—
Cr20Ni20Nb0.5	19,93	20,62	0,025	0,34	0,35	—	0,51	—
Cr20Ni20Ti0.4	20,15	20,38	0,005	0,39	0,48	—	—	0,37
Cr20Ni20Mo3	18,20	19,70	0,040	0,02	0,32	2,97	—	—
Cr20Ni20Nb2	19,45	20,20	0,080	0,31	0,54	—	2,02	—
Cr20Ni20Ti2	20,95	20,40	0,050	0,38	0,60	—	—	1,87

The alloys were forged and rolled in the form of rods with a cross section of 15 x 15 mm; the rods were then cut. The specimen dimensions were: 15 x 15 x 10 mm.

Since it was necessary to trace the effect of the variation in the crystal lattice parameter due to the possible internal intergranular adsorption of one element or another, a technique developed earlier was used to compare crystal lattice parameter of the solid solution in one and the same specimen; the latter was submitted to thermomechanical treatment in order to produce first the macrograin state and then the micrograin state. The observation of the variations in the crystal lattice parameter on one and the same specimen eliminates the influence of a possible nonuniformity in concentration from one specimen to another. A few test series were run on different specimens to verify the reproducibility of results for one and the same alloy.

As previously indicated, the greater the difference in grain size the greater the variation in concentration in the mass of the grain. The parameters of the crystal lattice of the solid solution in macrocrystalline and fine-grained states differ accordingly. The lattice parameter of the specimen in the macrocrystalline state will

correspond to a higher concentration of the horophile element, but in the fine-grained state, the lattice parameter will, inversely, vary in the direction corresponding to a reduction in the concentration of the horophile element.

Originally we investigated specimens some of which were annealed at 1250° and had a coarse grain and the others of which were annealed at 950° and had a fine grain. Next, the grain of the macrocrystalline specimen was ground by cold rolling to a cross section of 10 x 10 mm and then annealed at 950° to remove stresses. In the fine-grained specimens, the grain was coarsened by collective recrystallization at 1250°. After the specimens were X-rayed they were subjected to a reversal operation: the structure in the fine-grained specimens was coarsened by annealing at 1250°, and the macrocrystalline specimens were converted to fine-grained by rolling to a cross section of 10 x 10 mm. The subsequent thermomechanical treatment similarly resulted in a reduction of the coarse grain and in a coarsening of the fine grain in the specimens.

The specimens of each alloy selected were subjected to this treatment.

The grain size was checked after each annealing by photomicrography at a magnification of 130X. Here the cross-sectional area of the grain varied 100 - 1000-fold.

The measurement of the crystal lattice parameter was carried out by the method of reversed roentgenography. The X-rays were taken in the beams of K_β -Cr.

Repeated measurements of the distances between the lines on the roentgenograms have produced a maximum difference of 0.3 mm. This corresponds to the maximum error in measuring the crystal lattice parameter of the analyzed solid solutions which is 0.0010 Å.

In determining the parameter of the crystal lattice, the error is calculated according to the following formula:

$$\frac{\Delta a}{a} = - \cot \theta \Delta \theta,$$

$$\text{whereas } \Delta \theta = \pm \frac{\Delta L}{L} \cdot \frac{\sin 4(\frac{\pi}{2} - \theta)}{4},$$

where a is the lattice parameter;

θ is the angle of reflection; and

L is the distance between the symmetrical lines on the roentgenogram.

Examination Results

The observed variations in the parameter of the crystal lattice in the solid solution of Cr20Ni20 without the special admixtures and with the admixtures of molybdenum, niobium, or titanium are given in Table 2. These variations represent the difference in the parameters of the crystal lattice for the macrograin and fine-grained structures of the alloy tested.

The parameter measurements of several specimens of each alloy were taken with repeated reducing and coarsening of the grain by means of a specific thermomechanical treatment; the variations of the parameter exceed the measurement error.

The variation of the parameter with either an increase or decrease in grain size was reproduced in all cases and for each alloy. The observed variations in the size of the parameter of the crystal lattice reflect the variations in concentration that actually occur in the solid solutions with the change in grain size.

In order to clarify the general character of influence of the above admixtures on the parameter of the crystal lattice, measurements were also taken of the lattice parameter of the Cr20Ni20 base with relatively admixtures of molybdenum, niobium, or titanium (see Table 1). The obtained values for the parameter of the specimens with solid solutions having a macrograin structure are given in Table 3.

Table 2

The variations in the parameter of the crystal lattice of the solid solution of Cr20N120 with and without admixtures

Conventional make of steel	No. of specimen	Number of thermomechanical treatments*	Variation in parameter $\Delta a \cdot 10^4$ Å**	Remarks
Cr20N120	1	5	14	In all cases the parameter varies toward a decrease when the grain is coarsened and varies toward an increase when the grain size is reduced.
	2	5	20	
	3	1	18	
	4	3	19	
	5	5	25	
Cr20N120Mo0.6	1	3	20	
	2	3	29	
	3	1	25	In all cases the parameter varies toward an increase when the grain is coarsened and varies toward a decrease when the grain size is reduced.
	4	4	28	
Cr20N120Nb0.5	1	5	45	
	2	1	40	
	3	1	64	
Cr20N120T10.4	1	3	25	
	2	3	19	
	3	3	26	

*The thermomechanical treatment was conducted in succession for either reducing or coarsening the grain in the microstructure of the specimen.

**The mean variation value of the parameter with the change in grain size is 10 - 100-fold; the absolute dimensions of the grains in various tests varied from 4 to 400 μ.

Table 3

Conventional make of steel	Parameter of crystal lattice (mean value a, Å)
Cr20Ni120Mo3	3.5984
Cr20Ni120Nb2	3.5871
Cr20Ni120Ti2	3.5956
Cr20Ni120	3.5825

Discussion of Results

The measurements of the crystal lattice parameter conducted on several specimens show that the results are entirely reproducible.

The lattice parameter of the macrograin structure of the austenitic alloy Cr20Ni120 (without special admixtures) is lower than that of the fine-grained structure. Since the parameter of the crystal lattice of the investigated triple solid solution increases with the reduction in the concentration of nickel, it is obvious that the concentration of nickel in the grain decreases with the reduction in grain size, insofar as the total amount of nickel increases in the intergranular transitional zones as the total volume of the latter is increased. Consequently, the transition of nickel from the grain to the intergranular zones causes the increase of the parameter of the crystal lattice in the mass of the grain.

This provides a reason for concluding that the nickel in this solid solution is a positively active horophile element which participates in the internal intergranular adsorption.

The variations in the crystal lattice parameter of the solid solutions of Cr20Ni120 base with small admixtures of molybdenum, niobium, or titanium are opposite (with the change in grain size) to those observed in a solid solution without these additions. The parameter of the crystal lattice for a macrograin state is in these cases greater than that for a fine-grained state. He[illegible]he variation

in the parameter from its absolute value in alloys with small additions is greater than in the Cr20N120 alloy selected as base. The greatest variation of the parameter of the crystal lattice occurred in the alloy with the admixture of niobium (Cr20N120Nb0.5).

In this case, the variations of the parameter show that the admixtures of molybdenum, niobium, and titanium are adsorption-active. As in the first case, the concentration of the horophile element (Mo, Nb, or Ti) decreases in the mass of the grain when the latter is reduced due to the withdrawal of the horophile impurity to the intergranular zones. Here, however, in cleaving the structure of the solid solutions the diffusion of the horophile element in the intergranular transitional zones causes the reduction of the parameter in contrast with the analogous case of such a diffusion of horophile nickel in the Cr20N120 alloy. When the grain in the structure of alloys with small additions of molybdenum, niobium, or titanium is coarsened (the overall expanse and total volume of the intergranular transitional zones become smaller), a corresponding amount of the horophile element returns to the mass of the grain, and we have a greater parameter of the crystal lattice than in a fine-grained structure. The fact that the increase in concentration of such impurities as molybdenum, niobium, or titanium in the grain causes the increase of the crystal lattice parameter as compared to that in alloys without these additions is obvious from the nature of variation of the crystal lattice parameter in alloys containing a high amount of introduced additions, of the order of 2 to 3 percent (see Table 3).

Thus, it may be assumed that the adsorption activity of additions in the alloys containing them (molybdenum, niobium, or titanium) predominates over the adsorption activity of nickel.

Conclusions

The observed variations in the parameter of the crystal lattice of alloys with the change in grain size suggest the conclusion that nickel, molybdenum, niobium, and titanium in the tested alloys are adsorption-active (horophile) elements. This leads to an increase in chemical nonuniformities in the alloys which may help to decelerate the processes of plastic deformation in them. This behavior of the admixtures may be one of the factors increasing the heat resistance of alloys.

BIBLIOGRAPHY

1. Arkharov, V. I., Works of the Institute of Physics of Metals of the Academy of Sciences USSR, Ural Branch, Issue 8, Sverdlovsk, Press of the Academy of Sciences USSR, 1946.

2. Arkharov, V. I., and Skornyakov, N. N., Reports of the Academy of Sciences USSR, 89, 1953.

* * *

The Influence of Small Admixtures on the Creep of Solid Solutions

By V. A. Pavlov, E. S. Yakovleva, and M. V. Yakutovich

This article cites the findings on the hardening effect of small admixtures on the grain boundaries. The properties of the grain boundaries must strongly affect the creep of alloys* since in this case the deformation is to a great extent localized at the grain boundaries (1-3). In this connection, we carried out an investigation on the creep of aluminum and ferrum-chromium-nickel alloys, alloyed by various elements forming with them solid solutions.

Investigation of Aluminum Alloys

The study was conducted on alloys of aluminum with copper, magnesium, silver, and zinc. Three series of alloys were made using a 99.99-percent pure aluminum base; and two series of 99.97-percent pure aluminum (Table 1).

Table 1

The chemical composition of aluminum alloys

Aluminum purity, percent	Alloying element	Percentage of alloying element						Average grain size, mm
99.99	Zinc	0,00	traces	0,02	0,08	0,46	0,87	0,12
99.99	Silver	0,00	traces	0 03	0,17	1,03	2,05	0,2—0,3
99.99	Copper	0,00	0,017	0,034	0,09	0,46	0,8	0,12
99.97	Magnesium	0,00	0,04	0,07	0,48	0,79	5,8	0,06—0,08
99.97	Copper	0,00	0,03	0,09	0,48	1,30	2,44	0,06—0,08

*See the article by V. I. Arkharov and M. V. Yakutovich in this collection.

The specimens had the shape of wires with 2.0- and 1.7-mm diameters. The calculated length was 25 mm. Prior to the test, all specimens were subjected to recrystallization annealing; the temperature was so selected as to impart to each series of alloys the same grain size after the annealing.

The test on creep was conducted on the tension-testing machine, permitting the testing of six specimens simultaneously. The overall view of the machine is shown in Figure 1. The test temperature was taken below the recrystallization temperature. The alloys made with the 99.99-percent aluminum base were tested at 250°, and the alloys made with the 99.97-percent aluminum base at 300°. The creep test of the latter alloys was conducted at a constant tension, equaling 0.67 kg/mm^2. The alloys made with the 99.99-percent pure aluminum base were tested at various tensions ranging from 0.2 to 0.6 kg/mm^2.

The measuring of length was carried out on a measuring microscope accurate of 0.01 mm, at a relative measuring error of 0.04 percent. To measure the length, the specimens were periodically unloaded, taken from the machine, and transferred to the microscope stage.

The next loading of the samples was carried out after attaining the required temperature in the furnace and holding at this temperature for 1 hour.

The temperature was measured with a chromel-alumel thermocouple, placed at the middle of the calculated length of the specimen, at a distance of 1 mm from its surface. The constancy of the temperature during the test was maintained by means of a thermocontroller accurate to ±1°.

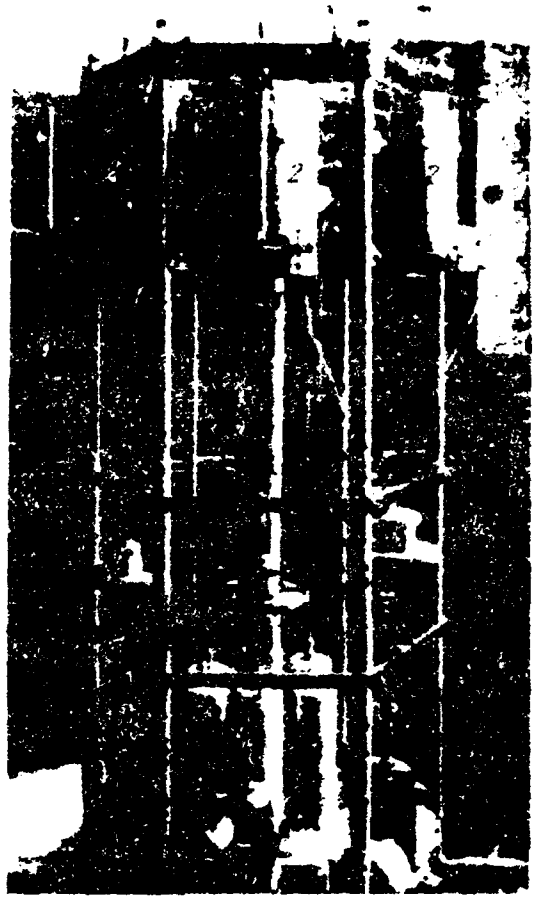

Figure 1. Creep testing equipment.
(1) Specimen; (2) furnace;
(3) load.

On the basis of these measurements we plotted the primary flow curves in coordinates of elongation time and proceeded to their further study.

Test Results

Figures 2 and 3 give the characteristic creep curves for four aluminum alloys (99.97-percent pure) with magnesium and copper. The dotted line on each graph shows the region where the flow curves of the pure aluminum specimens pass.

From the examination of the curves on Figure 2a we see that the alloy containing 0.07 percent magnesium

flows considerably faster than pure aluminum. The spread of the flow curves is as great as that of aluminum. The alloy containing 0.79 percent magnesium (Figure 2b) flows at a slower rate than aluminum, and the spread of the flow curves is insignificant.

The alloy of aluminum with 0.09 percent Cu flows at a faster rate than pure aluminum, but that containing 2.4 percent Cu (Figure 3) at a rate much slower than aluminum. Similar curves were obtained for alloys of other compositions. For a quantitative comparison of the creep of various alloys, mean elongation values were found from the flow curves for each alloy after 48, 72 and 96 hours of testing.

Figure 4 gives a combined graph of the mean elongation values for all tested aluminum alloys. The graph shows clearly that the alloys differ sharply from each other in behavior. The low-concentration alloys (below 0.5 percent Mg and 0.5 percent Cu) have an increased flow rate as compared to pure aluminum. The alloy containing 0.07 percent Mg has the highest flow rate. After 72 hours of testing, this alloy has elongated 20-fold in comparison with aluminum. From the aluminum-copper alloys, the alloy containing 0.09 percent Cu has the highest flow rate. After 96 hours of testing, its elongation is 5.5-fold in comparison with that of aluminum.

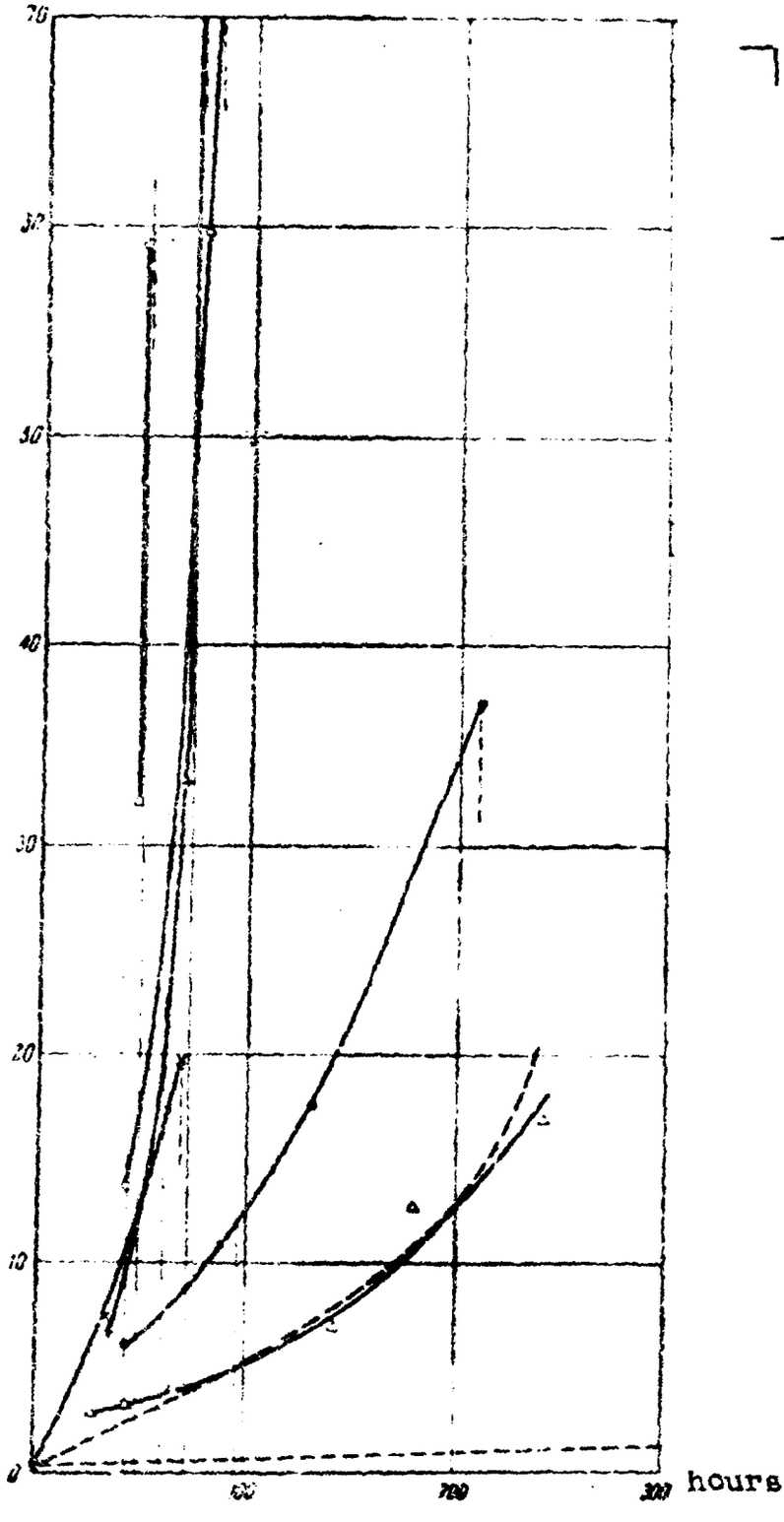

Elongation, percent

Figure 2a. Flow curves of aluminum alloys containing 0.07 percent Mg.

At high-admixture concentrations, the flow rate of the alloys drops and becomes lower than that of pure aluminum. The alloy containing 5.8 percent Mg is an exception. At 300° this alloy approaches the solubility limit of magnesium and aluminum. It is possible that the solid solution of magnesium and aluminum breaks up during flow, and this may result in the increase of the flow rate of the alloy. The observed strong variation in the flow rate of the alloys by alloying them with hundredths of one percent of the admixture provides reason for assuming that the great spread of the flow curves of pure aluminum is associated with the small fluctuations in the degree of purity in the volume of the initial material.

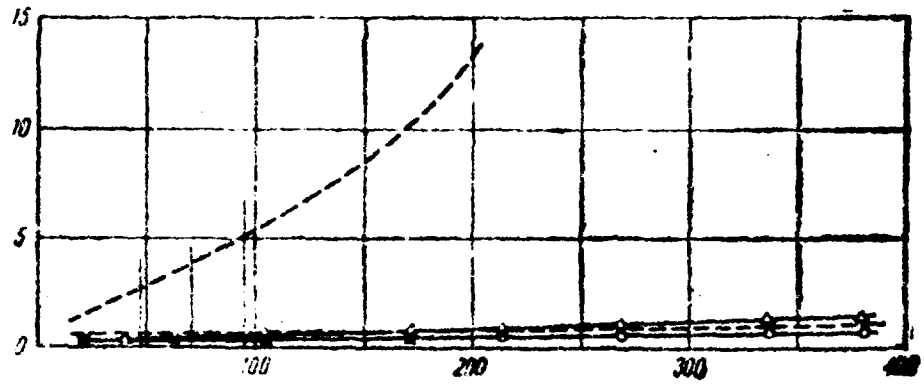

Figure 2b. Flow curves of aluminum alloys containing 0.79 percent Mg.

Aluminum-zinc alloys were tested for creep at the same stresses.

The elongation values were determined for all alloys after a 50-hour test*. Figure 5 gives the dependence of this elongation on concentration in the zinc alloy at four different stresses. It is obvious from this figure that the effect of the zinc addition somewhat varies with the reduction in stress.

*Curve 5 in Figure 5 is given because the alloys containing 0.08 percent zinc failed at a tensile stress of 600 g/mm^2 before the end of the 50-hour test.

At higher stresses, the first small zinc addition exerts a hardening effect; the next one resoftens the alloys. A further increase in the amount of zinc once again causes the hardening of the alloy.

At medium stresses the addition hardens the alloy. A resoftening effect of a small addition is also observed, but to a lesser degree than that at high stresses. A further increase in admixture results in hardening the alloy.

At much lower stresses the addition exerts only a hardening effect. However, the alloy is not hardened strongly to concentration. The first small addition hardens the alloy substantially, the next somewhat less. Consequently, there still is a relative resoftening. A further increase in the amount of the admixture changes the creep of the alloy slightly, but its tendency to harden is still noticeable.

Similar curves for aluminum-silver and aluminum-copper alloys are of the same nature. In the region of small concentrations we observe a relative resoftening of the alloy (Figure 6).

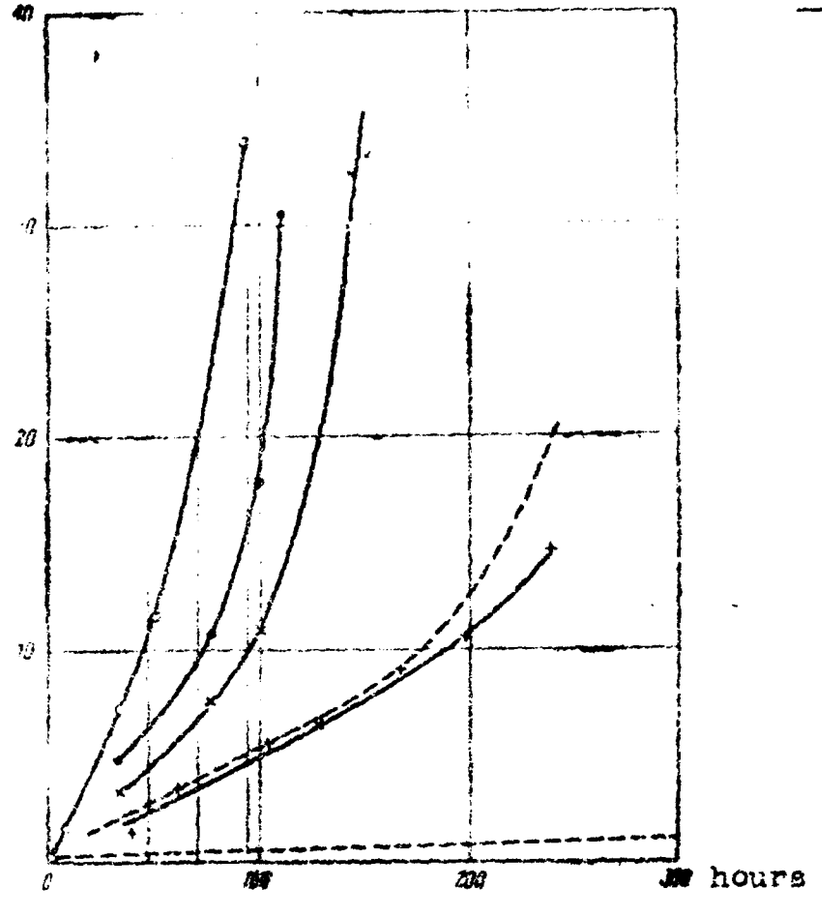

Figure 3. Flow curves of aluminum alloys containing 0.09 percent Cu (a) and 2.4 percent Cu (b).

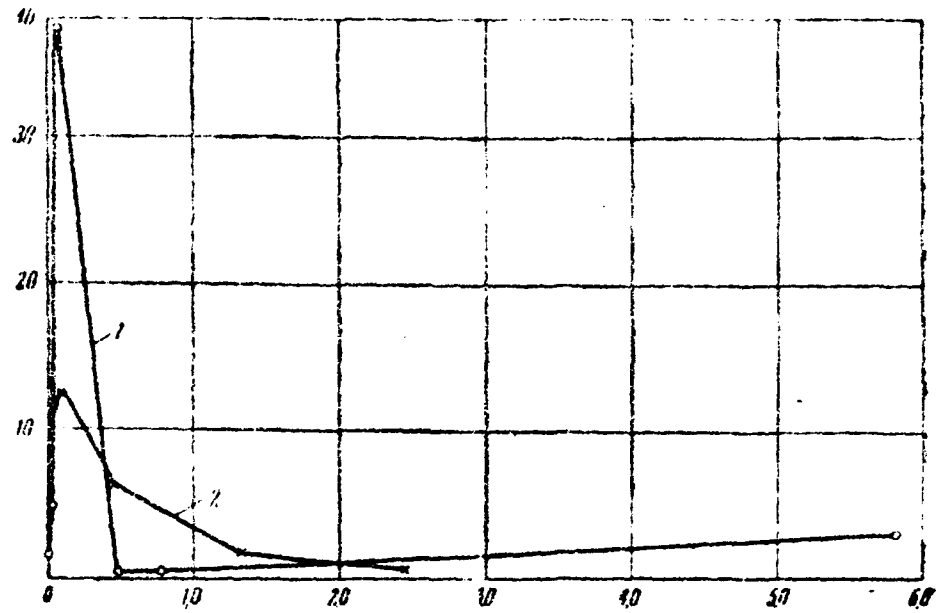

Figure 4. The dependence of elongation of aluminum alloys.
(1) On the concentration of magnesium (after 72 hours of flow);
(2) on the concentration of copper (after 96 hours of flow)

Elongation, percent

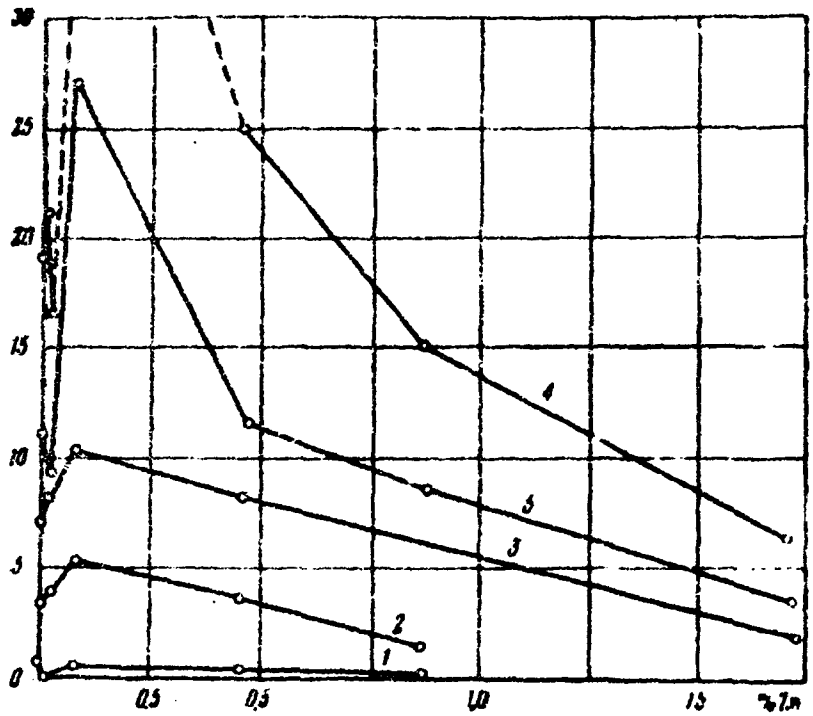

Figure 5. The dependence of elongation of aluminum alloys on the concentration of zinc after 50 hours of flow at a stress of:
(1) 200 g/mm^2; (2) 400 g/mm^2; (3) 500 g/mm^2; (4) 600 g/mm^2; (5) 600 g/mm^2 (after a 30-hour test)

Elongation, percent

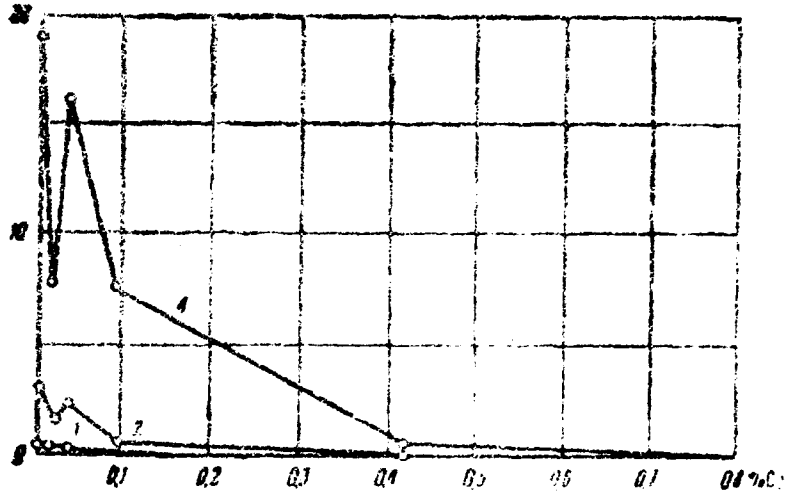

a

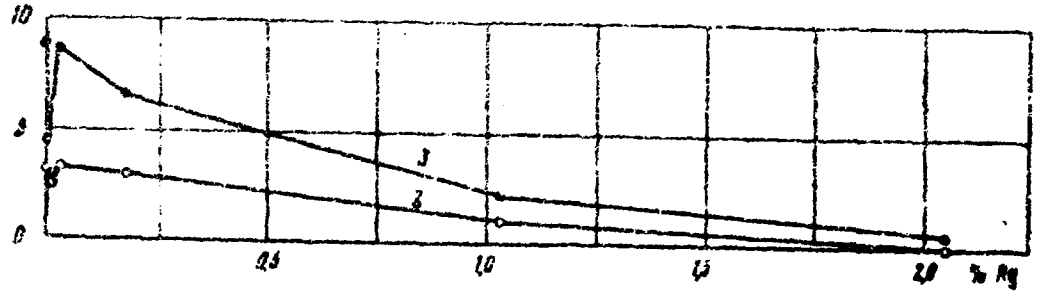

b

Figure 6. The dependence of the elongation of aluminum alloys after 50 hours of flow on the concentration of silver (a) and copper (b) at a stress of:
(1) 200 g/mm^2; (2) 400 g/mm^2; (3) 500 g/mm^2; (4) 600 g/mm^2

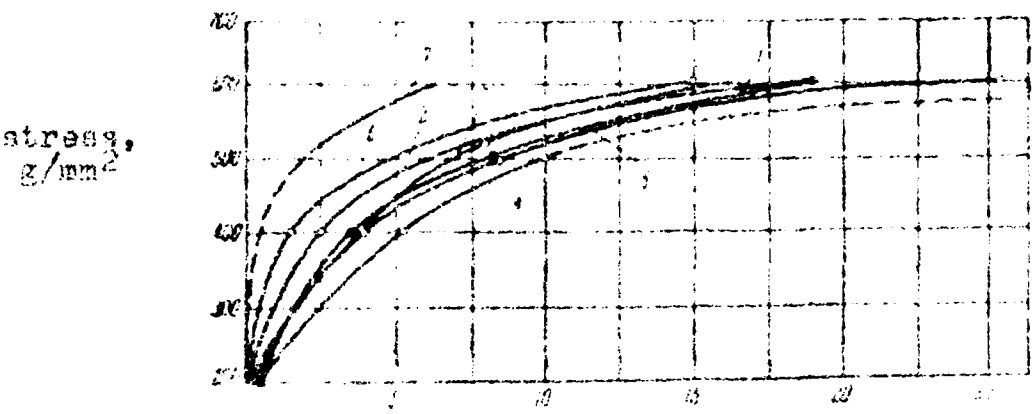

Figure 7. The dependence of the elongation of aluminum-zinc alloys on stress after 50 hours of flow:
(1) 0.00 percent of zinc; (2) traces of zinc; (3) 0.02 percent Zn; (4) 0.08 percent of Zn; (5) 0.46 percent Zn; (6) 0.87 percent Zn; (7) 1.72 percent Zn

It follows from the given curves that the variation of the mechanical properties of the alloy with the concentration of the alloying element is not monotonous and the influence of small admixtures varies qualitatively when turning from high stresses to low ones. The latter becomes particularly obvious if we are to plot the dependence of elongation on stress for one and the same instance of time (50 hours) for alloys containing a different amount of any alloying element. As we see from Figure 7, in the region of high stresses, pure aluminum appears to be stronger than the alloy with the addition of 0.08 percent Zn. In the region of low stresses, all alloys are, on the contrary, stronger than pure aluminum. The flow rate of the specimens of the original 99.99-percent pure aluminum has an extremely strong spread. It is therefore difficult to give a reliable estimate of both the hardening and resoftening effects of the alloying elements.

The Investigation of Ferrum-Chromium-Nickel Alloys

A study was made on ferrous alloys with a constant content of chromium and nickel alloyed with various amounts of molybdenum and titanium (Table 2).

Table 2

The chemical composition of ferrum-chromium-nickel alloys, percent*

Conventional grade of the alloys	Chromium	Nickel	Molybdenum	Titanium
Cr20N120	19,50	20,00	—	—
Cr20N120Mo0.25	19,50	19,80	0,26	—
Cr20N120Mo0.67	20,10	20,60	0,67	—
Cr20N120Mo1.25	19,90	20,30	1,25	—
Cr20N120Ti0.09S	19,90	19,88	—	0,09S
Cr20N120Ti0.03	19,30	19,68	—	0,03

The alloys were tested in a hardened state (hardening temperature 1250°). The average linear grain size of the alloys was 0.1 to 0.2 mm.

*Carbon content 0.02 to 0.04 percent; silicon 0.02 to 0.06 percent; manganese 0.2 to 0.3 percent; sulfur and phosphor less than 0.08 percent. [Translator's note: This figure is not clear in the original; it is either 0.08 or 0.03.]

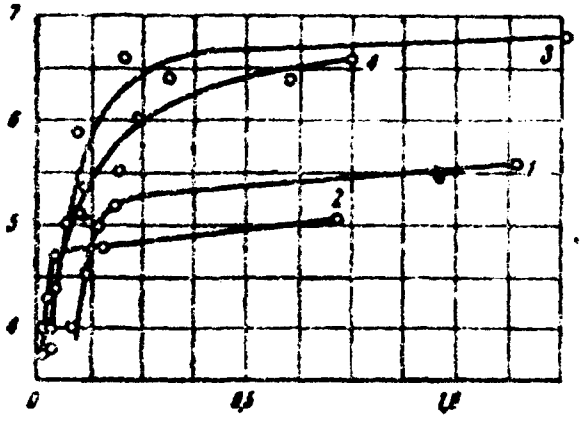

Figure 8. The dependence of the elongation of alloys, alloyed with molybdenum on stress after 250 hours of flow:
(1) Cr20Ni120; (2) Cr20Ni120Mo0.26;
(3) Cr20Ni120Mo0.67; (4) Cr20Ni120Mo1.25

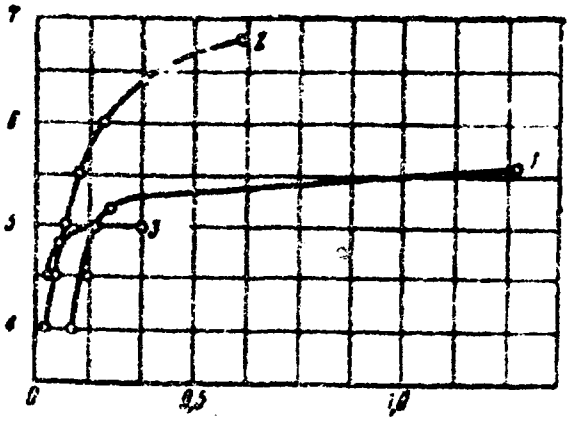

Figure 9. The dependence of the elongation of alloys alloyed with titanium on stress after 250 hours of flow:
(1) Cr20Ni120; (2) Cr20Ni120Ti0.095;
(3) Cr20Ni120Ti0.03

The testing of the alloys was conducted on TsKTI-2 machines (Central Institute of Boilers and Turbines). The specimens had a calculated length of 100 mm and a 10 mm diameter. The elongation was measured by means of an extensometer accurate to 1 micron. All tests were conducted at the same temperature of 700°, at various stresses.

The flow rate during the tests did not exceed $5 \cdot 10^{-3}$ percent per hour.

The elongation of all tested alloys after 250 hours of testing at various stresses was determined from the primary flow curves. Examining the curves given in Figures 8 and 9 we see that the Cr20N120 (without an admixture) is stronger at high stresses than the alloys containing 0.26 percent Mo or 0.03 percent Ti, but on the contrary, it is weaker in the regions of low stresses than the alloys with the mentioned admixtures, which is the same as in the case of aluminum alloys. A hardening of alloys over the entire investigated range of stresses is observed at a higher amount of alloying elements. A similar qualitative variation in the effect of small admixtures was revealed by I. A. Oding in ferrum-chromium-nickel alloys with additions of titanium by changing from low testing rates to high ones (4) and by varying the concentration of admixtures in steel (5). The hardening effect of small admixtures in our tested ferrum-chromium-nickel alloys in the regions of low stresses is more clearly pronounced than in aluminum alloys, since the elongation measuring technique made it possible to study more closely the region of low flow rates.

If we plot the dependence of the elongation of the Cr20N120 alloy on the concentration of molybdenum after a 250-hour test at various stresses, we will obtain the curves given in Figure 10.

Comparing the trend of the curves in Figure 10 with those for aluminum alloys (Figures 4-6), we see that the nature of the dependence of the elongation on concentration is the same.

This likeness in the behavior of the investigated alloys in flow in various stress ranges permits us to find a single treatment of the observed relationships.

Elongation, percent

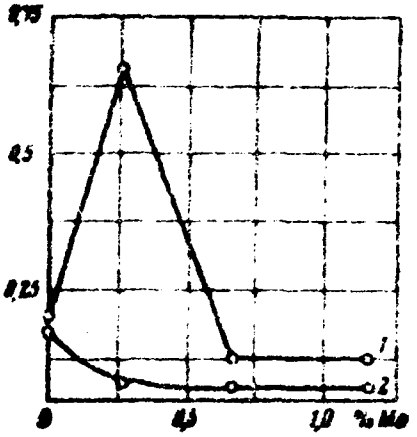

Figure 10. The dependence of elongation on the content of molybdenum in the Cr20Ni20 alloy after 250 hours of flow and stresses. (1) 5 kg/mm^2; (2) 4.5 kg/mm^2

Discussion of Results

The alloying of metal with admixtures forming solid solutions causes a strong variation in the resistance of the alloy to creep. Raising the amount of introducible admixtures will not produce a monotonous change in the properties.

A maximum variation in these properties is observed in the region of low stresses. In some cases this variation is so substantial that the properties of the metal are found to be changed in the direction opposite to the effect of the same element at all other concentrations. The inconsistency of the influence of the amount of the introducible alloying element becomes evident to a varying extent under various deformation conditions; in particular, it is observed in the flow of the alloys under the effect of high stresses.

The observed phenomenon is, obviously, associated with the nonuniform distribution of the admixture and with the difference in the distribution of the deformation over the grain of the metal under various conditions of strain.

The nonuniformity in the distribution of the

admixture in metals is inevitable, since the metals always have regions of rains with a distorted lattice (grain boundaries, slugs, individual distortions in the grain volume).

The appearance of foreign atoms in the distorted regions of the lattice may lead to its partial correction, while the appearance of the same atoms in the sound regions of the lattice may lead to its distortion. It is therefore possible to produce both hardening and resoftening of the alloy by varying the amount of the alloying element in the range of the relatively small concentrations.

The deformation proceeds irregularly in the various grain regions of the metal. The degree of irregularity varies with the conditions of strain. At high flow rates the main share of deformation falls onto the volume of the grain and the small share on to its boundaries. At low rates, the leading role is played by the local deformation along the grain boundaries. It is therefore natural that under various strain conditions the nonuniform distribution of the admixture in the metal will show on its properties to an unlike degree.

When the flow occurs under the effect of low stresses, the introduction of the first small amounts of the admixture will cause a reduction in the flow rate. This may be explained by the hardening of the grain boundaries, which is associated with the concentration of the admixture at the boundaries (1).

The irregular influence of the admixture on the behavior of the alloys is observed during the flow under the effect of high stresses. A certain content of admixture will cause a strong increase in the flow rate. This is, obviously, associated with the change in the properties of the very grains. This influence of admixture on the grain volume has already been observed in the region of relatively small concentrations.

BIBLIOGRAPHY

1. Hanson, D., and Wheller, A., J. Inst. Met., Vol. 55, 1931.

2. Medean, D., J. Inst. Met., Vol. 80, 1952.

3. Yakovleva, E. S., and Yakutovich, M. V.,

Reports of the Academy of Sciences USSR, 90, 1953.

4. Oding, I. A., "Vestnik mashinostroyeniya" (Herald of Machine Construction), No. 2, 1942.

5. Geeh, J. J., Iron and Steel Inst., Vol. 155, 1947.

* * *

The Influence of Small Additions of Titanium, Molybdenum, and Tungsten on the Mechanical Properties of Ferrum-Chromium-Nickel Alloys

By E. S. Yakovleva

This work gives an account of the results obtained from the study of the effect exerted by small amounts of solid-state soluble alloying elements on the mechanical properties of ferrum-chromium-nickel alloys at elevated temperatures. The investigation was conducted by the method of measuring the short-term and prolonged hardness.

It has been established experimentally that the usual hardness (H_u) is associated with the temporary hardness of the material by a simple relationship (1). But the lasting hardness (H_D) is, in the opinion of a number of researchers, qualitatively correlated with the characteristics of lasting toughness and creep. The correlation between the lasting hardness and these characteristics is mainly observed during accelerated tests -- but even so, not on all alloys (2-5).

We know that the distribution of plastic deformation over the grain volume is not uniform.

At high rates and elevated temperatures the deformation covers the entire grain volume, while at low rates it localizes to a considerable extent in the narrow boundary zone of the grains. Therefore, if the properties of the volume and grain boundaries are not alike, the accelerated testing, which reflects the properties of the grain itself, and a slow testing reflecting the properties of the grain boundary will yield strongly differing test results.

The alloying of the alloy with an admixture will cause a change in the properties of both the grains and their boundaries. It follows from the above that hardness and lasting hardness cannot give a comprehensive reflection of all the variations taking place in the metal during

alloying; they must, however, reflect the variation in the properties of the grain itself. The latter fact, as well as the rapidity with which test results on hardness were obtained, made it possible in this study to apply this technique for developing the influence of small admixtures on the mechanical properties of the grains of solid solutions. The hardness measurements were conducted on a lever-type instrument the diagram of which is given in Figure 1.

The specimen 1 is placed at the end of the traveling rod 2. The other end of the rod rests in a ball on the arm of the lever 3. The carriage with loads 4 travels over one arm of the lever and applies the load to the specimen. The other end of the lever rests on the indicating probe 5 which gives the indentation depth of the indentor. The indentor 6 has the shape of a cylinder with a pobedit* tip on one end. This end of the indentor comes in contact with the specimen; the opposite end rests against the lid 7 of the heat resistant tube which is rigidly secured to the frame. The thermocouple 8, which measures the temperature during the test, is inserted in the tube through a side hole.

The initial pressure, equal to 1.07 kg, is applied by the indentor to the specimen by the spring of the indicator 5 through the lever.

After setting the specimen, the heat-treatment furnace is moved down over the heat resistant tube. The lower end of the heat resistant tube is cooled by running water in order to protect the ball and the lever from the heat.

*Translator's note: "Pobedit" is the brand name of a hard alloy consisting of 71 to 97% tungsten carbide (Wc), 3 to 12% cobalt, and 5 to 21% titanium, and is equivalent to some of the American grades of carbide metals used for tips.

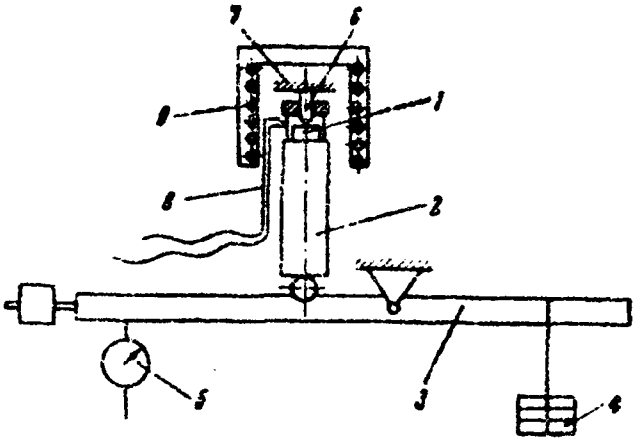

Figure 1. Lever-type instrument for measuring the hardness.
1 -- Specimen; 2 -- rod which holds the specimen; 3 -- lever;
4 -- carriage with load;
5 -- indicator probe; 6 -- indentor;
7 -- lid of heat resistant tube;
8 -- thermocouple; 9 -- furnace

The dimensions of the specimens were 10 x 10 x 5 mm or were the shape of a 5-mm thick disk with ϕ = 10 mm. The surface where the hardness was to be measured was preliminarily polished on paper No. 4/0. Two specimens were tested at each temperature; if there was a considerable spread between the hardness values, a third specimen was tested and the mean hardness value obtained.

The indentor tip had either the shape of a small ball with a diameter of 2.5 mm or of a blunt cone with a 90° span and a 0.97-mm curvature radius at the apex. The indentor had to be given this shape, since a sharper apex did not hold out the working loads: it failed. Of interest was not the hardness itself but its variation caused by the effect of the additions; we were therefore not necessarily interested in the absolute hardness values, and so were able to use an indentor of a nonstandard curvature. In order to eliminate distension and cracking while operating at 600 to 800°, the pobedit was submitted to a special chemothermal treatment.

The full-load magnitude was so selected that the immersion depth would not exceed 0.1 [?] of the specimen thickness, i.e., less than 0.5 mm deep. When a ball-type

indentor was used, the immersion depth was so selected as to have the indentation diameters within a range of 0.2 to 0.6 d (d is the diameter of the small ball); that is to say, the condition of a weak dependence of the hardness on the magnitude of load applied would be satisfied. The multiplying factor of the indicator had a 0.0031-mm immersion depth. The lasting hardness was determined after holding the specimen under a constant load for 60 minutes.

Test Results

Ferrum-chromium-nickel alloys alloyed with molybdenum (Table 1) were tested in two states: hardened from a temperature of 150° and then stabilized for one hour at 900°, i.e., in aged state. The test temperatures were in both cases the same: 500, 600, and 700°.

Table 1

The chemical composition of ferrum-chromium-nickel alloys alloyed with molybdenum, percent.

Cr	Ni	Mo	C	Si	Mn
18,60	37,20	0,25	0,043	0,16	0,27
19,83	35,50	0,60	0,048	0,05	0,22
19,00	35.10	1,30	0,028	0,26	0,25
19,20	35,10	0,00	0,023	0,18	0,27

Figure 2 gives the dependence curves of temporary hardness H_o, lasting hardness H_D, and the difference of $H_o - H_D$ on the content of molybdenum for both the stabilized and hardened states of these alloys. In the stabilized alloy, the addition of 0.25 percent Mo causes a substantial reduction of H_o and H_D at all testing temperatures.

The next addition of molybdenum, in the amount of 0.6 percent under the same conditions, has an opposite effect -- it hardens the alloy. A further raise of the molybdenum amount in the alloy causes some resoftening. The introduction of 0.25 percent Mo into the hardened alloy reduces the temporary hardness at all three temperatures and the lasting hardness at two (500 and 600°) temperatures.

At 700°, there is almost no variation in the lasting hardness with the concentration. The difference $\underline{H_0} - \underline{H_D}$ drops somewhat for both alloy states with the introduction of the first 0.25 percent addition of Mo. As we further raise the content of molybdenum in the alloy, there is almost no variation in the difference $\underline{H_0} - \underline{H_D}$. At 700° only the alloy in a stabilized state shows a small increase in creep with an increase of the molybdenum content in the alloy.

Examining the hardness curves of the alloys we arrive at the following conclusions.

1. A small addition of molybdenum in the amount of 0.25 percent softens the alloy, a larger addition of 0.6 percent and more hardens it.

2. The influence of alloying with molybdenum is more evident on alloys in a stabilized state. In hardened states, the process of aging which takes place during the deformation hides the effect of molybdenum. This can be observed particularly at high test temperatures (700°).

Ferrum-chromium-nickel alloys alloyed with titanium (Table 2) were tested in a hardened state at 500, 600, and 700° temperatures.

Table 2

The chemical composition of ferrum-chromium-nickel alloys alloyed with titanium, percent.

Cr	Ni	Ti	C	Si	Mn	S	P
21,24	40,11	0,06	0,06	0,25	0,15	0,008	0,008
20,56	40,24	0,30	0,05	0,44	0,17	0,006	0,012
21,04	39,58	0,57	0,06	0,38	0,25	0,008	0,008
20,04	39,85	—	0,05	0,13	0,17	0,007	0,015

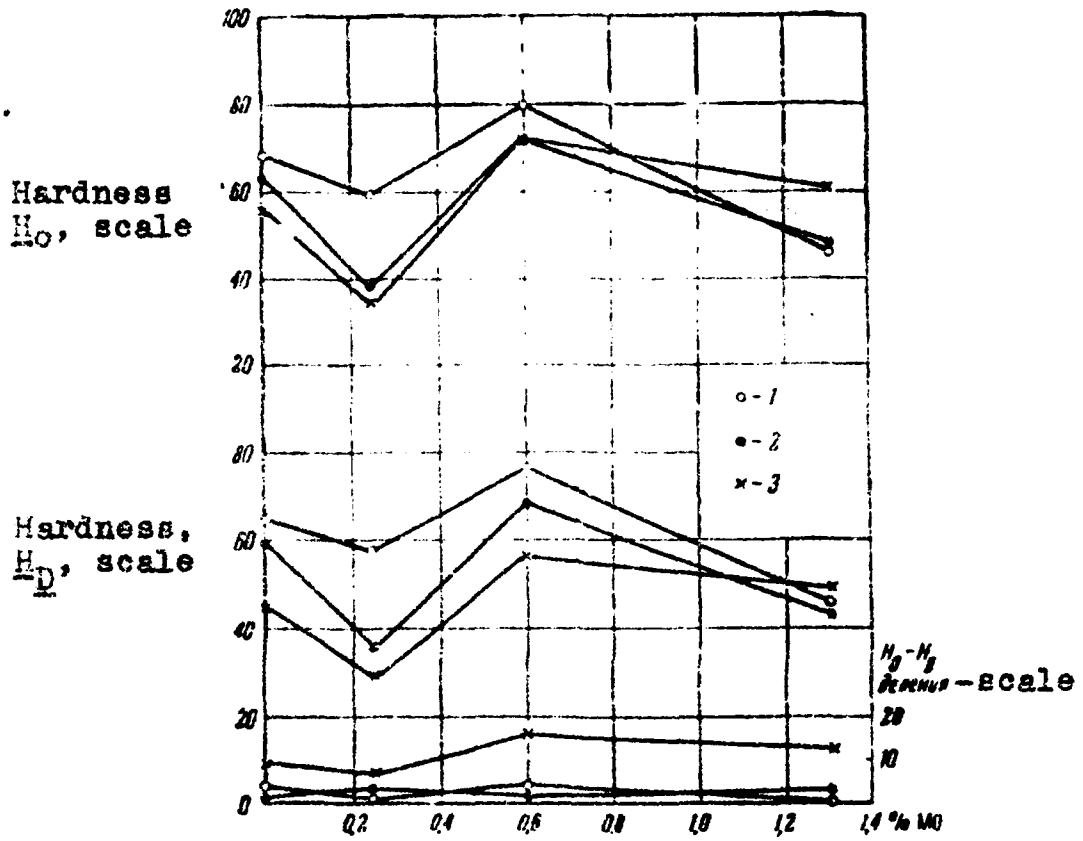

а

Figure 2. The dependence of hardness (H_O), lasting hardness (H_D), and the difference H_O - H_D of ferrum-chromium-nickel alloys in stabilized (a) states on the content of molybdenum; the following are the test temperatures:
1 -- 500°;
2 -- 600°;
3 -- 700°

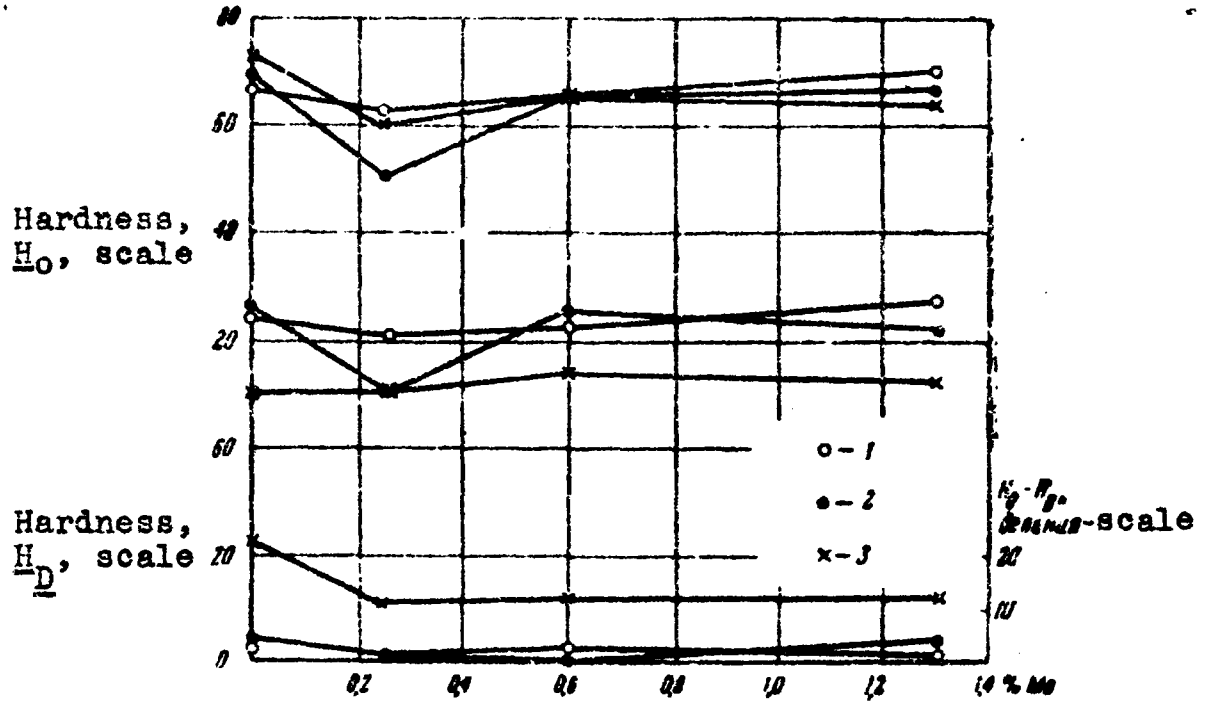

b

Figure 2. The dependence of hardness (H_O), lasting hardness (H_D), and the difference $H_O - H_D$ of ferrum-chromium-nickel alloys in hardened (b) states on the content of molybdenum; the following are the test temperatures:

1 -- 500°;
2 -- 600°;
3 -- 700°

Figure 3 gives curves for the dependence of temporary hardness H_o, lasting hardness H_D, and the difference $H_o - H_D$ on the content of titanium in the alloy. We can see from these curves that the addition of 0.06 percent Ti reduces both the temporary and the lasting hardness at all test temperatures.

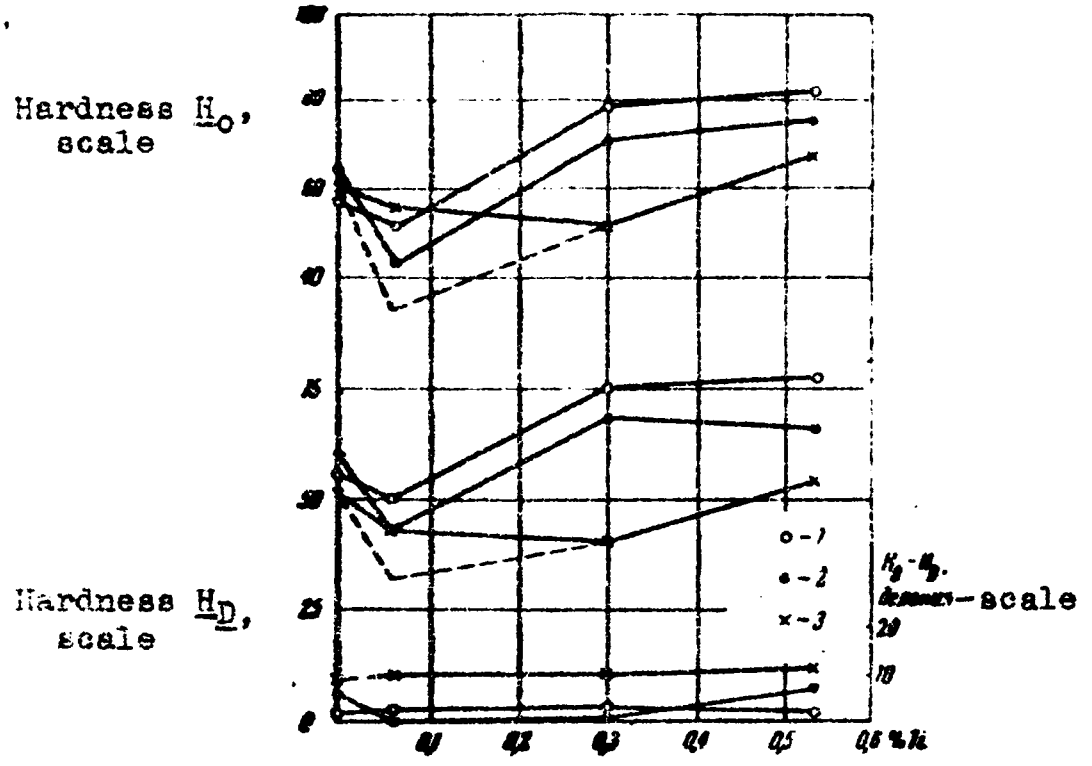

Figure 3. The dependence of hardness (H_o), lasting hardness (H_D), and the difference $H_o - H_D$ of a ferrum-chromium-nickel alloy in a hardened state on the content of titanium; test temperature: 1 -- 500°; 2 -- 600°; 3 -- 700°.

The next addition of 0.3 percent Ti hardens the alloy at 500 and 600° and slightly softens it at 700°. A further increase in the content of titanium up to 0.57 percent hardens the alloy at all temperatures.

The difference $H_o - H_D$ at 500 and 600° is very small in all tested alloys.

At 700° the flow of the alloy is more evident and has approximately the same rate at all concentrations. The value of $\underline{H_0}$ and $\underline{H_D}$ for the alloy containing 0.06 percent titanium, at 700°, was found to be higher than the hardness obtained at 500 to 600°; this is probably caused by the aging process taking place at this temperature.

Consequently, titanium influences the mechanical properties as follows:

1. A small addition of 0.06 percent Ti resoftens the alloy; all following additions harden it.

2. Alloys with titanium show almost no flow at 500 and 600° temperatures; the flow observed at 700° is approximately the same at all concentrations of titanium.

A similar variation in the effect of titanium and molybdenum was revealed in testing these alloys for creep*.

Table 3

The chemical composition of ferrum-chromium-nickel alloys alloyed with tungsten, percent.

Cr	Ni	W	C	Si	Mn
19,6	29,72	0,48	0,047	0,041	0,23
19,48	20,12	1,10	0,048	0,06	0,23
19,35	20,28	2,25	0,051	0,15	0,28
20,20	24,60	0,00	0,031	0,21	0,41

Ferrum-chromium-nickel alloys alloyed with tungsten (Table 3) were tested in a hardened state at 650, 700, and 750° temperatures.

*See the article by V. A. Pavlov, E. S. Yakovleva, and N. V. Yakutovich in this collection.

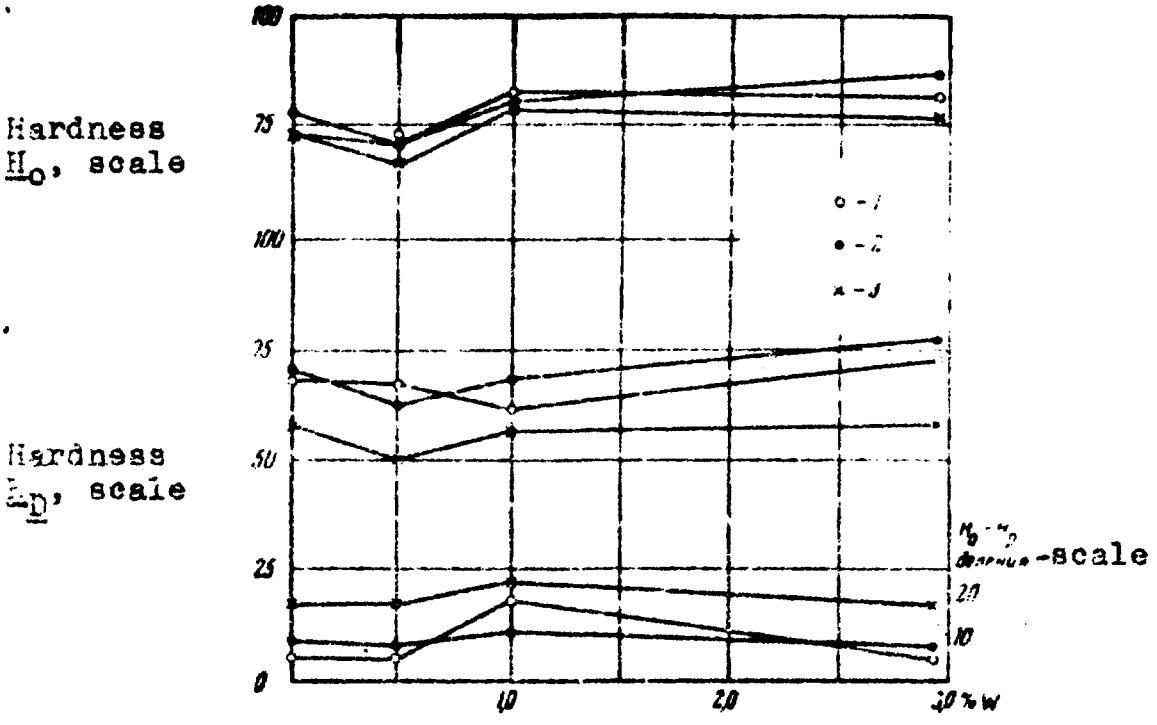

Figure 4. The dependence of hardness (H_o), lasting hardness (H_D), and the difference $H_o - H_D$ of a ferrum-chromium-nickel alloy in a hardened state on the content of tungsten; testing temperature:
1 -- 650°; 2 -- 700°; 3 -- 750°.

Figure 4 gives curves for the dependence of temporary hardness H_o, lasting hardness H_D and the difference $H_o - H_D$ on the content of tungsten.

We can see from the curves that tungsten added in small amounts somewhat resoftens the alloy; a further increase in the content of tungsten hardens it.

The difference $H_o - H_D$ varies little with the content of tungsten; it increases somewhat when the test temperature is raised.

Most probably, the trend of relaxation curves in the temperature range 650 - 750° is directed by similar effects of small amounts of tungsten; this has been

observed by Kolesnikov, Moiseyev, and Yakutovich* in relaxation tests of alloys of identical compositions.

Conclusions

1. The lasting hardness of ferrum-chromium-nickel alloys alloyed with small amounts of molybdenum, titanium, and tungsten have variations of an identical nature.

The first small addition of each of the investigated elements reduces the hardness -- resoftens the alloy; inversely, a subsequent increase in the content of admixture hardens it.

2. As had been expected, hardening effects of small additions on the grain boundaries were not observed with this technique.

BIBLIOGRAPHY

1. Davidenkov, N. N., Nekotoryye problemy mekhaniki materialov (Certain Problems of the Mechanics of Materials), Lenizdat, Leningrad, 1945.

2. Bochvar, A. A., Izv. AN SSSR, OTN (News of the Academy of Sciences USSR, Department of Technical Sciences), No. 10, 1947.

3. Mirkin, I. L., and Livshits, Plant Laboratory, No. 9, 1952.

4. Ginzburg, Ya. S., Plant Laboratory, No. 3, 1952.

5. Borzdyka, A. M., Metody goryachikh mekhanicheskikh ispytaniy metallov (Methods of Hot Mechanical Testing of Metals), Metallurgizdat (State Scientific and Technical Press for Literature on Ferrous and Nonferrous Metallurgy), 1955.

* * *

*See their article in this collection.

The Distribution of Deformation in the Grains of Aluminum and Aluminum-Zinc Alloys at Creep

By E. S. Yakovleva

V. A. Pavlov, E. S. Yakovleva, and M. V. Yakutovich have shown in their work* on a number of alloys that the introduction of small amounts of the alloying element into a solid solution will cause a strong variation in its flow rate; the variation of the flow rate is not monotonous with the concentration of the introducible admixture.

This nonmonotonous influence is most clearly evident at high flow rates. In such a case the effect of small concentrations of the alloying element often has a sign opposite to the effect of the same element at all other concentrations.

The authors associate this alloying influence with the fact that various grain regions change their share of participation in the deformation process as a result of the nonuniform distribution of the introducible element in the grain of the metal.

Our investigations were the first attempt at experimental detection of the variation in the distribution of deformation over the grain of the metal by alloying it with small admixtures soluble in the solid solution. We selected aluminum as the test metal and zinc as the alloying element.

We had previously studied in detail the creep of aluminum-zinc alloys in a wide range of concentrations of the solid solution (from 0.02 to 1.7 percent Zn). The investigation showed that alloying of aluminum with zinc in an amount of 0.02 percent hardens the alloy at all tested flow rates. However, introducing zinc in the amount of 0.08

*See their article in this collection

percent markedly resoftens it at high flow rates and causes a relative resoftening of the alloy at medium flow rates. And so the present work takes as its object of study aluminum 99.99 percent pure and both alloys indicated. It is known that deformation in the grain of the metal is not uniform. Slippage traces, twinning, plasticity, and displacements along the grain boundaries are the localization sites of deformation. Both the nature and degree of localization of deformation of the metal vary with the variation in the conditions of strain. Thus, for instance, clearly pronounced rectilinear slippage traces lose their rectilinearity and denseness with the increase in temperature and reduction in deformation rate. At sufficiently high temperatures and low flow rates, the slippage traces disappear altogether, but then the displacement over the grain boundaries becomes clearly pronounced (1).

We have studied the distribution of deformation in the indicated materials after their flow at 250° at rates of 10^{-1} to 10^{-3} percent per hour.

The origination of local deformation in the metal grains is accompanied by clearly pronounced fractures appearing on the bright surface of the metal. We can therefore judge to some extent the nature of distribution of deformation in the grain of the metal by the surface contour of the specimen. It is difficult to trace the details of the distribution of deformation by a simple microscopic observation of the surface of the deformed specimen. A closer study of the distribution pattern of the deformation in the grain can be made by using the interference method. This method was repeatedly employed to study the surface of deformed specimens. It makes it possible to give a qualitative as well as a quantitative evaluation of the distribution of deformation in the grain (2, 4).

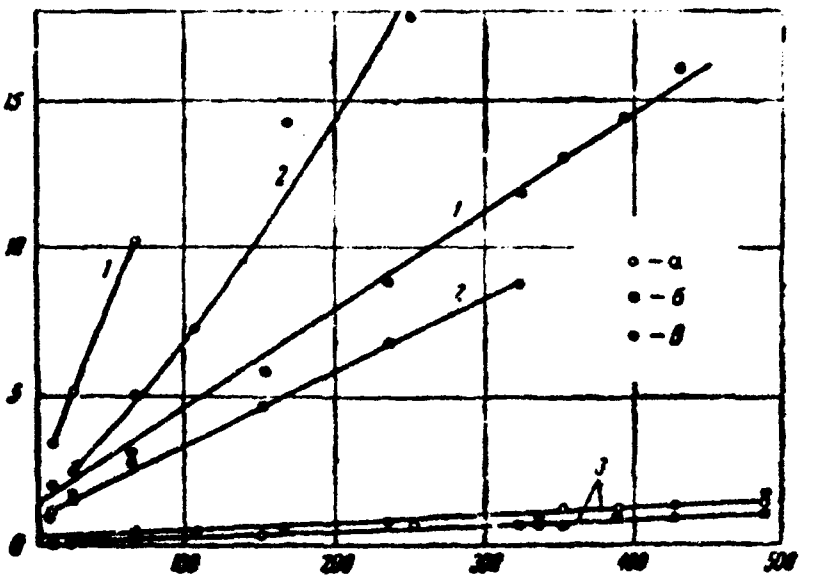

Figure 1. Flow curves of aluminum and the two of its alloys with zinc at stresses:
1 -- 500 g/mm^2; 2 -- 400 g/mm^2;
3 -- 200 g/mm^2 (a -- aluminum without zinc; b -- 0.02 percent Zn;
c -- 0.08 percent Zn).

We used for this study the Linnik interferometer, type IZK-2, with a 150X magnification. The observations were conducted in white light. On the undeformed surface of the specimen the interference lines (fringes) had the appearance of a pack of parallel straight lines. The direction of the strips and the distance between them varied with the appearance of some roughness on the surface of the specimen. The formation of a steplike surface produced a sharp displacement of the strips (fringes). Following further the course of the fringes into the grains of the deformed metals, we have attempted to get an idea of the nonuniformity in the distribution of deformation in them.

The tested specimens had the shape of strips measuring 50 x 2 x 1 mm. Prior to deformation, one wide side of the specimen was polished, and afterwards the

Specimen was annealed to recrystallization, after annealing, the polished surface of the specimen showed no marked orientation. The mean of grain diameter had an average linear size of 2 mm. The annealed specimens were secured in the chuck of the testing machine and then stressed under the effect of a constant load at room temperature. The flow curves of the tested specimens are given in figure 1. The specimens were periodically unloaded and transferred to the interferometer stage for the study of the surface contours.

Observations results

Figure 2 gives the photographs of the surface of the aluminum specimen subjected to flow at a stress of 200 kg/mm^2 at a rate of 2.5×10^{-3} percent per hour in various phases of the elongation. The direction of elongation is indicated on the figures by arrows. The photographs show the following:

Figure 2. The surface of aluminum tested at a stress of 200 kg/mm^2 and at the following elongations:
a -- 0.45 percent;
b -- 1.41 percent; c -- 1.77 percent.

Figure 3. The surface of aluminum tested at a stress of 500 g/mm^2 and a 3.4 percent elongation.

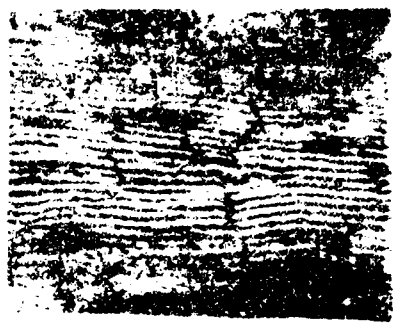

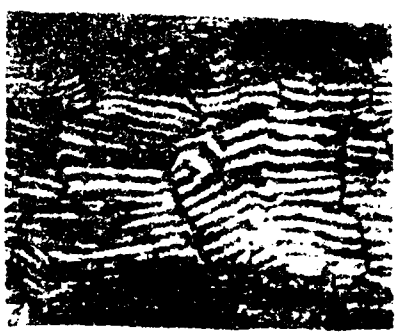

Figure 4. The surface of the aluminum-zinc alloy, containing 0.02 percent Zn, tested at a stress of 200 g/mm^2 at various elongation phases:
a -- 0.39 percent;
b -- 1.07 percent;
c -- 1.74 percent.

Figure 5. The surface of the aluminum-zinc alloy, containing 0.02 percent Zn, tested at a stress of 400 g/mm^2.

1. Under these conditions, the deformation is accompanied by the development of the grain boundaries, which appear in the form of thin black lines on the polished surface of the specimen. The interference lines (fringes) become displaced parallel to each other. The displacement increases with the extent of deformation. Consequently, at the grain boundaries, the grains become displaced with respect to each other. Besides, at a high degree of deformation the interference lines change their direction as they cross the grain boundaries. This means that the grains not only undergo displacement but also reciprocal rotation.

2. Within the grains, at low deformations the interference lines continue as a parallel pack; that is, if the deformation does occur in the grain, it occurs quite uniformly. As the deformation increases, both the distance between the strips and their direction in the various grain regions become different. This indicates that the deformation in the grain volume occurs unevenly.

In tests conducted at much higher stresses (400 and 500 g/mm^2), the specimens had considerably higher flow rates (on the order of 10^{-2} and 10^{-1} percent per hour); the initial elongation phases were therefore not studied. The surface observation of the specimen began with a 3.4 percent elongation (Figure 3).

We see from these figures that the contour of the surface is here considerably rougher than in the specimens deformed at a lower rate. It is possible that this is caused by the high degree of deformation. However, the nature of the distribution of deformation is still the same as before. We can see along the grain boundaries the reciprocal displacement and turn of the grains; within the grain, the deformation is distributed unevenly. At even greater deformations, the surface contour becomes so rough that its study by means of the interference lines becomes impossible.

Figure 4abc gives photographs of the surface of the aluminum-zinc alloy specimens, containing 0.02 percent Zn, at various elongation phases and at a stress of 200 g/mm^2. This alloy had a somewhat slower flow rate (by 30 percent) than that of pure aluminum. We see from the figures that this alloy (like aluminum) had a local deformation along the boundaries and a reciprocal turn of the grains. As for the deformation inside the grains, we can say that if it does occur, it is quite uniform over the volume. At any

rate, it is more uniform than in aluminum (see Figures 2c and 4c).

The same can also be said about the specimens of this alloy (Figure 5) elongated under the effect of much higher stresses (400 and 500 g/mm^2). True, the distribution of deformation in the grain is nonuniform, but it still is less than that in pure aluminum (see Figures 3 and 5).

A test was run on two specimens of an alloy containing 0.08 percent Zn. Their flow rates were close to those of pure aluminum. The distribution pattern of deformation in the grain differed somewhat from those observed in the earlier tested materials. Figure 6abc gives a specimen in which the difference was more sharply pronounced.

In the initial deformation stages the outlines of the grain boundaries were very weak (Figure 6a). As the deformation rose, the deformation along the grain boundaries increased but remained less than that in aluminum and in the alloy containing 0.02 percent Zn (see Figures 2c and 6c). There was a reciprocal turn of the grains near the boundaries but the turning angle varied in different regions of the grain. The interference line inside the grains were highly distorted (not less than those on the grain boundaries). All this indicates that the grain underwent a substantial deformation, unevenly distributed over the volume.

This alloy was also tested at a much higher stress, equal to 400 g/mm^2. Its flow rate under these conditions was higher than that in aluminum and in the alloy with 0.02 percent Zn. The study of its surface was conducted only at small deformations. Besides, the grain of the tested specimens was very uneven in size. These circumstances made it impossible to draw definite conclusions on the nature of distribution of deformation in the grain of the alloy at a higher flow rate.

It is obvious from the foregoing that we have made the most thorough study of the distribution of deformation in the grain of the metal during its flow under a 200 g/mm^2 load. The results of this investigation amount, briefly, to the following.

The grains of aluminum at a flow rate of the order of 10^{-3} percent per hour deform unevenly. A local plastic deformation occurs at the grain boundaries increasing with

elongation of the specimen. The deformation inside the grain occurs without visible slippage traces. At the initial elongation stages it is evenly distributed over the grain volume and is, probably, small in absolute magnitude. At high degrees of elongation, various grain regions undergo deformations different in magnitude.

The alloy, alloyed with 0.02 percent Zn, flows slower (by 30 percent) than pure aluminum; consequently, this addition causes the hardening of aluminum.

There are no variations in the extent of localization along the grain boundaries, and in the grain volume the deformation is more evenly distributed than in aluminum. It follows from this that the introduction of zinc in the amount of 0.02 percent hardens both the boundaries and the volumes of the grains.

Figure 6. The surface of the aluminum-zinc alloy, containing 0.02 percent Zn, tested at a stress of 200 g/mm² at various elongation stages:
a -- 0.39 percent;
b -- 1.41 percent;
c -- 1.75 percent.

The alloy containing 0.08 percent Zn flows faster than that containing 0.02 percent Zn. Its flow rate is close to the flow rate of aluminum. Thus, this alloy is found to be resoftened in comparison with that containing 0.02 percent Zn. This behavior of the alloy is accompanied by a change in the distribution pattern of deformation in the grain of the metal. The local deformation along the grain boundaries is considerably lower, whereas the nonuniformity in the distribution of deformation in the grain is higher than in the alloy containing 0.02 percent Zn and in that of aluminum. Consequently, the increase in the flow rate occurs at the expense of the higher deformation of the grain volume. The boundaries remain hardened and, most probably, to a higher extent than in the alloy containing 0.02 percent Zn.

Conclusions

A relationship has been established between the variation in the properties of aluminum caused by its alloy with zinc and the distribution of deformation in the grain of the alloy. The observed dependence makes it possible to draw certain conclusions on the nature of the variation in the properties of the grain of aluminum by alloying it with zinc.

1. The first small addition of Zn (0.02 percent) causes a reduction in the flow rate without a noticeable change in the extent of localization of deformation along the grain boundaries. Since we know that, at low flow rates (on the order of 10^{-3} percent per hour), a substantial share of deformation is localized along the grain boundaries, the observed reduction in the flow rate may be mainly caused by the zinc, which hardens the grain boundaries.

2. The next addition of zinc (0.08 percent) causes an increase in flow rate accompanied by a reduction in the extent of localization at the grain boundaries and by an increase in the nonuniformity of deformation inside the grain. This nature of variation in the distribution of deformation with a simultaneous increase in the flow rate of the alloy indicates the hardening process which takes place in the volume of the grain.

BIBLIOGRAPHY

1. Yakovleva, E. S., and Yakutovich, M. V.,

Reports of the Academy of Sciences USSR, 90, No. 6, 1953.

2. Kurnosov, D. G., Tronina, N. M., Yakutovich, M. V., Journal of Technical Physics (ZhTF), 18, Issue 2, 1948.

3. McLean, D., J. Inst. Metals, Vol. 80, 1952.

4. McLean, D., J. Inst. Metals, Vol. 83, 1954.

* * *

The Set-Up for Testing the Relaxation of Stresses at Elongation

By V. S. Averkiyev, G. N. Kolesnikov, A. I. Moiseyev, and M. V. Yakutovich

I. General Requirements for Testing the Relaxation of Stresses

In order to make an experimental study of net relaxation we must be able to:

(1) preset, and maintain, a certain definite deformation of the specimen;

(2) observe and record the variation in the force acts upon the specimen;

(3) maintain to a certain accuracy the temperature assigned for the specimen.

The relaxation of stresses can generally be observed below the elasticity limit as well as above it. It is more difficult to maintain the constancy in the length of the specimen in the region of elastic deformations on account of their small size (on the order of 0.01 to 0.1 percent). Assuming that the permissible measurement error in the elastic region is 1 percent, it will thus follow that we must maintain the deformation to an accuracy of 0.0001 to 0.001 percent, and maintain the temperature ranges of the specimen such that the variation in its dimensions caused by thermal expansion remains within the permissible variation limits of the specimen dimensions. Consequently, the temperature of the specimen must be maintained accurate to 0.1 - 1° C.

The set-up for tests on relaxation of stresses must include the following basic elements:

(1) a loading system which provides the necessary deformation (initial stress acting upon the specimen);

(2) a system providing the maintenance of the assigned

deformation of the specimen during the experiment;

(3) a system which permits the measuring (either directly or indirectly) of the variation in the load acting upon the specimen (automatic registration of the variation in load is desirable in due course);

(4) systems which produce and maintain the temperature at the preset regime during the experiment.

Naturally, in an actual set-up for tests on relaxation stresses, individual structural parts and assemblies may be components of other systems. Thus, for instance, the spring may be used simultaneously as a part of the loading and measuring systems as well as of the system providing the maintenance of the preset deformation.

The above classification of elements covers various set-up designs for tests on relaxation of stresses. For instance, in the widely used tests of the relaxation of stresses in the ring of equal resistance to bend (I. A. Oding (1, 2)), the wedge acts as the loading system as well as the system which maintains the preset deformation. The measuring microscope is a system enabling the indirect measurement of stresses. Finally, the tubular furnace serves as a system which presets and maintains the temperature.

Our further report will deal only with the method of testing relaxation of stresses at elongation.

II. A General Study on the Performance of the Individual Elements of the Set-Up for Tests on Relaxation of Stresses

A rational system of the individual elements of the set-up can be selected after a detailed study on the performance of these elements*.

1. Loading system

The loading of the specimen can be accomplished by various methods: such as a spring, a traveling load, a variable load, a hydraulic press, etc. The basic condition

*Some useful recommendations can be found in the study by Shevenar (3).

for conducting the test on relaxation of stresses is maintaining constant deformation of the specimen after its loading to a certain initial stress σ_0. In the process of testing, the load acting upon the specimen must be reduced in due course. It is desirable to simultaneously utilize the loading system for measuring the variation in the magnitude of the load in the process of testing. At this point the system is presented with a number of additional requirements; in particular, it must be connected with a mechanism controlling the variation in the deformation of the specimen and directing the variation in the load acting upon the specimen.

In designing the loading system, the following general requirements must be met:

(1) the functional diagram must be very simple;

(2) the system under prolonged operation must be reliable;

(3) the variation in load magnitude must be smooth (not jumplike);

(4) the readings in the load-measuring instrument must be sufficiently accurate and sensitive;

(5) the variation range for the stresses and deformations assigned for the specimen must be sufficiently wide;

(6) there must be freedom of operation of the components of the system with respect to the temperature and properties of the tested material;

(7) the highest unloading rates must be attained;

(8) there must be a simply functioning connection between the shifting of any loading point and the load (a linear or close-to-linear connection is desirable). This connection must be independent of the properties of the specimen and the material of the loading system as well as of the room and specimen temperatures.

These conditions are more than anything else met by the application of the traveling load or the spring. The hydraulic loading method which is widely used in the machines that test static elongation is not suitable for this purpose because of its unreliability under the

conditions of prolonged operation (4), the jerky nature of the variation in loading (4), and the difficulty of carrying out the loading at high rates under the conditions of the test on relaxation of stresses.

The traveling-load loading system

The system with the traveling load moving along one of the levers of the loading system is of special interest for measuring the stresses; in principle, it can provide high loading rates extremely necessary in the initial period of relaxation. The deficiency of the system, however, is that it cannot be used as an unloading system.

In loading with a traveling load, its mass (consequently, also the motor capacity, which moves the load) will depend on the preset maximum load of the specimen and on the gear ratio of the lever system. If the maximum load is preset, the reduction in the weight of the traveling load will increase the gear ratio of the lever system; this is advantageous in the sense of reducing the weight of the traveling load and facilitating its travel, but it is not advantageous in this sense: that it increases the angle of inclination of the lever with the load. In fact, if one end of the specimen is secured, and the effect of the load, which travels over one of the levers of the system, is transmitted to the other end of the specimen, then the lever with the load must inevitably assume an inclined position in the process of loading, as a result of the variation in the length of the specimen; this position will remain constant in the procedure of the test itself.

When the machine is operated in the elastic deformation regions of the tested material the inclination angles of the lever with the load will not be too great; however, in the plastic deformation regions of the specimen, these angles will be great (Table 1).

Table 1

The angle of inclination of the lever measuring 300 mm with the load at various deformations of 100-mm long specimens (in degrees)

The arm ratio of the levers	At an elastic deformation of the specimen, equal to 0.1%	At a plastic deformation of the specimen, equal to 2%
1 : 100	2	42
1 : 1000	20	>90

The quantity $>90^{\circ}$ indicates that it is impossible to assign for the specimen a deformation equal to 2 percent at the given correlations between the parameters.

This rough calculation is made under the assumption that the specimen is 100 mm long and the length of the load carrying arm of the lever is 30 cm (for structural reasons, the use of long arms is inexpedient).

It follows from the above discussions that a traveling-load loading system (having one end of the specimen hinged) will not allow the presetting of a high deformation in the plasticity region of the specimen. Consequently, this system is useless for operating in the region of high initial deformations.

However, in the case of small deformations the traveling-load design can be used simultaneously for both loading and measuring the variation in the load in the process of testing. In the case of high deformations, this design can be used only as an element of a system which measures the load and maintains constant deformation; in this case the initial loading of the specimen requires an independent mechanism.

Loading system with a spring

Loading by means of a spring is simple in principle but causes great difficulties if relatively high rates of loading and unloading are needed. (In particular, an

increase in rate requires an increase in motor capacity, strongly complicates the commutation of electrical circuits, etc.)

The variation in the elastic properties of springs, usually occurring in time, can be reduced by a preliminary aging of the spring material.

The variation in the stiffness of the springs under the influence of the variation in the room temperature by 10° C is relatively small -- on the order of several decimal fractions of one percent.

The great advantage of a loading system with a spring is the possibility of using it simultaneously for both measuring the load and maintaining the preset deformation constant.

We will henceforth discuss only this system and for convenience will use the term "loading system" without each time emphasizing its dual designation.

Selecting the dimensions of the specimen

The determination of the dimensions of the specimen is the starting point in the construction of the testing machine; all things considered, the fundamental data of the machine such as the overall size, etc., depend on those dimensions. In selecting the specimen dimensions we must proceed from the most favorable combination of several conditions. On the one hand, it is desirable that the length and the diameter of the specimen be large. The longer the the specimen, the easier it is to maintain constant deformation to an assigned accuracy. The greater the cross-sectional dimensions the more crystallites there are per cross section of specimen. Consequently, there is less (macroscopically) nonuniformity of the specimen and better reproducibility of test results.

On the other hand, it is perhaps advantageous to have the length and diameter of the specimen smaller: the smaller the specimen dimensions, the easier it is to maintain the assigned temperature and to adjust it according to the length of the specimen, the smaller the overall size of the furnace and the machine as a whole, the simpler the production technology of the specimens, the less the consumption of material necessary for the preparation of the specimens, etc.

The maximum load of the machine depends on the properties of the material in the strongest specimen and on its cross-sectional area. The length of the specimen defines the dimensions of the heat-treatment furnace, which, in turn, determines the dimensions of the machine.

The bracing of the specimen can be accomplished by three methods; namely, by the application of: (1) a head with a screw thread; (2) a head with a flat bearing surface; and (3) a tapered head. The dimensions of the heads for the specimens are determined from the condition of resistance to warping of the bearing surfaces. At one and the same permissible warping stress the diameter of the flat head is twice as large and the diameter of the tapered head is half as much again as the diameter of the head with the screw thread. The dimensions of the heads for the tractive forces will depend on the dimensions of the specimen heads. It is not to our advantage to increase the diameter of the specimen head, since this will lead to the increase in the heat transfer by the ends of the specimen and will create conditions unfavorable to its heating. Besides, a specimen with a small working diameter and a large head diameter is not economical in preparation.

Centering the specimen

To obtain a uniaxial stressed state in the case of uniaxial elongation it is necessary to completely eliminate the appearance of bend caused in the specimen by the application of the load.

The reduction in the magnitude of eccentricity of the load is usually accomplished by two methods: (1) maintaining the highest possible accuracy in the fabrication of the individual parts of the system which transmits the stress to the specimen; and (2) using special devices for centering the specimen; these devices come in various types (4, 6). The Hooke hinge and the spherical bearing are not very reliable for operating at elevated temperatures; consequently, they cannot be placed into the heating space of the furnace. In case they are used, they must be situated as close as possible to the specimen heads, i.e., next to the ends of the furnace.

Load reduction variants

The reduction of the load which is necessary for main-

taining constant the length of the specimen, can be accomplished in two variants:

(1) alternately reducing and increasing the load on the specimen within certain permissible limits; or (2) reducing the load in small steps.

The machine which employs the first variant records more fully the behavior of the specimen during the test, noting occasional variations in the working temperature of the specimen as well as variations in the specimen dimensions which result from the reduction of its length (for instance, phase transformation which occurs with the reduction in volume). However, with this variant the operation of the electric motor is very difficult.

The second variant greatly aids the operation of the electric motor but has a substantial drawback. If the dimensions of the specimen decrease, this decrease cannot be recorded on the diagram: the diagram will have the form of a horizontal straight line. Besides, when the working temperature of the specimen increases, the diagram will show a drop, which will not disappear even after a normal temperature has set in (consequently, this may be misinterpreted as a drop in stress).

These considerations speak in favor of the first variant for maintaining the length of the specimen.

Selecting the electric motor

The selection of the type and capacity of the electric motor depends on many factors: the maximum load, the gear ratio, maximum rates of loading and unloading, efficiency of transmission, magnitudes of permissible overloads of the motor in starting regime, duration of starting, adopted operating variant of the machine, reversal circuit and one-directional duration circuit (in case of an electrical reversal). In the latter case, a motor with two rotors and two independent stator windings is preferred.

Since the rates of relaxation during one experiment vary within wide limits, it is preferred that the motor be equipped with a gear-box transmission. It is also desirable to have a variable loading rate to determine its influence on the process of stress.

2. The system which maintains the preset deformation of the specimen

The system which maintains the preset deformation of the specimen is the most important unit of the relaxation machine. The following relatively independent parts may be singled out:

(1) a device which picks up and increases the deformation of the specimen (deformation amplifier);

(2) a device which sends electrical pulses to a relay system should the dimensions of the specimen deviate from the preset value (pulse transmitter system);

(3) a relay system which controls the electric motor of the loading system;

(4) loading system.

The set-up for measuring relaxation stresses can be considered as a closed self-oscillating feedback system (3). This opinion follows from studying the above variant for maintaining constancy in the deformation of the specimen by means of variable unloading and loading. The amplitude of self-oscillations is half the difference between the limits within which the length of the specimen (or the load which acts upon the specimen) varies. The lower these limits are, the more accurately is the length of the specimen maintained and the closer the conditions of testing are to net relaxation. Consequently, we must tend to reduce the amplitude of self-oscillations.

It can be expected that the following factors will influence the amplitude of self-oscillations:

(a) the rigidity of the components of the deformation amplifier;

(b) the sensitivity of the pulse transmitter system;

(c) resistances (friction, "sticking" of the contacts in the pulse transmitter) and the inertia of the individual components of the deformation amplifier;

(d) operating time of the pulse transmitter system and the relay system;

(e) loading and unloading rates;

(f) time necessary to establish the preset loading (or unloading) rate after receiving the switching pulse;

(g) rigidity of the elements of the loading system;

(h) inertia of the moving parts of the relaxation machine; and

(i) friction force in the connections of the loading system.

As the rigidity of the elements of the deformation amplifier is increased, the magnitude of elastic deformation of these elements necessary to create the force sufficient to overcome the resistances and produce the switching of the contact which controls the relay system decreases. The increase (or decrease) of the specimen length (speaking in approximate terms) continues until the contact is switched over. It follows from this that the reduction in the elastic deformation of the elements of the deformation amplifier (and, consequently, the increase in their rigidity) leads to the reduction in the amplitude of self-oscillations.

The increase in the sensitivity of the pulse transmitter system will also lead to a reduction in the elastic deformation of the components of the deformation amplifier and, consequently, to the reduction in the amplitude of self-oscillations. Although the resistance in the deformation amplifier (friction, "sticking" of the pulse transmitter contact) is small, it does, however, exert a great influence on the amplitude of oscillations of the length of the specimen. This is caused by the fact that the forces which the individual parts of the deformation amplifier exert upon each other are also small; as for the displacement of these parts with respect to each other, they are quite insignificant.

It is easy to see that the decline in resistance in the deformation amplifier will also lead to a reduction in the amplitude of oscillations of the dimensions of the specimen. The reduction in the operating time of the relay system acts in the same direction.

Generally speaking, the increase in loading and unloading rates results in the increase of the amplitude of self-oscillations. For instance, this will occur when the

operating times of both the pulse transmitter and the relay systems remain constant.

The other factors are evident to a much lesser extent. For instance, the time gap in establishing the loading (or unloading) rate after switching has a relatively little effect on the magnitude of the amplitude of oscillations in the dimensions of the specimen. We must, however, strive to reduce this time gap since its reduction will lead to a reduction of the total time gap between two successive loading (or unloading) phases, which will enable us to record more accurately the details of the relaxation curve.

As for the other three factors enumerated above, their role is practically negligible, inasmuch as the rates of the individual elements of the loading system under test conditions are low. These three factors, basically, influence the magnitude of the loading and unloading rates.

It follows from the above that in order to reduce the amplitude of self-oscillations at a preset loading-unloading rate, i.e., to increase the accuracy of maintaining the deformation, we must, on the one hand, reduce to a minimum (1) the resistance in the deformation amplifier and (2) the operating time of both the pulse transmitter and the relay systems; and, on the other hand, increase to a maximum (1) the rigidity of the components of the deformation amplifier and (2) the sensitivity of the pulse transmitter system. In other words, at a preset loading-unloading rate we must tend to reduce the total time gap between two successive loading (unloading) phases. However, reducing this time gap will place a burden upon the operating conditions of the relay system (particularly, the relay contacts) and the electric motor, which, being frequently switched will operate most of the time under starting regime conditions.

Let us dwell at some length on the analysis of the operating conditions of the individual elemonts of the system which maintain the constancy in the deformation of the specimen.

It should be noted, first of all, that the structure of the deformation amplifier must warrant the pick-up by the amplifier of only a deformation caused by the net elongation of the specimen, excluding, as far as possible, that share of deformation which is caused by the unavoidable bending at the elongation of the specimen.

The task of the deformation amplifier is to intercept the small specimen deformations; it is therefore necessary that the dimensions of the components of the deformation amplifier vary as little as possible during the test. The variation in the dimensions of the components of the deformation amplifier may occur as a result of: (1) thermal expansion, caused by the variation in the temperature of the components; (2) their plastic deformation; and (3) phase transformations taking place in the material of the component as the result of the variation in volume.

With respect to tht thermal conditions of the operation, all components of the deformation amplifier may be classified into two groups: (1) components operating in high-temperature regions; and (2) components operating at room temperature.

The influence of thermal expansion on the components operating in the high-temperature region can be reduced by using materials with lower coefficients of linear expansion and by increasing the accuracy in maintaining the temperature in the furnace. For the components operating at room temperature we can, apart from using material with low coefficients of linear expansion, in some cases also use compensating systems with materials of different coefficients of expansion. However, devices of the latter type will operate properly only at slow variations in temperature.

We can reduce the plastic deformation of the components by selecting an appropriate material as well as by a rational selection of shape and cross section with a view to reducing the specific forces (stresses). The problem of eliminating phase transformations in the components during operation can be solved by selecting the material.

Provisions must be made in the structure of the deformation amplifier for a simple and easy compensation for the variation in the length of the specimen, which is caused by the thermal expansion of the specimen during heating, its deformation in the process of loading, and errors made in preparing it.

The pulse transmitter system can be accomplished in several variants, such as electrical contact systems (fixed contact, slide contact, and mercury contact), systems with a capacitor, systems with a phototube, etc.

The most important factors in selecting a pulse transmitter system are: (1) sensitivity (the least variation in

the deformation of the specimen which leads to actuation) of the pulse transmitter system; (2) simplicity in making this system; (3) its reliable effect at prolonged operation.

If the accuracy in maintaining the deformation of the specimen is preset, then by increasing the sensitivity of the pulse transmitter system we reduce the amount of deformation to be increased by the amplifier.

The simplest transmitter system is composed of circuits employing a contact. In this case, the most important factor is the reduction in the output of the current switched off (or switched in) by the transmitter contact. A reduction in current increases the reliability of operation and sensitivity of the system and reduces the resistance ("sticking" of contacts) in the increaser of deformations.

The diagram of the relay system, which controls the electric motor, can be fully specified after both the pulse transmitter system and the capacity of the motor have been selected, and the operation time of the relay system is assigned.

3. The recording of diagrams

The diagram can be recorded by either joined broken lines or steps, depending on the variant selected to maintain the constancy of deformation. If the time scale is small, these broken lines will blend into one continuous curve of a definite width. This curve may have zigzags, i.e., deviations from an even ("smooth") course. The degree of perfection of the diagram (line width, absence of zigzags, etc.) is defined by: (1) the stiffness of the loading spring; (2) accuracy of maintaining the deformation; (3) operating reliability of the relay system, the deformation amplifier and the pulse transmitter system; (4) the degree of constancy in the temperature of the specimen; and (5) the influence of external vibrations on the operation of the pulse transmitter.

The relaxation diagram may be recorded by various means, such as photographic recording, pencil, pen, etc. The simplest and most reliable means of recording is either a pencil or a pen with ink. The photographic recording has a substantial drawback, which is rooted in the impossibility of observing the course of the curve during the test.

In order to conduct the tests in a wide range of initial loads it is desirable to use several scales in recording the stresses. Since the relaxation rate eventually drops, it is also necessary to have several scales in recording the time.

To reduce the harmful effect of outside vibrations on the clearness of the recording, provisions must be made for a shock-absorbing device; the influence of vibrations must also be taken into consideration when designing the increaser of deformations and the pulse transmitter.

4. The system which produces and maintains the temperature

The system which produces and maintains the temperature consists of two basic elements: (1) a temperature-producing device (furnace); and (2) a temperature-maintaining device (thermocontroller).

A detailed review of heating devices has been made by A. M. Borzdyka (7); the study produced the conclusion that the best heater is an electrical-resistance furnace.

Particular attention must be given to producing an identical temperature for the entire volume of the specimen, since some of the regions of specimens under different temperature conditions will relax to different degrees. The primary means of obtaining such a distribution of temperature are: (1) using furnaces which are (in comparison with the specimen) several times (3 to 4) longer than the specimen; and (2) using a system of unit-type heating coils with individual controls.

To mount the specimen we must either remove the furnace or remove the specimen together with the pull rods and the elements of the system which transmits the variation in deformation. The first variant can be accomplished only in two cases: (1) a dismountable furnace; or (2) a furnace which can be moved along the specimen.

It is more complicated to make a dismountable furnace, and it is still more difficult to ensure an identical temperature for the entire volume of the specimen in it. In the case of a furnace which moves along the specimen, the height of the machine must be at least twice as long as the length of the furnace. As for removing the specimen from the furnace along with the pull rods and the elements of the system transmitting the variation in deformation

(combined in one unit), this variant is, in our opinion, unsuitable, since at this point we reduce reliability by protecting the specimen from accidental bending.

The furnace must have a sufficiently high "thermal inertia" with respect to the specimen and as low as possible a "thermal inertia" with respect to the element of the thermocontroller, intercepting the variation in temperature.

The thermocontroller must have: (1) sufficient sensitivity to the variation in temperature; (2) simplicity in structure; and (3) reliability in continuous operation.

The thermal control can be accomplished by means of systems composed of a dilatometer, bolometer, thermocouple, etc. Dilatometric thermocontrollers are the simplest in design. The use of a bolometer and other temperature variation indicators requires more complex circuits.

5. Electrical system

In regard to the electrical system of the entire set-up as a whole, it should be noted that in connection with the long duration of the test on relaxation and the relative complexity of the aggregates included in the set-up, it is desirable to automatize the operating process of the machine as much as possible and ensure the electrical protection of the individual units of the set-up as well as the warning of inadmissible deviations from the normal operating regime.

III. The Description of the Machine Used in Tests on Relaxation of Stresses

Let us examine briefly the operating diagram of the machine for testing the relaxation of stresses (Figure 1).

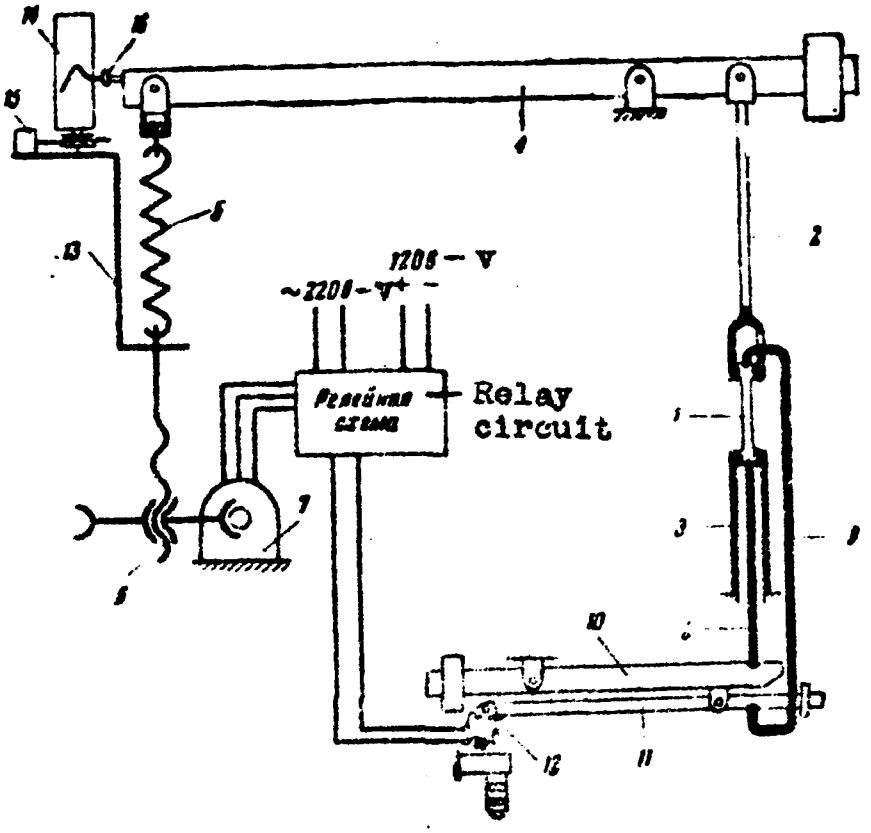

Figure 1. The diagram of the relaxation machine.

1 -- Specimen to be tested; 2 -- upper pull rod;
3 -- lower pull rod; 4 -- load lever;
5 -- load spring; 6 -- transmission system;
7 -- electric motor; 8 -- quartz rod;
9 -- quartz arch; 10 -- the upper lever of the increaser of deformations;
11 -- the lower lever of the increaser of deformations; 12 -- the lower lever of the deformation amplifier; 13 -- bracket;
14 -- diagram recording cylinder;
15 -- Warren motor; 16 -- pencil.

The electric motor 7 extends spring 5 through the transmission system 6. The stress created in stretching spring 5 is transmitted by lever 4 to the specimen 1 through pull rod 2. The specimen is secured by its ends to the pull rods 2 and 3. The variation in the length of the specimen 1 is transmitted by the quartz rods 8 and 9 to levers 10 and 11. The quartz rod 8 which runs inside the lower pull rod 3 rests with its upper end against the tapered hollow in the lower end of the specimen, and with its lower end in the counterbore of lever 10. The quartz rod 9 has hooks at both ends. The upper hook of the rod 9 enters the tapered hollow of the upper end of the specimen. The lower hook of rod 9 supports the short arm of lever 11.

As the length of specimen 1 changes, quartz rod 9 turns lever 11 in one or the other direction; this will either lock or unlock electrical contact 12 situated on the long arm of lever 11.

Contact 12 controls the relay system (circuit) connected with the electric motor 7. As the length of specimen 1 increases, contact 12 locks, and the electric motor unoads the spring; as a result, the load which acts upon the specimen and, consequently, the length of the specimen decrease. As the length of the specimen decreases, the contact 12 rises and unlocks the circuit of the relay system. The electric motor loads the spring; the load which acts upon the specimen and, consequently, the specimen length increase. This cycle repeats itself uninterruptedly during the entire test period.

The recording cylinder is situated in cantilever 13. Cantilever 13 is tightly connected with the bracing point of the lower end of spring 5. Cylinder 14 is rotated around its vertical axis by either a clock-work or by electric motor 15.

Pencil 16, drawn to cylinder 14 by a soft spring, is attached to lever 14.

As spring 5 is loaded it displaces the cylinder with respect to the pencil by the amount of the elastic elongation of the spring. This amount is in proportion to the load which acts upon the specimen. Consequently, the cylinder records the diagram in the coordinates: load vs. time.

To heat the specimen, we move down the tubular furnace equipped with a thermoregulator (not shown in this diagram).

The relaxation set-up can be subdivided into the following units: (1) loading system; (2) deformation amplifier; (3) recording device; (4) furnace; and (5) thermoregulator.

1. Loading system

The loading system consists of two parts, described below.

The lower pull rod (Figure 2) is secured to the frame by means of two nuts. The pull rod 1 has an ear 2 with holes and grooves for the deformation amplifier 3, the quartz arch 4, and quartz rod 5. The upper end of pull rod 1 is equipped with a thread (M-9) for securing the specimen. Pull rod 1 has a through-opening along its axis for the quartz rod 5.

The lower end of the upper pull rod 6 is threaded (M-9) for securing the specimen; in addition, the pull rod 6 has a through-opening for the upper end of the quartz arch (see Figure 3). The upper end of the upper pull rod 6 (Figure 2) is held in the suspension device 7 by means of a spherical rib. The suspension device 7 of the upper pull rod 6 is secured by means of a shaft on a ball bearing built into the load lever 8 which transmits the stress produced by spring 9 upon the specimen.

The arm ratio of the load lever is 1 : 8.

The shaft of load lever 8 is secured on ball bearings mounted into stands 10 which rest upon the front columns 11 of the machine. The short arm of lever 8 has a traveling counterweight 12 for balancing the lever. On its long arm the load lever carries a single-row ball bearing with a shaft secured to a suspension device with swivel 13 for spring 9.

The upper end of the loading spring is inserted in the hole of the swivel. The swivel rests on the suspension device through a ball-thrust bearing.

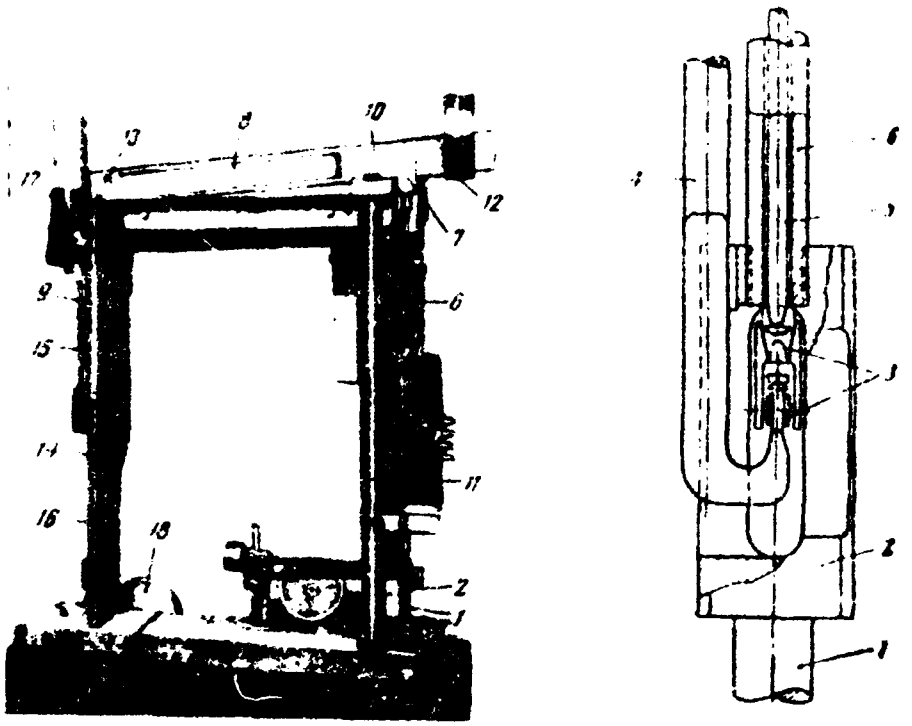

a b

Figure 2. Relaxation machine.

a -- Overall view; b -- lower pull rod unit;
1 -- lower pull; 2 -- ear;
3 -- the levers of the deformation amplifier;
4 -- quartz arch; 5 -- quartz rod; 6 -- upper pull rod; 7 -- suspension of the upper pull rod;
8 -- load lever; 9 -- load spring; 10 -- stands;
11 -- front columns; 12 -- counterweight;
13 -- swivel suspension; 14 -- carriage rod;
15 -- carriage; 16 -- rear columns;
17 -- cylinder; 18 -- pulley.

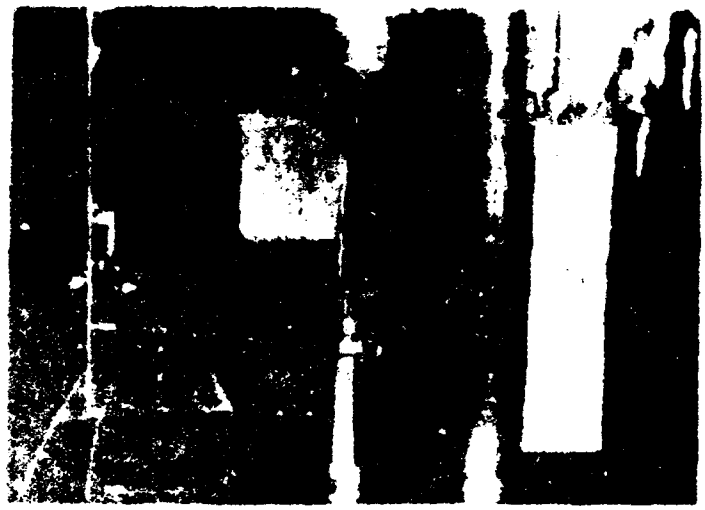

Figure 3. Mounted specimen with the attached thermocouples.

The lower end of spring 9 is inserted into rod 14 of the carriage. The upper end of the carriage rod is secured with nuts to carriage 15 which travels over the rear columns of the frame 16.

Carriage 15 has on its upper end a cantilever for the recording mechanism 17.

The lower end of the carriage rod is placed into a wormwheel with a nut; the wormwheel is rotated by a wormscrew at the end of pulley 18. The wormscrew is set into motion by the electric motor through a flexible transmission.

The motor of the actuating mechanism, type PR of PR-1 (3), is secured to the table with shock absorbers of sponge rubber. The motor represents an induction-type motor with two rotors mounted on one axis and with two independent stators. Each of the rotors can rotate in only one direction (one to the right and the other to the left); as a result, each of the stator windings "rests" approximately half of the operating time. To ensure greater reliability of operation, the motors are equipped with water cooling.

The highest load applied to the specimen is 1,000 kg, which, with our specimen dimensions (a 4.5 mm diameter

[in the working section), amounts, approximately, to 63 kg/mm^2.

Prior to mounting, the springs were extended to maximum working conditions and aged at 230° for three hours.

The elastic travel of the loading spring at highest load is equal to approximately 160 mm.

The highest loading-unloading rate is 50.9 kg/min (or 3.2 kg/mm^2 per minute respectively).

2. Deformation amplifier

The function of the deformation amplifier is to transmit the small changes in the length of the specimen and increase them by a factor of 25.

The deformation of the specimen is picked up by quartz arch 15 and quartz rod 14 (Figure 4) placed with their upper ends in the tapered grooves (counterbores) which are situated at the ends of the specimen, on its axis. This eliminates the influence of specimen bending on the amount of deformation perceived.

The deformation amplifier is constructed in the form of a system consisting of two light-weight (hollow) levers 7 and 8 made of invar [?]. The levers have counterweights which are so mounted as to ensure the tightening of the quartz rods 14 and 15 to the specimen with a load equal to 50 kg. The upper lever 8 is secured on ball bearings 17 on a shaft built on to carriage 18 which can move over the guiding column 19 and can be secured in the necessary position by a screw.

The guiding column 19 is mounted on base 20 which is fastened to the frame of the machine by means of screws.

The lever 8 terminates in part 11 which carries ball bearings 12 and has a counterbore 3 for the end of quartz rod 14.

The shaft of lever 7 is secured on ball bearings 12. The arm ratio of lever 7 is 1 : 25. One end of lever 7 has an electrical contact 22; the other end, in addition to weight 13, has a special device to compensate the [thermal expansion of part 11 and measure the variation in]

the length of the specimen (at heating, loading, etc.).

The lever 7 carries lever 4 tightened to a metal tubing 6 by spring 10. The plunger 24, situated in the hole of lever 7, rests with one end upon lever 4 and has on the other end a counterbore for the end of the quartz arch 15.

The compensation of thermal expansion occurs automatically due to the fact that the lengths of both the metal tubing 6 and the brass screw are so matched that the expansion of part 11 is compensated by the difference in expansion between tubing 6 and screw 5.

The variation in the dimensions of the specimen, transmitted by quartz rods 14 and 15, is compensated by means of screw 5 displacing plunger 24.

The micrometer screw 1 situated strictly on the vertical which runs through shaft 17 is secured to carriage 18 by means of insulation layer 23. Screw 1 is equipped with electrical contact 2 which may be connected with contact 22 (in our set-up, these contacts act as a pulse transmitter).

The quartz arch and the quartz rod are shown in Figure 5.

The set-up consists of four machines. The better of these machines ensures the maintenance of the length of the tested specimen to an accuracy of ±0.2 microns, which amounts (at a 100-mm calculated length of the specimen) to a relative accuracy of ±0.0002 percent in maintaining the constancy of the length; when the machine is not that good, this quantity is somewhat higher.

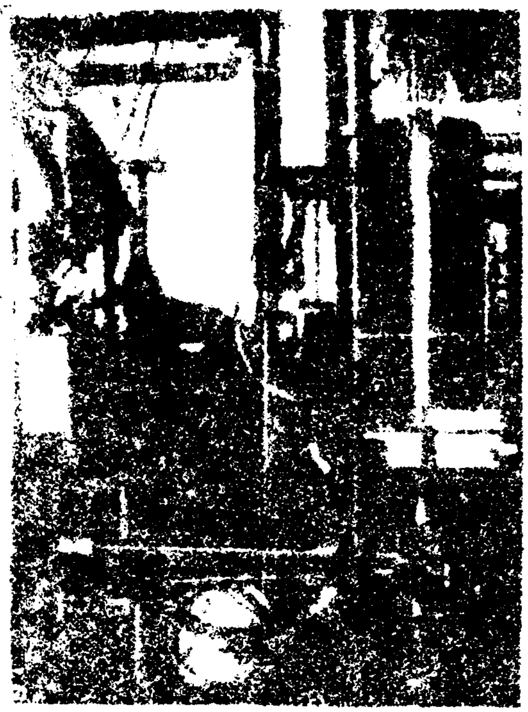

a

[illegible] -- [illegible] of [illegible]; [illegible] -- [illegible] ... -- [illegible] amplifier [illegible]; [illegible] -- [illegible]; [illegible] -- the contact of the [illegible] lever [illegible], [illegible] -- counterweight of upper lever; [illegible] -- lever of compensating device; [illegible] -- [illegible]; [illegible] -- [illegible]; 7 -- lower [illegible]; [illegible] -- upper lever; [illegible] -- axis of lever of compensating device, [illegible] -- spring [illegible] lever of compensating device, 11 -- part of the upper lever with the ball bearings and counterweight; 12 -- ball bearings of axis of lower lever; 13 -- counterweight of lower lever; 14 -- quartz rod, 15 -- quartz rod; 16 -- counterweight of upper lever;

17 -- ball bearing of axis of upper lever; [illegible] -- [illegible] of information amplifier; [illegible] -- [illegible] button; [illegible] -- [illegible] of information amplifier; [illegible] -- [illegible]; [illegible] -- contact of lower lever of information amplifier; [illegible] -- [illegible]; [illegible] -- [illegible]; [illegible] -- thermocontroller rod, [illegible] -- thermocontroller lever; 27 -- clamp.

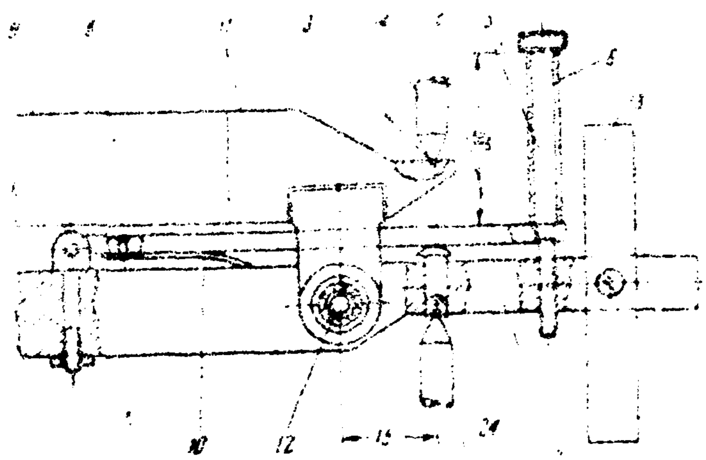

b

Figure 3. Quartz arch (to the right) and quartz rod (to the left).

3. A recording device

The recording cylinder (Figure 4) is fastened on the continuation of the carriage 11 and represents cylinder 17 (with clock-work) put on the axis of the wormwheel; the wormwheel is connected with the Warren motor. A sheet of paper is pasted around the cylinder. The holder with pencil is inserted in the cylindrical hole of the longer arm of the lever. The holder is drawn to the cylinder by a small cylindrical spring.

The cylinder can rotate at two different speeds; that is, by means of a clock-work or by the clock-work and Warren motor combined.

The recording scales of the diagram according to the stress axis and the time axis are given in Table 2.

4. Furnace

The heating element of the tubular electrical furnace is a nichromova wire wound around a tube of EYal-1-type heat-resistant steel over a thin layer of coating (10 percent clay, 90 percent magnesite, diluted in water containing two to three percent

water glass). The winding is divided into three sections which may be switched in successively (Table 3).

Parallel to the central and lower sections there are connected rheostats; by varying their resistance we vary the magnitude of current which passes through the central

and lower sections. This makes it possible to achieve a uniform distribution of temperature over the length of the specimen.

5. Thermoregulator

The furnace is equipped with a dilatometric-type thermoregulator consisting of two elements, one of which is the furnace tube and the other of which is the quartz rod which takes part in the elongation. The relative variation in the length of the tube and the rod increases 100-fold by means of a two-stage lever system. The travel of the lever system caused by the thermal expansion (or contraction) of the tube causes the closing (or opening) of the electrical contact, which, in the end, results in a reduction (or increase) in the magnitude of current passing through the winding of the furnace.

We should pause to discuss for a moment the method of fastening the quartz rod 25 (see Figure 4a). This rod must have thickenings (heads) at its ends. The lower end of the rod is led into a yoke on the short arm of the thermoregulator lever 26. The upper thickened end of the rod rests upon a brass tube which is put on the rod. This tubing may be tightly secured by clamp 27 at the upper end of the furnace.

The thermoregulator permits the temperature to be maintained to an accuracy of $\pm 0.17^{\circ}$ C provided the voltage oscillations in the network, which feed the furnace windings, are small. In the case of substantial voltage oscillations in the network the accuracy of maintaining the temperature of the specimen constant is impaired, and it reaches ± 1 and 1.5° C.

Table 2

The recording scales of the diagrams according to the stress axis and time axis

No. of machine	Stress corresponding to 1 mm on the diagram, kg	Time corresponding to 1 mm on the diagram, hour	
		With the Warren motor and the clock-work	Using only the clock-work
1	6.01	$4.08 \cdot 10^{-3}$	0.109
2	6.05	$4.19 \cdot 10^{-3}$	0.705
3	6.10	$4.26 \cdot 10^{-3}$	0.724
4	5.98	$4.17 \cdot 10^{-3}$	0.538

Table 3

Structural specifications for the winding of the heat-treatment furnace

Section	Number of turns	Spacing of winding, mm	Relative density of winding
Upper	22	4.6	2
Central	16	9.4	1
Lower	32	3.2	3

IV. The Electrical Circuit System of the Machine That Tests Relaxation of Stresses

The following circuits may be singled out in the electrical system of the control board: (1) furnace heating circuit; (2) thermoregulator circuit; (3) deformation

amplifier circuit (pulse transmitter); (4) electric motor circuit; (5) Warren motor circuit; (6) d-c potentiometer; and (7) signaling and safety circuit.

Figure 6 shows a schematic electrical diagram of one of the panels and wiring diagrams of both the board panel and the relay unit.

1. Furnace heating circuit

The furnace may be connected into a 120- or a 220-v a-c circuit (see Figure 6a).

The current passing through the circuit is measured with an ammeter and controlled with rheostats II and III. A portion of the current is shunted by rheostat IV by means of normally closed relay contacts R6. Tube 15 (furnace), which indicates the presence of current in the furnace, is connected in parallel to rheostats II and III. The central and lower heating sections are shunted by rheostats V and VI, respectively.

2. Thermoregulator circuit

The thermoregulator relay R6 is fed by the current (25 to 30 v) from the d-c potentiometer 1. The thermoregulator contacts VS close or open the relay circuit R6. The contacts of the R6 relay connect or disconnect the shunt rheostat IV circuit. To reduce sparking and, consequently, charring, the contacts of thermoregulator VS are shunted by the resistor R1 = 240 ohms.

In case of overheating of the furnace the lower contacts N of the thermoregulator close the circuit of relay R1 whose contacts close the emergency relay R8 circuit.

The 20,000-ohm resistor R3 serves as a spark arrester in the relay R1 contacts.

The (0.5μF) capacitor C1 serves as a spark arrester in the relay R6 contacts.

3. Deformation amplifier circuit

The lower lever of the deformation amplifier, by either closing or opening the contacts 13 and 14, passes or interrupts the current in the polarized relay R2.

Relay R2 is fed from the potentiometer 1 at a voltage of 1.5 to 1.8 v. The input power consumed by relay R2 and, consequently, cut off in contacts 13 and 14 amounts in all to ~0.006 v. The 10,000-ohm resistor R2 acts as a spark arrester on the contacts of the deformation amplifier.

When the contacts of the deformation amplifier are open, the relay R2 contacts 2B and 4B are open. At this point the normally closed contacts of the intermediate relay R7 close (through the normally closed contacts of the emergency relay R3) the coil of the loading motor relay R4. The contacts of relay R4 close the stator circuit of the motor which actuates the rotor toward loading the specimen.

When the contacts of the deformation amplifier are closed, the current passes from the potentiometer through relay R2 and close contacts 2B and 4B (the 30,000-ohm resistor R4 shunts contacts 2B and 4B for spark arresting); at this point the relay R7 contacts open the coil circuit of the unloading motor relay R5.

The contacts of relay 7 are shunted for spark arresting by resistors R5 and R6, 2400 ohms each.

The contacts of relay R5 close the stator circuit of the motor, which actuates the rotor toward unloading the specimen.

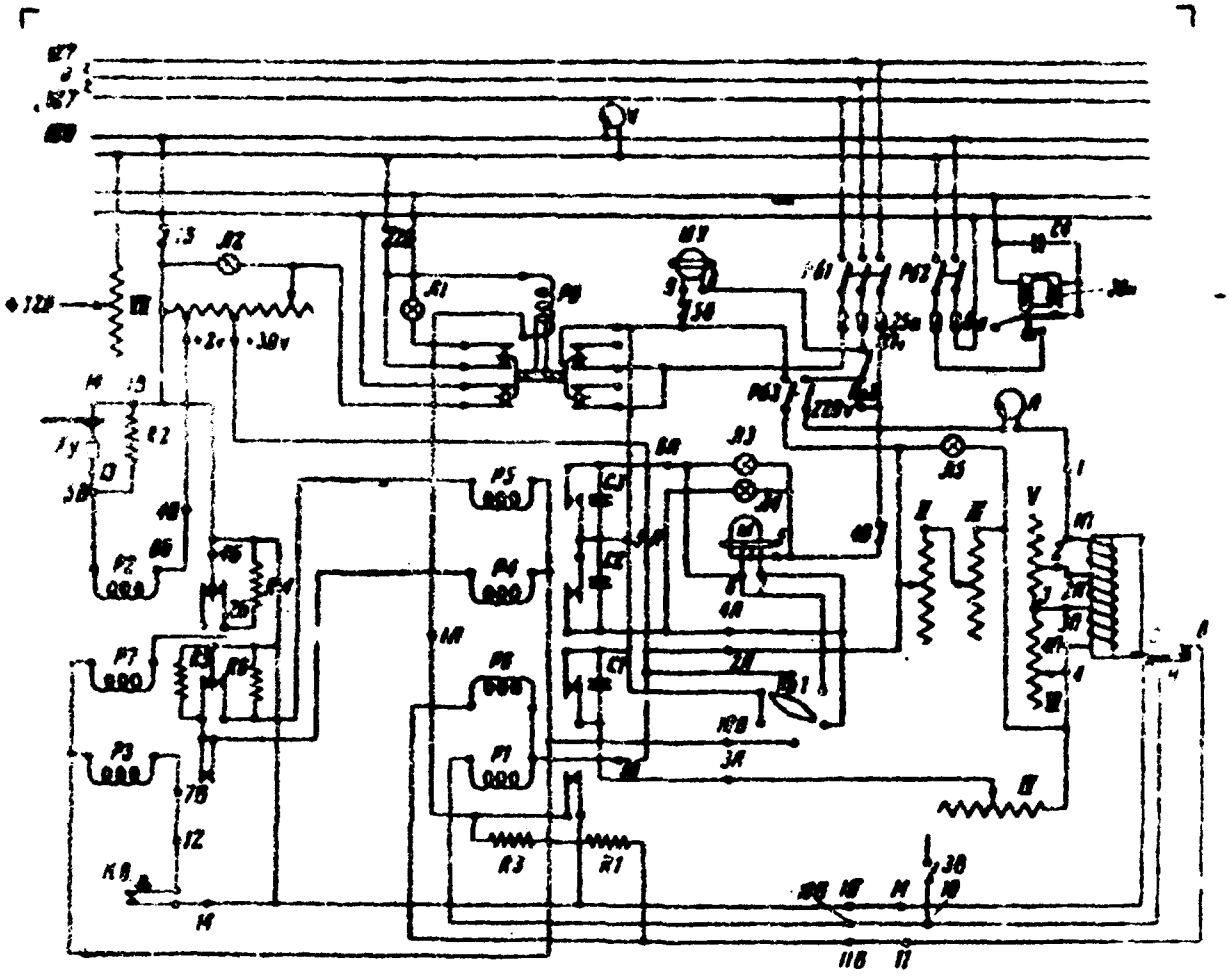

a

Figure 6. Relaxation Machine

a -- Schematic diagram of electrical circuits; b -- wiring diagram of the board; c -- wiring diagram of the relay unit of the machine; R1 -- relay interjacent to the emergency relay (general); R2 -- control relay of the mechanical amplifier of deformation (its contacts are 2B and 4B); R3 -- emergency relay (of the motor); R4 -- motor relay (loading); R5 -- motor relay (unloading); R6 -- thermoregulator relay; R7 -- relay (intermediate) of the mechanical amplifier of deformation; R8 -- emergency relay (general); R1, R2, R3, R4, R5, and R6 are spark-arresting resistors; C1, C2, C3, and C4 -- spark-arresting capacitors; L(T)1, L2, L3, L4, and L5 -- signal lamps; I -- d-c potentiometer; II and III -- ballast rheostats of the furnace;

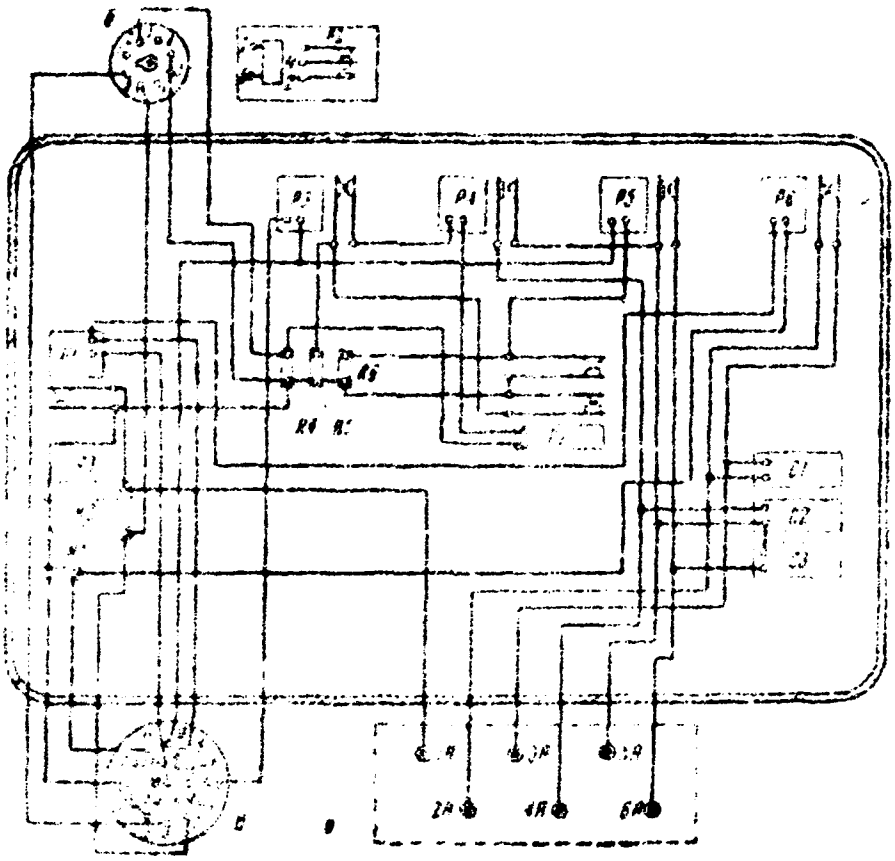

c

IV -- rheostat, shunting the ballast rheostats; V and VI -- shunt rheostats of the central and lower sections of the furnace; VII -- d-c ballast rheostat; V -- d-c voltmeter; A -- a-c ammeter; Zvn -- electrical signal bell; MW (MU) -- Warren motor; M -- electrical motor (5, 6, 7 -- its contacts); Rbl -- knife switch (master); Rb2 -- signal knife switch; Rb3 -- furnace knife switch; Prl -- four-position switch of electric motor; Pr2 -- two-position switch; 1v, 2v -- d-c switches; 3v -- emergency switch; 4v -- electric motor switch; 5v -- Warren motor switch; CA (KU) -- contacts of mechanical amplifier of deformation;

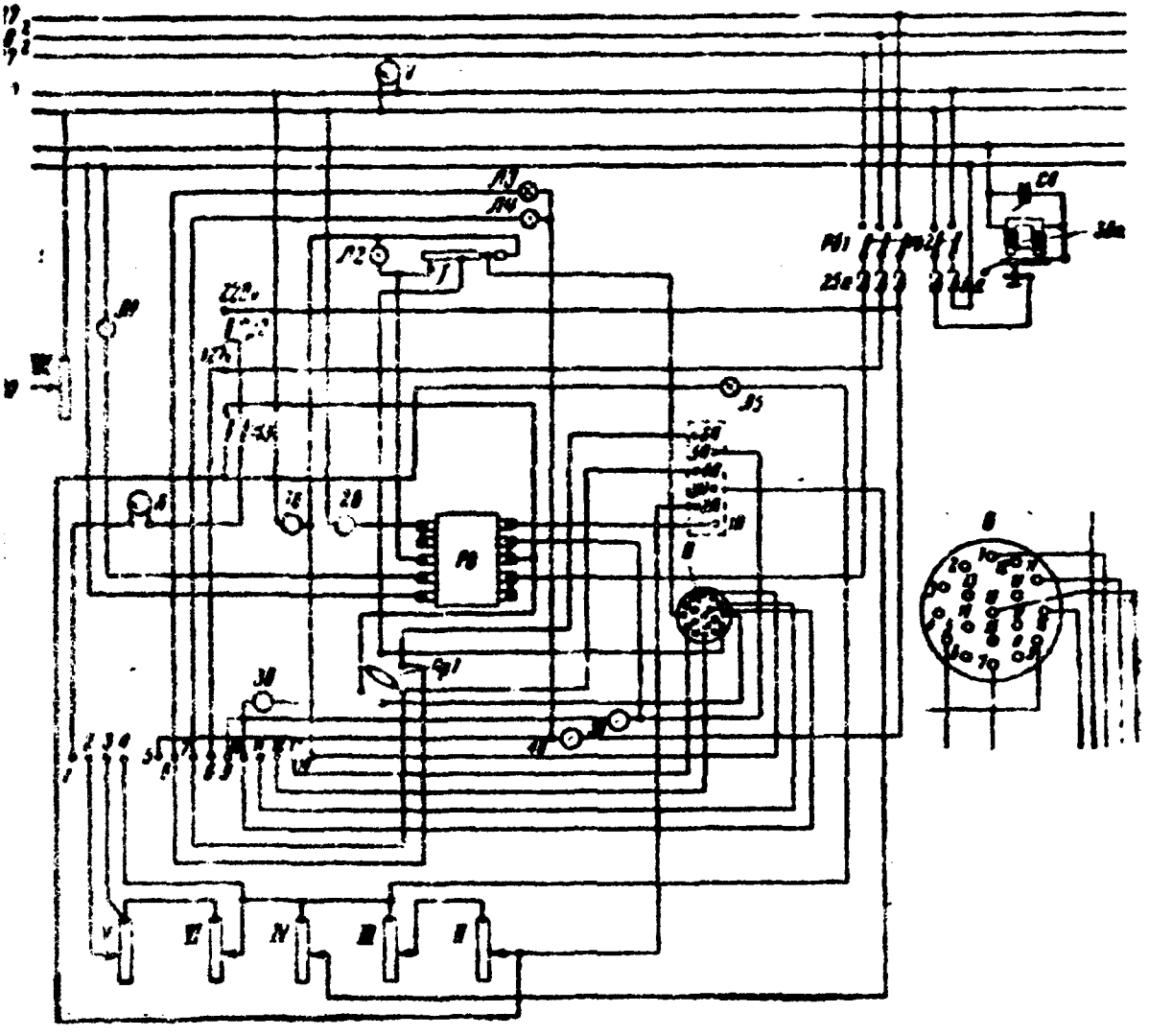

b

C (K), v -- contact of load lever screw; V, S, N -- thermoregulator contacts; 1 to 14 -- distributing board contacts; 1A to 6A -- contacts of relay unit panel; 2B to 8B -- contacts of tube socket of relay unit B; 1B to 18B -- contacts of the coupling of the relay unit B; 1P to 4P -- electric furnace contacts.

[illegible] Electric [illegible]

The [illegible] for [illegible] type Pr1 [illegible] rotor [illegible] of the [illegible] (see Figure [illegible]) [illegible] unloading [illegible] stators [illegible] from the [illegible]-v a-c [illegible].

The [illegible] switching [illegible] normally [illegible] the relay [illegible] of relays [illegible] capacitor [illegible] addition, by [illegible] 13 and 14, [illegible] simultaneously the [illegible] and absence of current in each of the circuit windings of the stator.

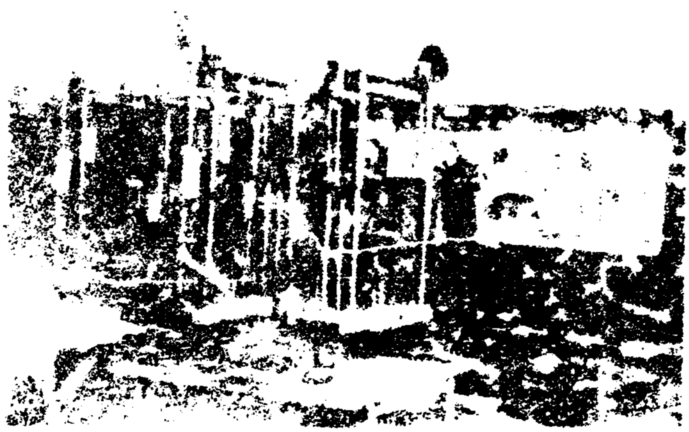

Figure 7. The overall view of the relaxation machines and the control board.

In the electric motor circuit there is a four-position switch Pr1. The switch Pr1 set in "automatic" position connects the electric motor circuit by means of relays R4 and R5; with the switch in "loading" position, relays R6 and R7 are on and the winding of the loading stator is off; with the switch in "unloading" position, only the winding of the unloading stator is on. With the switch Pr1 in "neutral" position, all the circuits of the

electric motor are on.

5. Warren motor circuit

The Warren motor is fed from the 120-v a-c network. It is connected and disconnected by switch 5v.

6. Direct-current potentiometer circuit

The relay system is fed from potentiometer 1 whose circuit is switched in by switches 1 and 2. Signal lamp L2 indicates the presence of voltage on the potentiometer. The potentiometer shows readings for 2-, 30-, and 120-v voltages.

The ballast rheostat VII is employed to maintain constant voltage during the experiment. The voltage constancy is checked by the d-c voltmeter.

7. Signaling and safety circuit

The 120-v a-c current is fed to the signal straps through the knife switch Rb2 and the bell circuit.

In case the furnace becomes overheated, the emergency relay R8 cuts off both a-c and d-c currents on the board of the machine and closes the circuits of emergency lamp L1 and the Zvn bell, whose coil is shunted by the 0.6 μF capacitor for spark arresting on the bell contacts. In order to connect the supply of current o the board, we must press a special button on relay R8.

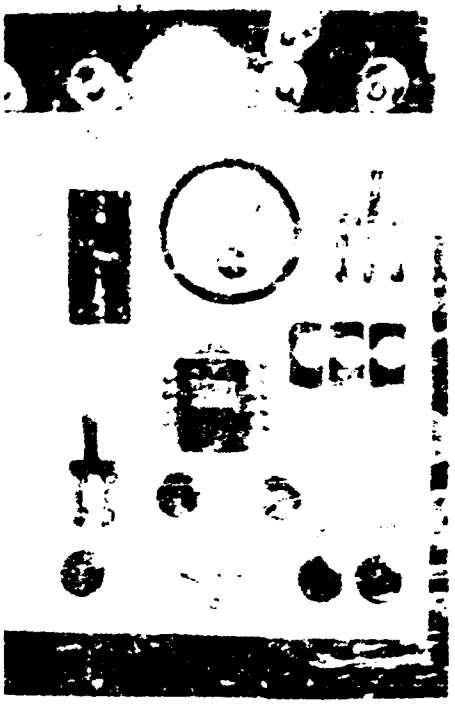

Figure 8. View of one panel of the control board of the relaxation machine.

1 -- a-c master knife switch; 2 -- a-c ammeter; 3 -- two-position furnace switch from 120 to 220 v; 4 -- emergency relay (master); 5 -- 25-amp fuses; 6 -- furnace knife switch; 7 -- d-c on-off switches; 8 -- the four-position of the electric motor; 9 -- on-off switch of the electric motor; 10 -- Warren motor on-off switch; 11 -- furnace signal lamp; 12 -- electric motor signal lamps; 13 -- d-c indicating lamp; 14 -- emergency signal lamp.

When the specimen is overloaded (if the relay of the deformation amplifier is not actuated), the load lever of the machine presses the button K of switch which closes the coil circuit of the emergency relay R3. The contacts of the emergency relay R3 open the coil circuit of the relay R4 of the loading motor.

To prevent a short-circuit, there are 25-amp fuses in the a-c circuit and 5-amp fuses in the d-c circuit.

The entire control of the electric circuits of the

four relaxation machines is centralized on the general control board (Figure 7); on the same board, there are, in addition, all the signal lamps and emergency relays. A view of one of the panels of the control board is shown in Figure 8.

V. Measurement Errors in Testing Relaxation of Stresses

1. The accuracy of maintaining the length of the specimen constant

Let us assume that the width of the line of the diagram Δz depends completely on the accuracy $\Delta\varepsilon$ at which the set-up maintains the constancy of deformation in the specimen. Then, taking the width of line Δz which has actually been measured for a case when the test was conducted at room temperature and the time recording was made by using a large scale (approximately, one turn of the cylinder per hour), we will have:

$$\Delta z = \pm \Delta z m l_0 / 2SE = \pm 0.00019 \text{ mm},$$

where $\Delta z = 0.2$ mm is the width of the line of the diagram;

$m = 6.0$ kg/mm is the scale of stresses;

$l_0 = 100$ mm is the working length of the specimen;

$S = 16$ mm^2 is the cross-sectional area of the specimen;

$E = 2.0 \cdot 10^4$ kg/mm^2 is the modulus of normal elasticity of the material of the specimen at a testing temperature of 20° C.

On the other hand, we can proceed from the average number of revolutions in one direction of the Δn of the wormwheel of the loading system (during the loading-unloading process). The number Δn will be related to the to the accuracy of maintaining deformation by the following expression:

$$\Delta\varepsilon = \frac{ihml_0\Delta n}{2SE} = \pm 0.00017 \text{ mm},$$

where

$i = 1/110$ is the gear ratio of the wormwheel;

$h = 4$ mm is the travel pitch of the carriage screw;

$\Delta n = 5$ revolutions is the average number of revolutions of the wormwheel in one direction.

When tests are conducted at an elevated temperature and a small time scale is used, we must also take into account the variation in the dimensions of the specimen caused by variations in its temperature. The error in maintaining the constancy in the length of the specimen which depends on the thermal expansion of its Δl in the most unfavorable case, when the temperature variations reach $\pm 1^\circ$ C, will equal:

$$\Delta \underline{l} = \pm \underline{l_0 \alpha \Delta t} = \pm 0.0016 \text{ mm},$$

where $l_0 = 100$ mm is the working length of the specimen;

$\alpha = 16.0 \cdot 10^{-6}$ is the coefficient of linear expansion (for high-alloyed chromium-nickel steels); and

$\Delta t = \pm 1^\circ$ C is the accuracy in maintaining the temperature.

In most cases it is possible to maintain the temperature to a greater accuracy, approximately $\pm 0.25^\circ$ C; this agrees with the error of thermal expansion on the order of ± 0.0004 mm.

In fact (in complete accordance with the above calculations), in conducting the test in the region of high temperatures, the total width of the line of the diagram in the sector of the most unfavorable condition amounted to about 2 mm, and in most cases to 0.6 mm.

2. Measurement error in the variation of load and time

Proceeding from a frequently observed diagram line width of 0.6 mm, it must be assumed that the error in the reading of stresses from the diagram

$$\underline{m/Sb} = 0.114 \text{ kg/mm}^2$$

will be equal approximately to 0.3 mm. This corresponds to the average measurement error of the stress $m/Sb = 0.114$ kg/mm^2 effective in the specimen, where

$m = 6.0$ kg/mm^2 the scale of stresses;

S = 16 mm^2 is the cross-sectional area of the specimen; and

b = 0.3 mm is the error in the reading of stresses on the diagram.

If we assume that the time-reading accuracy on the diagram is 0.2 mm, then the measurement error in time will be equal to the values given in Table 4.

Table 4

Errors in time measurement according to the diagram of relaxation of stresses, sec.

No. of machine	With the Warren motor and the clock work	Operating only with the clock-work
1	±2.9	±7.8
2	±3.0	±5.4
3	±3.0	±5.4
4	±3.0	±3.6

3. Evaluating the influence of the variation in room temperature on the stiffness of the loading spring

To evaluate the influence of the variation in room temperature on the stiffness of the loading spring, we may take advantage of the well-known formula relating the elongation of the helical spring to the load applied to it:

$$P = Gd^4/64ir^3f = kf$$

where P is the stress produced by the spring;

G is the modulus of tangential elasticity;

d is the diameter of the spring wire;

i is the number of turns in the spring;

r is the radius of the turn in the spring;

f is the elongation of the spring;

k is the stiffness factor.

Let us assume that at a small variation in temperature the modulus of tangential elasticity depends linearly on temperature, namely: it drops with the increase in temperature while the linear dimensions of the spring grow with the temperature, i.e.,

$$\underline{r} = r_0(1 + \alpha\Delta\underline{t})$$

$$\underline{d} = d_0(1 + \alpha\Delta\underline{t})$$

$$\underline{G} = G_0(1 - \beta\Delta\underline{t})$$

where α is the coefficient of linear expansion;

β is the thermal coefficient of the modulus of elasticity in shear; and

Δt is the variation in temperature.

From here we can easily determine the relative variation of the stiffness factor $\Delta k/k \cdot 100$ (expressed in percent) with the variation in temperature.

Taking $$\Delta \underline{k}/\underline{k} \cdot 100 \cong (\alpha - \beta) \cdot \Delta \underline{t} \cdot 100.$$

$$\alpha = 1.6 \cdot 10^{-5};$$

$$\beta = 2.5 \cdot 10^{-4}; \text{ and}$$

$$\Delta \underline{t} = 10^{\circ} \text{ C};$$

we obtain $$\Delta \underline{k}/\underline{k} \cdot 100 = -0.23 \text{ percent.}$$

Conclusions

1. A study has been made of the general requirements of a set-up for testing relaxation of stresses at elongation.

2. A description is given of this set-up; it was planned and built at the Institute of Physics of Metals of the Academy of Sciences USSR (AN SSSR), Ural Branch; it was designed for testing specimens 100 mm long and 4.5 mm in diameter at temperatures up to 900° C. The length

of the specimens was maintained automatically to an accuracy of ±0.2 micron and the temperature to an accuracy of ±1° C. The maximum load is 1,000 kg. The diagram of stresses with respect to the test time was recorded automatically.

3. An analysis of measurement errors in testing relaxation of stresses is given.

BIBLIOGRAPHY

1. Oding, I. A., "Vestnik mashinostroyeniya" (Herald of Machine Construction), No. 5-6, 7-8, 9-10, 1946.

2. Oding, I. A., Relaksatsiya i polzuchest' metallov (Relaxation and Creep of Metals, Central Scientific Research Institute of Heavy Machinery (TsNIITMASh), Moscow, 1946.

3. Chevenard, P., Rev. Met., Vol 39, No. 11, 12, 1942.

4. Davidenkov, N. N., Mekhanicheskiye svoystva i ispytaniya metallov (Mechanical Properties and Testing of Metals), "Kubuch" Press, Leningrad, 1933.

5. Davidenkov, N. N., Mekhanicheskoye ispytaniye metallov (Mechanical Testing of Metals), "Kubuch" Press, Leningrad, 1930.

6. Shaposhnikov, N. A., Mekhanicheskiya ispytaniya metallov (Mechanical Tests on Metals, State Scientific and Technical Press of Literature on Machinery (Mashgiz)), Moscow-Leningrad, 1951.

7. Borzdyka, "Zav. Lab." (Plant Laboratory), No. 5, 1935.

8. Motornyye ispolnitel'nyye mekhanismy (Actuating Mechanisms for Motors), DR, DR1, PR, PR1, Oborongiz (State Press of the Defense Industry), 1946.

* * *

Concerning Shearing and Diffusion Plasticity in the Process of Relaxation of Stresses

By G. N. Kolesnikov and A. I. Moiseyev

Relaxation of stresses is customarily called the spontaneous reduction of stresses which eventually takes place when total deformation remains permanent. We have today a sufficiently well-accepted conception that the primary reason for relaxation of stresses is the nonuniform and nonsynchronous course of plastic deformation in the material.

We know that at relatively low temperatures plastic deformation is accomplished by two processes: slip and twinning*. In the case of high temperatures, many authors (3-10) assume, parallel to slip, the existence of another type of plastic deformation, diffusion plasticity. Specifically, A. A. Bochvar (7) concludes that diffusion plasticity can be accomplished by three different mechanisms, which he calls: (1) amorphous diffusion; (2) soluble-precipitation; and (3) recrystallization. He, as well as several other authors, is justified in assuming that, at an assigned constant temperature, the greater the relative role of diffusion plasticity, the lower the rate of deformation.

The fundamental distinction of twinning and slip from diffusion plasticity is the fact that both slip and twinning are group processes ("collective", "cooperative"); in other words, the elementary acts of these processes are accomplished by the regular dislocation of entire groups of atoms along definite crystallographic planes and directions. The elementary act of diffusion plasticity represents a process of an independent migration of individual atoms which coincides with the elementary act of diffusion (self-diffusion).

*To this same type of "collective" processes we also refer the process of complex slip described by M. V. Klassen-Neklyudova (1) and A. V. Stepanov (2).

The conception of the existence of diffusion plasticity is, as a matter of fact, supported by four groups of established experimental facts.

1. In pure metals, the preceding plastic deformation (preset at a low temperature) affects oppositely the magnitude of the subsequent plastic deformation at low and high temperatures. A pure metal, preliminarily deformed (in the region of a relatively low temperature), will at a subsequent straining by some assigned stress (at the same temperature region) experience a plastic deformation, less in magnitude than a metal that had not undergone a preliminary deformation. But if we carry out the subsequent deformation at a sufficiently high temperature, the opposite relationship will be observed, i.e., the material that had not undergone a preliminary plastic deformation, will experience a lower deformation (11).

2. It is generally known that the variation in the grain size of a polycrystalline material affects diversely the magnitude of plastic deformation at low and high temperatures.

3. The distribution of plastic deformation over the polycrystalline specimen at its deformation in the region of low temperatures and of high deformation rates differs from the distribution obtained at the deformation of the specimen in the region of high temperatures and low deformation rates. In the first case, the deformation is mainly concentrated in the volume of the grain, and in the second case, it is mainly localized at the grain boundaries (12-15). Most convincing in this respect are the experiments conducted on bicrystals (12, 16). These experiments show that, at low temperatures and high deformation rates, plastic deformation occurs mainly in the sectors of the crystals removed from the boundaries, but that in the regions adjoining the boundary the deformation is hampered. In the case of high temperatures and low deformation rates, plastic deformation is localized at the grain boundaries and is almost unobservable in the sectors of the crystal removed from the boundary.

4. Some authors (17, 18) point out that the activation energy of self-diffusion in a number of metals concurs, within the limits of an experimental error, with the activation energy of plastic deformation by creep.

The above qualitative relationships can easily be explained on the basis of our conceptions of diffusion plasticity. That is, the intensity of the course of the diffusion processes must increase with the rise in temperature. Further, in considering this problem from the viewpoint of contemporary conceptions of the elementary act of diffusion in a crystalline body, it must be expected that the elementary acts must arise more easily in the sectors of the crystal where the crystal lattice is most distinct from that of an ideal, i.e., near the nonuniformity of the crystal and, particularly, at the grain boundaries. On the other hand, the elementary acts of the "cooperative" processes (slip and twinning), which also originate near the structural nonuniformities of the crystalline body, propagate to distances which are the greater dimensions of the undistorted sector of the crystal where the elementary act occurs.

In addition to the above there are some other experimental data which speak in favor of the existence of a process of diffusion plasticity; for instance, data referring to the damping of oscillations at elevated temperatures in a mono- and a polycrystalline material (19-21).

Although all that has been said above is based on experimental data obtained under deformation conditions different from those obtained in tests on relaxation of stresses, it is nevertheless obvious that plastic deformation which causes relaxation of stresses must be accomplished through microprocesses of the same types as in other cases of deformation. Indeed, from a phenomenological standpoint, relaxation of stresses can be considered as a special case of deformation of the specimen, in which the variation in the load applied to the specimen obeys a certain definite law in such a way that the total deformation (the sum of elastic and plastic deformations) of the specimen remains invariable (22). However, some authors have suggested (23-28) that the mechanism of plastic deformation at relaxation of stresses is essentially different from that of the plastic deformation under other deformation conditions (creep).

On the processes of creep and diffusion plasticity

According to present conceptions, diffusion plasticity is caused by independent (chaotic in nature) dislocations of individual atoms, while creep is a group phenomenon which consists of a coordinated simultaneous

dislocation of entire groups of atoms along definite planes and directions of the crystal lattice. Proceeding from these conceptions, it may be expected that so substantial a difference in the mechanism of these processes must manifest itself in the difference of the kinetics of their course.

It may be assumed that these processes are characterized by different dependencies of the rates of plastic deformation on stress, different magnitudes of activation energy, and different dependencies of the activation energy on stress.

In the opinion of Ya. I. Frenkel (29), the activation energy for a group process must be greater than that for the process of self-diffusion, while for a diffusion plasticity process the activation energy must be of the same order as the activation energy for a self-diffusion process.

At present there is still no detailed theoretical analysis of the dependence of deformation rate on stress for the case of diffusion plasticity in a crystalline body.

Some authors (5, 17) note that the activation energy of plastic deformation at creep is close in magnitude to that of diffusion (self-diffusion). On the basis of this fact, they conclude that in the case of creep the fundamental role is played by diffusion plasticity.

I. A. Oding (4) accepts the linear dependence of the activation energy of the diffusion plasticity on stress, assuming that the activation energy decreases with increase in stress. In fact, we can expect that the change in the specific volume caused by the superposition of stresses must manifest itself on the magnitude of the activation energy; in other words, that the activation energy will depend on that part of the tensor of stresses that causes the change of the volume. It may further be assumed that the dependence of the activation energy on stress can be expressed in the first approximation by a linear function. Theoretically, however, the order of the magnitude of the term depending on stress and appearing in the expression for the activation energy is absolutely vague. In other words, the question of how strongly the magnitude of activation energy for the process of diffusion plasticity (diffusion process) must depend on stress remains obscure. It can be assumed that this dependence must be weak.

I. Ya. Dekhtyar (30) suggested the following form of an expression for the dependence of the rate of diffusion plasticity on temperature and stress:

$$U_g = 2\delta K_0 e^{-\frac{Q_1}{RT}} \operatorname{sh}\frac{\sigma_1 V_a}{2RT}, \qquad (1)$$

where U_g is the flow rate or the rate of diffusion plasticity;

$\frac{1}{2}\delta$ is the distance between the initial (equilibrium) position of the atom and the vertex of the potential barier;

K_0 is the magnitude depending on the frequency of atomic vibrations;

Q_1 is the activation energy of the self-diffusion process;

R is the gas constant;

T is the absolute temperature;

σ_1 is the (internal) effective stress in the moving atoms;

V_a is the volume of crystal to suit one gram-atom;

e is the base of natural logarithms.

We will introduce the designations

$$A = 2\delta K_0; \quad \alpha = \alpha V_a \sigma_0 / 2Q_1;$$

where σ_0 is the yield strength at slip when $T = 0^\circ$; $\sigma_1 = \alpha\sigma$, where

σ is the external stress acting upon the specimen; and

α is the coefficient of local overstrain.

After some transformations and taking logarithms, we obtain the dependence of the log of plastic deformation rate on stress.

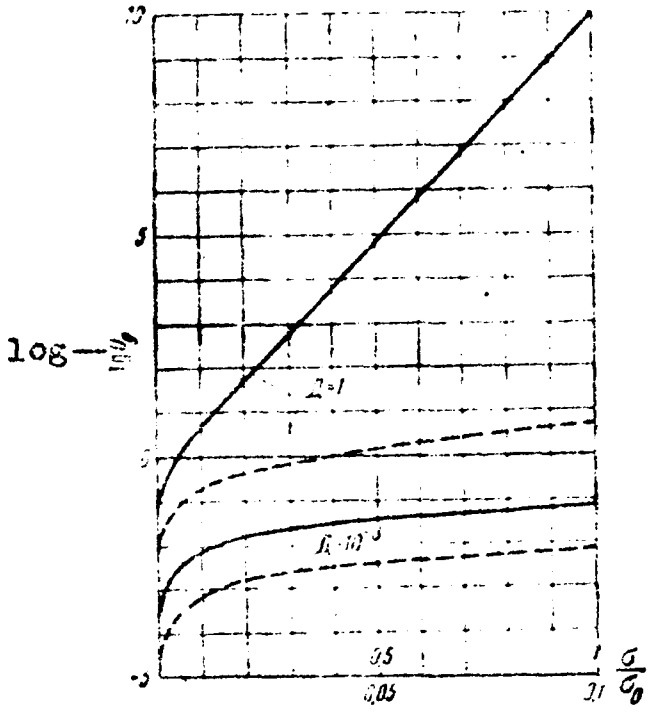

Figure 1. The relationship between the log of plastic deformation rate and stress, determined from Expression (2) for $Q_1/RT = 24$, $Д = 1$ and $Д = 10^{-3}$ (continuous lines correspond to the upper scale on the axis of abscissas, dotted lines correspond to the lower).

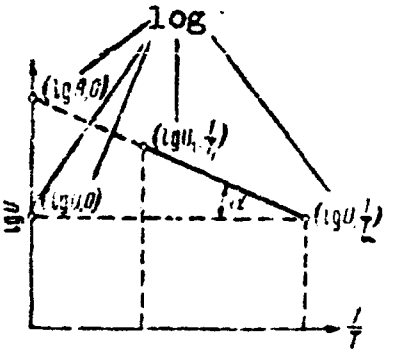

Figure 2. Schematic graph of the relationship between the log of deformation rate and the reciprocal of the absolute temperature; Log A is the initial ordinate.

$$\lg U_\varepsilon = \lg \frac{A_\varepsilon}{2} - \frac{Q_1}{RT}\left(1 - Д\frac{\sigma}{\sigma_0}\right)\lg e + \lg\left(1 - e^{-2Д\frac{Q_1}{RT}\frac{\sigma}{\sigma_0}}\right). \qquad (2)$$

For the values $\log A_\varepsilon/2 = 10$; $Q_1/RT = 24$; $Д = 1$, the curve which depicts Expression (2) is given in Figure 1. If T = constant, then, as obvious from Figure 1, in changing by one order (in the region of small stresses), the log of deformation rate decreases approximately by unity. In the region of high deformations the log of deformation rate rapidly descends with the reduction in stress, varying almost linearly. If we take $Д = 10^{-3}$ and the same value of Q_1/RT as above, then with the

decline in stress by one order the log of deformation rate will descend over the entire considered region of stresses ($\sigma \leq \sigma_0$) by one logarithmic unity (Figure 1).

From the viewpoint of kinetic theory, the constnat A_θ is proportional, on the one hand, to the number of sites, where the elementary acts of plastic deformation may originate, and, on the other hand, to the mean quantity of macroscopically observed plastic deformation which corresponds to the course of one elementary act.

Let us now stop to consider the experimental determination of the activation energy and the constant A_θ.

If in the expression for the process rate there appears only one exponential term which depends on the reciprocal of the absolute temperature, then the dependence under consideration in the coordinates -- log of rate and reciprocal of temperature -- is depicted by a straight line, whose tangent of the inclination angle is proportional to the activation energy Q and the initial ordinate gives the value for Log A (Figure 2). In an experimental determination of these values for any process we usually plot on the graph the log of the process rate on the axis of the ordinates, and plot the reciprocal value of absolute temperature on the axis of abscissas. Then after locating on the graph the absolute value of the tangent of inclination angle which equals

$$\operatorname{tg}\alpha = -\frac{d\lg U}{d\frac{1}{T}}, \tag{3}$$

we obtain the experimental value of the activation energy from the expression

$$Q_\theta = \frac{R \operatorname{tg}\alpha}{\lg e}. \tag{4}$$

The experimental value of the constant A_θ is found from the same graph by determining the initial ordinate which is equal to the Log A_θ. For instance, for the case of diffusion plasticity, described by Eq. (2), we have

$$Q_\theta = Q_1\left[1 - \Lambda\frac{\sigma}{\sigma_0}\left(1 + \frac{2}{e^{\frac{2\Lambda Q_1}{RT}\frac{\sigma}{\sigma_0}} - 1}\right)\right]. \tag{5}$$

$$\lg A_0 = \lg \frac{A_g}{2} + \lg\left(1 - e^{-\frac{2\Pi Q_1}{RT}\frac{\sigma}{\sigma_1}}\right) - \frac{Q_1 2.7 \frac{\sigma}{\sigma_0} \lg e}{RT\left(e^{\frac{2\Pi Q_1}{RT}\frac{\sigma}{\sigma_1}} - 1\right)}. \qquad (6)$$

It is obvious from Figure 3 that in this case Log A_0 will descend with the reduction in stress, varying approximately by one logarithmic unity when the stress changes by a factor of 10.

Let us now examine the relationship between the deformation rate, the stress, and the temperature for the case of deformation by slip.

Experimentaly, for monocrystalline specimens, i.e., in the case when there is minimum participation of diffusion plasticity, we observe a strong dependence of the activation energy on stress (31, 32). In particular, G. N. Kolesnikov (31), while investigating the flow of aluminum monocrystals of approximately the same orientation, found that the activation energy for the slip process varies from 20,600 cal/mole at a shearing stress of 600 g/mm^2 to 72,000 cal/mole at a stress of 150 g/mm^2.

It follows from this that in the case of slip the activation energy strongly increases with the reduction in the applied stress; moreover, the values of the activation energy which correspond to small stresses obviously exceed the activation energy of the process of self-diffusion*; according to the indication in literature, this activation energy for aluminum is equal to 37,500 cal/g-atom (17).

Present theoretical conceptions of the process of slip also lead to a strong dependence of the activation energy on stress.

*The activation energy of the process of self-diffusion is obviously determined without taking into account the cyclic diffusion (33).

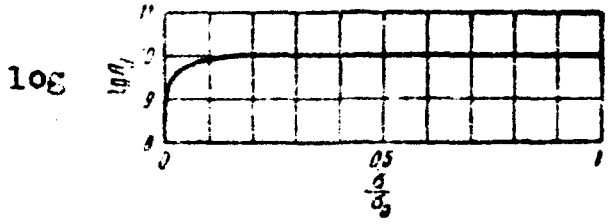

Figure 3. Relationship between value of log A_θ and stress, determined from Expression (6) for $Q_1/RT = 24$ and $A = 1$.

As an example, let us examine the Bekker-Orovan equation (34), since this is the simplest of a number of expressions suggested by various authors, and since the analysis of other relationships produced results which are not much different. Slightly modified, this expression will be written as follows:

$$U_c = A_c\left[e^{-\frac{v\sigma_1^2(1-\frac{\sigma}{\sigma_0})^2}{2GkT}} - e^{-\frac{v\sigma_1^2(1+\frac{\sigma}{\sigma_0})^2}{2GkT}}\right], \qquad (7)$$

where U_s = the rate of plastic deformation by slip;

A_s = the constant proportional to the number of sites where elementary acts of slip may originate and the constant of the mean macroscopic deformation of the specimen corresponding to the course of one elementary act;

v = the volume covered by the variation in stress;

σ_1 = theoretical shearing strength;

σ_0 = yield strength at absolute zero temperature;

σ = effective stress;

G = modulus of tangential elasticity;

k = Boltzmann constant;

T = absolute temperature;

e = the base of natural logarithms.

We will introduce the designations $\frac{\nu\sigma_1^2 N}{2G} = Q_0$, $kN = R$,

where Q_0 = the activation energy of the process of slip at zero stress;

N = Avogadro's number;

R = universal gas constant.

After a few transformations and taking logarithms, we obtain the expression

$$\lg U_c = \lg A_c - B\left(1 - \frac{\sigma}{\sigma_0}\right)^2 \lg e + \lg\left[1 - e^{-4B\frac{\sigma}{\sigma_0}}\right], \qquad (8)$$

where

$$B = \frac{Q_0}{RT}.$$

The general course of the log of rate-stress curve at a constant temperature is shown in Figure 4; in plotting this graph, we assumed the values of log A_e = 10 and B = = 20.

In all our further discussions, we will consider σ_0 the given constant value.

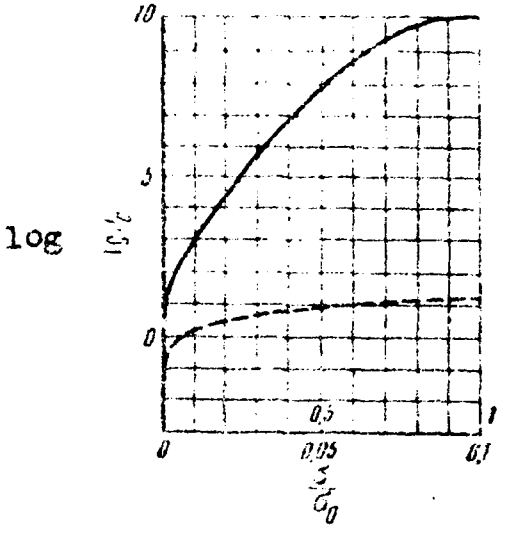

Figure 4. Relationship between the log of plastic deformation rate-stress, determined from Expression (8) (the continuous line corresponds to the upper scale on the axis of abscissas, the dotted line to the lower).

As can be seen from the graph, in the region of relatively high stresses there is a strong (close to parabolic) dependence of the log of plastic deformation rate on stress. But in the region of relatively small stresses, the trend of the curve is similar to the trend of the curve examined earlier for the case of diffusion plasticity. Particularly, as the stress changes by one order, the log of the plastic deformation rate varies by one logarithmic unity.

It is interesting to note that when only one type of process (diffusion plasticity by slip) occurs, the dependence curve of the log of rate on stress has a curvature of one sign, and its convexity faces the positive direction of the axis of ordinates.

In accordance with the fundamental propositions of the theory of slip, the activation energy, i.e., the value proportional to the minimum isothermic work necessary for the origination of one elementary act, is expressed as follows: $Q_o (1 - \sigma/\sigma_o)^2$. In other words, the activation energy must rapidly increase with the reduction of applied stress; specifically, according to the parabolic law. Within the bounds of this theory, this dependence will be the actual dependence of activation energy on applied stress.

Meanwhile, if we are to determine the activation energy experimentally from the tangent of the inclination angle of the curve of the log rate of plastic deformation vs. the reciprocal of temperature, we obtain a different relationship between the activation energy and stress even if we remain within the bounds of this theory. This is explained by the fact that Expression (7) contains two exponential terms which depend on temperature. The range of the temperature variation within which the tests are conducted is usually not wide, and with the variation of the temperature within that range Expression (8), depicted in coordinates (Log$\dot{\varepsilon}$, 1/T), will differ little from a straight line. It would therefore appear that the magnitude of activation energy determined from the tangent of the inclination angle would give the true dependence of the activation energy on stress. However, this is not so. In fact, let us determine the activation energy from Expression (8), using Expressions (3) and (4). Then, for Q_o -- which will be thus determined and will further be called, conventionally, "effective" activation energy -- we obtain:

$$Q_\sigma = Q_0\left[\left(1-\frac{\sigma}{\sigma_0}\right)^2 - \frac{4\frac{\sigma}{\sigma_0}}{e^{4B\frac{\sigma}{\sigma_0}}-1}\right]. \qquad (9)$$

Particularly, in an extreme case of a stress tending to zero, we will have

$$\lim_{\frac{\sigma}{\sigma_0}\to 0} Q_\sigma = Q_0 - RT < Q_0. \qquad (10)$$

It is already obvious from the latter relationship that (within the bounds of this theory) the activation energy determined from the tangent of the inclination angle will be less than the true value of the activation energy.

Figure 5 shows the trend of the curve for ratio Q_σ/Q_0 vs. ratio σ/σ_0 calculated for various values of parameter B. The dotted curve depicts the trend of the "true" activation energy (its further extent shows that its trend coincides with the trend of the curve referred to for the value B = 20).

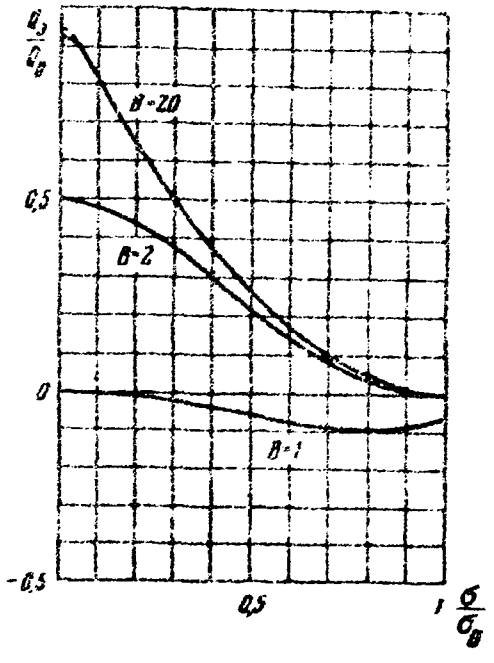

Figure 5. The relationship between the activation energy and the stress, determined from the Bekker-Orovan Expression (8) for various values of parameter B.

The following conclusions can be made from examination of this graph: (1) the "true" as well as the "effective" activation energies increase with the decrease in stress; (2) the lower the value of parameter B and the lower the stress, the more the "effective" activation energy deviates from the "true".

Assuming that Expres , is valid, our discussions show the following:

(1) the "true" activation energy can either be equal to or greater (but not smaller) than the "effective" activation energy determined from the tangent of the inclination angle;

(2) the "effective" activation energy will be the closer to the "true" activation energy as the stress is the higher and the parameter B the greater, i.e., the lower the temperature in comparison with the Q_0/R value. Besides, it follows from the above discussions that in using activation energy values determined from experimental data we must be cautious in judging the validity of either theory when there is reason to assume that the rate of the process under study cannot be expressed by one exponential term which depends on temperature.

Analogous discussions can proceed concerning the initial ordinate log A_e. Indeed, as has already been said, in considering the dependence of the log of rate on the reciprocal of temperature in a narrow interval of temperatures, we will obtain for each value a segment of the straight line. Continuing these segments to their intersection with the axis of ordinates, we will be able to determine the value of the initial ordinate log A_e for every stress. Generally speaking, these values will not represent constants and will depend on the magnitude of stress.

The initial ordinate (see Figure 2) can be determined from the following expression:

$$\lg A_e = \frac{Q_0}{\mu T} \lg e + \lg U. \qquad (11)$$

If we use Expressions (8) and (9), we can determine the dependence of log A_e/A_0 on stress for our case in the form

$$\lg \frac{A_e}{A_0} = -\frac{4B\frac{\sigma}{\sigma_0}\lg e}{e^{4B\frac{\sigma}{\sigma_0}}-1} + \lg\left(1 - e^{-4B\frac{\sigma}{\sigma_0}}\right). \qquad (12)$$

Within the bounds of the theory under consideration, A_0 is an essentially constant value; the dependence of $\log A_e/A_0$ on stress will, therefore, characterize the dependence of A_e on stress.

Figure 6 shows the relationship between $\log A_e/A_0$ and stress for various values of parameter B. It follows from the graph that if the theoretical notions under consideration are correct, the experimentally determined initial ordinate $\log A_e$ for the case of slip must decrease at a relatively low rate with the reduction in stress. This ordinate remains approximately constant in the region of high stresses but decreases in the region of low stresses by one logarithmic unity with the variation in stress by one order; i.e., just as this takes place in the earlier case of diffusion plasticity. In other words, in both cases the value A_e must not decrease more rapidly than stress.

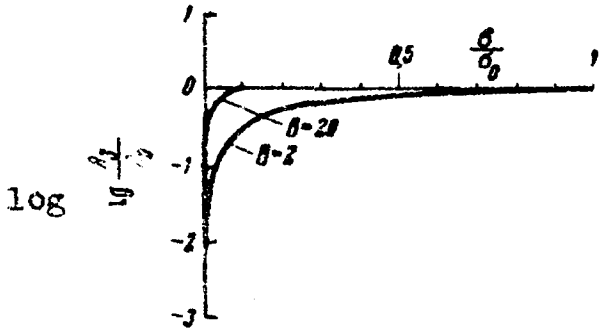

Figure 6. Relationship between $\log A_e/A_0$ and stress, determined from Expression (12) for various values of parameter B.

Let us turn now to the case of joint simultaneous participation of two processes in plastic deformation:

slip and diffusion plasticity.

Assuming that the resultant rate of plastic deformation U equals the sum of rates of both processes, we obtain

$$U = U_c + U_g. \tag{13}$$

Using for U_c and U_g Expressions (7) and (1) and introducing designations

$$\frac{A_c}{A_g} = A', \quad \frac{Q_1}{Q_c} = C, \text{ we obtain}$$

$$U = A_c e^{-B\left(1-\frac{\sigma}{\sigma_0}\right)^2}\left(1-e^{-4B\frac{\sigma}{\sigma_0}}\right)\left[1+\frac{1-e^{-2\pi BC\frac{\sigma}{\sigma_0}}}{2A'e^{-B\left[\left(1-\frac{\sigma}{\sigma_0}\right)^2-C\left(1-\pi\frac{\sigma}{\sigma_0}\right)\right]}\left(1-e^{-4B\frac{\sigma}{\sigma_0}}\right)}\right]. \tag{14}$$

After some transformations and taking a logarithm, we finally obtain

$$\begin{aligned} \lg U = \lg A_c - B\left(1-\frac{\sigma}{\sigma_0}\right)^2 \lg e + \lg\left(1-e^{-4B\frac{\sigma}{\sigma_0}}\right) + \\ + \lg\left[1+\frac{1-e^{-2\pi BC\frac{\sigma}{\sigma_0}}}{2A'e^{-B\left[\left(1-\frac{\sigma}{\sigma_0}\right)^2-C\left(1-\pi\frac{\sigma}{\sigma_0}\right)\right]}\left(1-e^{-4B\frac{\sigma}{\sigma_0}}\right)}\right]. \end{aligned} \tag{15}$$

As an example, Figure 7 gives the trend of the curve for log of total deformation rate vs. stress (to be more exact, vs. relation σ/σ_0) at a constant temperature. In calculating the trend of this curve, the following values were assumed: $\log A_B = 10$; $B = 80$; $C = 0.3$; $A' = 10^{10}$.

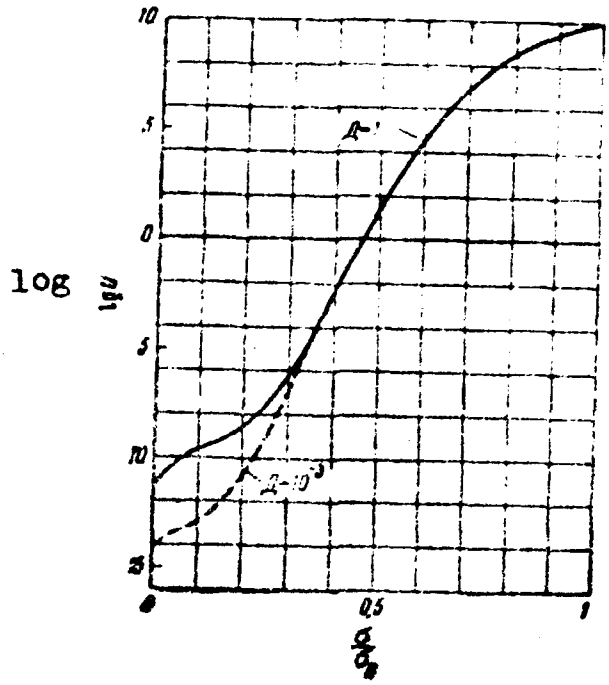

Figure 7. The relationship between the log of plastic deformation rate and stress, determined from Expression (15) for the simultaneous course of two processes ($B = 80$; $A' = 10^{10}$; $C = 0.3$; $\log A_g = 10$; $\alpha = 1$ and $\alpha = 10^{-3}$).

As can be seen from the graph, the individual segments of the given curve have curvatures of different signs, in contrast to the curves examined before (see Figures 1 and 4). In other words, the curve which corresponds to the simultaneous course of both processes (diffusion plasticity and slip) has a sector whose convexity faces the negative direction of the axis of ordinates.

Determining, just as before -- according to Eqs. (3) and (4) from Expression (15) -- the magnitude of "effective" activation energy Q_e, i.e., the magnitude of activation energy determined from the tangent of the inclination angle of the small sector of the curve, we obtain

$$\frac{Q_\sigma}{Q_0} = \left(1 - \frac{\sigma}{\sigma_0}\right)^2 - \frac{4\frac{\sigma}{\sigma_0}}{e^{4B\frac{\sigma}{\sigma_0}} - 1} + \tag{16}$$

$$+ \frac{\left(e^{2ABC\frac{\sigma}{\sigma_0}} - 1\right)\left[C\left(1 - A\frac{\sigma}{\sigma_0}\right) - \left(1 - \frac{\sigma}{\sigma_0}\right)^2 + \frac{4\frac{\sigma}{\sigma_0}}{e^{4B\frac{\sigma}{\sigma_0}} - 1}\right] - 2AC\frac{\sigma}{\sigma_0}}{2A'e^{-B\left[\left(1+\frac{\sigma}{\sigma_0}\right)^2 - C\left(1+A\frac{\sigma}{\sigma_0}\right)\right]}\left(e^{4B\frac{\sigma}{\sigma_0}} - 1\right) + e^{2ABC\frac{\sigma}{\sigma_0}} - 1}.$$

When $\sigma/\sigma_0 \to 0$, the limit value of this expression will equal

$$\lim\left(\frac{Q_\sigma}{Q_0}\right)_{\frac{\sigma}{\sigma_0}\to 0} = 1 - \frac{1}{B} - \frac{AC(1-C)}{4A'e^{-B(1-C)} + AC}. \tag{17}$$

It is appropriate to remind here of the physical meaning of the parameters appearing in Expressions (16) and (17):

$A' = A_s/A_d$ is the relation of the maximum possible values for the rate of slip and diffusion plasticity;

$B = Q_0/RT$ is the magnitude reciprocal to the absolute temperature of the experiment at the given value of σ_0;

$C = Q_1/Q_0$ is the relation of the values of the activation energy of diffusion plasticity and slip, at stresses equal to zero and at absolute temperature; and

$A = \alpha V_a \sigma_0/2Q_1$ is the magnitude proportional to the coefficient of local overstrain at given values for V_a, σ_0, and Q_1.

In particular: the value $A = 1$ corresponds to the local stresses of the order of the so-called theoretical shearing strength, i.e., the order that is numerically close to the modulus of tangential elasticity; the value $A = 10^{-3}$ corresponds to the local stresses which are of the same order of magnitude as the macroscopically applied stress.

Without going into a detailed analysis of this

expression, we will only point out that the "effective" activation energy that corresponds to the values of a stress close to zero satisfies the condition

$$Q_1 - RT \leqslant |Q_\sigma| \underset{\sigma \to 0}{\leqslant} Q_0 - {}_1RT.$$

i.e., this energy is not less than $Q_1 - RT$.

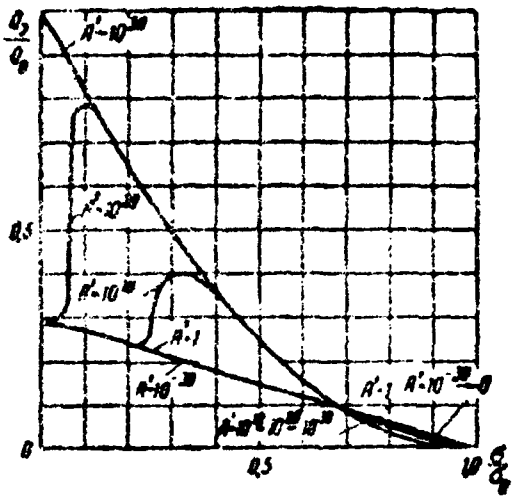

Figure 8. Dependence of activation energy on stress determined from Expression (16) for simultaneous course of two processes (B = 80; C = 0.3; A_1 = 1 at various values of A').

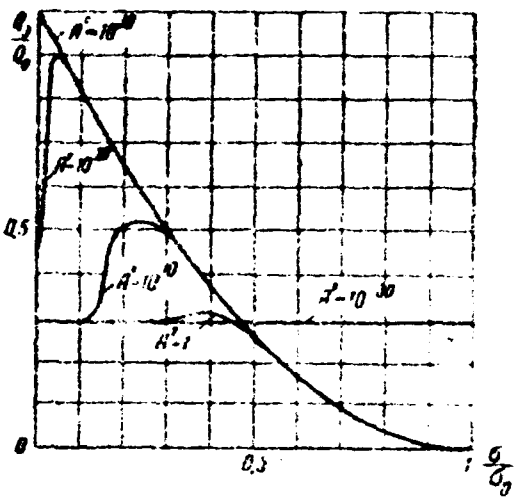

Figure 9. Dependence of activation energy on stress determined from Expression (16) for simultaneous course of two processes (B = 80; C = 0.3; $A_1 = 10^{-3}$ at various values of A').

Figures 8 and 9 give curves depicting the dependence of the "effective" activation energy on stress for two values of parameter A_1 (A_1 = 1 and $A_1 = 10^{-3}$) and for various values of parameter A' (from $A' = 10^{-3}$ to $A' = 10^{30}$). The values of parameter A', which correspond to the curves, are plotted next to them. When $A' = 10^{30}$, i.e., $A_s = 10^{30} A_g$ (or $A_s \gg A_g$), there is an absolute predominance of the slip process. In this case (see Figures 8 and 9), Q_e/Q_0 and, consequently, the "effective"

activation energy monotonously increases with the reduction in stress. For stresses close to zero, Q approaches the value equal to $Q_0 - RT$, i.e., for stresses that differ little from zero, the "effective" activation energy is close to the value of the activation energy of a process of slip equal to zero.

When $A' = 10^{-30}$, i.e., when $A_S = 10^{-30} A_D$ (or $A_S \ll A_D$), and there is an absolute predominance of the process of diffusion plasticity, the process of slip does not manifest itself. If the magnitude of the local stress-es is of the same order as the externally applied stress ($C = 10^{-3}$; see Figure 9), then the dependence of Q_e/Q_0 on σ/σ_0 in the considered variation of stresses ($0 \leq \sigma/\sigma_0 \leq 1$) is depicted by a horizontal straight line.

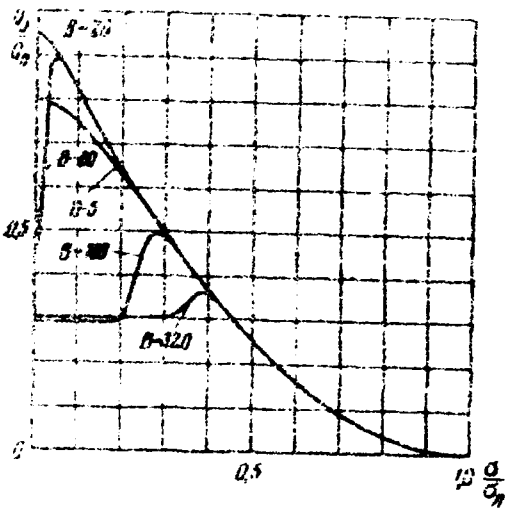

Figure 10. The relationship between the activation energy and stress, determined from Expression (16) for a simultaneous course of two processes ($A' = 10^{20}$, $C = 0.3$ and $\Delta = 10^{-3}$ for various values of quantity B).

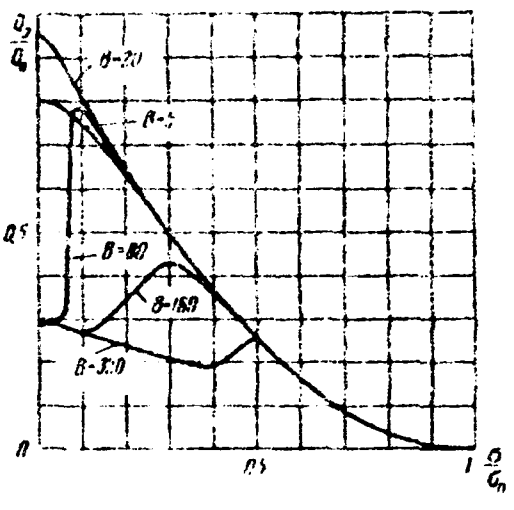

Figure 11. The relationship between the activation energy and stress, determined from Expression (16) for the simultaneous course of two processes ($A' = 10^{30}$, $C = 0.3$ and $\Delta = 1$ for various values of quantity B).

In other words, for all values of stress ($0 \leq \sigma \leq \sigma_0$), the "effective" activation energy is close to the value of the activation energy of diffusion plasticity in an unstressed material at an absolute zero temperature.

For the case $\Delta = 1$ which corresponds to high local stresses, Q_e/Q_o monotonously increases with the decrease in σ/σ_o (see Figure 8; $A' = 10^{-30}$).

With the decrease in stress, the "effective" activation energy, which in this case is close to the value of the activation energy of diffusion plasticity, increases and when $\sigma/\sigma_o = 0$, it reaches the value equal to $Q_1 - RT$, i.e., it becomes close to the value of activation energy in an unstressed material.

At values of $A' = 10^{10}$ and $A' = 10^{20}$, i.e., in cases when there is no absolute predominance of any of the processes of deformation (either slip or diffusion plasticity), the curves showing the dependence of Q_e/Q_o on σ/σ_o have a maximum. The right segment of these curves (where Q_e/Q_o increases with the reduction in stress) coincides on its either greater or smaller extension with the curve corresponding to the absolute predominance of the process of slip. With a further decline in stress, the curve showing the dependence of Q_e/Q_o on σ/σ_o goes down and, in the case where the values of A' are not too high, it emerges on the curve that corresponds to the absolute predominance of the process of diffusion plasticity. When the stress is zero, the "effective" activation energy can have values ranging between $Q_1 - RT$ and $Q_o - RT$, depending on the magnitude of parameter A'.

Figures 10 and 11 give curves showing the dependence of the "effective" activation energy on stress for two values of parameter Δ ($\Delta = 1$ and $\Delta = 10^{-3}$) and for various values of parameter B (from B = 5 to B = 320). When the values of this parameter are high (B = 320, 160, and 80), the curves showing the dependence of Q_e/Q_o on σ/σ_o have a maximum whose width and height grow with the reduction in the value of B. When the values of B are 20 and 5, the trend of the considered curves coincides with the trend of those corresponding to an absolute predominance of the process of slip. When the stress is reduced to zero, the limit value that the "effective" activation energy Q_e tends to then depends on the magnitude of parameter B (if the parameter A' is constant). In the case where the values of parameter B are high (B = 320 and B = 160), i.e., when $Q_o \gg RT$, the limit value coincides with the value $Q_1 - RT$, i.e., the limit value is close to the activation energy of the process of self-diffusion at a stress equal to zero. If the values of B are low (B = 20 and B = 5), the limit value equals $Q_o - RT$, i.e., close to the

activation energy of the process of slip at a stress equal to zero. When the values of B are intermediate (B = 80), the limit value lies between Q - RT and Q_0 - RT.

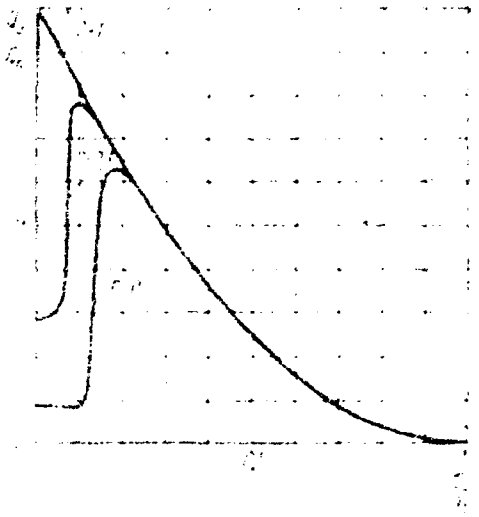

Figure 12. The relationship between the activation energy and stress, determined from Expression (16) for the simultaneous course of two processes ($A' = 10^{20}$, B = = 80, and $\Delta = 10^{-3}$ for various values of quantity C).

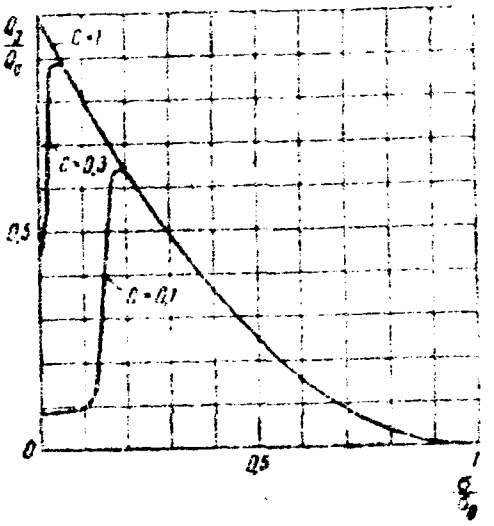

Figure 13. The relationship between the activation energy and stress, determined from Expression (16) for the simultaneous course of two processes ($A' = 10^{20}$, B = 80, and $\Delta = 1$ for various values of quantity C).

Figures 12 and 13 give curves showing the dependence of Q_e/Q_0 on σ/σ_0 for two values of parameter Δ ($\Delta = 1$ and $\Delta = 10^{-3}$) and for three different values of parameter C (C = 0.1, 0.3, and 1). Naturally, there is a maximum only for the curves corresponding to the values of $C = Q_1/Q_0 < 1$, i.e., in the case where the value of the activation energy of diffusion plasticity (at an absolute temperature and stresses equal to zero) is less than the value of the activation energy of the process of slip that corresponds to the same condition.

In completing the above conditions (when $C < 1$, and the parameters B and A are not too high and not too low),

and as the stress decreases the "effective" activation energy must first increase, pass through the maximum, and then decrease, gradually approaching a certain limit value. Such a dependence of the activation energy on the variation in stress is natural. In the presence of several processes possessing various activation energies (and a varying dependence of activation energy on stress), the experimentally observed value of the activation energy will be closer to the value of the activation energy of the process that will be predominant under these conditions.

If both the temperature and the value of stress are given, a relative share of the total rate of plastic deformation, which depends on the course of either process, will be determined by the value of the activation energy of this process at the given stress, by the greatest number of sites where the elementary act of the process can originate, and finally, by the magnitude of macroscopic deformation that results during the occurrence of one elementary act. In examining the trend of the curve $\lg A_e/A_s$ for the case of a simultaneous participation of the processes of slip and diffusion plasticity according to Expression (11), we obtain

$$\lg \frac{A_e}{A_c} = \lg U + \frac{Q_e}{RT} \lg e - \lg A_c. \qquad (18)$$

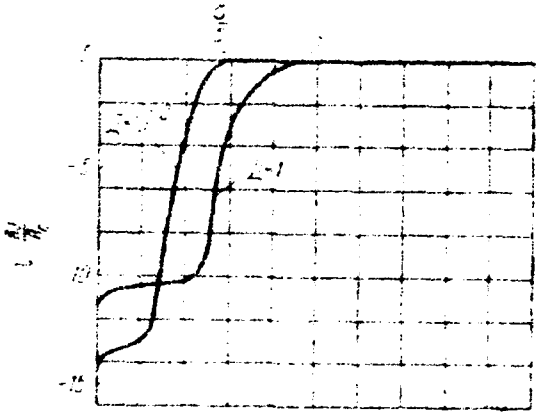

Figure 14. The relationship between the value $\log A_e/A_s$ and stress, determined from Expression (18) for the simultaneous course of two processes ($B = 80$, $C = 0.1$, $A = 1$, and $A = 10^{-3}$).

As an example, Figure 14 shows the trend of curve of log A_e/A_s vs. σ/σ_0 for parameter values: $B = 80$, $A' = 10$, $C = 0.1$, log $A_s = 10$, $\beta = 1$ and $\alpha = 10^{-3}$. From the examination of this graph, we can see that log A_e/A_s does not vary at first with a reduction in stress; then it begins to decline, and with a realtively small variation in stress, shows a variation by several logarithmic unities which corresponds to the decrease of log A_e/A_s by several orders. In other words, with the participation of two processes, the value A_e/A_s can strongly decline with a slight variation in stress; this has not been observed in the cases involving the course of one of the processes studied previously.

Of course, the discussions cited in this article have only a qualitative nature. They show, however, that the experimental study of the dependence of the rate of plastic deformation and the activation energy on stress may produce information necessary for the evaluation of the mechanism of the processes participating in plastic deformation.

On the mechanism of plastic deformation during the relaxation of stresses

The above-cited discussions do not take into account the variation in the state of the material during the process of deformation. In other words, the above relationships are, as a matter of fact, valid for a case when the state of the material remains constant in the process of deformation.

Inasmuch as the magnitude of plastic deformation occurring during the process of relaxation of stresses is small, we may assume that the state of the material changes little in the process of testing for relaxation and, consequently, will have little bearing on the behavior of the material during testing. In this connection, the dependences determined from the data of the relaxation tests will quite sufficiently satisfy the conditions of constancy in the state of the material in the process of deformation.

To determine the dependence of the rate of plastic deformation and the activation energy on stress, we used the results obtained in testing specimens of EI-395

Steel*.

The specimens were tested on the machines designed by the UFAN** (Academy of Sciences, Ural Branch) at various temperatures ranging from 665 to 790° and at an initial stress equal to 11 kg/mm^2; the duration of the tests amounted to 100 hours.

The selection of this steel was justified by the following considerations:

1. The EI-395 steel has a high yield strength (about 22.8 kg/mm^2 at 750°); the initial stress of 11 kg/mm^2 for all testing temperatures was, therefore, far below the yield strength.

2. The fact that the specimen material of this steel was submitted to a preliminary deformation at room temperature was contributory in the sense that it ensured to a considerable degree the occurrence of possible aging processes during the continuous heat-up of the specimen before the test. This has reduced a possible distorting influence of aging on the test results.

3. For this steel, there were data available (35) in literature on the value for the modulus of normal elasticity for the temperatures employed in our tests.

In order to plot the relationships sought for, it was necessary, first of all, to determine the dependence of the rate of relaxation on the operating stress from the initial diagrams for relaxation. The determination of the relaxation rate directly from the initial diagrams can lead to great errors in determining the rate value. As a matter of fact, on the diagram sectors corresponding to high relaxation rates, the curve is at a slight angle to the axis of loads; on the sectors corresponding to low relaxation rates, the curve makes a small angle with the time axis.

---

*The testing of this steel was carried out in accordance with the socialist-collaboration agreement with the Ural Plant for Construction of Heavy Machinery, imeni S. Ordzhonikidze.

**See the article by S. Averkiyev, G. N. Kolesnikov, A. I. Moiseyev, and M. V. Yakutovich in this collection.

It is known that the determination of the tangent for small angles involves great errors. We have therefore employed the method suggested by Shevenar (36).

With that end in view, we have first of all determined from the initial diagrams the values for the operating stress σ_t that had corresponded to the given duration of relaxation t. We then calculated the values for $\log (t + t_o)$, whereas the arbitrary value t_o was so selected that the used-up relaxation curve superposed in the coordinates $[\sigma, \log(t + t_o)]$ differed as little as possible from a straight line. Selecting the corresponding scales for the stress and $\log(t + t_o)$, we were able to dispose the replotted curve in such a way as to obtain an angle with the axis of coordinates similar to that of 45°.

It is evident that in these coordinates the tangent of the inclination angle at this point is expressed as $d\sigma/d \log(t + t_o)$. Determining for the replotted curve the tangents of the inclination angles at the points corresponding to the given stress values, it is possible to obtain the essential values for the relaxation rate with the help of expression

$$\frac{d\sigma}{dt} = \frac{\lg e \cdot d\sigma}{(t + t_o)\, d \lg (t + t_o)} \qquad (19)$$

The values for the common logarithm of the relaxation rate log $d\sigma/dt$ were determined from the obtained absolute values for the relaxation rate $d\sigma/dt$. The data obtained by processing the diagrams for log $d\sigma/dt$ are given in Table 1.

From the data of this table we plotted the dependence of the relaxation rate on the operating stress for each temperature (see Figure 15). The relatively wide spread of points on the curve corresponding to 750° is caused by the substantial variations in temperature during testing; these variations are related to the sharp variation in the voltage of the network.

The further processing has involved only the sectors of the curves where the value for the operating stress had exceeded 3 kg/mm^2.

These segments of the curves were used for the

Determination of the values for the rate of plastic deformation $d\varepsilon/dt$ that corresponded to the given values for the operating stress. The plastic deformation rate $d\varepsilon/dt$ is associated with the relaxation rate $d\sigma/dt$ by the relationship

$$\frac{d\varepsilon}{dt} = \frac{1}{E_t}\frac{d\sigma}{dt}, \qquad (20)$$

where E_t is the modulus of normal elasticity at testing temperature.

Therefore, to determine the log $d\varepsilon/dt$ we used the expression

$$\lg \frac{d\varepsilon}{dt} = \lg \frac{d\sigma}{dt} - \lg E_t \qquad (21)$$

Since the initial stress is approximately the same in all tests, each defined value for operating stress also fully agrees with a defined value of total plastic deformation experienced by the specimen at the instant the given value of operating stress has been determined. In other words, the values for the deformation rate determined in the above manner for various temperatures corresponded not only to one and the same operating stress but also to the same value of plastic deformation.

In calculating the values for the log of deformation rate, the curves corresponding to the testing temperatures 795 and 799° were combined into one, since the difference in testing temperature was not great. For this purpose the mean value for the relaxation rate was found from the relaxation rate values corresponding to both curves; the rate of plastic deformation was then calculated from the mean value of relaxation rate.

The values for log $d\varepsilon/dt$, so determined, are given in Table 2. Figure 15 gives curves showing the dependences of the log of the rate of plastic deformation on the operating stress for various testing temperatures. It is evident from Figure 15 that the curves (particularly those corresponding to low temperatures) have a distinctly pronounced segment whose convexity faces the negative values of the axis of ordinates.

Table 1

The relaxation of stresses in EI-695 steel at various temperatures

665°			695°			750°		
Time, hours	Stress, kg/mm²	log dσ/dt	Time, hours	Stress, kg/mm²	log dσ/dt	Time, hours	Stress, kg/mm²	log dσ/dt
0,000	11,25	1,25	0,00	10,52	—0,983	0,000	11,75	1,27
0,084	11,03	1,05	0,10	10,44	—0,958	0,008	11,40	1,45
0,1	10,99	0,69	0,19	10,21	—0,955	0,021	11,10	1,09
0,042	10,92	0,45	0,88	9,84	—1,20	0,042	10,92	0,88
0,063	10,84	0,25	1,58	9,45	—0,31	0,063	10,73	0,92
0,084	10,81	0,20	2,28	9,12	—0,49	0,084	10,50	0,88
0,126	10,77	0,12	3,68	8,80	—0,58	0,126	10,27	0,85
0,192	10,71	0,06	5,08	8,34	—0,57	0,170	9,97	0,78
0,30	10,35	—0,48	7,17	7,73	—0,68	0,890	7,99	0,17
1,62	10,16	—0,71	10,78	7,15	—0,84	1,60	7,22	—0,058
2,33	9,86	—0,58	16,16	6,74	—0,95	2,32	6,58	—0,22
3,08	9,72	—0,69	17,61	6,35	—0,95	3,06	6,32	—0,34
3,81	9,63	—0,78	21,14	6,12	—0,97	3,75	6,05	—0,42
4,5	9,43	—0,87	24,6	5,69	—1,00	5,18	5,52	—0,49
5,66	9,11	—0,95	28,1	5,38	—1,06	7,34	4,85	—0,71
7,1	8,73	—1,12	31,6	5,06	—1,11	11,02	4,46	—1,03
10,6	8,48	—1,21	35,1	4,77	—1,14	14,49	4,19	—1,05
13,5	8,26	—1,31	38,5	4,55	—1,19	18,07	4,07	—1,54
17,1	8,06	—1,34	42,0	4,24	—1,22	21,67	3,96	—1,69
21,1	7,72	—1,27	49,1	3,98	—1,34	29,02	3,72	—1,46
27,7	7,58	—1,47	56,1	3,70	—1,42	36,0	3,42	—1,38
34,5	7,07	—1,35	68,0	3,45	—1,46	44,6	3,05	—1,36
38,6	6,80	—1,35	70,0	3,18	—1,51	50,3	2,74	—1,40
48,6	6,45	—1,38	77,0	2,92	—1,57	58,1	2,38	—1,33
60,1	6,15	1,43	84,0	2,76	—1,67	65,3	2,20	—1,42
71,2	5,88	—1,48	90,9	2,66	—1,73	71,9	1,98	—1,68
84,1	5,66	—1,52	92,7	2,62	—1,74	79,0	1,90	—2,04
87,7	5,43	—1,51	—	—	—	86,2	1,86	—2,42
98,8	5,08	—1,49	—	—	—	99,7	1,83	—2,90

Table 1 (conclusion)

The relaxation of stresses in EI-395 steel at various temperatures

795°			799°		
Time, hours	Stress, kg/mm²	log dσ/dt	Time, hours	Stress, kg/mm²	log dσ/dt
0,000	10,46	1,65	0,000	11,00	1,92
0,004	10,30	1,58	0,004	10,65	1,77
0,012	10,00	1,46	0,012	10,28	1,60
0,020	9,65	1,40	0,020	9,97	1,48
0,040	9,40	1,24	0,040	9,46	1,30
0,061	9,15	1,15	0,061	9,10	1,21
0,101	8,74	1,02	0,100	8,51	1,09
0,171	7,90	0,87	0,167	7,88	0,96
0,279	7,25	0,65	0,275	6,95	0,76
0,386	6,96	0,44	0,382	6,32	0,59
0,494	6,72	0,29	0,486	6,16	0,46
0,709	6,35	0,15	0,703	5,70	0,21
0,925	6,0	0,041	0,921	5,40	0,068
1,249	5,73	—0,082	1,24	5,07	—0,13
1,783	5,45	—0,23	1,78	4,76	—0,35
2,320	5,20	—0,34	2,32	4,57	—0,46
2,856	5,00	—0,43	2,85	4,38	—0,55
3,396	4,81	—0,50	3,39	4,21	—0,52
4,470	4,47	—0,70	4,47	3,86	—0,61
5,550	4,36	—0,87	5,55	3,59	—0,68
7,700	4,14	—0,97	7,70	3,22	—0,79
9,880	3,91	—1,06	9,86	2,84	—0,85
11,99	3,69	—1,10	11,99	2,54	—0,92
14,08	3,46	—1,14	14,08	2,26	—0,98
16,29	3,42	—1,20	16,29	2,04	—1,04
21,67	3,05	—1,31	21,67	1,69	—1,17
27,02	2,71	—1,38	27,02	1,51	—1,20
32,42	2,45	—1,39	32,42	1,13	—1,19
37,82	2,08	—1,33	37,82	0,76	—1,16
40,47	1,88	—1,35	44,40	0,00	—1,12
53,97	1,69	—1,42			
64,67	1,18	—1,30			
75,47	0,49	—1,16			
81,70	0,00	—1,06			

Table 2

The logarithms of plastic deformation rate log dε/dt in relation to operating stress σ and testing temperature

σ, kg/mm²	log dε/dt				σ, kg/mm²	log dε/dt			
	797° (mean value)	750°	695°	665°		797° (mean value)	750°	695°	665°
11	−2,17	−2,80	—	−3,41	6	−3,78	−4,42	−4,99	−5,56
10	−2,50	−3,24	−4,19	−4,68	5	−4,27	−4,74	−5,13	−5,57
9	−2,84	−3,57	−4,48	−5,10	4	−4,75	−5,11	−5,30	—
8	−3,05	−3,86	−4,70	−5,40	3	−5,04	−5,50	−5,58	—
7	−3,32	−4,15	−4,86	−5,51					

According to the above discussions, this fact indicates the participation of two processes in the plastic deformation.

Figure 16 exhibits curves showing the dependence of the log of plastic deformation rate on the reciprocal of absolute temperature for various values of operating stress. Against each curve there is a constant value of operating stress, and, consequently, a constant value of plastic deformation (see above). Determining from these curves the value of the activation energy we were able to construct the curve for the dependence of activation energy on operating stress. The obtained values for the activation energy are summarized in Table 3.

Table 3

The dependence of the experimentally determined activation energy Q_e on the operating stress σ

σ, kg/mm^2	Q_e, cal/mol	σ, kg/mm^2	Q_e, cal/mol
11	47 500	6	60 300
10	75 400	5	44 700
9	76 400	4	28 900
8	77 100	3	20 300
7	73 000		

Figure 17 gives the curve showing the experimentally determined dependence of the activation energy on the operating stress. The spread of the experimental points in constructing the dependence of log $d\varepsilon/dt$ on $1/T$ has naturally resulted in the spread of values in determining the activation energy, since the rectilinear sector could have been plotted by various methods. The spread of values for the activation energy on Figure 17 is plotted by vertical segments.

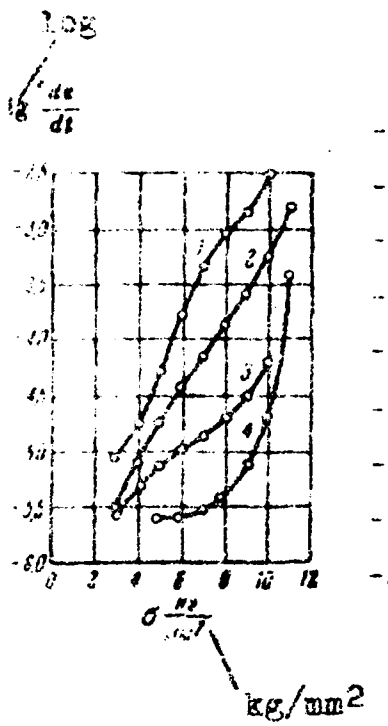

Figure 15. Curves of experimental dependence of the log of plastic deformation rate log dε/dt on stress:
1 -- σ_0 mean = = 10.73 kg/mm², T = 797°;
2 -- σ_0 = = 11.75 kg/mm², T = 750°;
3 -- σ_0 = = 10.52 kg/mm², T = 695°;
4 -- σ_0 = = 11.20 kg/mm², T = 665°.

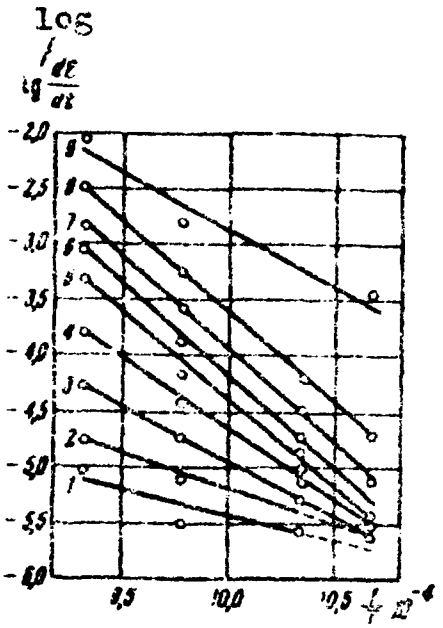

Figure 16. Curves of experimental dependence of the log of plastic deformation rate log dε/dt on the reciprocal of absolute temperature 1/T at an operating stress:
1 -- 3 kg/mm²;
2 -- 4 kg/mm²;
3 -- 5 kg/mm²;
4 -- 6 kg/mm²;
5 -- 7 kg/mm²;
6 -- 8 kg/mm²;
7 -- 9 kg/mm²;
8 -- 10 kg/mm²;
9 -- 11 kg/mm².

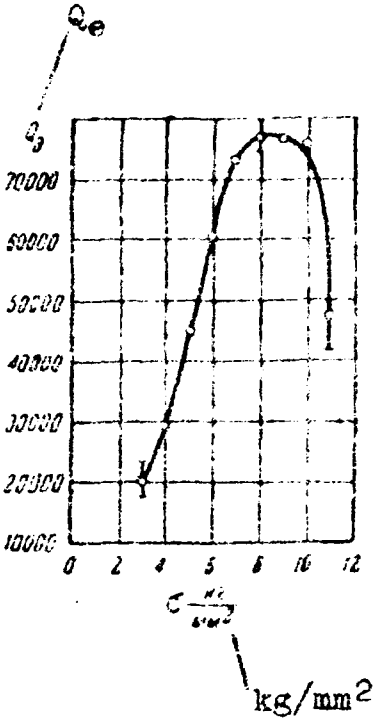

Figure 17. The experimental dependence of activation energy Q_e on σ.

Examining the curve shown in Figure 17 we see that with the decline in effective stress the activation energy at first grows, passes through the maximum, and then decreases. In accordance with the notions cited above, such a course of energy corresponds to the participation in the plastic deformation of two processes having different activation energy values and a different dependence of the activation energy on stress. At this point the value of activation energy which corresponds to a stress and an absolute temperature, both equal to zero, must be considerably below the value of the activation energy of the other process.

From the experimental data (see the curves in Figure 16) we determined the values for the initial ordinates log A_θ for various values of operating stress (Table 4). Figure 18 shows the dependence of log A_θ on the operating stress.

As can be seen from the graph in Figure 18, this curve is analogous by its nature to the curve for the dependence of activation energy on stress. There is no connection, however, between our previous discussions and the increase in the value of log A_θ with the reduction in stress (the right sector of the curve); this is obviously associated with the dependence of the activation energy Q_θ on temperature. It should be indicated that a similar behavior of the log A_θ value was observed by G. N. Kolesnikov (31) in studying the flow in the monocrystals of aluminum, i.e., in a case where no substantial participation of the process of diffusional plasticity could be expected.

Table 4

The dependence of the experimentally determined value of log A_e on the operating stress σ

σ, kg/mm^2	log A_e	σ, kg/mm^2	log A_e	σ, kg/mm^2	log A_e
11	7,32	8	12,35	5	4,64
10	12,60	7	11,26	4	1,02
9	12,44	6	8,34	3	—1,07

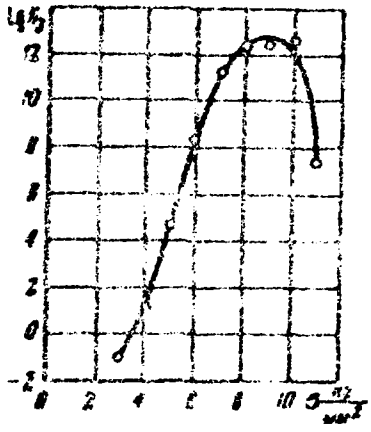

Figure 18. The experimental dependence of the log A_e value on stress σ.

It follows from what has been said above that the sharp drop of the log A_e value in the left portion of the curve representing the dependence of log A_e on stress can be explained by the participation in the process of plastic deformation of two different processes. The experimentally observed decrease of log A_e from 9 to 3 kg/mm^2 corresponds to a decrease of the value A_e by 10^{14}. It is obvious that such a strong variation of the value $A_e = A_s/A_g$ is attributable not so much to the difference in the values of the plastic deformations corresponding to the elementary act of one or another process, as to the substantial difference in the number of sites where the elementary acts of one or another process may originate.

From this viewpoint the experimentally observed variation in the value A_e substantiated the notions according to which the elementary acts of slip can originate in the entire volume of the grain whereas the elementary acts of diffusional plasticity can originate for the most part only in the grain regions having a distorted crystal lattice (such as the intergranular zones, etc.).

Conclusions

Summarizing the above, we arrive at the following conclusions.

1. The experimentally determined dependences of the rate of plastic deformation, activation energy, and the value log A_e on stress during the relaxation of stresses can be explained if we proceed from the notions on the participation of two processes in plastic deformation. At this point we must admit that, at stresses close to zero, the activation energy of one of the processes must be lower than that of the other processes.

2. On the basis of present conceptions of the physics of the mechanisms of plastic deformation, it is probably most correct to identify the process having a high activation energy -- at a stress close to zero -- with the process of slip, and to identify the other process with that of diffusional plasticity.

3. It follows from what has been said above that the predominant role in plastic deformation, occurring at the initial stage of the relaxation process under the conditions of our experiments, was played by the process of slip. With the reduction in the value of effective

stress, this role was gradually turned over to the process of diffusional plasticity. It is possible that in the case of very low initial stresses, when plastic deformation during the entire duration of the process of relaxation of stresses occurs only by diffusional plasticity, the latter will play the fundamental role even in the initial stage of the relaxation of stresses.

BIBLIOGRAPHY

1. Klassen-Neklyudov, M. V., News of the Academy of Sciences USSR, Department of Technical Physics (Izv. AN SSSR, OTN), No. 7, 1954.

2. Stepanov, A. V., and Donskoy, A. V., Journal of Technical Physics (ZhTF), Vol. 2, Issue 2, 1954.

3. Gorskiy, V. S., Fizicheskiy zhurnal Sovetskogo Soyuza (Journal of Physics of the Soviet Union), No. 8, 1935.

4. Oding, I. A., Izv. AN SSSR, OTN, No. 10, 1948.

5. Oding, I. A., "Vestnik mashinostroyeniya" (Herald of Machine Construction), No. 2, 1949.

6. Konobeyevskiy, S. T., Journal of Experimental and Theoretical Physics (ZhETF), Vol. 13, Issue 6, 1943.

7. Bochvar, A. A., Izv. AN SSSR, OTN, No. 5, 1948.

8. Frenkel, Ya. I., Vvedeniye v teoriyu metallov (Introduction to the Theory of Metals), Vtoroye izdaniye, (Second edition), Technical and Theoretical Literature Press (GIITL), Moscow -- Leningrad, 1950.

9. Yakutovich, M. V., O mekhanizme plasticheskoy deformatsiyi metallov (On the Mechanism of Plastic Deformation in Metals), Tr. In-ta fiziki metallov UFAN SSSR (Works of the Institute of Physics of Metals of the Academy of Sciences USSR, Ural Branch), Issue 12, Iz-vo AN SSSR (Press of the Academy of Sciences USSR), Moscow -- Leningrad, 1949.

10. Arkharov, V. I., Izv. AN SSSR, OTN, No. 11, 1951.

11. Shmid, Ye., and Boas, V., Plastichnost' kristallov (Plasticity of crystals), GONTI NKTP SSSR (State Institute

of Technology, the People's Commissarat of the Heavy Industry), Moscow -- Leningrad, 1938.

12. Yakovleva, E. S., and Yakutovich, M. V., Reports of the Academy of Sciences USSR, Vol. 90, No. 6, 1953.

13. Wilms, G. R., and Wood, W. A., J. Inst. Met., Vol. 16, 1949.

14. Crussard, C. H., Metal Treatment, autmn, 1947.

15. Hanson, D., and Wheeler, M. A., J. of the Inst. of Metals, Vol. 14, 1931.

16. King, R., Cahn, R. W., Chalmers, B., Nature, Vol. 161, No. 4096, 1948.

17. Dekhtyar, I. Ya., O mekhanizme diffuzii i polzuchesti v metallakh (On the Mechanism of Diffusion and Creep in Metals), Sb. nauchnykh rabot laboratorii metallofiziki (Symposium of Scientific Studies of the Laboratory of Physics of Metals), Press of the Academy of Sciences USSR, Kiyev, No. 2, 1950.

18. Osipov, K. A., Izv. AN SSSR, OTN, No. 9, 1940.

19. T'ing-Sui Ke, Phys. Rev., Vol. 72, No. 1, 1947.

20. T'ing-Sui Ke, Phys. Rev., Vol. 72, No. 1, 1947.

21. T'ing-Sui Ke, Journ. Appl. Physics, Vol. 20, No. 3, 1949.

22. Veynberg, B. P., ZhRFKhO (Journal of the Russian Physical and Chemical Society) chast' fizicheskaya (Section of Physics), Vol. 45, 2, 1913.

23. Johnson, E. A., Metallurgia, Vol. 29, No. 234, 1949.

24. Chit'kov, A. A., Hutnice' listy, racnik V Cislo 2, 1850.

25. Oding, I. A., Izv. AN SSSR, OTN, No. 12, 1949.

26. Oding, I. A., "Vestnik mashinostroyeniya", No. 3, 1948.

27. Oding, I. A., "Vestnik mashinostroyeniya", No. 5-6, 7-8, 9-10;
Oding, I. A., Relaksatsiya i polzuchest' metallov (Relaxation and Creep of Metals), TsNIITMASh (Central Scientific Research Institute of Heavy Machinery), Moscow, 1946.

28. Oding, I. A., Sorokin, O. V., and Sazanova, N. D., Reports of the Academy of Sciences USSR, Vol. 92, No. 3, 1953.

29. Frenkel, Ya. I., Journal of Experimental and Theoretical Physics (ZhETF), Vol. 9, Issue 10, 1939;
Frenkel, J., Journal of Physics, Vol. 11, No. 1, 1940.

30. Dekhtyar, I. Ya., O nekotorykh zakonomernostyakh diffuzii i mekhanicheskikh svoystv metallov (On Certain Relationships of Diffusion and Mechanical Properties of Metals), Sb. nauchnykh rabot laboratorii Metallofiziki, Izd-vo AN USSR (Press of the Academy of Sciences of the UkSSR), Kiyev, No. 3, 1952.

31. Kolesnikov, G. N., Plasticheskaya deformatsiya monokristallov alyuminiya v pervyy moment posle prilozheniya nagruzki (The Plastic Deformation in Crystals of Aluminum the Instant Following the Application of Load). Dissertatsiya (Dissertation). Institut metallofiziki i metallurgii Ural'skogo filiala AN SSSR (The Institute of Physics of Metals and Metallurgy of the Academy of Sciences, USSR, Ural Branch), Sverdlovsk, 1945.

32. Zener, K., and Khollomon, Dzh., Uspekhi fizicheskikh nauk (The Progress in the Physical Sciences), Vol. 31, Issue 1, 1947.

33. Zener, C., Acta Crystallographica, Vol. 3, part 5, 1950.

34. Orovan, E., Zs. f. Phys., Vol. 98, 1935.

35. Borzdyka, A. M., "Vestnik mashinostroyeniya", No. 2, 1948.

36. Chevenard, P., Rev. Met., Vol. 39, No. 11, 12, p. 321, 1942.

* * *

Relaxation of Stresses and Nonuniform Diffusional Mobility in Polycrystalline Austenitic Ferrum-Chromium-Nickel Alloys

By, V. I. Arkharov, S. I. Ivanovskaya, G. N. Kolesnikov, and A. I. Moiseyev

According to the idea which is the theme of the various studies in this collection, the high-temperature plastic deformation at low deformation rates is accomplished mainly by the diffusion mechanism and is localized in the boundary zones of the crystallites. This is particularly referred to relaxation processes at high temperatures.

It can be expected that there is a correlation between the intensity of relaxation and the diffusional mobility in the intergranular zones, and that the presence of an admixture in the heat-resistant alloy, capable of slowing down the relaxation, will at the same time reduce the diffusional mobility of the atoms in the alloy, at least of one of its chief constituents.

This will occur particularly when the impurity has a horophile nature, i.e., when it possess internal intergranular adsorption, since the influence of the impurity is intensified precisely in the regions where the plastic deformation develops.

Let us first dwell on a rough qualitative comparison of the results obtained in testing the diffusion of nickel in an austenitic alloy with those obtained in testing the relaxation of stresses in the same alloys.

The introduction of small additions of molybdenum and tungsten in alloys, containing 20 percent Cr and 10 percent Ni or 20 percent Cr and 20 percent Ni, has reduced the degree of the relative sharpness of the projections of the diffusional front along the intergranular zones. This fact could have been explained by a higher content of the alloying element in the intergranular zones as compared

to the body of the grain*.

From the standpoint of the notions related in the article by V. I. Arkharov and M. B. Yakutovich**, the concentration of the alloying element in the intergranular zones, which reduces the diffusional mobility, will entail the reduction in the intensity of the course of plastic deformation at the grain boundaries and also, consequently, the reduction in the intensity of relaxation of stresses, provided the latter is caused by the plastic deformation occurring in the boundary zones.

The data obtained from tests on relaxation of stresses on the same alloys confirm the above discussions. To prove this, let us turn to Figures 1-4 of the articley by G. N. Kolesnikov, A. I. Moiseyev, and M. B. Yakutovich***. These figures show curves which characterize the course of relaxation of stresses at various temperatures in ferrum-chromium-nickel alloys containing 20 percent Cr plus 10 percent Ni and also 20 percent Cr plus 20 percent Ni having various concentrations of either molybdenum or tungsten.

The examination of these figures shows that the curves corresponding to alloys with small additions of molybdenum and tungsten pass in the entire region of temperatures above the curves corresponding to alloys with neither molybdenum nor tungsten. This means that low concentrations of molybdenum and tungsten actually reduce the intensity in relaxation of stresses; consequently, the notions cited above are confirmed.

It is obvious that a maximum agreement of data on diffusional mobility with data on relaxation of stresses can be expected in a case in which the plastic deformation that occurs in the process of relaxation of stresses is concentrated near the grain boundaries, i.e., when the central sectors of the grain are practically not deformed.

It is natural that such deformation conditions may arise only at certain correlations between the stress effective in the specimen and the temperature of the

*See the article by V. I. Arkharov, S. I. Ivanovskaya, I. P. Polikarpova, and N. P. Chuprakova in this collection.
**Published in this collection.
***Published in this collection.

specimen; a substantial role is also played by the rate of the load increase in the process of loading.

In fact, the value of stresses sufficient to cause plastic deformation will be attained sooner in the regions of the grain adjoining the boundaries at slow (as a matter of principle, infinitely slow) loading of the material, because of overstresses which are created at the brain boundaries. The deformation will, therefore, begin precisely in these regions.

If the hardening coefficient is low (in principle, infinitely low), then, as we continue loading, a further increase of stresses effective in the grain regions more removed from the boundaries will become impossible. In other words, it will be impossible to increase the stress in the central grain regions to a point sufficient for the occurrence of plastic deformation.

The case is somewhat different at high (in principle, infinitely high) loading rates. While the rate of plastic deformation remains not too high, the occurrence of this deformation will not alter too much the distribution of stresses in the grain caused by the elastic deformation of the material. At a high loading rate, it is, therefore, possible to create stresses sufficient for the occurrence of an intensive plastic deformation even in the grain regions removed from the boundaries.

In applying the same external tension to specimens of two different materials having the same grain size but different yield strengths, it can be expected (if the loading rate is sufficiently high) that the plastic deformation will cover a greater portion of the grain volume in the material having a lower yield strength as compared to the material having a higher yield strength.

Since the yield strength decreases with the increase in temperature, it follows that a constant initial stress with an increase in test temperature will also result in an increase of the portion of the grain volume covered by the plastic deformation.

All tests on relaxation of stresses whose results are used in this article were conducted at one and the same value of initial stress (σ_0 = 13 kg/mm^2); the loading rate was the same in all cases and was equal to 3.2 kg/mm^2 per

minute; the temperatures of testing ranged from 350 to 800°.

The selected value of the initial stress for many of the tested materials at the highest test temperatures was above the yield strength of these materials. From what has been said, it can be expected that we will find the best agreement of results obtained in testing the diffusion of nickel in the investigated alloys with the results obtained in testing the relaxation of stresses on the same alloys if we use the data on relaxation of stresses taken at medium test temperatures.

In this case, the plastic deformation will cover a relatively small region of grain volume, adjoining the boundaries, while the intensity of plastic deformation will be high enough to cause a measurable value of relaxation of stresses.

Proceeding from the above, we used for the comparison the data referring to the relaxation of stresses at 550°.

The diffusional mobility of nickel in the intergranular transitional zones at a 550° temperature cannot be described in practice by the method of frontal diffusion employed in our study*; to obtain metallographic patterns suitable for measurements at this temperature would involve extremely protracted testing. For a comparison with the relaxation data, therefore, we had to use data on the diffusional mobility of nickel at a different (much higher) temperature. As has been experimentally established, the distinctions in the diffusional mobility of nickel along the intergranular transitional zones and through the grain mass are minimized with an increase in temperature. Therefore, using the experimental data on the degree of predominance of the intergranular diffusional mobility over the mobility in the grain mass at a temperature much higher than 550° could only minimize the correlation between the relaxation and diffusional data and, consequently, raise the importance of the value of the correlation sought for.

Even if the distinctions between the diffusional mobility along the intergranular zones and that in the grain mass are greater at lower temperatures, the width

*See the article by V. I. Arkharov, S. I. Ivanovskaya, I. P. Polikarpova, and N. P. Chuprakova in this collection.

here of the continuous diffusional zone as well as the width of the intergranular "projections" of the diffusional front decrease rapidly, and this makes measuring difficult and reduces accuracy.

The employed technique of metallographic investigation of diffusional mobility of nickel, mentioned in the article by V. I. Arkharov, S. I. Ivanovskaya, et al., produced the most reliable measurement results in tests conducted at 1100°. These results were used for comparison with the relaxation data.

As a characteristic for the intensity of relaxation of stresses at a 550° testing temperature we selected the ratio of stresses σ_{12}/σ_0, where σ_{12} is the stress effective in the specimen after 12 hours of relaxation and σ_0 is the initial stress value.

This value was compared with a, the "coefficient of diffusional mobility" of the atoms of nickel along the grain boundaries, a qualitative description of the relative intensity of the course of the diffusional processes in the intergranular zones as compared to the course of these processes in the grain body.

The data obtained for ferrum-chromium-nickel alloys either without additions or with small additions of molybdenum and tungsten, as well as the data for the alloys, in which some portion of nickel was replaced by cobalt or manganese, were used for the comparison.

All data are summarized in Table 1. On the basis of thes data we constructed a graph (Figure 1), in which we can distinctly see the correlation between the variation of the coefficient "a" value with the variation in the intensity of relaxation (despite the quite considerable spread between the points).

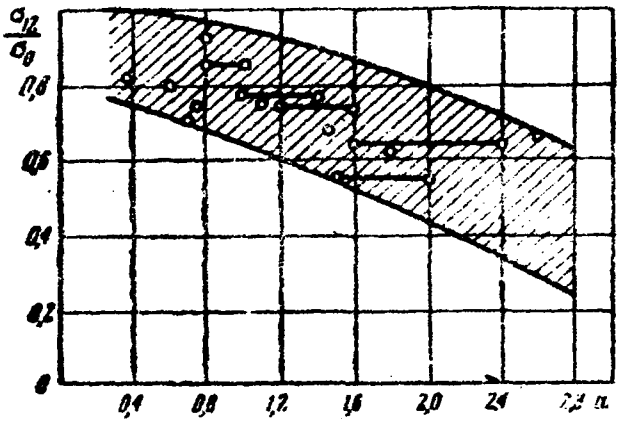

Figure 1. The graph showing the correlation of data on diffusional mobility and on relaxation of stresses ($\underline{a}$ = "coefficient of diffusion mobility", σ_0 = initial stress, σ_{12} = stress at the end of the test).

The decrease in the relative intensity of the course of diffusional processes along the intergranular zones agrees with the increase in ratio σ_{12}/σ_0, i.e., with the decrease in the intensity of the course of relaxation of stresses.

Table 1

The values of the coefficient of diffusion mobility a and the ratio of stresses σ_{12}/σ_0

Conventional grade of alloy	a*	σ_{12}/σ_0 (at 550°)**	Conventional grade of alloy	a*	σ_{12}/σ_0 (at 550°)**
9Cr20Ni10	1,5—2,0	0,55	4Cr18Ni20Mo3	0,80	0,92
5Cr20Ni11	1,6—2,4	0,64	7Cr20Ni21W1	1,10	0,75
5Cr21Ni10Mo1	1,0—1,4	0,77	4Cr20Ni15Ga5	0,35	0,83
4Cr18Ni10Mo2	0,8—1,0	0,85	8Cr21Ni20	1,2—1,60	0,74
11Cr18Ni10W1	0,70	0,70	4Cr19Ni18Co2	1,80	0,62
9Cr18Ni10W2	0,74	0,74	6Cr21Ni15Co5	1,47	0,68
8Cr19Ni10W4	0,60	0,79			

Conclusions

Summarizing the above we arrive at the following conclusions.

1. The results obtained in comparing the experimental data on the diffusion of nickel in the examined alloys with the data on the relaxation of stresses in the same alloys confirms the notions developed by V. I. Arkharov and M. B. Yakutovich. The addition of small positively active admixtures in the solid solution leads to the enrichment of the intergranular zones in the introduced admixtures to a degree comparative with the body of the grain. This will explain the reduction in the

*See the article by V. I. Arkharov, S. I. Ivanovskaya, I. P. Polikarpova and N. P. Chuprokova in this collection.
**See the article by G. N. Kolesnikov, A. I. Moiseyev, and M. B. Yakutovich in this collection.

diffusional mobility along the grain boundaries as well as the reduction in the intensity of the course of plastic deformation along the intergranular zones. In other words, this confirms the notions on the substantial role played by the intergranular zones at high deformation and on the possibility of affecting the mechanical properties of the metal as a whole with the help of small positively active admixtures.

2. The data examined in this article are not sufficient, however, to judge the participation of one or another mechanism of plastic deformation (slip or diffusional plasticity), since the hardening of the intergranular zone may lead to the deceleration of the development of both the diffusional plasticity and slip in this zone. A more definite opinion on this problem may be formed on the basis of the analysis of the experimental data on the relaxation of stresses related in the article by G. N. Kolesnikov and A. I. Moiseyev published in this collection.

* * *

Concerning the Influence of Phase Transformations on the Relaxation of Stresses

By G. N. Kolesnikov and A. I. Moiseyev

Phase transformations can be divided into three groups with respect to the variation in the specific volume caused by them.

The first group will include phase transformations causing an increase in specific volume, such as the martensitic transformation in steels (the increase in specific volume amounts to one to three percents (1)), the transformation $Sn\beta \rightarrow Sn\alpha$, causing the increase in specific volume up to 25 percent (2).

The second group will include phase transformations which occur without causing a variation in the specific volume or causing a slight variation, which is below an experimental error (all second-order phase changes).

The phase transformations involving a decrease in specific volume (transformation $Co\beta \rightarrow Co\alpha$ (3)) may be referred to the third group.

Unexpected properties which appear in metals and alloys as a result of phase transformations hold a great part of the attention of the theorists and the practical scientists.

At present, the interrelation and interdependence of phase transformations and plastic deformation has not been sufficiently studied.

On the basis of the data available in literature, the following conclusions may be made.

1. Phase transformations have a certain

temperature region where they are more intensive.

2. The intensity of phase transformations in alloys depends on the content of alloying elements (for instance, the content of carbon affects the segregation of martensite from austenite).

3. A great stimulative role in phase transformations is played by plastic deformation; phase transformations, in turn, influence the magnitude of total deformations. As a special case of the influence of phase transformations on the magnitude of total deformation, we will study the possible influence of phase transformations on the process of relaxation of stresses.

As we know, relaxation of stresses is called a special case of deformation, at which the total deformation remains constant for the entire duration of the experiment and is equal to the sum of elastic $\Delta\varepsilon_e$ and plastic $\Delta\varepsilon_p$ deformation (4).

The mathematical condition for the relaxation of stresses is usually written in the form of the expression

$$\Delta\varepsilon = \Delta\varepsilon_y + \Delta\varepsilon_n = \text{const}; \quad \Delta\varepsilon_y \neq \text{const}; \quad \Delta\varepsilon_n \neq \text{const}. \qquad (1)$$

In an experimental determination of the relaxation of stresses (usually, by means of some device) the given total deformation ($\Delta\varepsilon$) is maintained for a certain time during the experiment, while the instantaneous stress (effort) which acts upon the specimen is determined (measured or calculated). In this case, if we consider the possibility of a phase transformation and take into account that the relaxation machine is actually a sensitive dilatometer, then the condition for the net relaxation of stresses could be, more strictly, written in the form of expression

$$\Delta\varepsilon = \Delta\varepsilon_y + \Delta\varepsilon_n + \Delta\varepsilon_\phi = \text{const}, \qquad (2)$$

where $\Delta\varepsilon$ is the total length of the specimen which remains constant for the entire duration of the experiment;

$\Delta\varepsilon_e$ is the value of the elastic deformation of the

specimen;

$\Delta\varepsilon_p$ is the value of the plastic deformation of the specimen;

$\Delta\varepsilon_{ph}$ is the value of the variation in the linear dimensions of the specimen as a result of the change in the specific volume of the material of the specimen in the process of phase transformations.

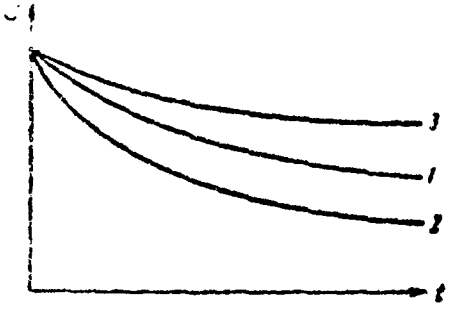

Figure 1. Curves for relaxation of stresses:
1 -- $\Delta\varepsilon_{ph} = 0$;
2 -- $\Delta\varepsilon_{ph} > 0$;
3 -- $\Delta\varepsilon_{ph} < 0$.

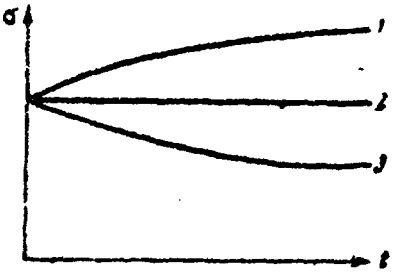

Figure 2. Curves for relaxation of stresses at $\Delta\varepsilon_{ph} < 0$:
1 -- $\Delta\varepsilon_p < \Delta\varepsilon_{ph}$;
2 -- $\Delta\varepsilon_p = \Delta\varepsilon_{ph}$;
3 -- $\Delta\varepsilon_p > \Delta\varepsilon_{ph}$.

Naturally, when there are no phase transformations in the material of the specimen, or when there are phase transformations causing changes in the specific volume that could be neglected, Expression (2) becomes Expression (1), since $\Delta\varepsilon_{ph} = 0$.

In order to simplify the further discussions, let us assume that at a given value of total deformation $\Delta\varepsilon$ the testing of the materials for the relaxation of stresses begins after reaching the given initial stress σ_0, and that the course of plastic deformation is the same in all cases.

If a phase transformation takes place in the material of the specimen in the process of relaxation of stresses causing an increase in specific volume, the term

$\Delta\varepsilon_{ph}$ will appear in Expression (2) with a plus sign ($\Delta\varepsilon_{ph} > 0$), and, then, with a given value of total deformation $\Delta\varepsilon$ the value for the elastic deformation $\Delta\varepsilon_e$ will be less than in the absence of a phase transformation. In this case, the experimental curve 2 for relaxation of stresses (Figure 1) will pass below curve 1 which corresponds to the recording of the process of relaxation of stresses without a phase transformation.

If a phase transformation takes place in the material of the specimen in the process of relaxation of stresses involving a decrease in the specific volume, term $\Delta\varepsilon_{ph}$ will appear in Expression (2) with a minus sign ($\Delta\varepsilon_{ph} < 0$), and at a given value of the total deformation $\Delta\varepsilon$ the value for the variation of plastic deformation $\Delta\varepsilon_p$ will be higher than in the absence of a phase transformation. Consequently, the experimental curve 3 for the relaxation of stresses (see Figure 1) will then pass above curve 1 which corresponds to the process without a phase transformation.

When $\Delta\varepsilon_p < 0$, there are three cases possible for the trend of the curve for the relaxation of stresses.

1. If $\Delta\varepsilon_p - \Delta\varepsilon_{ph} = 0$ -- ($\Delta\varepsilon_p = \Delta\varepsilon_{ph}$) -- no variation will occur in the value of stresses effective in the specimen in the process of relaxation of stress; the curve "relaxation of stresses" recorded on the machine will have the form of a straight line -- curve 2 (Figure 2).

2. If $\Delta\varepsilon_p - \Delta\varepsilon_{ph} > 0$ -- ($\Delta\varepsilon_p > \Delta\varepsilon_{ph}$) -- the curve 3 for "relaxation of stresses" (see Figure 2), recorded on the machine, will pass below the straight line 2; i.e., it will look approximately the same as a usual curve for relaxation of stresses, though at least a portion of the drop in stresses will be compensated for by the decrease in specific volume caused by the phase transformation.

3. If $\Delta\varepsilon_p - \Delta\varepsilon_{ph} < 0$ -- ($\Delta\varepsilon_p < \Delta\varepsilon_{ph}$) -- curve 1 for "relaxation of stresses" (see Figure 2), recorded on the machine, will pass above the straight line 2; i.e., in order to retain the condition of constancy of deformation (2), the stress affecting the specimen will not have to be reduced (as in the usual case), but rather increased to compensate for the reduction in the dimensions of the specimen resulting from the phase transformation which occurs causing a decrease in specific volume.

To confirm the above discussions, we can cite the experimental data by Ya. S. Gintsburg (5).

In plotting a curve for the relaxation of stresses in the coordinates log of stress vs. time (6), the second sector of the curve for relaxation of stresses is depicted in the form of a straight line (continuous curve in Figure 3). In the experiments conducted by Ya. S. Gintsburg, it was observed that under certain conditions of relaxation of stresses there is a third sector which deviates downwards from the straight line in the coordinates log of stresses vs. time (dotted line in Figure 3). Ya. S. Gintsburg points out that the presence of a third sector is always associated with the appearance of the β-phase, i.e., with the occurrence of phase transformation.

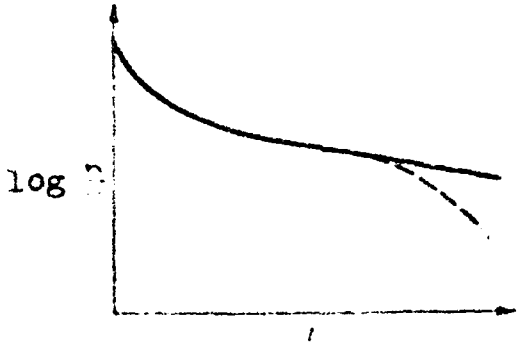

Figure 3. Curves for relaxation of stresses in coordinates: log σ vs. time.

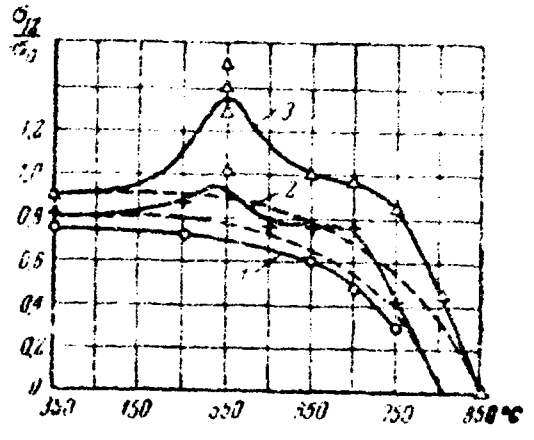

Figure 4. Curves showing the dependence of the coefficient of the relaxational variation of stresses on the testing temperature for alloys:
1 -- Cr20Ni20;
2 -- Cr20Ni20Ti0.42;
3 -- Cr20Ni20Ti1.87.

From the viewpoint of our discussions cited above, this abnormal case can readily be explained by the fact that under these conditions of deformation, in the process of relaxation of stresses, a phase transformation takes place in this material accompanied by an increase in specific volume; i.e., the increase in dimensions

following the increase in specific volume caused by the phase transformation is added in the process of relaxation of stresses to the increase of dimensions caused by the plastic deformation; thus, to maintain the total deformation of the specimen constant, a lower effective stress is required.

This study advises of certain results obtained in the investigation of relaxation of stresses in ferrum-chromium-nickel alloys, i.e., of an anomalous case of negative "relaxation of stresses" observed on a ferrum-chromium-nickel base with additions of titanium.

Table 1

The chemical composition of alloys, percent.

Conventional grade of the alloy	C	Si	Mg	Cr	Ni	Ti
Cr20Ni20	0,025	0,06	0,30	19,85	20,00	—
Cr20Ni20T10.42	0,058	0,32	0,32	20,00	20,14	0,42
Cr20Ni20T11.87	0,050	0,60	0,38	20,95	20,40	1,87

The alloys indicated in Table 1 were submitted to hardening from 1250° (holding time at this temperature is one hour) and then used for the preparation of specimens for relaxation of stresses at elongation.

The tests on relaxation of stresses were conducted on a machine designed at the Ural Branch of the Academy of Sciences (URAN) at temperatures ranging from 350 to 850° using the same initial stress of 13 kg/mm^2. The duration of the test was 12 hours.

The relaxation curve obtained in the test was used for the determination of the value for the stress σ_{12} effective at the end of the given testing time interval.

Next, as in the previously conducted studies* we determined the ratio σ_{12}/σ_0 representing the variation of stresses in the given material at the given conditions of testing, called "the coefficient of relaxational variation of stresses". Then we plotted a curve showing the dependence of the obtained coefficients of the relaxational variation of stress on the testing temperature. The comparison of these dependencies for various alloys makes it possible to characterize the relative heat resistance of the alloys.

Figure 4 shows the trend of the coefficients of relaxational variation in stress of the tested alloys depending on testing temperature. Curve 1 is referred to alloy Cr20Ni20 (without additions) and is monotonous over the entire region of testing temperatures. This trend of the curve showing the occurrence of relaxation of stresses depending on temperature is characteristic and normal since the intensity of relaxation of stresses increases with an increase in temperature. Curve 2 is referred to alloy Cr20Ni20Ti0.42; it has a slight maximum in the testing temperature region of 550°. The presence of a maximum on the curve of intensity of relaxation of stresses can only be explained by the fact that the phase transformation accompanied by a decrease in specific volume passes in the regions of temperatures which correspond to the maximum. Curve 3 is referred to alloy Cr20Ni20Ti1.87; it has a distinctly pronounced maximum in the testing temperature region of 550°. Here the value for the coefficient of relaxational variation in stresses σ_{12}/σ_0 in the maximum region even appears to be greater than one. This fact means that the effective instantaneous stresses are higher here than the initial ones. This can only be explained by an extremely sharp decrease in the dimensions of the specimen in the process of relaxation of stresses due to the reduction in specific volume during the phase transformation.

*See the article by G. N. Kolesnikov, A. I. Moiseyev and M. B. Yakutovich in this collection.

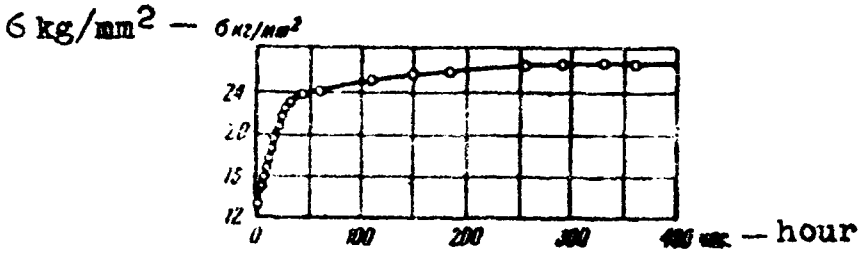

Figure 5. The anomalous curve of the "relaxation of stresses" (σ_o = = 13.63 kg/mm^2 and $\underline{t}$ = = 550°).

It may be assumed that in the absence of a phase transformation the curves showing the intensity of the relaxation of stresses for alloys with admixtures could have been analogous to a curve for an alloy without an admixture. Such assumed curves are indicated in Figure 4 by a dotted line.

The "relaxation curve" for alloy Cr20N120T11.87, obtained with automatic recording, is given in Figure 5. The anomalous curve for "relaxation of stresses" is shown in this figure in coordinates stress vs. time.

As we see from this figure, the instantaneous stress has kept continuously increasing with the duration of the test and amounted to 26.52 kg/mm^2 at the end of the 400th hour, i.e., twice as much as in the beginning of the test. The build-up of instantaneous effective stress was rapid at the beginning, but the rate was declining, and, then, beginning with the 350th hour, the build-up in stress practically ceased. This anomalous case in the trend of the curve for the "relaxation of stresses" can readily be explained by the process of relaxation of stresses occurring under the conditions of a phase transformation accompanied by a decrease in specific volume.

This macroscopic effect obtained in testing relaxation of stresses does not mean at all that the relaxation of stresses does not occur in this material under the given conditions. Relaxation of stresses is called a process of an eventual spontaneous reduction in stress during a constant deformation. Naturally, there was a process of relaxation of stresses in this case also, but the decrease

in the specific volume caused by the phase transformation has overlapped the effect of spontaneous relaxation of stresses.

From the above-cited discussions and experimental data it follows that phase transformations, which occur in metals, may show up substantially on the shape of the "relaxation curve".

We cannot expect high relaxation characteristics in alloys where the phase transformation occurs with an increase in specific volume.

From the viewpoint of industrial application those alloys which are of special interest have, as in the described ferrum-chromium-nickel alloys with admixtures of titanium, phase transformations occurring with a decrease in specific volume. In the end, the intensity in the reduction of stresses decreases in these alloys (which is exactly what the industry is interested in). In other words, from the industrial point of view, the degree of "relaxation of stresses" decreases; i.e., the "relaxation" characteristics of the alloys improve.

In the light of the cited discussions and experimental data, the task may be set forth of developing alloys with practically no variations in the external stresses under the given conditions of deformation (i.e., under the given degree of deformation, in a certain region of temperature and a certain time interval).

Furthermore, the problem of obtaining "antirelaxing" alloys is also not unsolved. Bolts made of such an "antirelaxing" alloy will not only not weaken any flange coupling in the course of time, but, on the contrary, such a flange coupling will eventually become more and more dense; it will appear as though the coupling were self-tightening and self-sealing.

In concluding, the following deduction can be made: the search for heat-resistant and "nonrelaxing" alloys can be conducted using alloys which have phase transformations occurring with a decrease in specific volume; as for the "antirelaxing" alloys, these can only be found among the alloys which have phase transformations occurring with a decrease in specific volume.

And another deduction follows from the cited discussions and experiments: the phenomenon of relaxation of stresses and its relationships must be studied in its simplest form on pure elements or, at any rate, on alloys representing solid solutions not subjected to phase transformations under all given conditions of temperature, stress, and duration of experiment; but if alloys are used, then it is altogether necessary to consider the possibility of side factors which may appear and overlap the plastic deformation in the process of relaxation of stresses in the form of phase transformations causing a variation in specific volume.

BIBLIOGRAPHY

1. Gulyayev, A. P., Metallovedeniye (Metal Studies), Oborongiz (State Press of the Defense Industry), Moscow, 1951.

2. Umanskiy, Ya. S., Finkel'shteyn, B. N., Blanter, M. Ye., Fizicheskiye osnovy metallovedeniya (The Physical Fundamentals of Metal Studies), Metallurgizdat (State Scientific and Technical Press for Literature on Ferrous and Nonferrous Metallurgy), Moscow, 1949.

3. Shteynberg, S. S., Metallovedeniye, Vol. 1, Metallurgizdat, Sverdlovsk--Moscow, 1952.

4. Oding, I. A., "Vestnik mashinostroyeniya" (Herald of Machine Construction), No. 5-6, 7-8, 9-19, 1946.

5. Gintsburg, Ya. S., "Zav. lab." (Plant Laboratory), No. 4, 1953.

6. Oding, I. A., and Tseytlin, V. Z., Dokl. AN SSSR, (Reports of the Academy of Sciences USSR), Vol. 71, No. 5, 1950.

* * *

The Investigation of Relaxation of Stresses in Ferrum-Chromium-Nickel Austenitic Alloys Containing Admixtures of Titanium and Niobium

By M. G. Gaydukov and V. A. Pavlov

The study of the relaxation of stresses in Cr20Ni20-type alloys containing additions of titanium and niobium is a continuation of the study of one of the sections of the complex investigation of the influence of small admixtures of certain alloying elements on the heat resistance of alloys.

Procedure and test material

The study of relaxation of stresses was conducted on machines designed at the Institute of Physics of Metals of the Ural Branch of the Academy of Sciences USSR. The duration of testing amounted to 50 hours at all temperatures (650, 700, and 750°). The temperature was maintained constant automatically, by the aid of a thermoregulator, accurate to ±1.5°. All tests were conducted at two initial stresses: 6 and 8 kg/mm^2. The variation of the stresses in the specimen was automatically recorded on a diagram by a clock-work. The following are the dimensions of the relaxation specimens: diameter 4.5 mm; working length 100 mm; the fastening tread M9 length 8 mm. The specimens were heat-treated in billets according to the following regime: heating-up to 1250°, holding for one hour, and water cooling.

The study of relaxation of stresses was carried out on two groups of Cr20Ni20Ti-type alloys (Table 1). The niobium content varied (from 0.25 to 1.0 percent) in the first group of alloys having a constant content of 0.2 percent titanium. The titanium content was increased to one percent in the second group of alloys, and so was the content of niobium, varying from 0.2 to one percent.

The intensity of relaxation of stresses was determined from the σ_{50}/σ_0 ratio, i.e., from the ratio of stress obtained after a 50-hour test to the initial stress at the

instant of loading. The lower the ratio σ_{50}/σ_0, the higher, consequently, the value by which the effective stress has decreased during the test, i.e., the higher the intensity of relaxation of stresses.

Test results

The test results of relaxation of stresses are given in the form of graphs (Figure 1-6) in the coordinates of "log of stress" vs. "duration of testing".

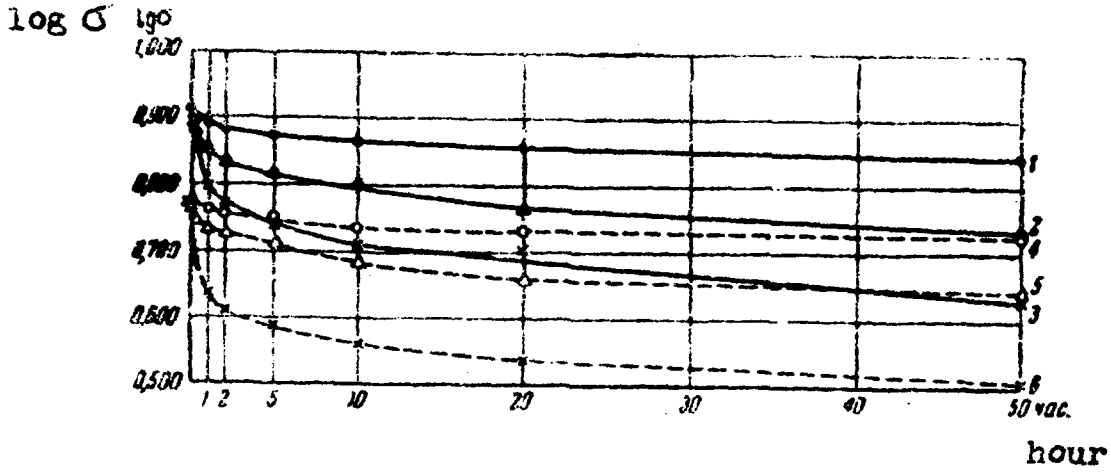

Figure 1. Curves for relaxation of stresses in alloy Cr20Ni20Ti0.2Nb0.2 at the following temperatures and stresses:
1 -- 650°, 8 kg/mm^2; 2 -- 700°, 8 kg/mm^2;
3 -- 750°, 8 kg/mm^2; 4 -- 650°, 6 kg/mm^2;
5 -- 700°, 6 kg/mm^2; 6 -- 750°, 6 kg/mm^2.

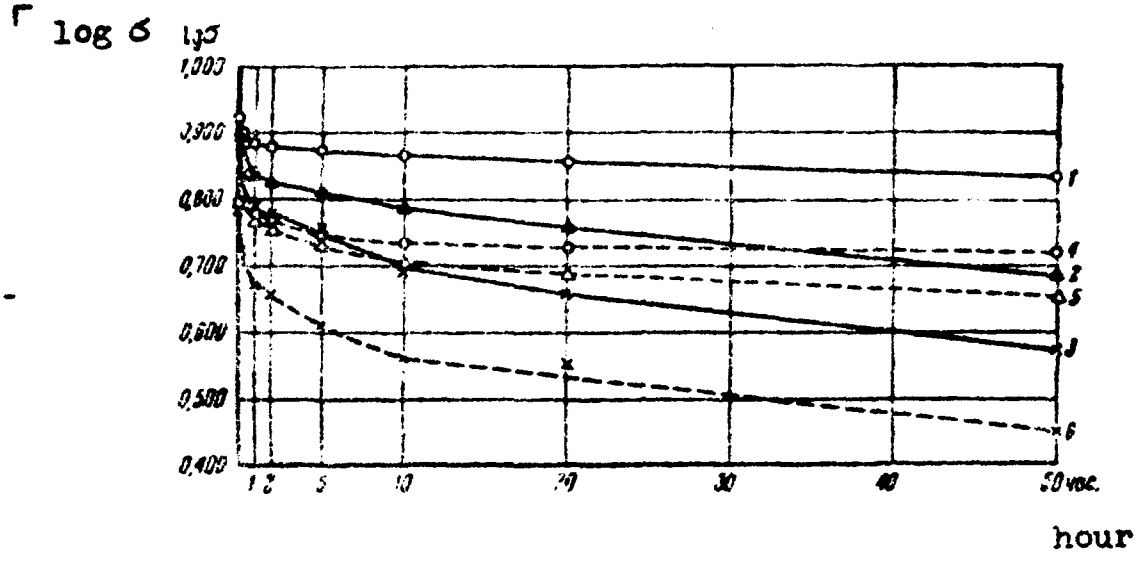

Figure 2. Curves for relaxation of stresses in the alloy Cr20Ni120Ti0.2Nb0.5 at the following temperatures and stresses:
1 -- 650°, 8 kg/mm2; 2 -- 700°, 8 kg/mm2;
3 -- 750°, 8 kg/mm2; 4 -- 650°, 6 kg/mm2;
5 -- 700°, 6 kg/mm2; 6 -- 750°, 6 kg/mm2.

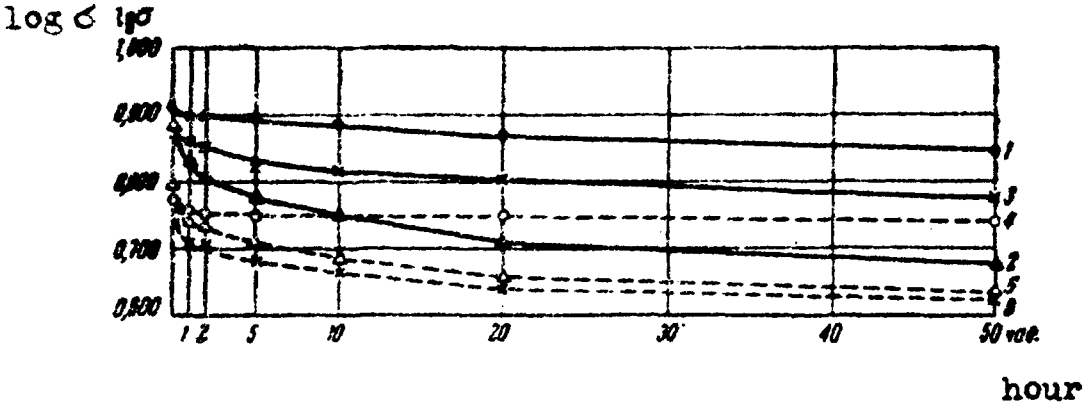

Figure 3. Curves for relaxation of stresses in the alloy Cr20Ni120Ti0.2Nb1.0 at the following temperatures and stresses:
1 -- 650°, 8 kg/mm2; 2 -- 700°, 8 kg/mm2;
3 -- 750°, 8 kg/mm2; 4 -- 650°, 6 kg/mm2;
5 -- 700°, 6 kg/mm2; 6 -- 750°, 6 kg/mm2.

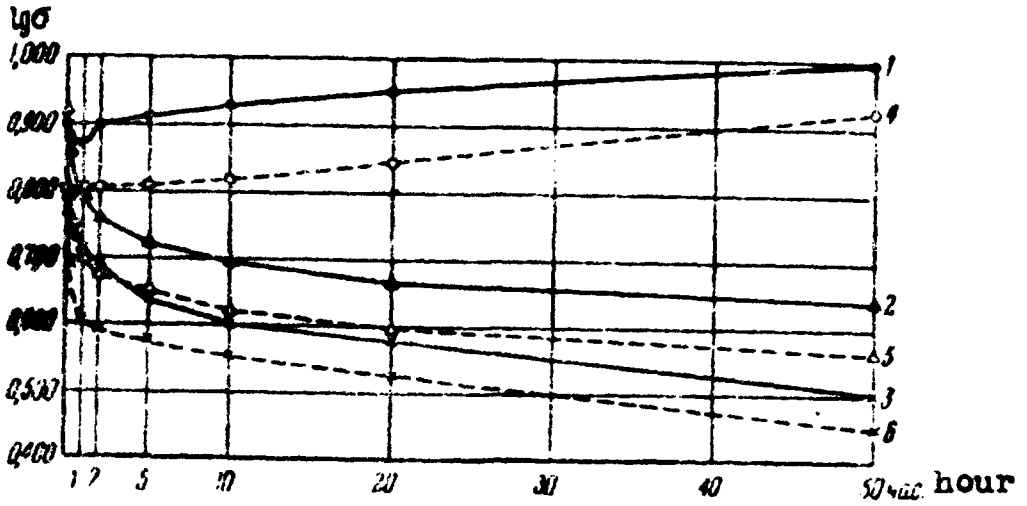

Figure 4. Curves for relaxation of stresses in the Cr20Ni120Ti1.0Nb0.2 alloy at the following temperatures and stresses:
1 -- 650°, 8 kg/mm2; 2 -- 700°, 8 kg/mm2;
3 -- 750°, 8 kg/mm2; 4 -- 650°, 6 kg/mm2;
5 -- 700°, 6 kg/mm2; 6 -- 750°, 6 kg/mm2.

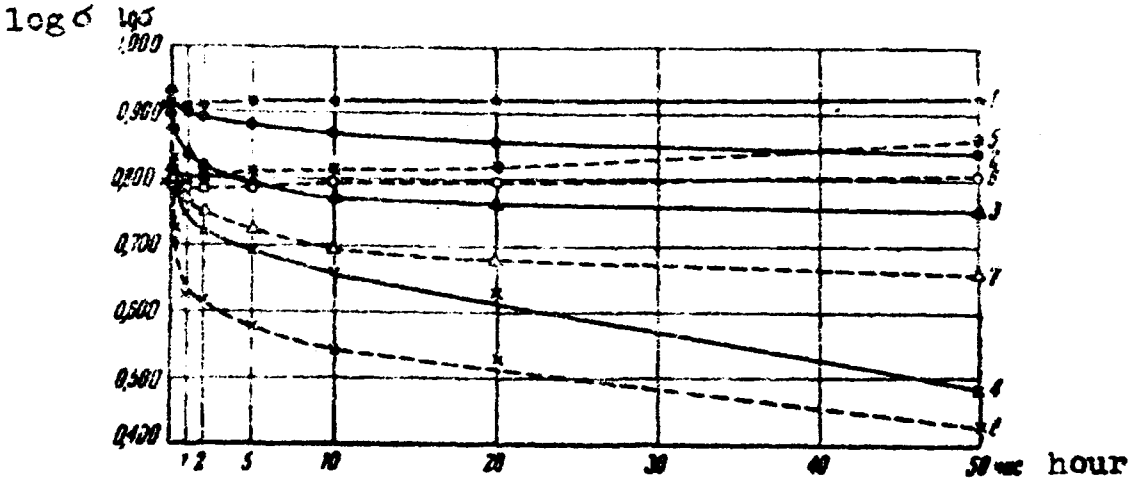

Figure 5. Curves for relaxation of stresses in the Cr20Ni120Ti1.0Nb0.5 alloy at the following temperatures and stresses:
1 -- 600°, 8 kg/mm2; 2 -- 650°, 8 kg/mm2;
3 -- 700°, 8 kg/mm2; 4 -- 750°, 8 kg/mm2;
5 -- 600°, 6 kg/mm2; 6 -- 650°, 6 kg/mm2;
7 -- 700°, 6 kg/mm2; 8 -- 750°, 6 kg/mm2.

We observe in alloy Cr20N120T10.2Nb0.2 a slight reduction in stresses at the temperature of 650° and at an initial stress of 6 kg/mm^2 (Figure 1). An increase in the tem[illegible]ature to 700 and 750° leads to a more intensive re-l[illegible]on of stresses; at 750° the sharpest reduction in s[illegible]sses takes place at the initial moment, during the f[illegible] hours of testing. Raising the initial stress to 8 [illegible]/mm^2 increases the intensity of stresses at all three temperatures.

Table 1

The chemical composition of the tested alloys, percent

Conventional grade of the alloy	C	Mn	Si	Cr	Ni	Ti	Nb
Cr20N120T10.2Nb0.2	0,029	0,30	0,39	18,90	19,61	0,15	0,25
Cr20N120T10.2Nb0.5	0,031	0,32	0,25	19,35	19,61	0,19	0,40
Cr20N120T10.2Nb1.0	0,033	—	0,43	19,20	19,20	0,38	1,00
Cr20N120T11.0Nb0.2	0,030	—	0,40	18,96	18,92	0,93	0,20
Cr20N120T11.0Nb0.5	0,029	—	0,58	19,48	19,00	0,79	0,40
Cr20N120T11.0Nb1.0	0,038	—	0,62	18,78	18,85	1,13	1,00

At an initial stress of 6 and 8 kg/mm^2 we observe in the Cr20N120T10.2Nb0.5 alloy a more intensive reduction of stresses than in Cr20N120T10.2Nb0.2 alloy at all testing temperatures, due, primarily, to the high intensity of relaxation on the second sector of the curves (Figure 2). As the testing temperature is increased from 650° to 750°, the relaxation of stresses on the second sector in the Cr20N120T10.2Nb0.5 alloy builds up more rapidly than in the Cr20N120T10.2Nb0.2 alloy.

The intensity of relaxation of stresses in the Cr20N120T10.2Nb1.0 alloy at 6 and 8 kg/mm^2 and at a 650° temperature is lower than in Cr20N120T10.2Nb0.2 and Cr20N120T10.2Nb0.5 alloys, but is higher at a temperature of 700° (see Figure 5). The intensity of relaxation of stresses on the second sector at 700° is approximately the same in Cr20N120T10.2Nb0.2 and Cr20N120T10.2Nb1.0 alloys and is slightly lower in the Cr20N120T10.2Nb0.5 alloy. As the temperature is increased to 750°, the intensity of relaxation of stresses does not increase in the Cr20N120T10.2Nb1.0 alloy at the initial stress of 6 kg/mm^2;

It even decreases at a stress of 8 kg/mm^2 (Figure 7). This takes place due to the reduction in intensity of relaxation of stresses on both the first and second sectors of the relaxation curve.

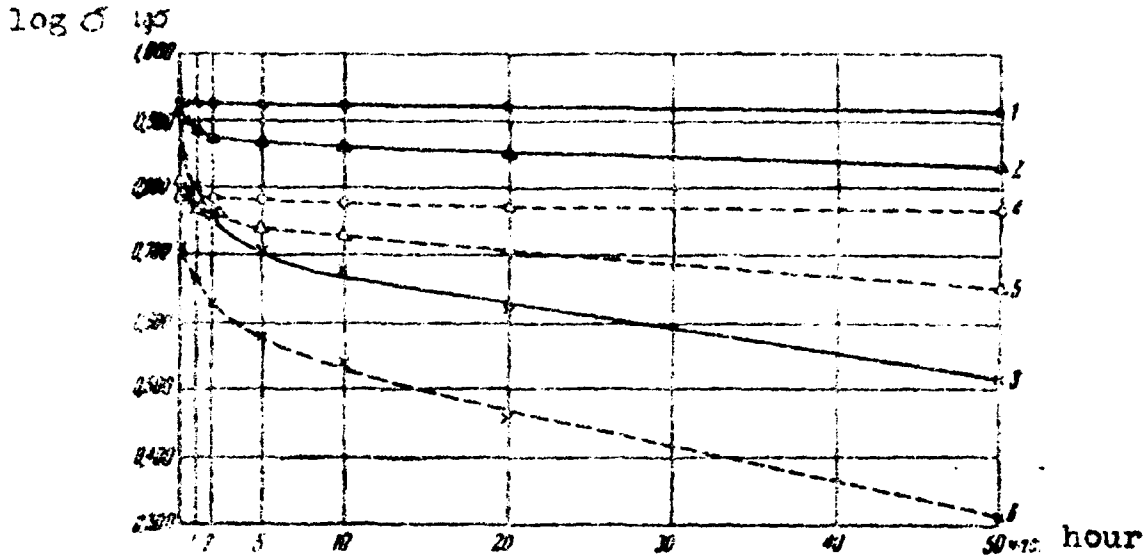

Figure 6. Curves for relaxation of stresses in the Cr20Ni120T11.0Nb1.0 alloy at the following temperatures and stresses:
1 -- 650°, 8 kg/mm^2; 2 -- 700°, 8 kg/mm^2;
3 -- 750°, 8 kg/mm^2; 4 -- 650°, 6 kg/mm^2;
5 -- 700°, 6 kg/mm^2; 6 -- 750°, 6 kg/mm^2.

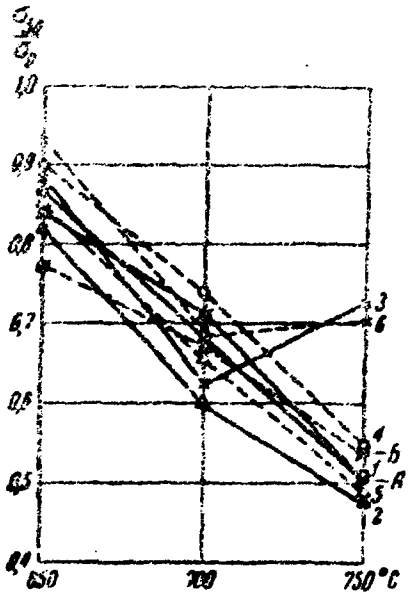

Figure 7. The intensity of relaxation for stresses in alloys:
A -- Cr20Ni120 at 8 kg/mm^2;
B -- Cr20Ni120 at 6 kg/mm^2;
1 -- Cr20Ni120T10.2Nb0.2 at 8 kg/mm^2; 2 -- Cr20Ni120T10.2Nb0.5 at 8 kg/mm^2; 3 -- Cr20Ni120T10.2Nb1.0 at 8 kg/mm^2; 4 -- Cr20Ni120T10.2Nb0.2 at 6 kg/mm^2;
5 -- Cr20Ni120T10.2Nb0.5 at 6 kg/mm^2; 6 -- Cr20Ni120T10.2Nb1.0 at 6 kg/mm^2.

In the next group of the ferrum-chromium-nickel alloys with titanium and niobium, the content of titanium was increased to one percent. The tests of the Cr20Ni20Ti0.2Nb0.2 alloy at 650° produced somewhat unusual results. While the test is on there occurs, not a reduction of the effective stresses but, on the contrary, an increase in stresses (Figure 4). At an initial stress of 6 kg/mm^2 and a temperature of 650°, the stresses gradually increased throughout the 50 hour period. At a much higher initial stress of 8 kg/mm^2 at the very initial moment of testing there is noted a slight reduction of stresses which stops very soon, and then the stresses already begin to increase as in the test at an initial stress of 6 kg/mm^2. A substantial reduction of stresses is noted on both the first and second sectors of the relaxation curve in the Cr20Ni20Ti1.0Nb0.2 alloy at 700 and 750°. As compared to the Cr20Ni20Ti0.2Nb0.2 alloy, the relaxation of stresses occurs more intensively in the Cr20Ni20Ti1.0Nb0.2 alloy on account of a greater reduction of stresses on the first sector of the relaxation curve.

A certain increase in stresses at 6 kg/mm^2 and a temperature of 650° is noted also in the Cr20Ni20Ti1.0Nb0.5 alloy (Figure 5). But even at an initial stress of 8 kg/mm^2 the sign of the variation of stresses in the process of testing changes, and the stresses decrease. The Cr20Ni20Ti1.0Nb0.5 alloy was tested additionally at a temperature of 600° and at initial stresses of 6 and 8 kg/mm^2; in both cases the effective stresses increase during the test.

At a temperature of 700° and an initial stress of 6 kg/mm^2 the stresses decrease during the test. The intensity of relaxation of stresses in the Cr20Ni20Ti1.0Nb0.5 is lower than in the Cr20Ni20Ti1.0Nb0.2 alloy at 700° and is higher at 750°. The increase of relaxation of stresses at 750° is caused by the higher intensity of the reduction of stresses on the second sector of the relaxation curve.

In the Cr20Ni20Ti1.0Nb1.0 alloy at 650°, the reduction of stresses occurs at a very low rate at both 6 and 8 kg/mm^2 initial stresses (Figure 6). A reduction in stresses is observed at 700°; however, the intensity of relaxation is lower than in Cr20Ni20Ti1.0Nb0.2 and Cr20Ni20Ti1.0Nb0.5 alloys; this occurs, primarily, on account of lower intensity in relaxation of stresses on the first sector of the relaxation curve. The intensity of relaxation of the Cr20Ni20Ti1.0Nb1.0 alloy at 750° is

approximately the same as in the alloys with a lower content of niobium, whereas the lower intensity of relaxation on the first sector is compensated for by a higher intensity of relaxation on the second sector of the relaxation curve.

Interpretation of results

The test data on relaxation of stresses in ferrum-chromium-nickel austenitic alloys alloyed with various amounts of titanium and niobium point to the complexity of the processes which take place in this group of alloys. The variation in the relaxation of stresses is caused by the composition of the alloys and by an additional factor -- the aging of the alloys during testing. The intensity of phase transformations varies nonsynchronously, depending on the temperature as well as on the magnitude of stresses applied.

In testing the alloys alloyed with titanium, G. N. Kolesnikov and A. I. Moiseyev* established not reduction of stresses but rather an increase during the test. Under the given testing conditions, when the length of the specimen was automatically maintained constant, the increase of stresses was explained by the occurrence of a phase transformation accompanied by a reduction in volume. In this study this phenomenon of the increase in the stresses during testing, apparently caused by the same reason, was established in alloys alloyed with titanium and niobium. An additional alloy, the Cr20Ni20Ti alloy with niobium, changes the intensity of the phase transformation and displaces the temperature maximum interval (Cr20Ni20Ti1.0Nb0.2 and Cr20Ni20Ti1.0Nb0.5 alloys).

Increasing the niobium content to one percent in the alloy containing 0.2 percent titanium will not lead to an increase in stresses in the process of testing; however, the temperature curve of the intensity in relaxation points to the occurrence of a phase transformation even with this composition of the alloy. For the Cr20Ni20Ti0.2Nb1.0 alloy this is also confirmed by the variation in the intensity of relaxation depending on stresses (Figure 7). Thus, in alloys containing 0.2 percent titanium and 0.25 percent niobium or 0.40 percent niobium, the intensity of relaxation increases (the ratio σ_{50}/σ_0 becomes lower) with an

*See their article in this collection.

increase of initial stress from 6 to 8 kg/mm^2 at all three testing temperatures. In an alloy with 0.2 percent Ti and 1.0 percent Nb the intensity of relaxation with an initial stress of 6 kg/mm^2 and 50 hours of testing remains at the same level with an increase in temperature from 700 to 750°; as we increase the temperature to 750° at 8 kg/mm^2, the intensity of relaxation of stresses decreases and becomes lower than at 700° or at 6 kg/mm^2. Thus, despite the increase in initial stress, the intensity of relaxation is not increased; this can only be explained by the phase transformation which builds up with the increase in stresses. The increase of the content of niobium in the Cr20Ni120Ti1.0 alloy to one percent will also change the dependence of the intensity of relaxation on stresses and reduce the intensity of relaxation of stresses at 8 kg/mm^2 as compared to the tests at 6 kg/mm^2 (Figure 8). Consequently, it may be assumed that the increase of niobium in the Cr20Ni120Ti1.0 alloy to 1.0 percent at temperatures of 700 and 750° (in the Cr20Ni120Ti0.2 at 750°) contributes to the development of phase transformation.

It is of interest to compare the data on intensity of relaxation of stresses in the Cr20Ni120Ti-type alloys, alloyed with titanium and niobium, with those of the Cr20Ni120 alloy. The test results of the Cr20Ni120 alloy at temperatures of 650, 700, and 750° and at initial stresses of 6 and 8 kg/mm^2 are shown in the form of curves in Figures 7 and 8*. Comparing the Cr20Ni120Ti alloys, alloyed with 0.2 percent Ti and the Cr20Ni120 alloy, we see that the intensity of relaxation in the Cr20Ni120Ti alloys has no marked distinction from the Cr20Ni120 alloy except for the Cr20Ni120Ti0.2Nb1.0 alloy at 750°. The intensity of relaxation of stresses of the Cr20Ni120Ti alloys alloyed with one percent of Ti is higher at a testing temperature of 750° than the relaxation of stresses of the Cr20Ni120 alloy. It may also be noted that increasing the content of niobium in the Cr20Ni120Ti1.0Nb alloys increases the intensity of relaxation at the same testing temperature of 750°. No explanation has yet been found for the phenomenon of increasing the intensity of relaxation of stresses in alloys alloyed with titanium and niobium at a certain temperature and under testing conditions. It is possible that this is associated with a definite variation in the cohesion forces during the alloying of the alloy with titanium and niobium or with the acceleration of the diffusional processes at

*These data were obtained by G. N. Kolesnikov and A. I. Molseyev.

750°. The intensity of relaxation of stresses of the Cr20Ni120Ti1.0Nb alloys at testing temperatures ranging from 600 to 700° is lower than that of the Cr20Ni120 alloy and is, obviously, defined by the influence of an additional factor -- the processes of phase transformations accompanied by a decrease in volume.

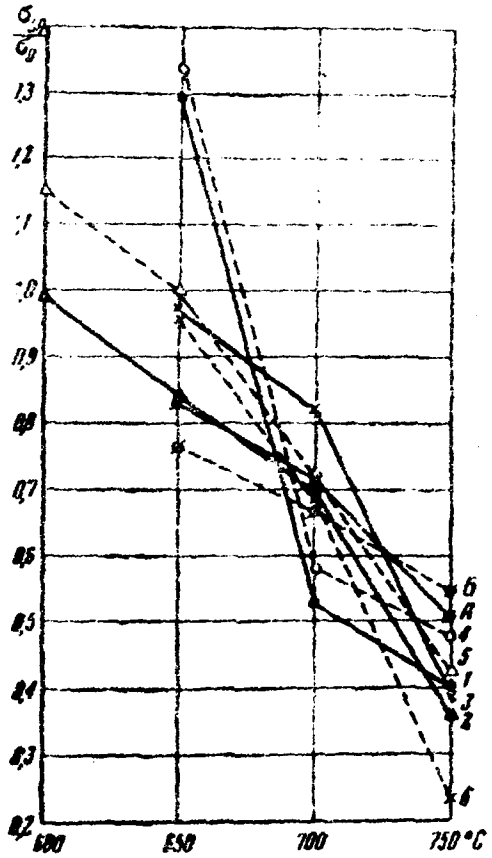

Figure 8. Intensity of relaxation of stress in the following alloys:
A -- Cr20Ni120 at 8 kg/mm^2;
B -- Cr20Ni120 at 6 kg/mm^2;
1 -- Cr20Ni120Ti1.0Nb0.2 at 8 kg/mm^2;
2 -- Cr20Ni120Ti1.0Nb0.5 at 8 kg/mm^2;
3 -- Cr20Ni120Ti1.0Nb1.0 at 8 kg/mm^2;
4 -- Cr20Ni120Ti1.0Nb0.2 at 6 kg/mm^2;
5 -- Cr20Ni120Ti1.0Nb0.5 at 6 kg/mm^2;
6 -- Cr20Ni120Ti1.0Nb1.0 at 6 kg/mm2.

Conclusions

1. The complex alloying of Cr20Ni20 alloys with titanium and niobium leads to a complex dependence of the intensity of relaxation of stresses on the composition and testing conditions.

2. In testing the Cr20Ni20Ti alloys alloyed with one percent of Ti, at definite temperatures, there develops a phase transformation accompanied by a reduction in volume. This results in a decrease in the intensity of relaxation of stresses, whereas in some individual cases an increase in effective stresses is observed rather than a decrease.

3. The increase in the content of niobium in the Cr20Ni20Ti alloys containing one percent of Ti displaces the maximum of phase transformation toward the lower temperatures.

4. A reduction in the intensity of relaxation of stresses is observed in the Cr20Ni20Ti0.2Nb alloy with a one percent content of niobium at a relaxation temperature of 750°, which is obviously related to the development of phase transformation.

5. Increasing the amount of titanium to one percent in alloys containing niobium increases the intensity of relaxation of stresses of the Cr20Ni20Ti1.0Nb alloys at a temperature of 750° as compared to the intensity of relaxation of stresses in the Cr20Ni20 alloy.

* * *

The Investigation of Creep in Ferrum-Chromium-Nickel Austenitic Alloys with Admixtures of Titanium, Niobium, and Tungsten

M. G. Gaydukov and V. A. Pavlov

Cr20Ni20 alloys, alloyed with titanium, niobium, and tungsten, were investigated in connection with the study of the general problem on the influence of small admixtures of certain alloying elements on the increase in heat resistance.

Test procedure

The tests on creep were conducted on TsKTI-2-type machines (designed by the Central Boiler and Turbine Institute). Regular-type specimens measuring 100 mm long (calculated length) with a 10-mm diameter were used. The variations in the diameter with respect to the length did not exceed 0.02 mm. The specimen billets measuring 20 x 20 x 250 mm were submitted to the following heat treatment: heating to a temperature of 1250°, holding at this temperature for one hour, and quenching in water. The temperature was measured during the test by three thermocouples, secured by hot junctions at both ends and at the center of the gage length of the specimen. After fastening the thermocouples, the gage length of the specimen was wrapped with several layers of asbestos cord to protect the thermocouple junctions from the heat radiated directly from the heated walls of the furnace. The difference in temperature over the length of the specimen did not exceed 2.5 to 3°; the mean variation of the temperature during the entire test period was of the order of 1.5 to 2°.

The deformation of the specimens was measured with indicators accurate to 0.001 mm.

The loading of the specimens was smoothly applied through the spring of a dynamometer, beginning with a preliminary loading for clearing the gaps in the loading system, and then applying the full load.

The duration of testing amounted to 250 hours. The

readings of the temperature and deformation given the indicators were taken off on the hour. The tests were conducted at a temperature of 700° at several different stresses. From the obtained initial deformation curves we plotted the curves showing the dependence of the total elongation (ε,%) on the stress applied for a tesing period of 250 hours.

Tests were made on three groups of alloys with a Cr20Ni20 base, alloyed with titanium (0.27, 0.77, and 1.09 percent), niobium (0.2, 0.5, and 1.1 percent), and tungsten (0.2, 0.5, and 2.95 percent); tests were also made on two groups of alloys, alloyed simultaneously with two elements (titanium and tungsten, the niobium content being unknown).

The chemical composition of the investigated alloys is given in the table.

The chemical composition of the alloys, percent

Conventional grade of the alloy	C	Mn	Si	Cr	Ni*	Ti	Nb	W
Cr20Ni120	0,016	0,11	0,17	20,81	20,30	—	—	—
Cr20Ni120Ti0.27	0,046	0,35	0,29	19,58	20,24	0,27		
Cr20Ni120Ti0.77	0,009	0,37	0,45	20,22	20,46	0,77	—	—
Cr20Ni120Ti1.1	0,020	0,40	0,43	20,23	20,34	1,09	—	—
Cr20Ni120Nb0.2	0,040	0,40	0,21	18,75	19,76	—	0,21	—
Cr20Ni120Nb0.2	0,032	0,32	0,14	19,60	19,0	—	0,20	—
Cr20Ni120Nb0.5	0,037	0,38	0,23	19,20	19,76	—	0,52	—
Cr20Ni120Nb0.5	0,038	0,24	0,29	20,08	18,78	—	0,53	—
Cr20Ni120Nb1.1	0,023	0,28	0,38	19,45	19,61	—	1,10	—
Cr20Ni120Nb1.1	0,018	0,24	0,38	19,87	19,99	—	1,05	—
Cr20Ni120W0.2	0,041	0,27	0,06	19,86	20,12	—	—	0,20
Cr20Ni120W0.5	0,047	0,23	0,04	19,62	19,72	—	—	0,48
Cr20Ni120W1.1	0,010	0,23	0,06	19,48	20,12	—	—	1,15
Cr20Ni120W3.0	0,051	0,28	0,16	19,35	20,28	—	—	2,95
Cr20Ni120Ti0.2Nb0.12	0,033	0,36	0,46	19,90	19,50	0,18	0,12	—
Cr20Ni120Ti0.2Nb0.33	0,038	0,18	0,37	18,84	19.22	0,18	0,33	—
Cr20Ni120Ti0.2Nb0.89	0,038	0,17	0,46	20,16	19,50	0,23	0,89	—
Cr20Ni120Ti1.0Mo0.17	0,038	0,25	0,39	20,17	19,50	1,04	0,17	—
Cr20Ni120Ti1.0Nb0.46	0,040	0,29	0,30	19.92	19,57	1,28	0,46	—
Cr20Ni120Nb0.5W0.3	0,051	0,23	0,41	19,42	19,64	—	0,51	0,30
Cr20Ni120Nb0.5W0.2	0,046	0,21	0,43	19,22	19,64	—	0,48	0,25
Cr20Ni120Nb0.5W0.5	0,051	0,22	0,46	19,53	19,52	—	0,58	0,54
Cr20Ni120Nb0.5W1.0	0,042	0,31	0,58	19,39	19,46	—	0,61	1,00
Cr20Ni120Nb0.5W1.0	0,033	0,22	0,42	19,68	19,45	—	0,39	1,00
Cr20Ni120Nb0.5W3.1	0,028	0,26	0,32	19,17	20,26	—	0,62	3,10
Cr20Ni120Nb0.5W3.1	0,025	0,25	0,32	19,17	20,26	—	0,59	3,15

*Translator's note: The original text gives "Mi", which is evidently a misprint, since we are discussing here a chromium-nickel base.

Test results

Some test results of Cr20Ni20 alloys alloyed with titanium are given in Figure 1. We have investigated alloys containing 0.27 to 1.1 percent titanium. Data on alloys alloyed with even a smaller amount of titanium (below 0.2 percent) are given in the paper by V. A. Pavlov, Ya. S. Yakovleva, and M. B. Yakutovich. From three alloys with a titanium content of 0.27, 0.77, and 1.1 percent, the highest heat resistance was obtained for the alloy alloyed with the smallest amount of titanium (0.27 percent).

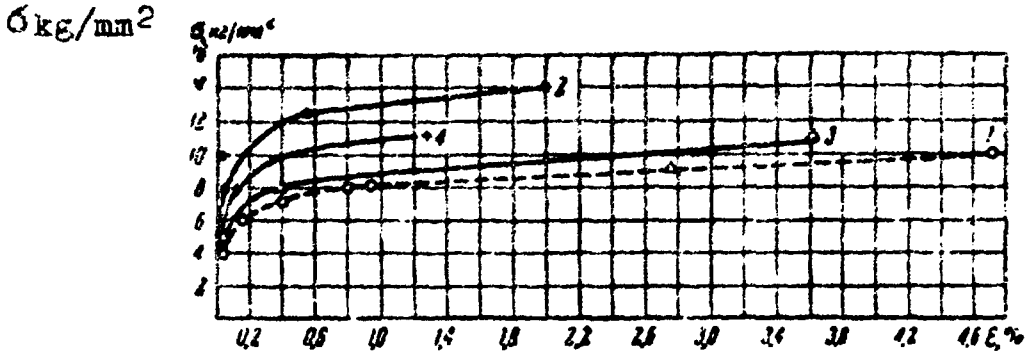

Figure 1. Curves for the creep of alloys alloyed with titanium:
1 -- Cr20Ni20; 2 -- Cr20Ni20Ti0.27;
3 -- Cr20Ni20Ti0.77; 4 -- Cr20Ni20Ti1.09.

Increasing the content of titanium to 0.77 percent leads to a relative resoftening of the alloy. At a temperature of 700°, the Cr20Ni20Ti0.77 alloy has a considerably lower heat resistance than the Cr20Ni20Ti0.27 alloy, which is slightly higher than the Cr20Ni20 alloy without titanium.

The heat resistance of the Cr20Ni20Ti1.1, containing 1.09 percent titanium, is also lower than that of the Cr20Ni20Ti0.27 alloy, but is already higher than the heat resistance of the Cr20Ni20Ti0.77 alloy. A phenomenon of negative creep was established in the Cr20Ni20Ti1.1 alloy under certain testing conditions. This phenomenon consists of the decrease in the length of the specimen during the test and may be explained by a phase transformation accompanied by a decrease in volume. In testing the relaxation of stresses in alloys containing 0.42 and

1.87 percent titanium, G. N. Kolesnikov and A. I. Moiseyev* established the presence of a maximum and have explained it by a phase transformation accompanied by a decrease in volume.

Comparing a number of tests on creep, conducted under various conditions, we may conclude that the intensity of the phase transformation depends to a considerable degree on the magnitude of the effective stresses. Under prolonged testing at low stresses of the order of 6 to 8 kg/mm^2, the specimen of the Cr20Ni120Ti1.1 alloy gradually lengthens. At a stress of 11 kg/mm^2 there was observed a considerable creep at the first moment of testing, which began to decrease immediately thereafter. After a certain period of creep damping we noted a period of negative creep, at which the length of the specimen decreased. The reduction in the length of the specimen evidently occurs as the result of a phase transformation accompanied by a reduction in volume.

The test data on the Cr20Ni120 alloys, alloyed with niobium, are given in Figure 2. Alloying with an amount of niobium up to 1.1 percent considerably increases the heat resistance of alloys. The heat-resistant properties of alloys containing niobium improve at all investigated admixture percentages of niobium (0.2, 0.5, and 1.1 percent Nb); however, the highest effect is obtained by a 0.2 percent admixture of niobium. The alloys containing 0.5 and 1.1 percent Nb have a somewhat lower heat resistance at low stresses than the alloy with 0.2 percent Nb.

Ferrum-chromium-nickel alloys with niobium, investigated in this study, are referred to austenitic alloys of the aging type. As has been established in the study by V. I. Arkharov, S. I. Ivanovskaya, I. P. Polikarpova, and N. P. Chuprakova*, the alloys with an admixtures of niobium exhibit a decomposition of the solid solution of austenite along the grain boundaries as well as in the grains themselves after the alloy has been hardened from a temperature of 1250°. It should be noted that the introduction of niobium into an alloy sharply reduces the plasticity of alloys at a high temperature.

*See their article in this collection.

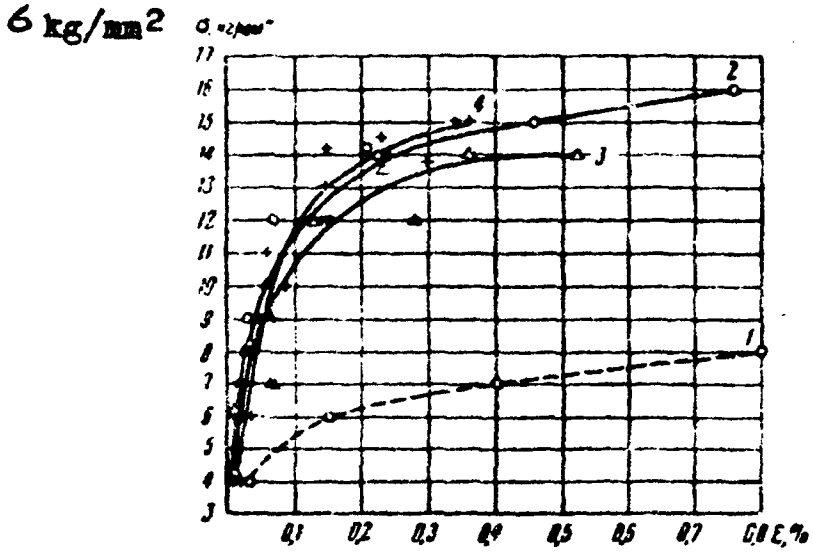

Figure 2. Curves showing creep of alloys alloyed with niobium:
1 -- Cr20Ni20; 2 -- Cr20Ni20Nb0.2;
3 -- Cr20Ni20Nb0.5;
4 -- Cr20Ni20Nb1.1.

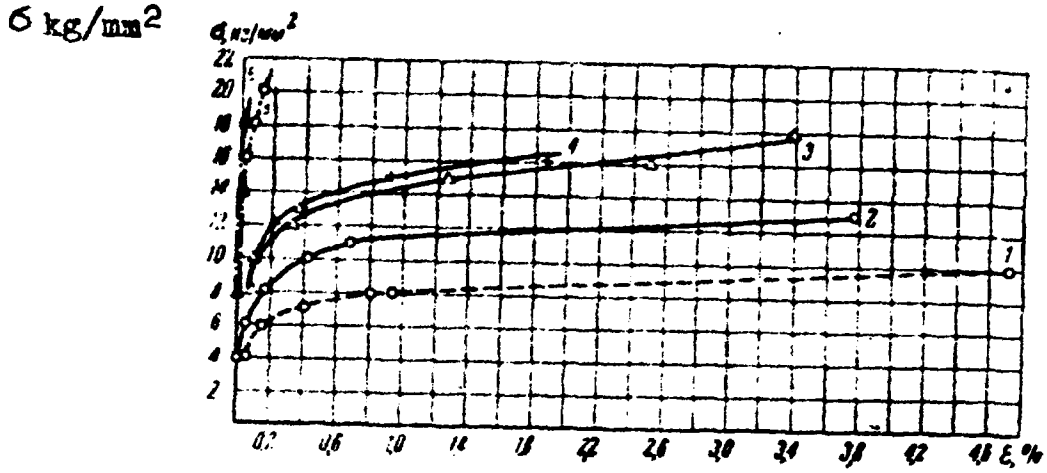

Figure 3. Curves showing the creep of alloys alloyed with titanium and niobium:
1 -- Cr20Ni20; 2 -- Cr20Ni20Ti0.2Nb0.12;
3 -- Cr20Ni20Ti0.2Nb0.33; 4 -- Cr20Ni20Ti0.2Nb0.89; 5 -- Cr20Ni20Ti1.0Nb0.17;
6 -- Cr20Ni20Ti1.0Nb0.46.

Next, we investigated two groups of Cr20Ni20-type alloys, alloyed with a combination of titanium and niobium. The first group includes alloys alloyed with 0.2 percent titanium and a varying content of niobium (from 0.12 to 0.89 percent); the second group includes two alloys alloyed with one percent of titanium plus 0.17 and 0.46 percent Nb, respectively. The test data are given in Figure 3. Alloying with 0.2 percent Ti and 0.12 percent Nb increases the heat resistance of the alloy as compared to that of the Cr20Ni20 alloy. Increasing the content of niobium to 0.33 and 0.89 percent in an alloy containing 0.2 percent Ti, leads to a further increase of heat resistance, approximately equal for both alloys.

An increase in the amount of titanium to 1.0 percent in alloys containing niobium sharply changes the nature of the behavior of alloys under a load at a high temperature. In many cases we noted a reduction in the length of the specimens during the test. In the alloy with 1.0 percent of Ti and 0.46 percent of Nb, the period of negative creep continued over the entire period of testing. From all earlier investigated alloys, Cr20Ni20Ti1.0 alloys exhibited the highest heat resistance; however, at this point we observed a considerable decrease in plasticity. The Cr20Ni20Ti1.0Nb0.17 alloy fails at a total elongation not exceeding 0.80 percent, while the Cr20Ni20Ti1.0Nb0.46 alloy fails at even a lesser elongation.

Tests were made on Cr20Ni20 alloys alloyed with tungsten in amounts of 0.2, 0.5, 1.15 and 2.95 percent (Figure 4). Alloying with 0.2 and 0.5 percent tungsten increases the heat resistance as compared to that of Cr20Ni20 alloys without tungsten at low stresses. As the stresses are increased to 7 kg/mm^2 the total deformation of the alloys containing small admixtures of tungsten over the entire 250 hours of testing is higher than the total deformation of the alloy without tungsten. When the tungsten content in the alloy is increased to 1.15 and 2.95 percent, the heat resistance of the alloy substantially increases, particularly at higher stresses of the order of 9 to 11 kg/mm^2.

A test was made on a group of alloys from the Cr20Ni20-type series containing 0.5 percent Nb and 0.2 to 3.1 W (Figure 5). All alloys with admixtures of niobium and tungsten have a much higher heat resistance in comparison with that of alloys alloyed with tungsten only.

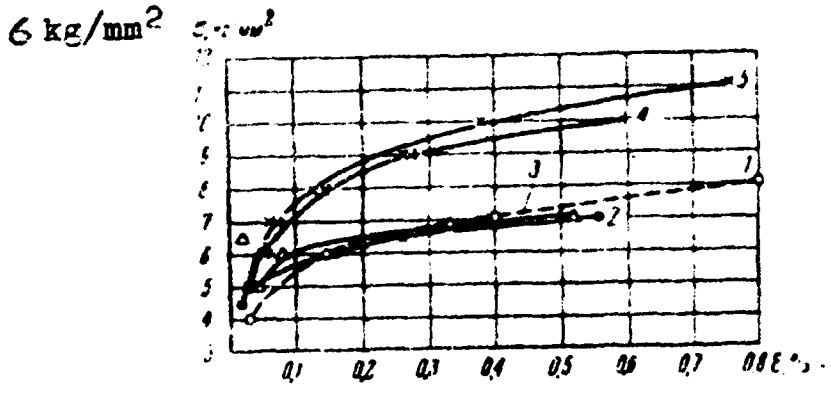

Figure 4. Curves showing creep in alloys alloyed with tungsten; 1 -- Cr20Ni120; 2 -- Cr20Ni120W0.2; 3 -- Cr20Ni120W0.5; 4 -- Cr20Ni120W1.1; 5 -- Cr20Ni120W3.0.

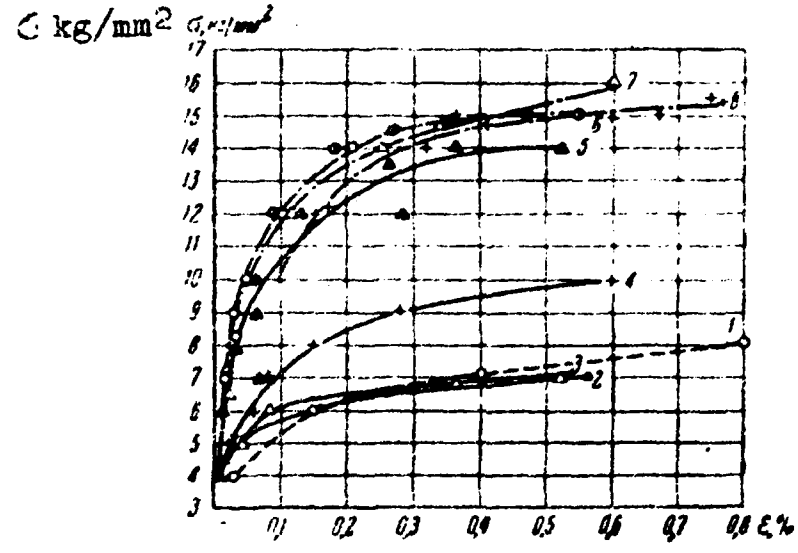

Figure 5. Curves showing creep in alloys alloyed with niobium and tungsten: 1 -- Cr20Ni120; 2 -- Cr20Ni120W0.2; 3 -- Cr20Ni120W0.5; 4 -- Cr20Ni120W1.0; 5 -- Cr20Ni120Nb0.5; 6 -- Cr20Ni120Nb0.5W0.2; 7 -- Cr20Ni120Nb0.5W0.5; 8 -- Cr20Ni120Nb0.5W1.0.

Increasing the content of tungsten in the Cr20Ni120Nb0.5 alloy produces an effect similar to the variation in heat resistance caused by the increase of the niobium content in a Cr20Ni120 alloy. At low creep rates (low stresses), the alloys with small admixtures of tungsten (Cr20Ni120Nb0.5W0.2 and Cr20Ni120Nb0.5W0.5) are more heat-resistant. At much higher creep rates the highest heat resistance is observed in alloys with a higher content of tungsten. The nature of the variation of the curves showing the dependence of creep rate on stresses confirms the analogy between the influence exerted by the variations in the concentration of niobium in Cr20Ni120W alloys and that of the variations in the concentration of niobium in Cr20Ni120Nb alloys on the heat resistance. Alloying the 0.2-percent-W alloy with 0.5 percent niobium increases the heat resistance of the alloy to the level of that in the alloy containing 0.2 percent Nb (Figure 6). But alloying a 3.1-percent-W alloy with 0.5 Nb produces an influence typical for the increase in the concentration of niobium in Cr20Ni120Nb alloys to 1.1 percent (Figure 7).

6 kg/mm^2

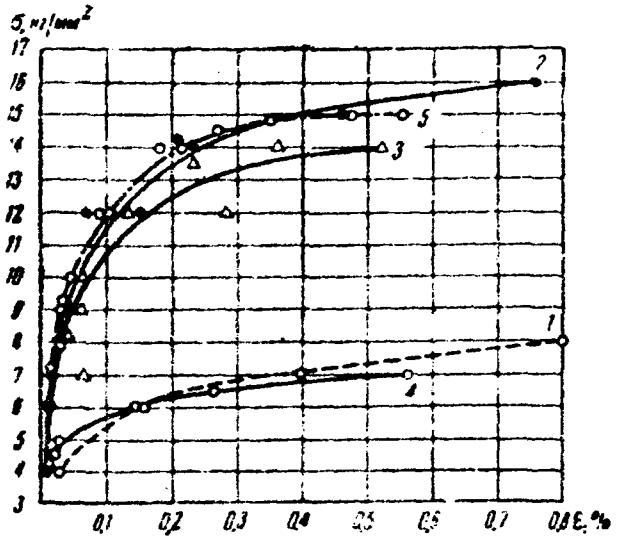

Figure 6. Curves showing creep in alloys alloyed with niobium and tungsten:
1 -- Cr20Ni120; 2 -- Cr20Ni120Nb0.2;
3 -- Cr20Ni120Nb0.5 4 -- Cr20Ni120W0.2;
5 -- Cr20Ni120Nb0.5W0.2.

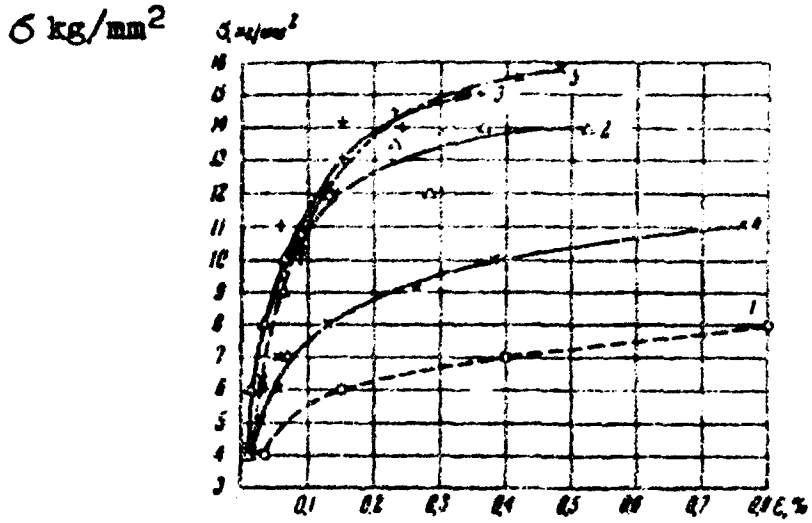

Figure 7. Curves showing creep in alloys alloyed with niobium and tungsten:
1 -- Cr20Ni20; 2 -- Cr20Ni20Nb0.5;
3 -- Cr20Ni20Nb1.1; 4 -- Cr20Ni20W3.0;
5 -- Cr20Ni20Nb0.5W3.1.

Since the investigated alloys containing niobium and tungsten have shown a sufficiently high heat resistance at low stresses, and since the total deformation over a 250-hour test at 700° amounted to less than 0.1 percent, the duration of testing was increased to 1,000 hours. Continuous tests, conducted on Cr20Ni20Nb alloys and on the Cr20Ni20Nb0.5W3.1 alloy confirmed the results obtained for 250 hours of testing. The creep rate of alloys, alloyed with niobium (0.2 to 1.1), is approximately the same at a 4 kg/mm² effective stress. At a stress of 6 kg /mm² the creep rate of Cr20Ni20Nb1.1 and Cr20Ni20Nb0.5W3.1 alloys is somewhat higher than that of the Cr20Ni20Nb0.2 alloy alloyed with the least admixture of niobium.

Interpretation of test results

Alloying the Cr20Ni20 alloy with the first smallest admixtures of titanium, niobium, and tungsten increases the heat resistance of alloys at low stresses of the order of 6 to 8 kg/mm² as compared to the heat resistance of the Cr20Ni20 alloy. The creep of alloys at high testing

temperatures and low initial stresses is mostly produced by the deformation along the grain boundaries. On the other hand, from the studies confirming the hypothesis of V. I. Arkharov*, we know that a number of alloying elements are mostly and principally concentrated in the boundary zones of the crystallites provided the total content of these elements in the alloys is small. This selective distribution of the alloying elements in the boundary zones of the crystallites strengthens the grain boundaries and increases the heat resistance of the alloys, which is confirmed by the results of this study.

Thus, increasing the concentration of the alloying elements to a definite level characteristic for the given element and the given alloy increases the heat resistance of alloys. However, the increase in heat resistance has generally an irregular nature which manifests itself in the relative resoftening of the alloys in case the concentration of the alloying elements is increased. Thus, the high creep rate at low stresses for the Cr20Ni20Nb1.1 alloy, in comparison with the Cr20Ni20Nb0.2 alloy, indicates that there has been a certain resoftening after the niobium content in the alloy had been increased to 1.1 percent; this could have been caused by a certain resoftening of the grain boundaries. The relative resoftening of alloys with a high niobium content at low creep rates (low stresses) can possibly be explained by either a redistribution of niobium caused by the increase of its concentration in the alloy or by a much stronger hardening of the volume of the austenite grains as compared to the grain boundaries.

This irregularity in the variation of heat resistance of the alloys, caused by an increase in the concentration of certain alloying elements, was observed by us in the investigated titanium alloys as well as in the alloys alloyed with a combined amount of titanium and niobium. In this connection, it is of interest to compare the data obtained on creep of alloys alloyed with titanium and niobium with the data of the alloys alloyed individually with either titanium or niobium. The first admixtures of either titanium (0.27 percent) or niobium (0.21 percent) produce the maximum influence on the increase in the heat resistance of the alloys. However, when the admixtures are alloyed in a combination, the percentage of each being

*See also the article by V. I. Arkharov and M. B. Yakutovich in this collection.

The same, the heat resistance of the Cr20Ni20Ti0.2Nb0.12 alloy is found to be below that of the alloys alloyed with either only titanium (Cr20Ni20Ti0.27) or with only niobium (Cr20Ni20Nb0.21) (Figure 8). When the content of niobium in Cr20Ni20Ti* alloys with 0.2 Ti is increased, the heat resistance of the alloys increases becoming higher than that of the Cr20Ni20Ti0.27 alloy but lower than that of the alloys with niobium alone (Figures 9 and 10).

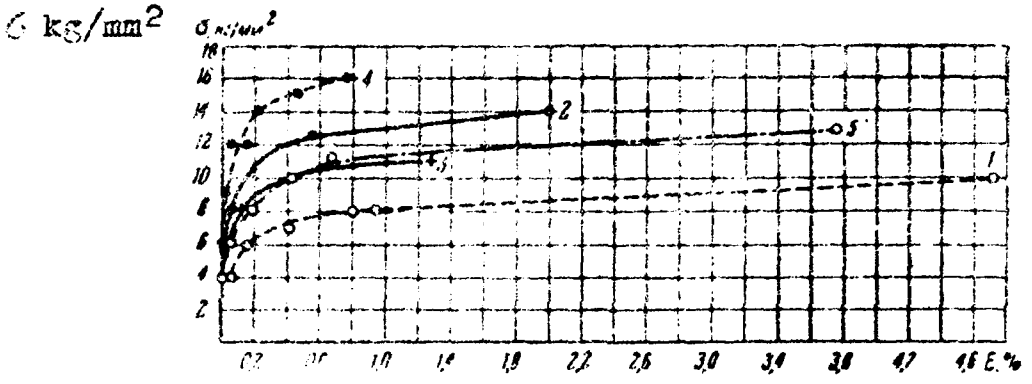

Figure 8. Curves showing creep of alloys alloyed with titanium and niobium:
1 -- Cr20Ni20; 2 --Cr20Ni20Ti0.27;
3 -- Cr20Ni20Ti1.09; 4 -- Cr20Ni20Nb0.2;
5 -- Cr20Ni20Ti0.2Nb0.12.

*Translator's note: The original text gives Ni20Ni20Ti which apparently is a misprint.

σ kg/mm²

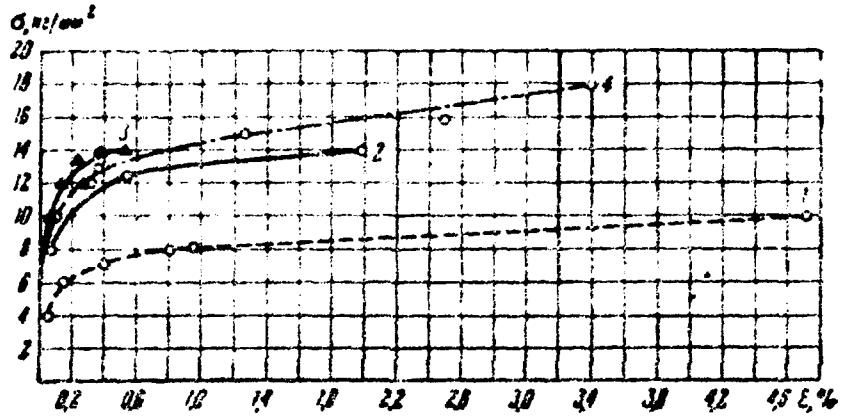

Figure 9. Curves showing creep of alloys alloyed with titanium and niobium:
1 -- Cr20Ni120; 2 -- Cr20Ni120Ti0.27;
3 -- Cr20Ni120Nb0.5; 4 -- Cr20Ni120Ti0.2Nb0.33.

σ kg/mm²

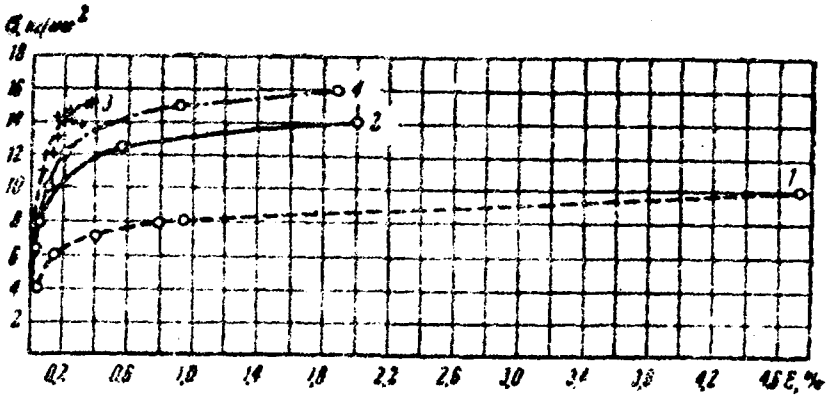

Figure 10. Curves showing creep of alloys alloyed with titanium and niobium:
1 -- Cr20Ni120; 2 -- Cr20Ni120Ti0.27;
3 -- Cr20Ni120Nb1.1; 4 -- Cr20Ni120Ti0.2Nb0.89.

Explaining these data, we must take into consideration the fairly complex composition of the investigated alloys, in which the variation in heat resistance caused by the concentration of the alloying elements depends on a number of important factors. These include: the variation in the austenitic solid solution itself; the variation in the intensity of the aging processes, since these alloys are classed as aging-type alloys (the negative creep confirms the occurrence of a phase transformation); the variations in the diffusional processes which produce a substantial influence on the heat-resistant properties of the alloys.

BIBLIOGRAPHY

1. Arkharov, V. I., Tr. In-ta fiziki metallov Ural SSSR (Works of the Ural Branch of the Academy of Sciences USSR), Issue 8, Sverdlovsk, 1946.

* * *

The Influence of Small Admixtures of Tungsten, Molybdenum, Titanium, and Niobium on the Oxidation Resistance of Certain Austenitic Cr20N120- and Cr20N135-Type Alloys at Temperatures Ranging From 1100 to 1300°

By Z. P. Kichigin

During the investigation of the mechanical properties of certain ferrum-chromium-nickel austenitic alloys it has developed that small admixtures of molybdenum, tungsten, titanium, and niobium improve the heat-resistant properties of these alloys*. It was of interest to find out how these admixtures affect the oxidation resistance of the alloys. With that end in view, we have taken a few of the alloys, the heat resistance of which we have already tested. The composition of the alloys is shown in Table 1.

*See the article by G. N. Kolesnikov, A. I. Moiseyev, and M. B. Yakutovich in this collection.

Table 1

The chemical composition of alloys, percent

Conventional grade of steel	Cr	Ni	C	Mn	Si	Mo	W	Ti	Nb
Cr20Ni20	19,85	20,0	0,025	0,30	0,08	—	—	—	—
Cr20Ni20Mo0.24	19,22	20,1	0,048	0,2	0,04	0,24	—	—	—
Cr20Ni20Mo0.65	20,1	20,2	0,031	0,22	0,014	0 65	—	—	—
Cr20Ni20Mo1.2	20,48	20,3	0,01	0,29	0,14	1,2	—	—	—
Cr20Ni20Mo0.17Nb0.4	19,97	20,5	0,037	0,20	0,18	0,17	—	—	0,4
Cr20Ni20Mo1.43Nb0.4	20,29	21,04	0,023	0,21	0,45	1,43	—	—	0,4
Cr20Ni20W0.2	19,48	20,2	0,041	0,29	0,06	—	0,2	—	—
Cr20Ni20W2.7	20,2	9,72	0,030	0,26	0,07	—	2,7	—	—
Cr20Ni20Ti0.09	20,25	18,45	0,024	0,35	0,09	—	—	0,09	—
Cr20Ni20Ti0.37	20,15	20,35	0,005	0,39	0,48	—	—	0,37	—
Cr20Ni20Ti1.87	20,93	20,40	0,050	0,38	0,60	—	—	1,87	
Cr20Ni20Ti0.11Nb0.5	19,20	29,96	0,045	0,20	0,36	—	—	0,11	0,48
Cr20Ni20Ti0.23Nb0.5	19,65	20,62	0,021	0,24	0,41	—	—	0,23	0,50
Cr20Ni20Ti0.6Nb0.5	18,95	20,91	0,026	0,25	0,32	—	—	0,60	0,49
Cr20Ni20Nb0.5	19,1	19,98	0,08	0,37	0,41	—	—	—	0,52
Cr20Ni35	19,87	35,6	0,038	0,45	0,27	—	—	—	—
Cr20Ni35W0.5	19,36	35, 6	0,040	—	0,34	—	0,5	—	—
Cr20Ni35W1.14	19,91	36,08	0,037	0,54	0,53	—	1,14	—	—
Cr20Ni35Nb0.5	19,55	35,68	0,065	0,37	0, 3	—	—	—	0,5
Cr20Ni35W0.2Nb0.58	19,63	36,36	0,028	0,38	0,56	—	0,20	—	0,58
Cr20Ni35W3Nb0.5	19,09	35,96	0,032	0,47	0,63	—	2,87	—	0,5

Method of investigation

The oxidation resistance was defined as the rate of oxidation, i.e., the ratio of the increase in the weight of the specimen after oxidation over a definite time interval at a constant test temperature to the area of the initial surface of the specimen.

Cylindrical specimens 10 mm high and 10 mm in diameter were made of the alloys. The oxidation was carried out in a porcelain tube placed into a horizontal silit furnace. Both ends of the porcelain tube were closed with rubber stoppers through which glass tubes were inserted for the admission and withdrawal of dry air. The air, used as an oxidation atmosphere for the specimen, was

desiccated and purified from CO_2 by passing it through sulfuric acid, calcium chloride, and soda lime (1). The rate of air stream was maintained constant by means of a flow meter.

The temperature was measured with platinum-rhodium thermocouple built into the furnace. The specimen was placed above the thermocouple. The furnace together with the inserted porcelain tube was brought up to the testing temperature. A quartz boat containing the weighted specimen was placed into the tube. The ends of the tube were then closed and the passing of dry air through the tube began. After the lapse of two hours the specimen was removed from the furnace and cooled in air on a porcelain plate. At this point careful attention was given not to lose any of the scale. After the specimen was cooled off it was weighed. The oxidation rate was investigated at 1100, 1200, and 1300° temperatures.

Table 2

Dependence of oxidation rate on temperature

Make of steel	Increase in the weight of the specimen, mg/cm^2		
	1100°	1200°	1300°
Cr20Ni120	2,8	3,0	3,5
Cr20Ni120Mo0.24	4,2	2,47	2, 3
Cr20Ni120Mo0.65	1,5	1,06	2,1
Cr20Ni120Mo1.2	2,17	2, 5	3,48
Cr20Ni120Mo0.17Nb0.4	2,6	9,6	50,5
Cr20Ni120Mo1.43Nb0.4	4,9	4,7	96,5
Cr20Ni120W0.2	0,63	1,37	2,8
Cr20Ni120W2.7	2 52	2,52	255,0
Cr20Ni120T10.09	1,5	3,3	3,2
Cr20Ni120T10.37	1,2	1,05	1,7
Cr20Ni120T11.87	1,06	2 5	3,4
Cr20Ni120T10.11Nb0.5	3,2	19,1	78,6
Cr20Ni120T10.23Nb0.5	4,6	4,9	37,0
Cr20Ni120T10.6Nb0.5	2,8	8,05	27,7
Cr20Ni120Nb0.5	1,7	1,48	16,4
Cr20Ni135	2,14	2,8	2,8
Cr20Ni135W0.5	1.67	1.25	20,3
Cr20Ni135W1.14	2.6	2,34	34,5
Cr20Ni135Nb0.5	1,3	3,6	13,0
Cr20Ni135W0.2Nb0.58	2,4	4,0	4,6
Cr20Ni135W3Nb0.5	1.67	1,45	25,0

Investigation results

The test results are given in Table 2. We can see from the tabular data that the influence of small admixtures on the oxidation resistance of alloys differs depending on the type of the added element, on its concentration, and on temperature.

Alloys with the admixture of molybdenum. The oxidation rate of Cr20Ni120-base alloys with admixtures of 0.2 and 1.2 percent Mo hardly differs at any temperature from the oxidation rate of the base (Cr20Ni120); however, the oxidation rate with an 0.6-percent-Mo admixture is

slightly lower than that of the base.

Alloys with the admixture of tungsten. The oxidation rate of the Cr20Ni20-base alloy with an admixture of 0.2 W at all testing temperatures is a little lower than the oxidation rate of the base. But the alloy with an admixture of 2.7 percent W at 1100 and 1200° oxidizes practically at the same rate as the base; however, as the temperature approaches 1300°, the oxidation rate rapidly increases and becomes many times higher than that of the base.

The oxidation rate of the Cr20Ni35-base alloy with an admixture of 0.5 percent W is somewhat lower at 1100 and 1200°, while at 1300° it is considerably higher in comparison with the oxidation rate of the base (Cr20Ni35).

The oxidation rate of the alloy of the same base with 1.14 percent W at temperatures of 1100 and 1200° is practically the same as in the base alloy; at 1300° it is considerably higher than that of the base.

Alloys with the admixture of titanium. The addition of 0.09 percent Ti to the Cr20Ni20 base has no effect on the oxidation rate of the alloy; the addition of 0.37 percent slightly reduces the oxidation rate of the Cr20Ni20 alloy at all testing temperatures. The oxidation rate of the alloy with 1.87 percent Ti at 1100 and 1200° is slightly lower, and at 1300° it is the same as the oxidation rate of the Cr20Ni20 base.

Alloys with the admixture of niobium. The oxidation rate of the Cr20Ni20 alloy with 0.5 percent Nb at 1100 and 1200° is a little lower than that of the base at these temperatures, while it is higher than the oxidation rate of the base at 1300°. The Cr20Ni35-base alloys with the addition of 0.5 percent niobium at 1100° oxidize a little less than the base; at 1200° the oxidation rate becomes slightly higher and at 1300° it becomes considerably higher than that of the Cr20Ni35 base.

Alloys with combined admixtures of molybdenum and niobium. The oxidation rate of the Cr20Ni20-base alloys with combined admixtures of molybdenum and niobium is markedly higher at 1100 and 1200° and is by far higher at 1300° as compared to the oxidation rate of the base (Cr20Ni20).

Alloys with combined admixtures of tungsten and niobium

The Cr20Ni35-base alloy with the combined admixtures of 0.2 percent W and 0.58 percent Nb had an oxidation rate slightly higher than that of this alloy without admixtures at all testing temperatures. At temperatures of 1100 and 1200° the Cr20Ni35 alloy with admixtures of 2.87 percent W and 0.5 percent Nb oxidizes a little less, and at 1300° a little more, than the base.

Alloys with combined admixtures of titanium and niobium. The oxidability of the Cr20Ni20 alloy with 0.11 percent Ti and 0.5 percent Nb at 1100° is slightly higher than that of the Cr20Ni20 base. As the temperature is raised to 1300°, the oxidability becomes many times higher than that of the base at these temperatures.

The oxidation rate of the Cr20Ni20 alloy with 0.23 percent Ti and 0.5 percent Nb at 1100 and 1200° is slightly higher and at 1300° much higher than that of the base.

The oxidation rate of the Cr20Ni20 with admixtures of 0.6 percent titanium and 0.5 percent niobium is almost the same as that of the base. At 1200° the oxidability of this alloy becomes noticeable and at 1300° it is considerably higher than that of the Cr20Ni20 base.

Conclusions

1. Small admixtures of molybdenum (up to 1.0 percent), tungsten (up to 0.2 percent), and titanium (up to 1.8 percent) have almost no marked effect on the oxidation resistance of ferrum-chromium-nickel alloys.

2. Niobium (up to 0.5 percent) reduces the oxidation resistance of ferrum-chromium-nickel alloys, particularly in the presence of Mo, W, or Ti in them.

3. A reduction in oxidation resistance is also caused by tungsten, its content being above 0.2 percent.

BIBLIOGRAPHY

1. Akimov, G. V., Gazovaya korroziya uglerodistykh staley (Gas Corrosion of Carbon Steels), Tr. TsAGI (Works of the Central Aero-Hydrodynamic Institute), Issue 30, Izd-vo TsAGI (Press of TsAGI), Moscow, 459.

* * *

The Effect of Internal Adsorption on Aging Processes and the Value of This Effect for Heat Resistance

By V. I. Arkharov

1. Gradation of the aging process of an alloy and the value of the latter for heat resistance

According to the most widely accepted notion, the prime condition for a high resistance of an alloy, parallel to the great atomic interaction forces in the crystal lattice, is the degree of nonuniformity of the alloy's crystalline structure, which is specific for each type of alloys. The local nonuniformities, which are either large or small, either more or less thickly distributed over the mass of the alloy, and either more or less sharply pronounced, are the sites where the plastic deformation is slowed down and damped.

In order to obtain for practical purposes the best mechanical properties, depending on the type of the alloy and the character of the atomic interaction in it, it is essential that there be an optimum degree of nonuniformity, i.e., an optimum combination of size factors, dispersion, shape, denseness, and uniformity of spatial distribution, physical and crystallographic nature of local nonuniformities, and bonding degree with the surrounding crystalline base of the alloy. There exists a wide gamma of nonuniformities which are distinguished by the above characteristics. The aging process of the alloy, i.e., the decomposition of the supersaturated solution, can be used as a basis for realizing this gamma.

There are reasons to assume that even in an unsaturated solid solution there are either more or less stable distribution nonuniformities of the atoms of the dissolved component among the atoms of the solvent in the common crystal lattice. Approaching the saturated state and, then, at a supersaturated state, these nonuniformities increase in respect to both the size of the regions they occupy and the concentration of the components; they pass through

stages of "pre-transitional" formations, Guinier-Preston zones, a partial or a complete break of the coherent bond with the surrounding crystal lattice, the nucleus crystal of the new phase getting isolated, and through the stage of further growth of these crystals (1).

2. Internal adsorption in solids

Apart from the structural nonuniformities inherent to the alloy in its given state, i.e., those effected by factors such as temperature, composition of basic constituents, and holding time for attaining equilibrium, there is one more type of nonuniformities related to the microstructure of the alloy and to the particular behavior of certain components. This particular behavior of the alloy is displayed when microstructural nonuniformities, which are the spots of increased potential energy of atomic interaction, cause the redistribution of the components between these spots (nonuniformities) and the surrounding, since such a redistribution minimizes the energy nonuniformity in the alloy.

The reduction of excess energy at the sites of structural nonuniformity can be achieved during such a redistribution by either increasing the concentration of some components or by reducing the concentration of others. The elements that enrich the sites of the structural and energy nonuniformities are called horophile, while those elements that are deprived of these nonuniformities are called horophobic. The horophile and horophobic properties depend on many factors that are not quite clarified yet; first of all, on the chemical type of the given dissolved element and the solvent in whose lattice this element is in a solid solution; next, on the concentration of the element (on an average -- over the entire alloy), on the crystallometric character of nonuniformity, on temperature, etc.

Obviously, the sharpest nonuniformity in concentration during its redistribution in the alloy containing energy nonuniformities will be observed in the presence of small quantities of strongly horophile elements in the alloy. This puts forward the problem of the physical nature of the strong influence of small and very small admixtures of certain elements on the properties of the alloys.

The phenomenon of redistribution of dissolved components caused by the structural (energy) nonuniformities and

producing a concentration nonuniformity (whereas the former are minimized due to the others), we call internal adsorption in solids.

We must emphasize here the community of our definition for the phenomenon of internal adsorption because there were tendencies to its narrow understanding. We examine structural energy nonuniformities of most diverse types and scales. The most sharply pronounced are the structural energy nonuniformities in the conjunction sites of crystallites of polycrystalline bodies, in other words, in intergranular transitional zones*. The variation in the concentration of some components which occurs independently in these zones and reduces their excess energy**, according to what has been said, we call intergranular internal adsorption.

Less pronounced are the structural energy nonuniformities in the sites of the elements of the so-called subcrystallite structure join crystal lattice of the solid solution surrounding them.

Of particular interest at present are the elements of the subcrystallite structure that originate and develop in the process of aging. These include the most initial formations, i.e., the stable groupings of the atoms of the dissolved components in still unsaturated solutions, pretransitional formations, Guinier-Preston zones coherently bound with the surrounding zones which had partially or completely broken the coherent bond and had thus become isolated crystals of the precipitating phase. Even though the structural energy nonuniformities are not very sharply pronounced in the conjunction of such elements of subcrystallite structure, it is possible on a general basis that they may also have an internal adsorption of some components.

The changes in concentration caused by adsorption in general, to one degree or another, affect the course of aging processes at the sites where these changes occur. It

*We contemplate the crystallites which are rather distinctive by either orientation or crystallographic character of the lattice.
**It is sometimes called incorrectly "surface" energy of intergranular "boundaries".

therefore seems important to consider in detail the problem of the influence of internal adsorption, in its broad understanding, on the aging processes of alloys and, in this connection, on the shaping of their heat-resistant properties.

3. The influence of the intergranular internal adsorption of the excess component on the aging process

Let us examine first the most simple case, when the excess component (that supersaturating the solid solution) in an aging binary alloy is adsorption-active, whereas the adsorption affects only the sharpest structural nonuniformities -- the intergranular conjunctions.

In this case, when the adsorption is positive, the concentration in the intergranular transitional zones may be considerably increased as compared to the mass of the crystallites. However, the closer the average concentration of the alloy to solubility at hardening temperature*, the lower the degree to which the nonuniformity in concentration is pronounced. When the intergranular internal adsorption is negative, in this case it is the opposite: the periphery of the crystallites is supersaturated to a lesser degree than the central section of each crystallite**. Here, the closer the averaged concentration of the alloy to solubility at hardening temperature the narrower the zone of impoverishment of adsorption.

Thus, during a positive adsorption in the intergranular transitional zones, due to an increased supersaturation, the conditions for the decomposition of the solid solution are more favorable; therefore it is just here where aging begins, in the first place, extending further down deep the crystallite. This difference in the kinetics of aging, particularly manifested in its initial stages, is minimized when the average concentration of the excess

---

*The adsorption enrichment of the structural energy zones of nonuniformity in the horophile element is to some extent related to its solubility (2) and is limited by it although in some cases it can, obviously, exceed it as, for instance, in the copper-ferrum system (3, 4).

**However, in some alloys, at a negative adsorption, the periphery of the crystallites may prove to be supersaturated.

component in the alloy is increased (retaining the same hardening temperature). This fact indicates that the initiatory role of the intergranular conjunctions here is related to the intergranular adsorption, but not just to the boundary distortions of the lattice which facilitate the structural rebuilding. During a negative internal adsorption more favorable conditions for aging are found in the mass of the crystallite; as for the periphery, where the supersaturation is lower, there aging will lag in the beginning. Increasing the average concentration in the alloy at the given hardening temperature up to the value of solubility at this temperature must lead to the contraction of the zone of adsorptional impoverishment near the intergranular conjunctions and to a more uniform distribution of the conditions for the decomposition of the solid solution over the crystallite which is supersaturated everywhere to the same extent except for the narrow intergranular transitional zones where the lagging of aging (if it is not compensated for by the accelerating effect of the usual distortions of the lattice in three zones) is not detected experimentally due to the narrow width of the intergranular transitional zones.

To confirm the above considerations we may cite the results of the study made by V. I. Arkharov, I. P. Borenova, and N. A. Kozina (5). In these tests they investigated the distribution of microhardness in individual crystallites of aluminum-zinc, aluminum-silver, and aluminum-copper alloys, hardened and aged to various stages.

In the Al - Zn and Al - Ag alloys, where the content of the second component was below its solubility at hardening temperature, aging (observed by the increased microhardness) began intensively and developed rapidly at the intergranular "boundaries", where it succeeded in going through the microhardness maximum while it was just beginning (to develop) in the center of the crystal. In the alloys of the systems with a higher content of the second component, which were hardened from the same temperatures as the alloys with a lower concentration, the difference in microhardness over the periphery and in the mass of the crystallites were found to be minimized.

In the Al - Cu alloy having a low copper content, the microhardness on the periphery of the crystallites at the beginning of aging appeared to be considerably reduced as compared to the mass, and the course of the variation of microhardness on both the periphery and in the mass of the

crystallites in respect to time was opposite to that in the Al - Zn and Al - Ag alloys. The decrease of microhardness (due to the set-in coagulation of the precipitated particles) in the mass of the crystallite was taking place at the time when the microhardness on the periphery was just beginning to build up.

In the Al - Cu alloy containing a higher amount of copper and hardened from the same temperature, the aging occurred uniformly in both the periphery and the mass of the crystallites.

Similar experimental facts show that intergranular internal adsorption is an important factor able to influence the aging course of alloys in general; it can, therefore, particularly have an effect on the formation of the properties of heat resistance, inasmuch as this formation is basically produced through aging.

4. The influence of the internal adsorption of the admixture of a third component on the decomposition of a binary solid solution

A more interesting case is aging in the presence of a third component in a disintegrating solid solution, the component being in low concentration and also adsorption-active (horophile).

Although the average concentration of the element admixture in the alloy is low, in the adsorption-enrichment zones it may appear increased. Due to this, the influence of the admixture on the properties of the alloy, which is insignificant structurally uniform in the mass of the crystallites, may substantially change these properties in the adsorption zones: in particular, the ability to age may thus appear substantially changed. The mechanism of such an effect is the same for structural-energy nonuniformities of all previously considered gradations; however, it may be assumed that of greatest interest is the study of this mechanism as applied to subcrystallite nonuniformities formed at the very beginning of the aging process. We will therefore not dwell upon cases in which the third component, i.e., the admixture, experiences an intergranular internal adsorption, but will turn to the most interesting case mentioned.

We know of many examples of a strong influence of small admixtures on the kinetics of aging of alloys; however

not all such cases can be given a simple explanation by the direct influence of the third component on the solubility of the excess component, i.e., on the supersaturation of the solid solution. Naturally, the admixtures which markedly reduce the solubility of the third element increase the supersaturation and stimulate the decomposition of the solid solution, while those that increase the solubility slow down the decomposition.

However, as it has been determined by our studies (6, 9), such an explanation is unsuitable for certain alloys, since the admixture used in its given (low) average concentration in alloys will either not change the supersaturation or will have an insignificant effect on it. Nevertheless, an admixture in these alloys has a quite marked effect on the aging process. At this point it turns out that the admixture has a horophile character.

An analysis of these cases leads us to the following two possible types of influence mechanism of horophile admixtures on the aging process, on the basis of notions on the internal adsorptions of these admixtures (6, 10).

1. The given admixture, being in a low concentration, does not greatly change the solubility of the excess component, but it can change it considerably with increase in concentration.

In this case the adsorption enrichment in the given admixture of the sites of structural nonuniformity will create in them seats of increased (or reduced) supersaturation, and, consequently, alleviated (or encumbered) nucleation centers of crystallization of the new phase. This may occur on the intergranular conjunctions as well as on the elements of subcrystallite structure, including here the "finest", i.e., the groupings of the atoms of the component precipitating during aging. The adsorption forms around these groupings, which exist at the earliest stages of the process (possibly even in unsaturated state of the alloy at a high temperature before hardening), as if "clouds" of atoms of the horophile system. Increasing the concentration of the admixture in such "clouds" while changing the solubility of the excess component will either facilitate (at a reduced solubility) or obstruct (at an increased solubility) the conversion of this grouping of atoms into a nucleus of crystallization.

Thus, in the considered mechanism of the phenomenon,

the influence of internal adsorption of the admixture on the kinetics of aging depends on its influence on the rate of nucleation of the centers of crystallization of the new phase. The admixture which, at a sufficiently increased concentration, reduces the solubility of the excess components, accelerates the nucleation of the centers of crystallization; the admixture, which increases solubility, will, on the contrary, decelerate the nucleation.

2. The given admixture, at a sufficiently increased concentration, affects the rate of diffusion of the atoms of the excess component in an aged solid solution.

In this case, the adsorption-enriched zones that surround the structural nonuniformities -- in particular, the "clouds" of the atoms of the admixture around the nucleating crystallization centers of the new phase (on all development stages of these centers, beginning with the initial groupings of atoms and ending with an isolated crystal) -- will affect the diffusion of the atoms of the excess component from the surrounding regions of the lattice of the solid solution to each center of crystallization. This means that the adsorption "clouds" affect the rate of growth of the nuclei.

The horophile elements (admixtures) which accelerate the diffusion of the excess component into the solid solution accelerate the growth of the crystallization centers of the new phase; but the admixtures that decelerate this diffusion will retard the growth of the centers of the new phase.

To confirm the above-stated considerations we can cite the results of a number of experimental investigations (6-12), where it has been established that the decomposition rate of the solid solution changes substantially under the effect of certain dissolved admixtures. Comparing with the disintegration rate of a binary alloy 94 percent Cu + 6 percent Ag, in an alloy of this composition plus 0.16 percent Be, the disintegration occurs considerably more slowly; in a similar copper-silver alloy with an addition of 0.17 percent Sb, the disintegration is strongly accelerated; in a similar alloy with an addition of 0.03 percent Fe, the integration is markedly accelerated, though to a lesser degree than in the case with antimony. The addition of cadmium also has a marked accelerating effect.

As our other studies have shown (3, 4, 11, 13, 14),

all these admixtures appear to be horophile in respect to copper as a solvent. On the other hand, it has been established (6, 8) that these admixtures, in indicated concentrations, have no marked effect on the solubility of silver in copper and, consequently, their effect on the kinetics of aging cannot be reduced to a variation in the supersaturation of the solid solution. At the same time, at <u>increased</u> concentrations in the admixture of beryllium, antimony, and ferrum, the solubility of silver in copper and, consequently, the supersaturation of the solid solution, somewhat change; the admixture of beryllium increases, while the admixtures of ferrum and antimony reduce, the solubility of silver in copper.

Parallel to this, it has been established that the rate of diffusion of silver in copper with a high content of antimony is very strongly increased as compared to the rate of diffusion in pure copper. The same effect, even though to a lesser degree, is observed in copper with an admixture of ferrum, while beryllium at its high concentration in copper strongly retards the diffusion of silver (11, 13).

The comparison of all these experimentally established facts (the horophile activity of the admixtures, their effect on the rate of aging, on the solubility of silver in copper, and on the rate of diffusion of silver in copper) leads to the conclusion that in these alloys the influence of the admixture on the kinetics of aging is caused by internal adsorption.

The adsorption influence on the kinetics of aging, apart from the copper alloys, was found in the aluminum-copper alloys we investigated containing horophile admixtures (6, 10), such as silver or zinc. The horophile activity of these elements in respect to aluminum follows from the results of our investigations conducted somewhat earlier (5); this can also be confirmed for silver -- in the micro-X-ray examinations made by the author of this article and by N. N. Skornyakov (6, 10), for zinc -- in micro-X-ray and autoradiographic studies made by French authors (15, 16).

At the same time, it has been established that the concentrations of either zinc or silver in aluminum employed in the study (6, 10), had no marked effect on the solubility of copper in aluminum (9), which eliminates one possible easy explanation of the effect of either zinc or silver on the rate of aging of the supersaturated solid solution

of copper in aluminum. It must be noted that at high concentrations of silver or zinc the solubility of copper in aluminum appears slightly increased. It must be concluded from this that the acceleration of aging of the aluminum-copper alloy affected by small additions of silver or zinc cannot be explained by the accelerating influence of the internal adsorption of the latter on the nucleation of the crystals of the new phase. As further tests have shown (17), increased concentrations of zinc or silver in aluminum produce an accelerated diffusion of copper into it. This offers the possibility of explaining the acceleration of the aging of the "aluminum-copper" alloy containing admixtures of either zinc or silver by the accelerating influence of the internal adsorption on the rate of growth of both the pre-transitional formations and the crystals of the new phase.

5. The possible value of the influence of internal adsorption on aging for heat resistance

The above-cited general theoretical considerations and experimental data show that the processes of aging, so important for the formation of high mechanical properties of alloys, are subjected to the influence of small admixtures on account of the internal adsorption of the latter.

There are numerous experimental data on the substantial influence of small admixtures on heat resistance, and there are reasons to assume that, at least in some cases (and maybe in most of them), this influence is related to internal adsorption which changes the kinetics of aging toward obtaining the prolonged stability of the grade of this process, which has an optimum combination of both dispersion and distribution of forming structural nonuniformities. Much is being done in searching for new formulas for heat-resistant alloys toward making their composition more complex and introducing several admixtures simultaneously into the alloy.

In this connection we must point out a very interesting and important phenomenon which complicates the picture of internal adsorption of the admixtures, and specifically, their tendency to some kind of "competition" in respect to a preferential concentration in the regions of various structural nonuniformities.

When there are two or several horophile admixtures in a solid solution, the latter can participate jointly in

the adsorption enrichment of the sites of structural energy nonuniformities only in some cases; in other cases, their participation in adsorption is unequal and not additive. At certain correlations in the concentrations of the admixtures the adsorption is experienced mainly by one admixture, while the other practically does not participate in adsorption. At other correlations in the concentration of the same admixtures they may change roles: the first will be deprived of adsorption activity while the other will enrich in adsorption the sites of increased energy.

In respect to intergranular internal adsorption, such a competition was revealed in our works on copper alloys (3, 4, 10, 14). In the presence in the copper solvent of small admixtures of antimony, berrylium, and ferrum in various combinations and various correlations of concentrations, it is possible to observe a different change of the crystal lattice parameter of the solid solution by varying the size of the crystallites. Since the influence of the content of antimony in solid solution on the parameter of its lattice is opposite to the influence of berrylium, it is easy to establish which of these admixtures changes its concentration in the mass of each crystal by varying the grain size, i.e., at the variation of the total amount of admixture which departs to the intergranular transitional zones due to adsorption. Thus, by the variation sign of the lattice parameter affected by either the decrease or the increase of the grain size of the alloy, it is possible to judge which of the admixtures (antimony or beryllium) experiences adsorption.

Iron has practically no effect on the lattice parameter of a copper solvent. In combination with either antimony or beryllium (or with both), the behavior of iron in copper-base alloys can also be traced by the character of the variation in the crystal lattice with the variation of the grain size of the alloy. The competition of admixtures with respect to their participation in adsorption we also traced for the same alloys by a different method -- the influence of foreign component (silver) on the character of its intergranular diffusion into the alloy; the results obtained were the same (3, 4).

Parallel to the phenomenon of competition between several horophile admixtures during their simultaneous presence in the solid solution, there is one more fact which complicates the internal adsorption. The adsorption activity (horophile activity) of any admixture depends on the

composition of the solvent, which may be not only the element but also the solid solution that includes in its composition several components, adsorption-passive. In particular, the horophile activity of an admixture depends in some cases on the concentration of the admixture. For instance, that is the way it is in the Fe - Pd system. According to our data (18, 20), at low concentrations, palladium is horophile in respect to iron, but in concentrations above 4 percent, palladium loses its activity.

In the light of the cited experimental data on the competition of the horophile admixtures as a function of the horophile activity of the composition of the alloy in general, the picture on the influence of the composition on heat resistance becomes clear.

In this connection we find it possible to introduce one new hypothesis that can serve as a basis in the search for an explanation of the complex dependence of heat resistance on the composition of the alloy, as well as in the search for a better formulation of alloys.

This hypothesis is reduced to the following. Horophile admixtures, taken individually, may be adsorption-active to a various degree in respect to different types of structural energy nonuniformities (for instance, intergranular transitional zones and subcrystallite nonuniformities, the periphery-type pre-transitional formations at aging or the periphery of the Guinier-Preston zones, etc.).

When there are more than one horophile admixtures present simultaneously in a solid solution, their competition may be displayed in various degrees for different types of structural energy nonuniformities. As a result, there may occur a redistribution of horophile admixtures at which various admixtures will be adsorbed on nonuniformities of various types: the sites with the greatest energy nonuniformities will be enriched mainly in one of the admixtures, while the others will enrich the regions or zones where the nonuniformities are less pronounced, etc.

At this point, it is important to take into account that in the course of aging there occurs a change in both scale and character of the structural energy nonuniformities on the periphery of the originating and developing structural formations in the mass of the lattice of the solid solution. Consequently, it may be expected that the competing horophile admixtures will rearrange themselves even

in the very process of aging, in its various stages.

We already know that there are alloys in which the internal adsorption of admixtures either accelerates or decelerates the processes of aging and the nucleation centers of the formation of the precipitating phase, as well as the growth of these centers; and we know that, combining various admixtures qualitatively or quantitatively, it may be possible to paralyze the adsorption effect of some and intensify the influence of the others.

Generally speaking, in an aging alloy there may be such a selection of admixtures where one of the admixtures will, through adsorption, accelerate the nucleation of the formation centers of the precipitating phase and their growth in the most initial stage of the process; but, then, on its course, it will be displaced by another competing admixture which is more active in respect to much sharper structural energy nonuniformities and thereby slow down the diffusion supply of the excess component to the growing formation.

Under these conditions it is possible to obtain an optimum of heat-resistant properties owing to the fact that the optimum dispersion degree of sufficiently closely distributed structural nonuniformities is rapidly attained at the beginning, whereas this state is further stabilized for a sufficiently protracted period due to the retardation of the growth of the nonuniformities on account of the redistribution of the admixtures in the adsorption zones around these nonuniformities. The optimum dispersion, the closeness, and the uniformity in distribution of the structural nonuniformities depend on the type of the alloy; there may be one set of requirements for the case of austenitic alloys and entirely different ones for aluminum-base alloys and so forth.

Here, it must also be taken into consideration that the character of the distribution of the originating structural nonuniformities over the various regions of one and the same crystal depends on the intergranular internal adsorption. An excessive concentration of the aging process at the intergranular conjunctions may cause a dangerous "intergranular" brittleness. On the other hand, as we have earlier noted (1, 21)*, the regions of the crystallite

*See also the article by V. I. Arkharov and M. B. Yakutovich in this collection.

adjoining the intergranular conjunctions are the sites of the most intensive high-temperature plastic deformation (diffusion plasticity). Therefore, hardening these regions by means of forming in them optimum structural nonuniformities by aging brought to a certain stage is essential to a greater degree than in the center of the grain. Attempts can also be made to control the course of aging in the various crystallite regions through a proper selection of horophile admixtures.

All considerations here cited lead to a conclusion of the necessity of widely expanded investigations of the internal adsorption in alloys in general.

It can be said that these investigations went through only the very initial stage. Now it has become clear that internal adsorption may play an important role in the formation of many properties of alloys, but it appears to be a more complex phenomenon than it had seemed at the beginning. Now there is already an awareness of the need of theoretical generalizations concerning the criteria of either horophile or horophobic activity, quantitative evaluation of the degree of adsorption activity of the components of solid solutions, the dependence of these characteristics on the concentration of the adsorption-active admixtures themselves, as well as of other components both inactive and active (the interaction with the latter causes a competition which is to be investigated both qualitatively and quantitatively). Then, investigations should be conducted on the influence of the horophile components of the admixtures (at an increased concentration) on the solubility of the "excess" component, which determines the aging of the alloy, as well as on the rate of its diffusion in the solid solution.

Considering the diversity of alloys and the admixtures employed with them, we must admit that the scope of the problems which arise is enormous.

However, we deem it necessary and urgent to carry out these investigations, since their results can (as we have attempted to show above) offer us one possible method of controlling the properties of alloys, and particularly of improving their heat resistance.

BIBLIOGRAPHY

1. Arkharov, V. I., Tr. In-ta fiziki metallov UFAN SSSR (Works of the Institute of Physics of Metals of the Ural Branch of the Academy of Sciences USSR), Iz-vo AN SSSR

(Press of the Academy of Sciences, USSR), Issue 16, 1955.

2. Arkharov, V. I., Tr. In-ta fiziki metallov UFAN SSSR, Issue 8, Iz-vo UFAN SSSR, 1946.

3. Arkharov, V. I., Ivanovskaya, S. I., and Skornyakov, N. N., Dokl. AN SSSR (Reports of the Academy of Sciences USSR), Vol. 89, 1953.

4. Arkharov, V. I., Ivanovskaya, S. I., and Skornyakov, N. N., Tr. In-ta fiziki metallov UFAN SSSR, Issue 16, Iz-vo AN SSSR, 1955.

5. Arkharov, V. I., Berenova, I. P., and Kozina, N. A., Dokl. AN SSSR, Vol. 98, 1954.

6. Arkharov, V. I., Varskoy, B. N., and Skornyakov, N. N., Dokl. AN SSSR, Vol. 89, 1953.

7. Arkharov, V. I., and Varskoy, B. N., Tr. In-ta fiziki metallov UFAN SSSR, Issue 16, Iz-vo AN SSSR, 1955.

8. Arkharov, V. I., Vangengeym, S. D., Magat, L. M., and Polikarpova, I. P., ZhTF (Journal of Technical Physics), 24, 1954.

9. Magat, L. M., and Noskova, N. I., Fizika metallov i metallovedeniye (Physics of Metals and Metallography), 1, No. 2, 1955.

10. Arkharov, V. I., and Skornyakov, N. N., Tr. In-ta fiziki metallov UFAN SSSR, Issue 16, Iz-vo AN SSSR, 1955.

11. Arkharov, V. I., and Gol'dshteyn, Tr. In-ta fiziki metallov UFAN SSSR, Issue 11, Sverdlovsk, Iz-vo UFAN SSSR, 1950.

12. Arkharov, V. I., and Polikarpova, I. P., ZhTF, Vol. 24, 1954.

13. Arkharov, V. I., and Gol'dshteyn, T. Yu., Dokl. AN SSSR, Vol. 66, 1949.

14. Arkharov, V. I., and Skornyakov, N. N., Dokl. AN SSSR, Vol. 89, 1953.

15. Berghezan, A., Lacombe, P., and Chaudron, G., Comp. Rend., 231, 1950.

16. Montariol, F., Albert, Ph., and Chaudron, G., Comp. Rend., 235, 1952.

17. Arkharov, V. I., and Noskova, N. I., Fizika metallov i metallovedeniye, 2, 1956.

18. Arkharov, V. I., Yefremova, K. A., Ivanovskaya, S. I., Shtol'ts, A. K., and Yunikov, B. A., Dokl. AN SSSR, Vol. 89, 1953.

19. Arkharov, V. I., and Yunikov, B. A., Dokl. AN SSSR, Vol. 94, 1954.

20. Arkharov, V. I., and Yunikov, B. A., Tr. In-ta fiziki metallov UFAN SSSR, Issue 16, Iz-vo AN SSSR, 1955.

21. Yakutovich, M. B., Tr. In-ta fiziki metallov UFAN SSSR, Issue 12, Iz-vo AN SSSR, 1950.

#2164 END

THIS PUBLICATION WAS PREPARED UNDER CONTRACT TO THE
UNITED STATES JOINT PUBLICATIONS RESEARCH SERVICE
A FEDERAL GOVERNMENT ORGANIZATION ESTABLISHED
TO SERVICE THE TRANSLATION AND RESEARCH NEEDS
OF THE VARIOUS GOVERNMENT DEPARTMENTS